
BEDEUTUNG DES KERN-ZYTOPLASMA TRANSPORTS FÜR DIE BIOLOGISCHE FUNKTION ZELLULÄRER PROTEINE
GEORG
SPEYER
HAUS

GEORG SPEYER HAUS

Untersuchungen zur Bedeutung des Kern-Zytoplasma Transports für die biologische Funktion zellulärer Proteine

Dissertation
zur Erlangung des Doktorgrades
der Naturwissenschaften

vorgelegt beim Fachbereich 14
der Johann Wolfgang Goethe-Universität
in Frankfurt am Main

von Shirley Knauer
aus Fürth / Bayern

Frankfurt im Juni 2005
(DF1)

Vom Fachbereich 14 (chemische und pharmazeutische Wissenschaften) der Johann Wolfgang Goethe-Universität als Dissertation angenommen.

Dekan: Prof. Dr. Harald Schwalbe

Gutachter: Prof. Dr. Rolf Marschalek
PD Dr. Roland Stauber

Datum der Disputation:

Der Zufall begünstigt nur den vorbereiteten Geist.

Louis Pasteur (1822-1895)

Für Claudia

I Contents

1 Zusammenfassung

Ein Hauptmerkmal eukaryoter Zellen ist ihre räumliche wie funktionelle Unterteilung in den Zellkern und das Zytoplasma. Im Gegensatz zu den Prokaryonten, die nur ein einziges zelluläres Kompartiment besitzen, können somit eine Vielzahl zelluläre Prozesse besser reguliert, und somit eine weitaus komplexere Ebene an intra- und interzellulärer Kommunikation erreicht werden. Dies erfordert jedoch die Existenz eines hoch spezifischen und effizienten Transportsystems, welches den Austausch von Makromolekülen zwischen den beiden Kompartimenten vermittelt.

Ziel dieser Arbeit war es, die Bedeutung des Kern-Zytoplasma-Transports für die biologische Funktion von Transkriptionsfaktoren sowie von Proteinen, welche am programmierten Zelltod beteiligt sind, aufzuklären. Zusätzlich sollten zelluläre Testsysteme entwickelt werden, die eine Identifizierung von molekularen Werkzeugen zur Interferenz mit dem Kern-Zytoplasma-Transport von Proteinen erlauben.

Um essentielle biologische Prozesse wie die der Signaltransduktion, Transkription und Translation zeitlich und räumlich effizient kontrollieren zu können, sind der Zellkern und das Zytoplasma durch die Kernhülle voneinander getrennt. Der Substanzaustausch durch die Kernhülle wird durch die kanalartigen, dynamischen Kernporenkomplexe vermittelt, welche aus lektinbindenden Proteinen, den so genannten Nukleoporinen aufgebaut sind (Übersicht in Pante, 2004). Es wird angenommen, daß neben Ionen und Metaboliten Makromoleküle bis zu einem Molekulargewicht von 60 kDa die Kanäle der Kernporen einem Konzentrationsgradienten folgend mittels freier Diffusion passieren können. Makromoleküle von mehr als 60 kDa werden hauptsächlich mittels eines aktiven Transportprozesses transportiert, welcher signalspezifisch und energieabhängig auch gegen ein Konzentrationsgefälle erfolgen kann, wobei der Kernporenkomplex als selektiver Transporter fungiert (Übersicht in Pemberton & Paschal, 2005). Der Transport wird durch Transportrezeptoren vermittelt, die ihre Substrate über spezifische Sequenzmotive erkennen und binden können, und selbst zwischen dem Zellkern und dem Zytoplasma wandern. Die Nukleoporine dienen hierbei hauptsächlich als stationäre Phase, an denen die mit Transportsubstraten beladenen Rezeptoren transient binden. Je nach Richtung der Translokation wird bei den Erkennungssequenzen zwischen nukleären Importsignalen (NLS) und nukleären Exportsignalen (NES) unterschieden. „Klassische“ NLSe bestehen aus einer Anhäufung basischer Aminosäuren (zur Übersicht siehe Bednenko *et al.*, 2003) und vermitteln über die Bindung an die Transportrezeptoren Importin-α und -β den Kernimport. Für eine Reihe von Transportsubstraten wird jedoch auch ein Kernimport direkt durch

Importin-β oder durch alternative Importrezeptoren diskutiert.
Im Gegensatz zum Kernimport ist der Kernexport molekular weniger gut verstanden. Die am besten charakterisierten Kernexportsignale sind reich an hydrophoben Aminosäuren, wie Leucin oder Isoleucin (zur Übersicht siehe Bednenko *et al.*, 2003). Leucin-reiche NESe vermitteln als Komplex mit Ran-GTP die Bindung an den Exportrezeptor Exportin-1 (CRM1). Die Bindung der Transportsignale sowie die anschließende Freisetzung der Transportrezeptoren wird durch die asymmetrische Verteilung von Ran in seinen verschiedenen nukleotid-gebundenen Formen reguliert. In neueren Arbeiten sind eine Reihe weiterer Exportrezeptoren identifiziert worden, denen eine Selektivität für gewisse Proteine und RNA-Spezies zugeschrieben werden.

Für eine Vielzahl von Molekülen ist der koordinierte und effiziente Ablauf nukleozytoplasmatischer Transportprozesse essentiell für die Ausübung ihrer biologischen Aufgaben. Insbesondere für Transkriptionsfaktoren stellt die Regulation ihrer subzellulären Lokalisation einen attraktiven Mechanismus zur Kontrolle ihrer Aktivität dar. Die komplexen Expressionsmuster der Homeobox-Gene in der embryonalen Retina erfordern ein ausgeklügeltes regulatorisches Netzwerk von Transkriptionsfaktoren (Ohtoshi *et al.*, 2004). Um eine mögliche Regulation der Aktivität dieser Transkriptionsfaktoren durch aktiven Kern-Zytoplasma-Transport zu untersuchen, wurde im Rahmen dieser Arbeit das intra- und interzelluläre Transportverhalten der sogenannten „paired-like CVC Homeodomain“ Proteine (PLC-HDPs) auf molekularer Ebene analysiert (Knauer *et al.*, 2005a). Mittels Deletionsmutagenese, Mikroinjektionsexperimenten und biochemischer Analysen konnte gezeigt werden, daß die Mitglieder der PLC-HDP Familie über den CRM1-Signalweg aus dem Kern exportiert werden und ein evolutionär konserviertes Leucin-reiches NES enthalten. Der Kernexport regulierte durch den verstärkten proteasomalen Proteinabbau im Zytoplasma die intrazelluläre Konzentration und extrazelluläre Sekretion der PLC-HDPs, und beeinflußte somit die transkriptionelle Aktivität der PLC-HDPs. Die hauptsächlich nukleäre Gleichgewichtslokalisation der PLC-HDPs wurde durch ein aktives NLS vermittelt, welches in der PLC-HDP Familie zu 100% konserviert ist. Die hohe Homologie des NLS zu bekannten Protein-Transduktionsdomänen (PTD) konnte auch funktionell verifiziert werden. Die Integrität beider Signale, NES und NLS/PTD, erscheint somit als Grundvoraussetzung für die Funktion der PLC-HDPs als mobile nukleozytoplasmatische „shuttle“-Proteine mit dem Potential zur unkonventionellen Sekretion und zum interzellulären Transfer. Neben der Kontrolle auf der Ebene der Transkription, scheint der Kern-Zytoplasma-Transport somit einen zusätzlichen konservierten Kontrollmechanismus für die präzise Feinregulation der transkriptionellen Aktivität der PLC-HDPs darzustellen, um das komplexe Expressionsmuster innerhalb der Retina-Entwicklung zu gewährleisten.

Neben intrazellulären Transportsignalen können auch posttranslationelle Modifikationen einen regulatorischen Einfluß auf die Lokalisation von Proteinen haben. Beispielsweise wird der nukleozytoplasmatische Transport der STAT Transkriptionsfaktoren durch Phosphorylierungen reguliert (McBride & Reich, 2003), und auch andere Modifizierungen wie Sumoylierung (Endter *et al.*, 2001) und Acetylierung (Yuan *et al.*, 2005) können einen Einfluß auf den Kerntransport von Proteinen haben. Das Gleichgewicht zwischen der Acetylierung und Deacetylierung von Proteinen wird durch die sogenannten Histon-Acetyltransferasen (HATs) und Histon-Deacetylasen (HDACs) reguliert (Kouzarides, 1999). Chemische HDAC-Inhibitoren (HDACi) können das Expressionsmuster verschiedenster Gene beeinflussen, deren Genprodukte wichtige regulatorische Funktionen während der Differenzierung, des Zellzyklus, der Apoptose oder der Signaltransduktion ausüben. Um die molekularen Wirkmechanismen der HDACi zu verstehen, wurde in der vorliegenden Arbeit (Krämer *et al.*, 2005) der Einfluß von HDACi auf Signaltransduktionskaskaden und auf die Apoptoseinduktion untersucht. Es zeigte sich, daß die durch HDACi verursachte Apoptose mit der Expression des STAT1-Proteins korrelierte, und die ektope Expression von STAT1 in STAT1-defizienten Zellen die HDACi vermittelte Apoptose auslösen konnte. HDACi induzierten nicht nur die STAT1-Expression, sondern bewirkten außerdem dessen Acetylierung. Acetyliertes STAT1 zeigte eine verbesserte Bindung an NF-κB p65, und die STAT1/NF-κB p65 Komplexe wiesen eine verminderte nukleäre Lokalisation und reduzierte DNA-Bindung auf, was letztendlich eine verminderte Expression anti-apoptotischer Zielgene zur Folge hatte. Diese Arbeit zeigte, daß die Interaktion zwischen STAT1 und dem NF-κB Signaltransduktionsweg durch HDACi-induzierte Änderungen im Acetylierungszustand von STAT1 reguliert werden, und durch Beeinflussung der intrazellulären Lokalisation letztendlich die biologische Aktivität von Signaltransduktionswegen verändert werden kann.

Nicht nur indirekt über die Aktivierung von Signaltransduktionsketten, sondern auch direkt spielt der Kern-Zytoplasma-Transport eine wichtige Rolle innerhalb der Apoptose. Der programmierte Zelltod kann sowohl durch interne als auch durch externe Stimuli ausgelöst werden (Übersicht in Krammer, 2000), und erfordert letztendlich den Zugang von Effektorproteinen zum Zellkern. Deregulierte Apoptosevorgänge spielen eine wichtige Rolle bei einem breiten Spektrum humaner Erkrankungen einschließlich Krebs. Neben den Mitgliedern der Bcl-2 Proteinfamilie (Cory & Adams, 2002) kann die enzymatische Aktivität der Caspasen auch durch die sog. „Inhibitoren der Apoptose" Proteine (IAPe) (Deveraux & Reed, 1999) reguliert werden. Besondere Beachtung fand in den letzten Jahren das IAP Survivin, welches in den meisten Tumoren stark exprimiert wird und an der Resistenz von Tumoren gegenüber Radio- und Chemotherapie beteiligt zu sein scheint (Altieri, 2003d).

Neben seiner anti-apoptotischen Aktivität spielt Survivin außerdem als sog. „chromosomal passenger“ eine wichtige Rolle während der Zellteilung (Lens *et al.*, 2003). Diese duale Rolle weist Survivin als ein attraktives Ziel für die Entwicklung neuer Krebstherapeutika aus.
In der vorliegenden Arbeit wurde daher untersucht, ob und in welcher Weise der Kern-Zytoplasma-Transport eine Rolle für die biologische Funktion von Survivin spielt (Knauer *et al.*, 2005b). Die Überexpression von Survivin konnte in Kopf-Hals-Tumoren und in kolorektalen Karzinomen sowohl auf RNA als auch auf Proteinebene verifiziert werden. Dabei zeigte sich, daß Survivin sowohl im Zytoplasma als auch im Zellkern von Tumorproben detektiert werden konnte, was auf eine dynamische intrazelluläre Lokalisation hinwies. Diese Annahme konnte durch die Identifizierung eines evolutionär konservierten CRM1-abhängigen Leucin-reichen NESs bestätigt werden. Interessanterweise war die Integrität des NES essentiell für eine geordnete Zellteilung, da Survivin durch die NES-vermittelte Interaktion mit CRM1 an die Mitosemaschinerie lokalisiert wurde. Zusätzlich zeigte sich, daß der Kernexport wichtig für den durch Survivin vermittelten Schutz gegenüber Chemo- und Radiotherapie induzierter Apoptose war, da die NES-vermittelte zytoplasmatische Lokalisation von Survivin eine optimale Interaktion mit der Apoptosemaschinerie zu ermöglichen scheint. Die klinische Relevanz dieser Ergebnisse wurde durch die Beobachtung untermauert, daß eine vorwiegend nukleäre Lokalisation von Survivin, welche durch Störung des nukleären Exports in Zellkulturexperimenten induziert werden konnte, mit einer längeren Überlebensdauer in Kolonkarzinompatienten korrelierte. Somit scheint der Kernexport essentiell für die duale biologische und auch tumorfördernde Aktivität von Survivin zu sein. Die spezifische Interferenz mit dem Kernexport von Survivin stellt daher einen vielversprechenden Ansatz für die Entwicklung neuer Anti-Krebs-Therapien dar.

Die Ergebnisse dieser Studie und eine Vielzahl von Beispielen aus der Literatur belegen, daß nukleozytoplasmatische Transportprozesse essentiell für die biologische Funktionen von Proteinen sind, welche eine zentrale Rolle für eine Reihe von Krankheitsprozessen spielen. Der Ansatz, die gerichtete Modulation nukleozytoplasmatischer Transportprozesse als therapeutische Strategie zu verfolgen, rückte daher in den letzten Jahren vermehrt in das Interesse von akademischer und industrieller Forschung (Kau *et al.*, 2004). In diesem Zusammenhang ist die Verfügbarkeit zellbasierte Testsysteme von besonderer Bedeutung, um eine effiziente Identifizierung und Validierung von Inhibitoren dynamischer intrazellulärer Prozesse zu gewährleisten.

Im Rahmen dieser Arbeit wurden neuartige Biosensoren generiert, welche es ermöglichen, den signal-spezifischen Kern-Zytoplasma-Transport molekular zu charakterisieren, und die zugleich als Grundlage für die Entwicklung zell-basierter Testsysteme zur Identifizierung chemischer Transportinhibitoren dienen können. (Knauer *et al.*, 2005c). Die autofluoreszierenden Translokations-Biosensoren setzten sich aus Glutathion-S-Transferase (GST), Mutanten des grün-fluoreszierenden Proteins (GFP) sowie rationalen Kombinationen aus nukleären Import- und Exportsignalen zusammen. Diese hauptsächlich im Zytoplasma lokalisierten Indikatormoleküle wandern kontinuierlich zwischen Kern- und Zytoplasma. Die Inhibition des Kernexports führte zu einer quantitativen nukleären Translokation, welche fluoreszenzmikroskopisch bereits in lebenden Zellen detektiert und automatisch quantifiziert werden konnte. Dieses System erlaubt es nicht nur, den Einfluß der Expression oder der siRNA-vermittelten Degradation von Proteinen auf den Kern-Zytoplasma-Transport zu untersuchen, sondern auch chemische Substanzen auf deren inhibitorische Aktivität zu testen bzw. Inhibitoren aus Substanzbibliotheken zu identifizieren.

Zudem wurden die Transport-Biosensoren zu Protein-Translokations-Biosensoren (PTB) weiterentwickelt, welche es erlauben, Protease-Aktivität sowie Protein-Protein-Interaktionen *in vivo* zu erforschen.
Zur Generierung der Protease-Biosensoren wurde in die Transport-Biosensoren zusätzlich eine Proteasespaltstelle vor dem NES integriert. Intrazelluläre Proteasen bewirken die proteolytische Abspaltung des NES, wodurch die Kernakkumulation des Biosensors induziert wird. Die Funktionalität des Systems als Apoptose-Sensor konnte durch die Integration der Casapase-3 Schnittstelle experimentell verifiziert werden.
Eine dritte Anwendung des Translokationsprinzips stellt das sog. „Two-Hybrid“ Protein-Interaktions-System dar. Ein primär zytoplasmatisch lokalisiertes „Beute“-GFP-Fusionsprotein, welches kontinuierlich zwischen Zytoplasma und Zellkern wandert, beinhaltet die zu testenden Proteindomäne. Durch Koexpression mit dem am Nukleolus verankertem „Köder“-BFP-Fusionsprotein, welches eine zweite Proteindomäne enthält, findet im Falle einer effizienten *in vivo* Protein-Interaktion eine Translokation des „Beute“-GFP-Fusionsprotein an den Nukleolus statt, die fluoreszenzmikroskopisch bereits in lebenden Zellen detektiert werden kann. Die Spezifität sowie die generelle Anwendbarkeit der PTB wurde durch die Analyse unterschiedlicher Klassen von Protein-Interaktionsdomänen (ID), wie z.B. der „Leucin-Zipper“-ID der Transkriptionsfaktoren Jun und Fos, der basischen „Helix-loop-Helix-Zipper“ ID der Transkriptionsfaktoren Myc und Max sowie der „coiled-coil“ ID der leukämieassoziierten Bcr-Abl-Proteinkinase nachgewiesen (Knauer *et al.*, 2005c; Knauer & Stauber, 2005). Das Translokations-System erlaubt neben der Verifizierung der *in*

vivo Protein-Interaktion auch eine effiziente Kartierung von ID, wie am Beispiel der Proteine p53 und Mdm2 gezeigt werden konnte (Knauer & Stauber, 2005). Im Gegensatz zu auf Enzym-Komplementation basierenden Testsystemen erwies sich das PTB-System als effizient und reversibel, und somit auch zur systematischen Identifizierung synthetischer Protein-Protein-Interaktions-Inhibitoren geeignet.
Die im Rahmen dieser Arbeit entwickelten Biosensoren nutzen somit die nukleäre Akkumulation der vormals zytoplasmatischen Indikatormoleküle als gemeinsamen „Read-out". Durch die gerichtet Integration regulatorischer Sequenzen konnten drei Klassen von Biosensoren entwickelt werden, welche zum Studium von Kerntransportprozessen, der Aktivität intrazellulärer Proteasen und von Protein-Protein-Wechselwirkungen angewendet werden können. Die vorgestellten Testsysteme erscheinen auch für die Entwicklung von zellbasierten Testsystemen geeignet, um eine systematische Identifizierung von niedermolekularen potentiell therapeutisch relevanten Inhibitoren durchzuführen.

Die vorliegende Arbeit unterstreicht nicht nur die allgemeine zellbiologische Bedeutung des nukleozytoplasmatischen Transports, sondern verdeutlich auch dessen Potential zur Entwicklung neuer Therapien gegen Krankheiten.

2 Introduction

One defining key feature of eukaryotic cells is their spatial and functional division into the nucleus and the cytoplasm. In contrast to prokaryotes that only possess one cellular compartment, numerous fundamental biological processes can be regulated more sophisticatedly, and thus a much more complex level of intra- and intercellular communication can be achieved. To efficiently control fundamental biological processes like signal transduction, transcription and translation in a time and space dependent manner, the nucleus, comprising most of the cell's genetic material, and the cytoplasm, where protein synthesis takes place, are separated by the nuclear envelope and transport occurs through the nuclear pore complexes. This type of regulation requires the existence of a highly specific and efficient transport machinery for the controlled transport of macromolecules between both compartments. Ordered regulation of bidirectional nucleo-cytoplasmic transport is critical for normal cell function and essential for cellular homeostasis. Deregulation of nucleo-cytoplasmic transport has been observed in many disease conditions, and the cellular transport machinery is also taken advantage of by intracellular parasites, such as viruses. Thus, besides the academic interest in a detailed understanding of the molecular regulation of nucleo-cytoplasmic transport, targeted intervention with transport is now considered also an attractive opportunity for the development of novel therapeutics.

Therefore, this work aimed to unreveal the impact of nucleo-cytoplasmic transport on the biological function of transcription factors as well as proteins involved in programmed cell death. Additionally, cell-based assay systems should be developed, which allow the identification of molecular tools for the interference with nucleo-cytoplasmic transport of proteins.

3 Nucleo-cytoplasmic transport

All nucleo-cytoplasmic transport processes take place through the nuclear pores that are embedded in the nuclear envelope (reviewed in Fahrenkrog *et al.*, 2004; Pante, 2004). Ions, metabolites, and other small molecules up to a size of 60 kDa are able to passively diffuse through the pore channels, whereas larger molecules or complexes must be actively transported in an energy-dependent manner (Pante & Kann, 2002). This active transport can also occur against a concentration gradient, and is mediated by soluble transport factors, that in turn shuttle between the nucleus and the cytoplasm. Importantly, even molecules that are theoretically small enough for passive diffusion are actively and selectively transported, and often play crucial roles for cellular homeostasis (Görlich & Kutay, 1999), since regulated transport appears to be more efficient and more amendable for specific regulation.

3.1 Composition and structure of the nuclear pore complex

The complex macromolecular structure that acts as the passageway for transport is a large dynamic multi-protein assembly called the nuclear pore complex (NPC) (Pante, 2004). It is embedded in the double membrane of the nuclear envelope and has an estimated molecular mass of 125 MDa in vertebrates (Reichelt *et al.*, 1990). Although the NPC performs a function analogous to membrane channels, it does not span the individual bilayers but instead forms an aqueous channel at the site where the inner and outer nuclear membrane are continuous. Figure 3.1.1.A shows an electron microscopical (EM) cross-section of a vertebrate nuclear pore (Stoffler *et al.*, 1999) with a double-layered nuclear membrane around the pore and a high electron density in the central plane of the nuclear membrane. It extends approximately 120 nm in width and 200 nm in heights (figure 3.1.1.A). In vertebrates the NPC is composed of about 30 different proteins that are collectively termed nucleoporins (NUPs) (reviewed in Fahrenkrog *et al.*, 2004; Pante, 2004). Owing to the eight-fold rotational symmetry of the NPC and the relatively small number of proteins that build up the nuclear pore, it can be assumed that most of the NUPs are present at a copy number of either 8 or an integer multiple of 8 per pore. The 8-fold symmetry around a central axis can also be observed in the conventional transmission electron microscopical (CTEM) top view of nuclear pores shown in figure 3.1.1.B (Reichelt *et al.*, 1990). The schematic organization of the nuclear pore complex is depicted in figure 3.1.1.C. It is composed of a central body

consisting of eight spoke-like segments sandwiched between nucleoplasmic and cytoplasmic rings. The spokes project radially from the wall of the pore membrane and surround a central tube called the central transporter. Each spoke is composed of numerous struts and attached to its neighbors by four coaxial rings: an outer spoke-ring in the lumen of the nuclear envelope adjacent to the pore membrane, a nucleoplasmic ring, a cytoplasmic ring, and an inner spoke-ring surrounding the central transporter. A considerable portion of each spoke traverses the pore membrane and resides in the lumen of the nuclear envelope. Together these structures comprise the central core. Peripheral elements project from this core toward the nucleoplasm and cytoplasm. These include numerous proximal filaments on both faces of the cylindrical central core, whose presence is inferred from the large number of symmetrically disposed filamentous nucleoporins. In addition, fibers extend into both cytoplasm and nucleus. The eight cytoplasmic filaments are attached at the cytoplasmic ring, and the nuclear filaments originate at the nuclear ring and conjoin distally to form a basket-like structure below the body of the NPC, reaching approximately 120 nm into the nucleoplasm (figure 3.1.1.A), thus connecting with elements of the nucleoskeleton. The body of the NPC thereby forms a central channel through which macromolecules are transported.

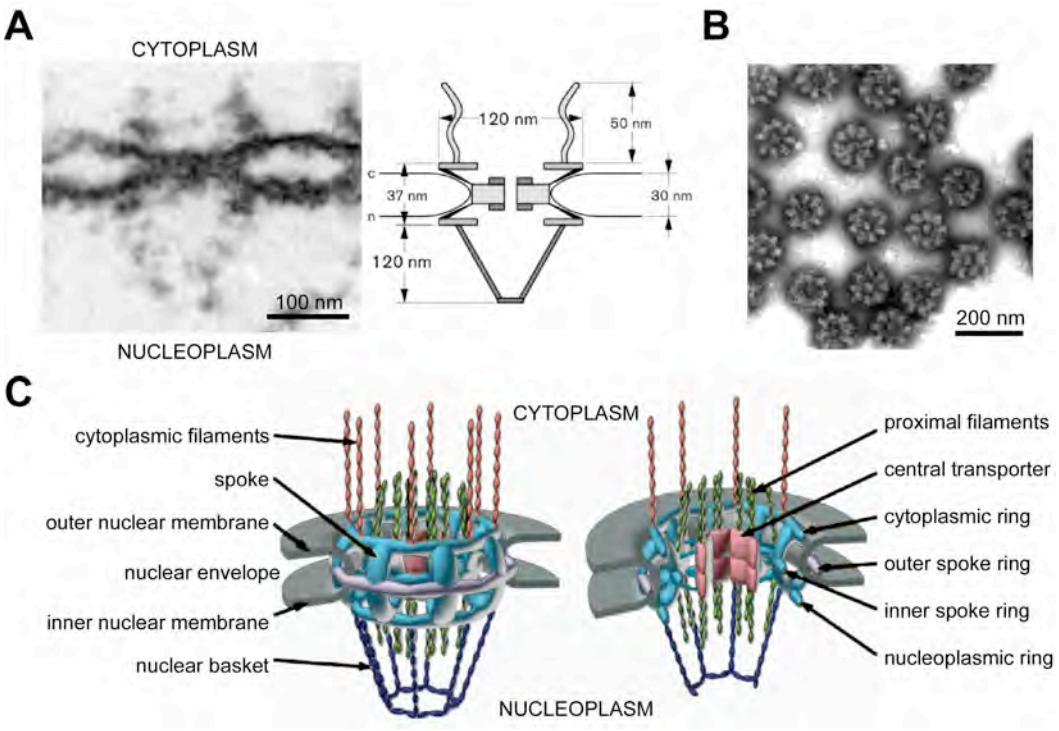

Figure 3.1.1. **Structure of the nuclear pore complex.** (A) EM cross-section of a vertebrate NPC (*Xenopus laevis*) and the respective schematic comparison (Stoffler *et al.*, 1999) (B) CTEM top view of negatively stained vertebrate NPCs (*Xenopus laevis*) (Reichelt *et al.*, 1990). (C) Organization of a vertebrate NPC. Structural elements are marked by arrows (Rout & Aitchison, 2001). See text for further explanations.

Nucleoporins can be assigned to two different groups: NUPs without phenylalanine-glycine (FG)-repeats, which form the basic scaffold of the nuclear pore (Doye & Hurt, 1997), and FG-repeat containing NUPs (see table 3.1.). Those interact with the transport receptors, importins (IMPs) and exportins (EXPs), and are considered to guide the transport receptor-cargo complexes through the pore.

Investigations on the composition of the NPC revealed distinct subcomplexes of nucleoporins. The relative positions of individual NUPs in the NPC structure have been determined by immuno-electron microscopy (Fahrenkrog *et al.*, 2000; Rout *et al.*, 2000; Stoffler *et al.*, 1999), revealing a defined network of NUP-NUP subcomplexes. Thus, the NUPs seem to have specific substructural localizations within the NPC architecture, with distinct protein compositions on the cytoplasmic and the nucleoplasmic faces (see table 3.1. and figure 3.1.2.), which may reflect distinct functions during NPC assembly and transport (reviewed in Suntharalingam & Wente, 2003).

Table 3.1. **NPC Components in Vertebrates.**

Nucleoporin	Localization	Motif(s)
NUP153b	Nuclear	FXFG
NUP62	Symmetric	FG, FXFG
NUP50b	Nuclear-biased	FXFG
NLP1/hCG1 (45)	Cytoplasmic	FG
NUP58, NUP45	Symmetric	FG
NUP35	Symmetric	
NUP35	Symmetric	
NUP54	Symmetric	FG
NUP88	Cytoplasmic	
NUP107	Symmetric	
NUP75/NUP85	Symmetric	
NUP93	Symmetric	
NUP98b	Cytoplasmic-biased	GLFG
NUP98b	Cytoplasmic-biased	FG, GLFG
NUP98b	Nuclear-biased	GLFG
NUP160	Symmetric	
NUP133	Symmetric	
NUP96	Symmetric	
NUP155	Symmetric	
NUP155	Symmetric	
NUP214/CAN	Cytoplasmic	FG
NUP188	Symmetric	
NUP205	Symmetric	
hGle1b,d (85)	Cytoplasmic-biased	
Rae1/Gle2b (41)	Symmetric	WD
Tpr (266)	Nuclear	
Tpr (266)	Nuclear	
Seh1 (40)	Symmetric	WD
Pom121	Pore membrane	FG, TM
Gp210	Pore membrane	TM
NUP358/RanBP2	Cytoplasmic	FXFG
ALADIN (60)	?	WD
NUP37	?	WD
NUP43	?	WD

Table based on the general NUP nomenclature. The numerical designation reflects the predicted mass in kDa. For a subset where this is not the case, the predicted mass is in parentheses. A NUP having two different names is indicated by "/".

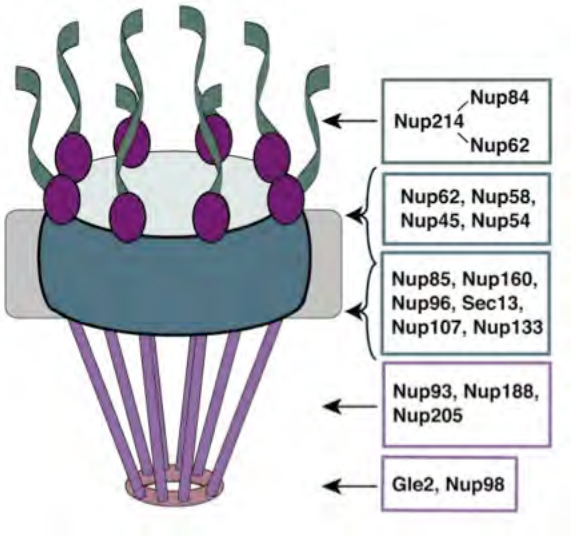

Figure 3.1.2. **NUP Subcomplexes in Vertebrate NPCs.** The boxes show the reported NUP-NUP subcomplexes. Defined NUP-NUP interactions are indicated by the dashes, whereas commas indicate that the association network is not fully known. Their relative surface-accessible localizations are indicated: purple or green box: asymmetric, only on the designated side; blue box: symmetric with two sets, one on each side. Figure adapted from (Suntharalingam & Wente, 2003). See text for further explanations.

3.2 The Ran-GTPase cycle

As the process of active transport is mediated by mobile transport receptors interacting with NUPs, it additionally needs diverse soluble factors that are able to shuttle between the nucleus and the cytoplasm as well. One of these soluble factors, which plays an important role in conferring directionality to nucleo-cytoplasmic transport events, is the small Ras-like GTPase (guanosine-5'-triphosphatase) Ran (Izaurralde *et al.*, 1997; Nachury & Weis, 1999). Furthermore, Ran acts in diverse cellular processes like mitotic spindle assembly, the regulation of cell cycle progression, and post-mitotic nuclear assembly (Dasso, 2002). In contrast to the majority of the members of Ras superfamily, Ran localizes predominantly to the nucleus. Similar to other Ras-like GTPases, Ran occurs in to different bound states inside the cell (reviewed in Görlich & Kutay, 1999; Kuersten *et al.*, 2001). Either it is bound to guanosine triphosphate (GTP), or it is complexed to guanosine diphosphate (GDP) (figure 3.2.). A steep Ran-GTP/Ran-GDP gradient has been measured across the nuclear envelope, being the key for dictating the bidirectionality of transport. This gradient with nuclearly

enriched Ran-GTP is generated by the cellular compartmentalization of the regulators of the Ran cycle. The existence of these specific factors is necessary because of the low intrinsic GTP-hydrolysis und nucleotide exchange activity. Specifically, the guanine-nucleotide exchange factor of Ran (RanGEF or RCC1), which regenerates Ran-GTP, is nuclear and associated with the chromatin (Azuma & Dasso, 2000; Dasso, 2001). In contrast, the main GTPase-activating protein (RanGAP) and its co-activators, the Ran-binding proteins RanBP1 and RanBP2, which stimulate GTP to GDP + P_i hydrolysis, localize to the cytoplasm (Dasso, 2001). As a direct consequence, nuclear Ran is predominantly bound to GTP whereas cytoplasmic Ran is immediately converted to a GDP-bound state. Interestingly, an increase of Ran-GTP levels in the cytoplasm of permeabilized HeLa cells could partially invert the direction of transport (Nachury & Weis, 1999).

It was also suggested that, in addition to the Ran cycle, the NPC itself could provide a further mechanism to ensure transport directionality (Ben-Efraim & Gerace, 2001). Given that several nucleoporins implicated in binding to importins and exportins have distinctive locations in the structure of the NPC, the asymmetric design of the NPC may also be important to efficiently drive nuclear import and export.

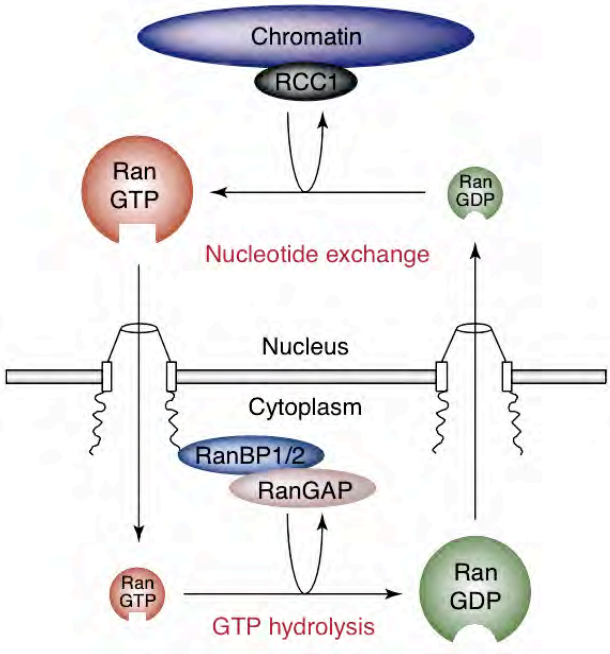

Figure 3.2. **The Ran-GTP/GDP cycle.** Figure modified from (Kuersten *et al.*, 2001). See text for details.

3.3 The protein family of karyopherins

Most nucleo-cytoplasmic transport processes are mediated by a group of homologous transport receptors, the karyopherins. They belong to the family of importin-β-like proteins, named after the first characterized member importin-β (Görlich *et al.*, 1995). In vertebrates, there exist at least 20 different karyopherins (table 3.3.), which recognize their various cargoes via transport signals present in them (reviewed in Pemberton & Paschal, 2005). Depending on the direction of transport, karyopherins are divided into importins und exportins, with the potential to recognize either substrates with an nuclear import/localization (NLS) or nuclear export signal (NES), respectively. Importins bind their cargo in the cytoplasm and transfer it to the nucleus, whereas exportins interact with their substrates in the nucleus and mediate their export to the cytoplasm. Human importin-13 takes an exceptional position within the karyopherins (Mingot *et al.*, 2001), mediating both export and import of its substrates, and is therefore also called transportin. All karyopherins consist of a N-terminal Ran-GTP-binding site and a C-terminal domain mediating the interaction with their cargoes. At the same time, the karyopherins can interact with the FG-repeats of the NUPs and thereby enable the translocation of the complexes through the pore. Despite their detailed characterization, the exact molecular mechanism how specificity and activity of the karyopherin-cargo interaction is achieved and controlled is still not completely understood.

Table 3.3. **Members of the human karyopherin-β family.**

Karyopherin	Cargo
Import	
Importin-β1	Many cargoes, cargoes with basic NLSs via karyopherin-α, UsnRNPs via snurportin
Karyopherin-β2	hnRNPA1, histones, ribosomal proteins
Transportin SR1	SR proteins
Transportin SR2	HuR
Importin 4	Histones, ribosomal proteins
Importin 5	Histones, ribosomal proteins
Importin 9	Histones, ribosomal proteins
Importin 7	HIV RTC, Glucocorticoid receptor, ribosomal proteins
Importin 8	SRP19
Importin 11	UbcM2, rpL12
Export	
CRM1/Exportin 1	Leucine-rich NES cargoes
Exportin-t	tRNA
CAS	Karyopherin α
Exportin 4	eIF-5 A
Exportin 5	microRNA precursors
Exportin 6	Profilin, actin
Exportin 7	p50Rho-GAP, 14-3-38
Import/Export	
Importin 13/Transportin	Rbm8, Ubc9, Pax6, hnRNPA1 (import); eIF-1 A (export)
Uncharacterized	
RanBP6	undefined
RanBP17	undefined

Table adapted from (Pemberton & Paschal, 2005).

3.4 Energetics of nucleo-cytoplasmic transport

In the past, it has been suggested that the translocation through the pore needs hydrolysis of adenosine or guanosine triphosphate (ATP or GTP, respectively). In the meantime, this assumption was refuted by different findings. E.g., for the import of a classical NLS by importin-α und importin-β (see 3.5.1), no hydrolysis of GTP appears to be required (Schwoebel *et al.*, 1998). The NES-mediated export (see 3.5.2) by the export receptor CRM1 obliges Ran-GTP, but not Ran-GTP hydrolysis (Englmeier *et al.*, 1999). However, this does not apply to the whole export and import cycle. Thus, the reloading of Ran with GTP appears to be essential for the release of the export cargo from its exportin via Ran-GTP-hydrolysis, for the reimport of Ran-GDPs by the nuclear transport factor NTF2 as well as for the dissociation of the import complex, each exhausting one molecule of GTP. The energy needed for nucleo-cytoplasmic transport could by supplied indirectly via the hydrolysis of Ran-GTP. Other energy-consuming steps are suspected during the transport of very large macromolecules, like mRNA containing ribonucleoproteins (mRNPs) or ribosomes. e.g. Also processes like the unwinding of the RNA or other conformational changes of the transport substrates, as well as the detachment of proteins not to be cotransported, could for example demand energy (Adam, 1999; Görlich & Kutay, 1999; Vasu & Forbes, 2001). Clearly, additional work has to be performed to clarify the energy requirements of general and substrate specific transport processes.

3.5 Mechanisms of translocation through the nuclear pore

Any NPC translocation model will have to account for the observation that the same NPC is strongly bidirectional *in vivo*, mediating both import and export. Moreover, the mechanism will need to accommodate for rapid transport rates of up to 1000 macromolecules per second per NPC (Suntharalingam & Wente, 2003). At present, different translocation models are discussed, most of them assume a facilitated diffusion that is controlled via the association and dissociation of the transport complexes with FG-repeat containing NUPs (reviewed in Suntharalingam & Wente, 2003).

The first step is the recognition of the cargo, followed by docking of the transport factor-cargo complex at the NPC. The key tenets of all the proposed NPC translocation models are based on the transport factors having dual interactions with the cargo and the NPC.

The FG-containing NUPs may form the physical and mechanistic basis of the NPC permeability barrier. The FG repeat domains have remarkably unstructured and random coil properties (Denning *et al.*, 2003), resulting in a dynamic meshwork of filaments that excludes macromolecules that do not directly interact (figure 3.5.A). The specific interactions may facilitate random movement through the network and the NPC.

Debate has centered on several discrete models that propose either affinity-gating, selective phase partitioning, or affinity-gradient mechanisms. In the affinity-gating scenario (Rout & Aitchison, 2001), passive diffusion into the narrow NPC central region is sterically prevented by the FG-rich filaments. The FG binding sites at the NPC create a high concentration of transport complexes, thereby increasing the probability that the complex will enter into the NPC, overcome the entropic barrier, and translocate through the NPC by Brownian-based random diffusion. Molecules with no affinity for FG NUPs would not achieve an effective concentration at the NPC, and thus be excluded. The model assumes the binding of the transport receptor to the FG-repeats to be necessary and sufficient for the subsequent translocation through the pore. It doesn't explain however, how larger objects that actually exceed the physical size of the narrow pore channel are able to pass.

A key difference in the selective phase model (figure 3.5.B) is the assumption that the diameter of the central channel is large enough to also allow passage of large receptor-substrate complexes (Pante & Kann, 2002; Ribbeck & Görlich, 2002). The channel is not completely open, but is protected by a so called selective phase that is composed of the NUPs in this model. A hydrophobic network results from weak interactions between the FG domains themselves, thereby building a permeability border (figure 3.5.B, inset). The FG binding sites on the shuttling receptors allow selective passage through the hydrophobic environment, excluding hydrophilic macromolecules. However, by binding the FG repeats, the transport factor/cargo complexes would locally dissolve the hydrophobic network and selectively partition into and through the central region of the NPC, rendering the barrier permeable. These sequential association and dissociation of the transport complex to and off the different NUPs then mediates the direction of transport. What argues against this model is the fact that the translocation process itself is fully reversible and mediated in both directions (Ribbeck & Görlich, 2001). In the affinity gradient model (figure 3.5.C), the FG-NUPs would provide a series of sequential binding sites of progressively increasing affinities for the translocating macromolecules from one NPC side to the other (Ben-Efraim & Gerace, 2001). Again, molecules that do not interact with FG-NUPs would not engage in such cycles of association and dissociation, and would thus not be transported

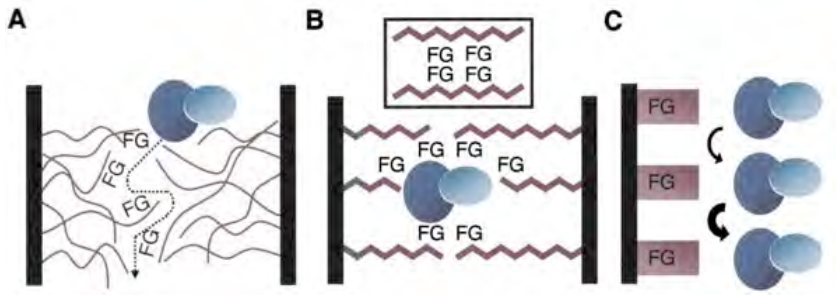

Figure 3.5. **Different NPC translocation models** (A) Dynamic filamentous network model (Denning *et al.*, 2003). (B) Selective phase model (Ribbeck & Görlich, 2001). (C) Affinity-gradient model (Ben-Efraim & Gerace, 2001). Not specifically shown is the affinity-gating model (Rout & Aitchison, 2001). See text for explanations.

3.5.1 Import processes

Protein translocation through the NPC is thought to occur by an essentially similar mechanism for all importin-β related receptors, except for the fact that, in some situations, additional adaptors are required to bridge the cargo/receptor interaction (reviewed in Goldberg, 2004; Harel & Forbes, 2004; Pemberton & Paschal, 2005). Import processes can be divided into classical NLS-mediated protein import, the import of RNA-binding and ribosomal proteins.

The most-studied pathway is the import of classical NLS-containing proteins. Classical protein import is mediated by one or two clusters of basic amino acids (aa), the simple or classical basic nuclear localization signal, and the bipartite NLS (Kalderon *et al.*, 1984; Robbins *et al.*, 1991). E.g., the simian virus 40 (SV40) large T-antigen harbors a classical NLS, consisting of the aa-sequence PKKKRKV. An example for a bipartite NLS can be found in the protein nucleoplasmin, with the recognition sequence KRPAAIKKAGQAKKKK. The two groups of basic amino acids (shown underlined) are separated by a 9 aa spacer in this case (Görlich & Mattaj, 1996). The import of many nuclear proteins is thought to be mediated by the basic NLS. Both types of classical import signals are recognized by the heterodimeric importin-β/importin-α complex in the cytoplasm. Thereby, importin-α acts as an adaptor between the NLS-bearing protein and importin-β, recognizing and binding the NLS-containing cargo and importin-β in the cytoplasm. The binding of importin-α to importin-β is thereby mediated via its N-terminal importin-β binding domain (IBB) (Görlich & Kutay, 1999). After formation of the trimeric complex, importin-β mediates docking at the NPC via direct

interaction with the FG-repeat sequences of the NUPs. Translocation of the complex occurs in the presence of Ran-GDP and free GTP, and is terminated via binding of Ran-GTP to importin-β in the nucleus, which releases the complex from the NPC and dissociates importin-α from importin-β. Free importin-α has a lower affinity for the NLS cargo, and release from importin-β is therefore believed to trigger release of the NLS cargo as well. Thereafter, the importin-β-Ran-GTP complex as well as importin-α bound to its exportin (CAS) together with Ran-GTP, are re-exported to the cytoplasm for another round of import.

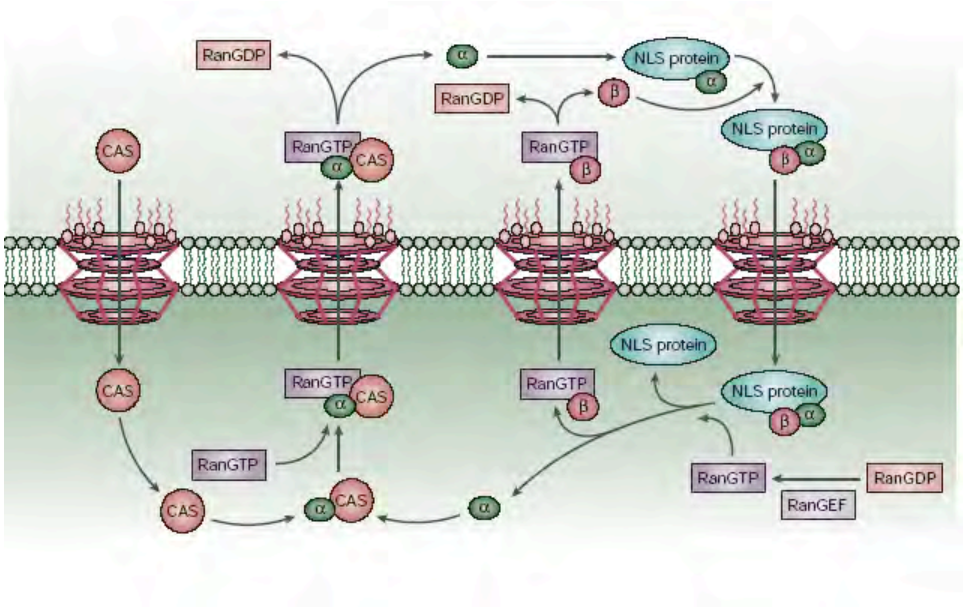

Figure 3.5.1. **Schematic representation of the transport cycles of importin-α and -β.** Figure modified from (Kau *et al.*, 2004). See text for further explanations.

In higher eukaryotes, several importin-β homologues exist, some of which interestingly show a tissue- and development-specific expression. Additionally, they reveal different binding specificities to NLS-bearing cargo proteins (Nachury *et al.*, 1998). This suggests that import processes can be regulated specifically for different tissue types. In addition, there is increasing evidence that active import of cargos containing basic NLSs can be mediated by importin-β in the absence of importin-α (Palmeri & Malim, 1999; Strom & Weis, 2001). For example, uridine-rich small nuclear ribonuclear proteins (UsnRNPs), which are polymerase type II transcripts from small nuclear RNA (snRNA) that are synthesized inside the nucleus and thereafter exported into the cytoplasm for maturation, are reimported into the nucleus via

a bipartite NLS by an importin-β-dependent mechanism that does not involve importin-α (Palacios *et al.*, 1997).

Another example for a complex nuclear translocation process is the import of heterogeneous nuclear ribonucleoproteins (hnRNPs). The so called “M9 domain” of hnRNP A1 not only serves as a recognition sequence essential for import, but also has been postulated to also mediate re-export. Spanning 38 aa, the M9 signal exceeds the length of the classical SV40 NLS (Siomi & Dreyfuss, 1995). The receptor recognizing this transport signal, transportin, also belongs to the importin-β family (see also table 3.3.) (Pollard *et al.*, 1996). Similar to importin-β/-α-mediated transport, the import complex, consisting of hnRNPA1 and transportin, is dissociated by Ran-GTP inside the nucleus (Izaurralde *et al.*, 1997). Thus, a continuous shuttling of hnRNPA1 between the nucleus and the cytoplasm occurs, with the involved exportin not yet identified.

Also ribosomal proteins, which are synthesized in the cytoplasm, must be transported into the nucleus and afterwards directed to the nucleolus. To date, it is still unclear whether these proteins are imported individually or as preformed complexes, and whether they contain distinct nuclear import and also nucleolar localization sequences (Rosorius *et al.*, 2000).

3.5.2 Export processes

As one hallmark of nucleo-cytoplasmic transport is the bidirectionality, the existing import reactions into the nucleus face a comparable amount of export processes into the cytoplasm. These transport processes in the reverse direction are mediated by exportins, and are regulated in a converse manner (reviewed in Goldberg, 2004; Kau *et al.*, 2004; Pemberton & Paschal, 2005).

Since in eukaryotes transcription and translation are taking place in two different compartments, the RNA molecules synthesized in the nucleus have to be exported into the cytoplasm. As most RNAs are transported as ribonucleoprotein particles, it was assumed that export is mediated via RNA-binding proteins containing nuclear export signals. The best characterized signal mediating export is the leucine-rich NES, which was first discovered within the Rev-protein of the human immunodeficiency virus type 1 (HIV-1) (Fischer *et al.*, 1995). The HIV-1 Rev protein is an essential viral protein responsible for the efficient export of unspliced and partially spliced viral mRNAs required for the production of the viral structural proteins.

Leucine-rich NESs conform to the still loosely defined consensus sequence Ω-x_{2-3}-Ω-x_{2-3}-Ω-x-I/L, (Ω = V,F,M or W; x is any amino acid) (Fornerod & Ohno, 2002; La Cour *et al.*, 2004). The presence of regularly spaced, large hydrophobic amino acids such as leucine or isoleucine as well as the spacing itself are critical features of the signals. Leucine-rich NESs have been identified in an increasing number of disease relevant cellular and viral proteins (table 3.5.2.) (Heger *et al.*, 2001; La Cour *et al.*, 2004; Rosorius *et al.*, 1999), implicated in transcription control, cell cycle control and RNA transport.

Table 3.5.2. **Examples of viral and vertebrate leucine-rich NESs.**

Protein	**NES-sequence**
Minute virus of mice (MVM) NS2	**M**TKK**F**–GT**L**T**I**
Protein kinase inhibitor PKI	**L**ALK**L**–AG**L**D**I**
HIV-1 Rev	**L**–PP**L**–ER**L**T**L**
HTLV-1 Rex	**L**SAQ**L**YSS**L**S**L**
MAP kinase kinase MAPKK	**L**QKK**L**–EE**L**E**L**
Adenovirus type 5 E1B-55K	**L**YPE**L**RRI**L**T**I**
Tumor suppressor protein p53	**M**FRE**L**NEA**L**E**L**
Double minute 2 Mdm2	**I**SLS**F**DES**L**A**L**
Inhibitor of NF-κB I-κBα	**M**VKE**L**–QE**I**R**L**
Cyclin B1	**L**CQA**F**–SD**V**I**L**
Transcription factor IIIA TFIIIA	**L**–PV**L**–EN**L**T**L**
Signal transducer and activator of transcription STAT1	**L**AAE**F**-RH**L**Q**L**
NES consensus	**Ω**x_{2-3}**Ω**x_{2-3}**Ω**x**L/I**

Conserved hydrophobic aa residues reported to be essential for function are marked in bold.
Ω denotes amino acids V,F,M or W; x is any aa.

A major step towards the identification of the export receptor of leucine-rich NESs was the observation that the fungicide antibiotics leptomycin B (LMB) blocks export of Rev (Wolff *et al.*, 1997). LMB, a Streptomyces metabolite, inhibits the cellular target protein CRM1 (chromosome region maintenance) by direct binding (Fornerod, 1997; Fukuda *et al.*, 1997). The inhibition of CRM1 by LMB depends on the highly conserved nucleophilic cysteine residue 528 (Cys528), to which LMB covalently binds in a "Michael-type" reaction (figure 3.5.2.1.) (Kudo *et al.*, 1999). Thus, LMB serves as a potent tool to identify proteins that are exported via the CRM1-pathway.

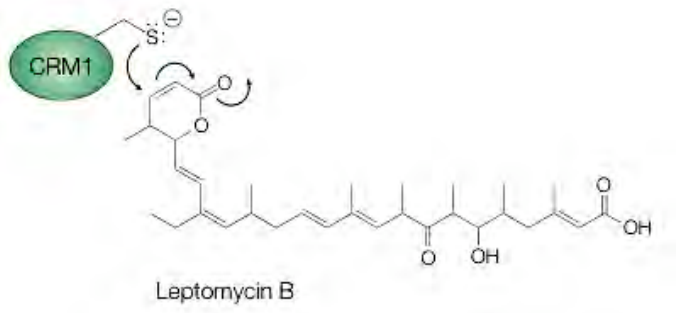

Figure 3.5.2.1. **Michael-type addition of LMB with the Cys528 of CRM1.** Figure taken from (Kau *et al.*, 2004).

Mechanistically, CRM1 binds to substrates containing a leucine-rich NES in the nucleus, forming a trimeric complex with Ran-GTP. This complex is then transferred to the cytoplasm by a mechanism involving binding of CRM1 to the NPC. Once in the cytoplasm, GTP hydrolysis results in the dissociation of Ran from the complex, allowing CRM1 to release its cargo. Free CRM1 then reenters the nucleus to bind and export additional cargo molecules (figure 3.5.2.2.).

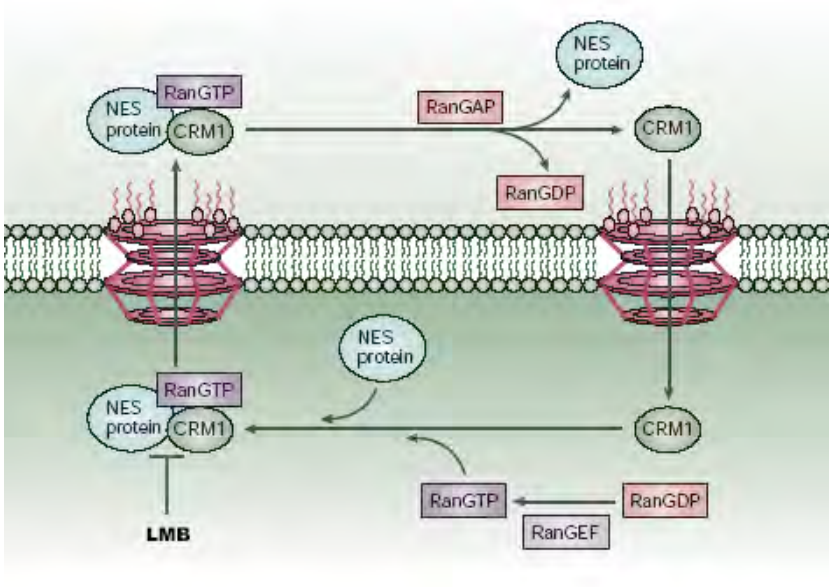

Figure 3.5.2.2. **Schematic representation of the transport cycles of CRM1.** Figure modified from (Kau *et al.*, 2004). See text for further explanations.

Although the orchestration of export is still unclear, NESs can be grouped into specific classes according to their activity *in vivo* (Heger *et al.*, 2001; Rosorius *et al.*, 1999), although most NESs bind to CRM1 with relatively low affinity *in vitro* (reviewed in Kutay & Guttinger, 2005). The different activities of the individual NESs can be regulated either by the NES-conformation itself or by additional cofactors favoring the formation of specific NES-CRM1 complexes. Efficient binding of weak NESs to CRM1 in the nucleus was for example suggested to be stimulated by a CRM1-specific cofactor, RanBP3, a nuclear Ran-GTP-binding protein (Englmeier *et al.*, 2001; Lindsay *et al.*, 2001).

In addition to leucine-rich NESs, also other nuclear export signals appear to exist, since nuclear export has been described for proteins lacking leucine-rich NESs. For example, the Ran binding protein Yrb1 in yeast, not harboring a leucine-rich NES, is exported via binding to the yeast CRM1 homologue (Künzler *et al.*, 2000). Another protein that uses the CRM1 export pathway for recycling and does not contain a classical leucine-rich NES is Snurportin, a factor involved in small nuclear ribonucleoprotein (snRNP) import (Paraskeva *et al.*, 1999). However, since the definition of active nuclear export still awaits a standardized experimental definition, some of these reports have to be considered with caution.

3.6 Regulation of nuclear transport

Nuclear transport is regulated at multiple levels, via a diverse range of mechanisms, and in response to a variety of signals such as hormones, cytokines and growth factors, cell-cycle signals, developmental signals, immune challenge and stress (see Poon & Jans, 2005 and references therein). Although several mechanisms have been suggested through which the regulation of nuclear import and export pathways can occur, the complex orchestration and specificity of transport is not yet understood.

Post-translational modifications and masking/unmasking of the specific transport signals can modulate the accessibility and affinity of target signal recognition by the transport receptors, and thus appear to contribute to the coordinated control of nucleo-cytoplasmic transport (Poon & Jans, 2005). In addition, alterations in the expression levels of components of the nuclear transport machinery also appear to be a determinant of transport efficiency, having central importance in development, differentiation and transformation.

Post-translational modification of signaling molecules through phosphorylation/dephosphorylation can be mediated by kinases/phosphatases. As kinases/phosphatases can be regulated by many different cellular signals, signal-responsive phosphorylation/dephosphorylation to modulate subcellular localization represents a direct

link between extracellular signals or signals within the cell, and response in terms of nuclear import or export of specific signaling molecules such as cell-cycle regulators, kinases and transcription factors. A key step by which the efficiency of nuclear transport may be regulated is that of importin-NLS/exportin-NES interactions. Intra- or intermolecular masking of NLSs/ NESs within cargo proteins to prevent importin/exportin recognition appears to be a common mechanism to regulate the efficiency of nuclear transport. Intramolecular masking occurs when the accessibility of the NLS/NES is inhibited by the charge or conformation of the NLS/NES-containing protein (Figure 3.6.A). Intramolecular masking can also be effected by phosphorylation close to the targeting sequence, as it is the case for the NLSs of the nuclear factor of activated T cells (NF-AT) 2. Intermolecular masking occurs when the binding of a heterologous protein prevents NLS-importin- or exportin-NES-interaction (Figure 3.6.B). Examples are the transcription factor NF-AT4, where at high Ca^{2+} concentrations, the phosphatase calcineurin binds to and masks the NES, or NF-κB p65, where the NLS is masked due to binding of the specific inhibitor protein I-κB. Nuclear localization of the tumor-suppressor p53 is regulated by a number of mechanisms, one of which is tetramerization in the nucleus in response to DNA damage, resulting in masking of the NES in the tetramer. Ligand binding can also mask NESs/NLSs, as shown for the NES of the androgen receptor, which lies in the ligand binding domain of the molecule. Intermolecular masking of targeting signals can also occur via RNA or DNA binding. In the case of the HIV-1 Rev protein, binding of mRNA masks its NLS. This ensures mRNA release in the cytoplasm before another round of Rev nuclear import to ferry HIV-1 mRNA out of the nucleus. The physiological role of this may be an alternative mechanism to Ran-GTP-mediated cargo release in the nucleus, as it also seems to be the case for STAT1 (Poon & Jans, 2005).

In addition to NLS/NES masking, the binding affinity of importins/exportins for NLSs/NESs can be regulated positively by phosphorylation, where phosphorylation sites close to the targeting signal enhance importin/exportin binding. E.g., this accounts for the NLS of the SV40 T-Ag, the NLS of the Drosophila morphogen Dorsal, or the NES of the transcription factor Pho4 (Figure 3.6.C). That importin-binding affinity is of critical importance in a human context is demonstrated by the analysis of mutations within either one of the dual NLSs of the sex-determining factor SRY (Harley *et al.*, 2003) that lower the binding affinity, impair SRY nuclear import and result in XY females (Swyer syndrome). Similarly, mutations in the protein Dorsal that prevent phosphorylation and thereby enhancement of nuclear import are lethal (Briggs *et al.*, 1998). These studies underline the critical importance of regulated importin-NLS interaction for developmental processes.

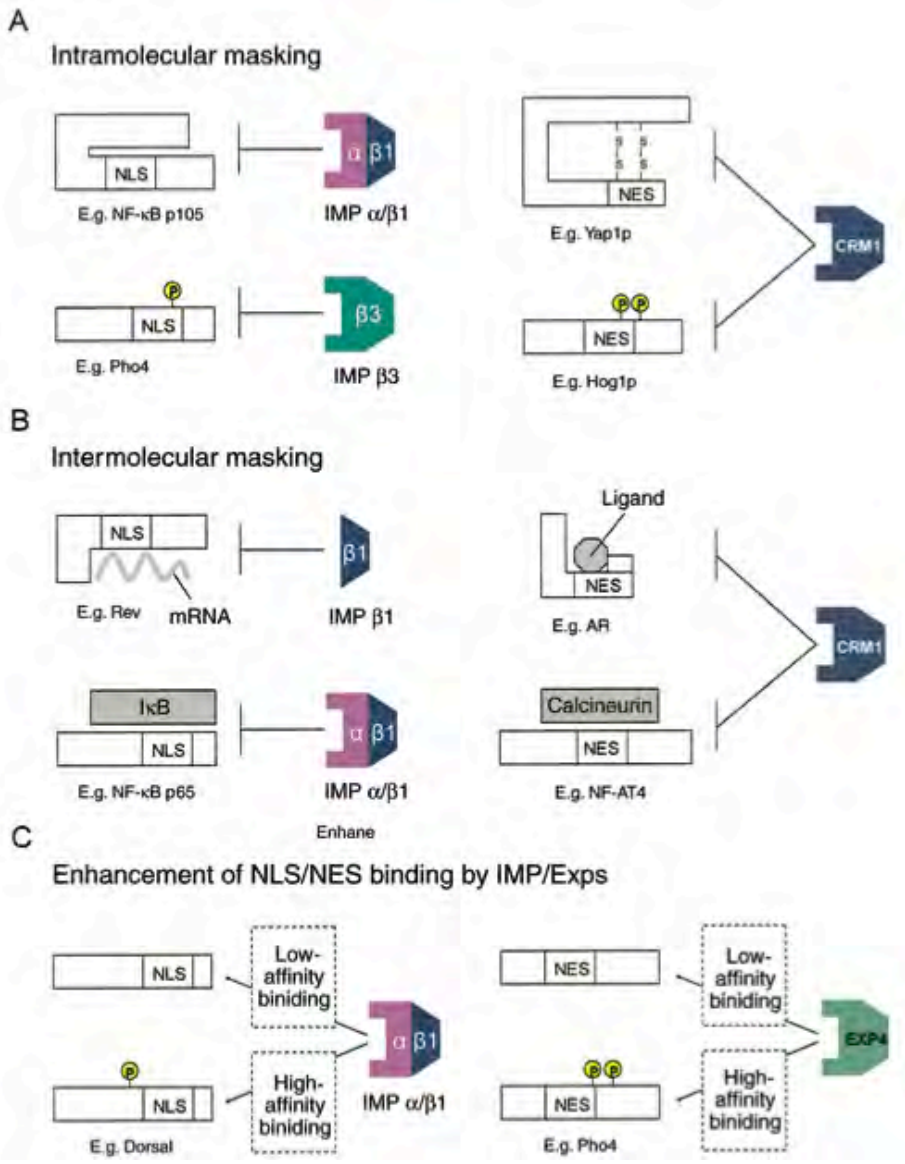

Figure 3.6. **Mechanisms of nuclear transport regulation.** (A) Selected examples of intramolecular masking, where targeting signals are prevented from importin-(IMP)/exportin (EXP) recognition by the conformation of the protein containing it. (B) Selected examples of intermolecular masking, where targeting signals are protected from IMP/EXP recognition by binding of a heterologous molecule. (C) Selected examples of the enhancement of IMPs/EXPs binding to NLSs/NESs by phosphorylation. Figure modified from (Poon & Jans, 2005). See text for further explanations.

Another mechanism of regulating nuclear transport is through modulation of the binding of NLS/NES-containing cargo to specific cytoplasmic or nuclear factors that serve to anchor or retain cargoes in cytoplasmic or nuclear compartments, thereby preventing nuclear transport and leading to cytoplasmic or nuclear retention. Proteins that are regulated via cytoplasmic retention, are, for example, the glucocorticoid receptor (GR) complexed with the heat-shock protein Hsp90, or the tumor-suppressor p53 bound to the ubiquitin ligase p53-associated Parkin-like cytoplasmic protein (Parc). Binding interactions with both nuclear and cytoplasmic anchor/retention factors may contribute to signal transduction-responsive control of the subcellular localization of signaling and other molecules in the nucleus (Poon & Jans, 2005).
As indicated above, the modulation of the expression level of components of the nuclear transport machinery represents an additional regulatory mechanism. In particular importins appear to be specialized to mediate the nuclear import of particular transport cargoes. Further, it seems likely that importin/cargo complexes or proteins such as β-catenin or the STAT proteins may take specific paths through the NPC by binding to only a subset of FG-repeat-containing NUPs. Thus, the presence or absence of a particular importin or NUP may determine whether specific nuclear import/export cargoes can efficiently enter or exit the nucleus, making the tissue/cell type-specific expression of components of the nuclear transport machinery a critical determinant of the nuclear import efficiency for a given cargo.

3.7 Functional implication of nucleo-cytoplasmic transport

The following chapter will give a brief introduction into several functional implications of nucleo-cytoplasmic transport, focusing mainly on proteins and mechanism that have been investigated in this work.
Active transport signals have been identified in an increasing number of cellular and viral proteins executing heterogeneous biological functions involving RNA transport (Cullen, 2003b), transcription (Knauer *et al.*, 2005a; McBride & Reich, 2003), apoptosis (Ferrando-May, 2005), or cell cycle control (Phippard & Manning, 2003). Since nucleo-cytoplasmic transport is crucial for normal cell function, defects in this process can also lead to various disease conditions including cancer (reviewed in Kau *et al.*, 2004; Poon & Jans, 2005). However, regulated subcellular transport also provides an attractive way to control the activity and stability of regulatory proteins and RNAs. Recently, interfering with nucleo-cytoplasmic transport in general as a novel therapeutic principle has attracted major interest by academia and industry (reviewed in Kau *et al.*, 2004; Pagliaro *et al.*, 2004).

3.7.1 RNA-transport

Eukaryotic cells transport the different classes of RNAs, like rRNAs, tRNAs, mRNAs and snRNAs, by distinct but in some cases partially overlapping nuclear export pathways (see Cullen, 2003b and references therein). In contrast to the export of proteins, which are mostly transported individually, most RNAs are transported as a complex with appropriate ribonucleoprotein particles (RNPs).

Virology has made several key contributions to our current understanding of how mRNAs are exported from the nucleus (figure 3.7.1.). Initial evidence identifying the karyopherin CRM1 as a nuclear RNA export factor derived from efforts to identify the cellular cofactor for the HIV-1 Rev protein, which is essential for the nuclear export of the incompletely spliced HIV-1 mRNA species expressed late in the viral life cycle (Pavlakis & Stauber, 1998). The HIV-1 replication requires the cytoplasmic expression of unspliced, singly spliced and fully spliced viral mRNAs. In the absence of Rev function, only fully spliced viral mRNAs are exported from the nucleus. In contrast, incompletely spliced viral mRNAs, encoding primarily the viral structural proteins, are retained in the nucleus by cellular proteins that normally prevent the nuclear export of cellular pre-mRNAs. However, Rev is responsible for the CRM1-mediated export of the incompletely spliced viral mRNAs by binding to the cis-acting Rev response element (RRE) present on these RNAs. In addition to HIV-1, other retroviruses and also adenovirus encode adapter proteins that recruit CRM1 to late viral mRNAs, e.g., the human T-cell leukemia virus (HTLV) Rex protein (Heger *et al.*, 1999) or the adenovirus type 5 E1B-55K protein (Krätzer *et al.*, 2000). One common reason why these viruses exploit the CRM1 pathway for mRNA transport is that eukaryotic cells have a stringent proofreading mechanism to ensure nuclear retention of incompletely spliced RNAs, which has to be overcome.

CRM1 also appears to be responsible for the export of cellular UsnRNAs and all rRNAs (see Cullen, 2003b, and references within). The small nuclear ribonucleoprotein particles are RNA-protein complexes that play a critical role in the splicing of nuclear pre-mRNAs. In higher eukaryotes, the UsnRNA components of the snRNPs are synthesized in the nucleus, then assembled into mature snRNPs in the cytoplasm and reimported into the nucleus by the snurportin1/importin-β-heterodimer. The snRNAs that undergo this cytoplasmic assembly step are cotranscriptionally 7-methylguanosine (m7G) capped, whereas the cap serves as the critical export signal. For export, the m7G cap is bound by the nuclear cap-binding complex (CBC), consisting of the cap-binding proteins CBP20 and CBP80. This complex

does not directly interact with CRM1, but with an additional factor, PHAX (phosphorylated adapter for RNA export), which in a phosphorylated form binds Ran-GTP-bound CRM1.

Ribosomes are RNPs that consist of a large (60S) and a small (40S) subunit, and are essential for protein synthesis inside the cytoplasm. The two subunits, each encompassing different rRNAs and ribosomal proteins, are assembled and processed in the nucleolus, a specialized subnuclear structure, and are then separately exported to the cytoplasm. Export of both subunits depends on Ran, and nuclear export of the 60S pre-ribosomal subunit is mediated by the Nmd3-dependent recruitment of CRM1. Nuclear export of the 40S pre-ribosomal subunit is also CRM1 dependent, but neither Nmd3 nor CRM1 directly bind to the 40S subunits. Recruitment of CRM1 to nuclear 40S pre-ribosomal subunits therefore probably depends on an hitherto unidentified adapter that has an analogous role to Nmd3.

In contrast, tRNA export is mediated by a own transportin of the importin-β family, exportin-t or XPO-t. Exportin-t binds directly and specifically to mature tRNA molecules in the presence of Ran-GTP, but very poorly to tRNAs that bear incorrect 5'- or 3'-ends, or that are inappropriately modified (Cullen, 2003b).

Recently, it has been discovered that eukaryotic cells transcribe a wide range of other small non-coding RNAs. Recent advances have revealed that so called microRNAs (miRNAs) function in a variety of regulatory pathways, including cell proliferation, apoptosis, hematopoiesis and organogenesis (reviewed in Ambros, 2001; McManus, 2003). Recent studies have shown that exportin-5 (Exp5), a Ran-dependent importin-β-related transport receptor, mediates nuclear export of miRNA precursors (pre-miRNAs) (Kim, 2004), resembling the transport of small viral RNAs, e.g., the adenovirus VA mRNA (Cullen, 2003a).

In contrast, mRNA export is generally mediated by a distinct nuclear export pathway that is independent of the Ran system and karyopherins, and is both complex and still incompletely understood (reviewed in Izaurralde, 2004). However, a few human mRNAs might be subject to nuclear export by CRM1. E.g., AU-rich elements (AREs) that are present in the 3'-untranslated regions of several genes involved in cell signaling, bind the protein HuR, which in turn interacts with the nucleo-cytoplasmic shuttle protein APRIL, which contains a leucine-rich NESs and interacts with CRM1. Functional analysis of members of the human nuclear export family (NXF) has also suggested that some cellular mRNAs might be exported by CRM1.

The key mediator of bulk mRNA export is instead a heterodimer of the tip associating TAP and a small cofactor termed NXT. RNA binding is achieved via recruitment of the protein UAP56, which in turn binds to ALY that then interacts with TAP and its partner NXT.

Although UAP56, TAP and NXT are all essential for poly(A)+ RNA export, ALY appears to be dispensable, thus suggesting the existence of other intermediate factor(s). TAP differs from CRM1 in not being a member of the karyopherin family, and TAP-mediated nuclear export does not require its interaction with any karyopherin nor the Ran-GTPase as a cofactor. Thus, these findings explained the previous observation that, in contrast to all other nuclear RNA-export pathways, nuclear mRNA export was independent of Ran function. Instead, the TAP-NXT heterodimer interacts directly with components of the NPC via an essential domain located at the C terminus of TAP. Although TAP is ubiquitously expressed, a closely related protein, NXF3, displays a highly tissue-specific expression pattern. Although NXF3, like TAP, is a nucleocytoplasmic shuttle protein that can export nuclear mRNAs when tethered via a heterologous RNA-binding motif, NXF3 lacks the C-terminal NPC-binding domain that is crucial for TAP function. This conundrum was resolved by the demonstration that NXF3, unlike TAP, contains a leucine-rich NES that binds CRM1. NXF3 associates with poly(A)+ mRNA *in vivo* and, therefore, might function as a tissue-specific CRM1-dependent nuclear mRNA-export factor.

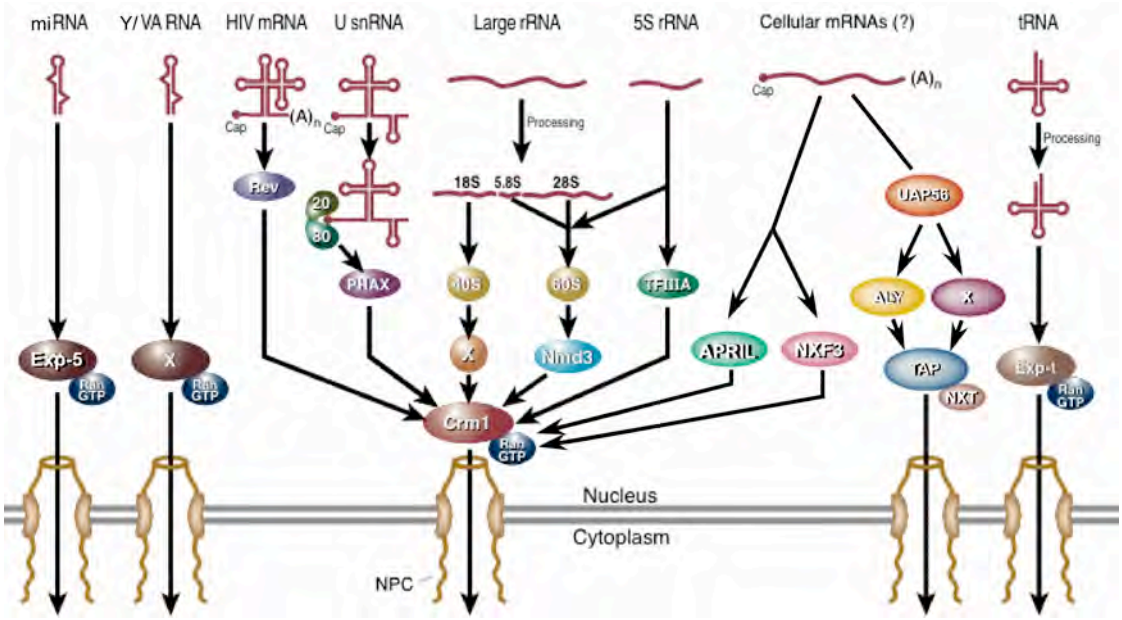

Figure 3.7.1. **Karyopherin-mediated nuclear RNA export pathways.** This depiction provides an overview of the key factors involved in mediating the nuclear export of different classes of RNA. Hypothetical factors that remain to be identified are indicated by 'X'. Figure modified from (Cullen, 2003a; Cullen, 2003b). See text for details.

3.7.2 Transcriptional activation

A key juncture in the control of cell differentiation and growth is found at the level of gene expression. Transcription factors are gene regulatory proteins endowed with sequence-specific DNA recognition and protein interaction motifs, and as such have the ability to positively or negatively influence the rate and efficiency of transcript initiation. Since transcription factors lie at the heart of almost every fundamental developmental and homeostatic organismal process, defects in transcription factor function can lead to various types of malignancy. On the other hand, transcription factors also represent prime targets for disruption in malignancy. Often, transcription factors are latent in the cytoplasm and are transported into the nucleus upon signal mediated activation. Thus, modulating their nucleo-cytoplasmic transport as well as their interactions with transcription regulatory proteins provides a multistep mechanism for controlling and interfering with gene expression in eukaryotes.

3.7.2.1. Homeodomain proteins

Ordered development depends on the fine-tuned activity of transcription factors in a temporal and spatial controlled manner. Among other mechanisms, regulated stability and subcellular localization provides an intracellular way to control the activity of transcription factors (Affolter *et al.*, 1999). Homeodomain proteins (HDPs) have been shown to exert key developmental functions since defects in the evolutionary conserved homeobox genes were shown to cause many human disorders and aberrant animal phenotypes (Zhao & Westphal, 2002). Homeobox-containing genes encode transcription factors and are characterized by the homeodomain (HD), a motif that directs specific DNA binding to regulate the expression of target genes. Homeodomain proteins (HDPs) are grouped into several subclasses according to the primary structure of their HD and its flanking sequences (Galliot *et al.*, 1999 and references therein). In concordance with their role as transcriptional regulators, homeoproteins localize predominantly to the nucleus, although several reports characterize HDPs also as nucleo-cytoplasmic shuttle proteins (Affolter *et al.*, 1999). For example, Maizel *et al.* suggested that nuclear export of the Engrailed protein influenced intracellular localization and also extracellular secretion (Maizel *et al.*, 2002).

3.7.2.2. The STAT family of transcription factors

The STAT family of transcription factors, named after their dual role as signal transducers and activators of transcription (reviewed in Levy & Darnell, 2002) are characterized by a modulatory structure comprising a coiled-coil domain for protein interaction, a DNA-binding domain recognizing the GAS family of enhancers, an SH2 (src homology 2) domain for dimerization, and a transactivation domain (TAD). The STAT proteins are latent in the cytoplasm until they are activated by extracellular signaling proteins that bind and activate specific cell-surface receptors, the Janus kinases (Jaks), which in turn phosphorylate STAT proteins. Phosphorylated and thereby activated STAT proteins dimerize, and are transported into the nucleus via importin-α5 to drive transcription. In the nucleus, dephosphorylation of STATs is thought to trigger conformational changes that expose the NES and induce export back to the cytoplasm, thereby terminating target gene expression. As STAT proteins are often deregulated in malignancies (Levy & Darnell, 2002), nucleo-cytoplasmic transport processes that affect their transcriptional regulation are currently considered a highly relevant target for therapeutic intervention (McBride & Reich, 2003).

3.7.2.3. Nuclear factor-κB

Transcriptional modulators of the nuclear factor-κB (NF-κB)/Rel family hold a central role in the inducible expression of a high number of genes involved in inflammation, host defense, cell survival, proliferation, and thus also tumorigenesis (Perkins, 2004). Their common characteristic is a so-called Rel homology domain, which is responsible both for binding to a consensus DNA sequence and for homo- or heterodimerization. The most abundant forms of NF-κB are p65/p50 heterodimers and p65/p65 homodimers. In most cases, NF-κB dimers are kept inactive by cytoplasmic retention due to binding to the inhibitors of NF-κB (I-κBs), mostly I-κBα. I-κBα is thought to mask the NLS of NF-κB, thereby preventing the interaction of NF-κB with the nuclear import machinery. Moreover, the non-conventional NLS of I-κBα itself, located within the second ankyrin repeat, appears to be blocked when I-κBα is bound to NF-κB. Thus, the NLS of NF-κB is unmasked upon degradation of its inhibitor and the transcription factor can be imported into the nucleus, where it binds to specific promoter elements. Besides a number of other genes, NF-κB is also inducing the transcription of DNA encoding its own inhibitor. After translation in the cytosol, I-κBα is imported into the nucleus, where it is assumed to dissociate NF-κB from promoter regions. The newly formed NF-κB/I-

κBα complex is then transported back to the cytosol by the means of a classical NES of I-κBα (Tam *et al.*, 2000). However, it was also postulated that NF-κB contains a NES by itself, which would allow an I-κBα-independent nuclear export. The finding that both molecules apparently contain NLS as well as NES domains still raise the question how the intracellular distribution of these proteins is regulated functionally in the course of activation and deactivation of the signaling pathway. This regulatory network became even more complex upon the demonstration that posttranslational modifications (e.g., phosphorylation, acetylation) and/or binding to regulatory proteins can influence the trafficking, stability and activity of the NF-κB and/or NF-κB/I-κBα complexes (Kiernan *et al.*, 2003; Zhong *et al.*, 2002).

3.7.2.4. The Myc/Max/Mad network of transcription factors

The Myc/Max/Mad network of transcription factors regulates many cellular functions, including proliferation, differentiation, and apoptosis. These proteins belong to the helix-loop-helix-zipper (bHLH-ZIP) family of transcriptional regulators and can form dimers in multiple combinations through interactions mediated by the helix-loop-helix leucine zipper dimerization interface. Different members of the Myc/Max/Mad family have distinct biological functions. Myc proteins promote cell proliferation, whereas Mad family proteins limit proliferation (reviewed in Hurlin & Dezfouli, 2004). Genes encoding Myc family proteins are mutated or deregulated in many types of cancer, whereas Mad family proteins can inhibit cell transformation. Myc and Mad family proteins form dimers with Max, and dimerization with Max is essential for the regulatory functions of Myc and Mad family proteins. Interestingly, a NES has been identified in the Mad4 protein (Grinberg *et al.*, 2004) and suggests that regulated subcellular localization might be an additional factor influencing the stoichiometry of Myc/Max and Mad/Max complex formation, which ultimately may have an profound impact on the cellular response.

3.7.2.5. The AP1 transcription factor

Likewise, it has been suggested that the transcription factors c-jun and c-fos, which constitute the AP1 transcription factor, are actively imported into the nucleus via a Ran/Imp-β-mediated mechanism, which however does not require importin-α (Forwood *et al.*, 2001). AP1 is involved in regulation of gene transcription linked to cell proliferation and is thought to

be associated with the development of a more malignant cancer phenotype (van Dam & Castellazzi, 2001). Like the bHLH family, the interactions between basic leucine zipper (bZIP) family members are mediated by the coiled alpha helices. These factors can homo- and heterodimerize, but only the Jun/Fos heterodimer displays a high affinity for the AP1 site (Vogt, 2002).

3.7.2.6. p53 and Mdm2

The p53 protein is a transcription factor regulating many cellular processes, including cell cycle, DNA repair, apoptosis, angiogenesis, and thus acts as major tumor suppressor, with loss of normal p53 function by mutation occurring in almost all cancers (Vogelstein *et al.*, 2000; Vousden & Prives, 2005).

Regulated nuclear export of p53 is a major mechanism governing its stability and ability to promote G1 arrest and apoptosis (Vousden & Prives, 2005). However, although one NLS and even two NESs have been identified in p53, the mechanisms that control p53 nucleo-cytoplasmic transport have not been fully clarified (O'Brate & Giannakakou, 2003). Various models for p53 nuclear export have been proposed, but recent data indicate that Mdm2-mediated mono-ubiquitination of p53 promotes its nuclear export (Brooks *et al.*, 2004), while poly-ubiquitination promotes its degradation in the nucleus. Because p300 has been shown to promote p53 poly-ubiquitination, it was suggested that p300/CBP binding, besides acetylation, regulates p53 nuclear export by controlling its ubiquitination (Xu & Massague, 2004).

Mdm2-mediated p53 degradation depends on the interaction between the two proteins, and the ability of p53 to be exported is greatly enhanced by the action of Mdm2, potentially by an additive effect of the Mdm2 NES (Gu *et al.*, 2001). Thus, inhibition of Mdm2 nuclear export stabilizes nuclear p53. Constant growth factor stimulation, which is evident in tumors, can promote relocation of Mdm2 to the cytoplasm and thereby attenuate the ability of p53 to induce cell cycle arrest and apoptosis (Vousden & Prives, 2005).

3.7.3 Apoptosis

Apoptosis is a key component in the development and maintenance of tissues within multicellular organisms, providing a tightly regulated and selective mechanism for the deletion of superfluous, infected, mutated or aged cells. Dysregulation of apoptosis

contributes to a variety of pathologic conditions, including cancer (reviewed in Gerl & Vaux, 2005; Meier *et al.*, 2000). As tumor cells show a disturbed equilibrium between proliferation and apoptosis, conventional cancer therapies take advantage of this apoptotic mechanism by employing ionizing radiation or chemotherapeutic drugs to damage DNA and induce selective apoptosis of rapidly growing cells. Apoptosis consists of two main pathways, the extrinsic and the intrinsic pathway (for reviews see Igney & Krammer, 2002; Jesenberger & Jentsch, 2002). The functional role of nucleo-cytoplasmic transport for apoptosis is implicated at several levels. First, the apoptotic demolition of the nucleus is accomplished by diverse pro-apoptotic factors, most of which are activated in the cytoplasm and have to gain access to the nucleoplasm during the cell death process. Secondly, signals generated in the nucleus by DNA damage have to propagate to all cellular compartments to ensure the coordinated execution of cell demise. The nucleocytoplasmic shuttling of signaling and execution factors is thus an integral part of the apoptotic programme. Several proteins implicated in apoptotic cell death have been shown to shuttle between the nucleus and the cytoplasm prior to or upon apoptosis induction. These include the apoptosis-inducing factor (AIF), adapter molecules like FADD, TRADD and Apaf-1, but also the caspases, which consist of a family of cysteine proteases that can be grouped into initiator (caspase-8 and -9) and effector caspases (caspase-3, -6 and -7) (see Ferrando-May, 2005 and references therein). The so-called caspase cascade, which is a sequence of subsequent proteolytic caspase cleavages, leads to the activation of caspases that in turn cleave cytoskeletal and nuclear proteins, finally resulting in cell death. Although an NLS has been identified in caspase-2, a requirement for active import of all caspases is not clear since also the NPC is an early target of caspase activity and thus caspases may gain indirectly access to the nucleus.

In addition, pro- and anti-apoptotic factors, such as members of the Bcl-2 family and the inhibitors of apoptosis (IAP) family, have been described to actively migrate between the nucleus and the cytoplasm.

The evolutionarily conserved IAP family is characterized by a signature region of about 70 aa termed baculovirus IAP repeat (BIR) domain and is mainly involved in anti-apoptosis.

Survivin, the smallest mammalian member of the IAP family (Salvesen & Duckett, 2002), contains a single BIR domain and exists as a stable homodimer in solution (Sun *et al.*, 2005). A single-copy survivin gives rise to the four alternatively spliced survivin transcripts survivin-2B, -3B, -ΔEx-3 and -2α (Altieri, 2003b; Caldas *et al.*, 2005, and references within). Although, the low molecular weight would allow survivin to access intracellular compartments by

passive diffusion, regulated subcellular localization has also been suggested for survivin (reviewed in Altieri, 2004). Survivin is cell cycle regulated, and involved in both control of apoptosis and regulation of cell division. It is undetectable in most normal adult tissues, but is highly expressed in cancer. As its expression correlates with reduced tumor cell apoptosis, abbreviated patient survival, accelerated rates of recurrences, and increased resistance to chemo- and radiotherapy, major therapeutic and prognostic interest has been focused on survivin (see Altieri, 2003a; Altieri, 2003d; Li, 2003, and references within). The protective effect of survivin is supposed to be due to its caspase-binding capacity and to depend also on its spindle association during cell cycle progression (Li *et al.*, 1999; Li *et al.*, 1998). However, critical gaps in the molecular understanding of the survivin pathway still exist that have hampered its full exploitation for cancer therapeutics.

3.7.4 Cell cycle

The cell cycle is one of the most comprehensively studied biological processes, particularly given its importance for growth and development and its implication in many human disorders (for review see Harper & Brooks, 2005). The mammalian cell division cycle is divided into two basic parts: interphase and mitosis, also called M-phase. Interphase is the time during which replication of chromosomes and centrosomes and cell proliferation occur in an orderly manner in preparation for cell division. While the cells double in size between each mitotic step, the DNA is synthesized only during a portion of interphase. The timing of DNA synthesis thus conventionally divides the cell cycle into four discrete phases - G1, S, G2 and M phase (figure 3.7.4.1.A). The two most dramatic phases are the DNA synthesis (S) phase, in which DNA replication takes place, and the chromosomes are faithfully duplicated, and mitosis (M), in which the replicated genome is divided equally between two new daughter cells by the separation of the daughter chromosomes. Preparations for S and M phase take place in the preceding G1 (gap 1) and G2 (gap 2) phase, respectively. Under unfavorable environments, cells can exit the G1 phase and enter the quiescent G0 phase, from where they can return to the cycle through the G1 phase when environmental cues permit.

Mitosis comprises different steps - prophase, prometaphase, metaphase, anaphase and telophase (figure 3.7.4.1.B) - and usually ends with cell division (cytokinesis). At prophase, chromosome condensation begins, centrosomes separate and the nuclear envelope breaks down. During prometaphase, chromosomes are captured by microtubules growing from the

separated centrosomes and bi-orient, congressing to the center of the spindle at metaphase. Cromosome alignment is finished with the end of metaphase. Anaphase marks the loss of cohesion between sister chromatids and their movement to opposite spindle poles, which move apart to further separate daughter nuclei reforming in telophase (not shown) prior to cytokinesis (not shown) and the return to interphase.

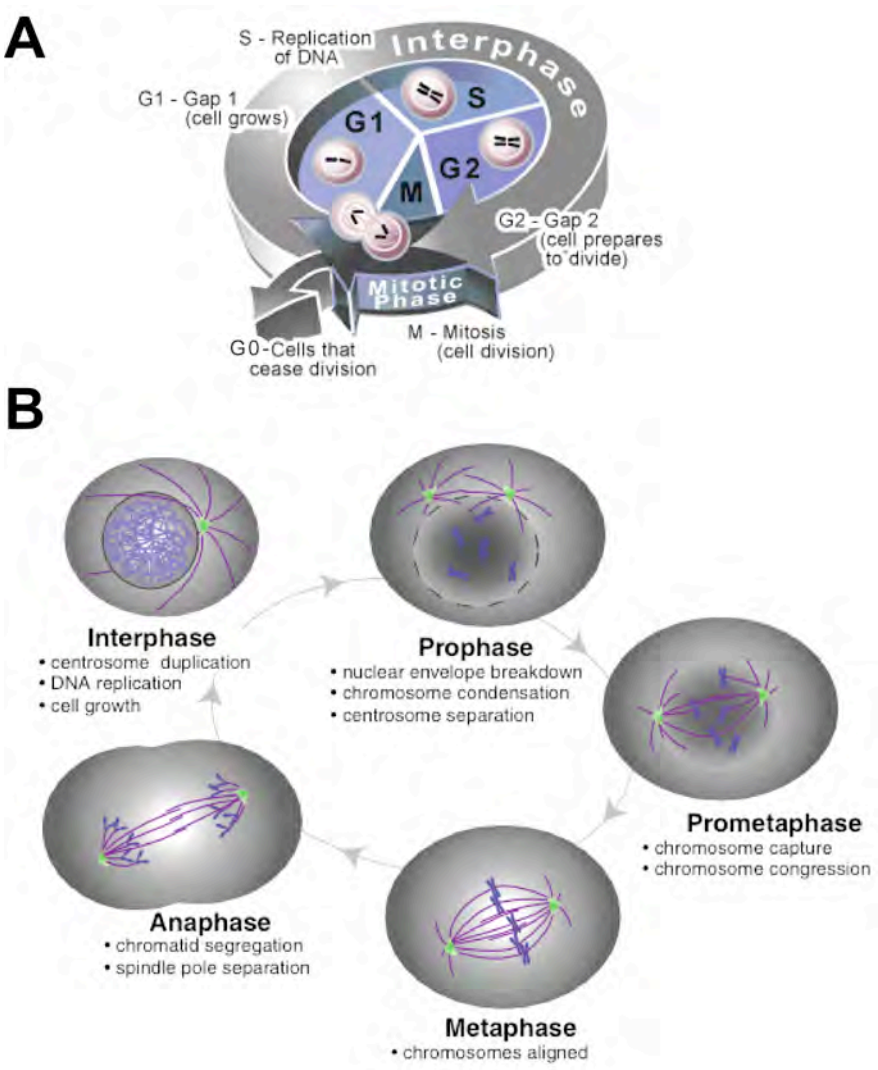

Figure 3.7.4.1. **The mammalian cell cycle.** (A) The phases of the cell cycle - G1, S, G2, and M (mitosis). (B) The stages of mitosis illustrating microtubule reorganization and chromosome translocation. Depiction modified from (Gadde & Heald, 2004). For further explanations see text.

To ensure that the original cell is copied with high fidelity, an elaborate control system using so called checkpoints is employed, preventing cell cycle events to occur prematurely or in the wrong order. Chromosome segregation is an important process in mitosis and must be

performed correctly to ensure that the two resulting daughter cells have the same DNA content. Missegregation of chromosomes results in aneuploidy, something that is frequently found in cancers, suggesting that the machinery surveying the chromosome segregation process has somehow been compromised during the development of these tumors. One of the cell cycle checkpoints, the mitotic spindle checkpoint, has also been shown to be defective in cancers with chromosomal instability.

The proper passage through the cell cycle is regulated by phosphorylation and degradation of cyclins and cyclin dependent kinases (CDK). While the cyclins C, D, and E are essential for the progression of the cycle into S phase, and synthesized during G1, cyclins A and B, are synthesized during S and G2 phases, which are essential for entry into mitosis. The activity of cyclin-dependent kinases is regulated by temporal synthesis and binding of cyclins, by the association and dissociation of CDK inhibitors (CDKIs), and by inhibitory and activating phosphorylation events (reviewed in Miele, 2004; Sherr & Roberts, 2004). The decision to continue cell cycle progression takes place in G2 phase, when cellular Ras induces the elevation of cyclin D1 levels. These levels are maintained through G1 phase and are required for the initiation of S phase, at which time cyclin D1 levels are automatically reduced to low levels. This reduction is required for DNA synthesis, and forces the cell to induce high cyclin D1 levels once again when it enters G2 phase. In this way, cyclin D1 is proposed to serve as an active switch in the regulation of continued cell cycle progression.

Regulated nucleo-cytoplasmic transport has a profound impact on the intracellular activity of cell cycle regulators. Controlled removal of cyclin D1 from the nucleus during S phase is essential for regulated cell division. GSK-3β-dependent phosphorylation of cyclin D1 promotes its interaction with CRM1 and thus, nuclear export (Alt *et al.*, 2000). In addition, the shuttling proteins p21 and p27 appear to be positive regulators of cyclin D1/CDK4 assembly and nuclear accumulation via inhibition of cyclin D1/CRM1 interaction (Alt *et al.*, 2002). Disturbance of this regulatory network results in cellular transformation and promoted tumor growth in mice (Alt *et al.*, 2000). While cyclin B1 is capable of shuttling from the nucleus to the cytoplasm throughout interphase, mitotic onset requires phosphorylation of cyclin B1 by Polo-like kinase1, thereby enhancing import and inhibiting export of the cyclin B1-CDK1 complex (Porter & Donoghue, 2003). Connor *et al.* also showed that the cell cycle dependent localization of p27 is regulated by CRM1/Ran-GTP-mediated nuclear export. This resulted in the incremental activation of cyclin E-CDK2 leading to cyclin E-CDK2-mediated phosphorylation and p27 proteolysis in late G1 and S phase (Connor *et al.*, 2003). Interestingly, LMB did neither inhibit p27-CRM1 binding nor prevent p27 export.

Strikingly, effectors and components of the nuclear transport machinery are not only active during interphase but play additional crucial roles during mitosis. Mitosis involves a dramatic reorganization of the nucleus, with changes in chromatin structure, assembly of the mitotic spindle, and the breakdown of the nuclear envelope. Recent evidence suggest that the Ran-GTPase/RCC1 system also controls changes in microtubule dynamics and chromatin structure (Arnaoutov *et al.*, 2005; Arnaoutov & Dasso, 2003; Weis, 2003). Generation of Ran-GTP by RCC1 on chromosomes causes the release of so called spindle assembly factors (SAFs) from inhibitory complexes with importins-α and -β that otherwise bind to a nuclear localization sequence (NLS) on a SAF (figure 3.7.4.2.) (Clarke, 2005). Interestingly, Ran-GTP can also function through CRM1, which interacts with kinetochores and recruits Ran-BP2 and Ran-GAP1. Thus, through the interactions with leucine-rich nuclear export sequences, proteins are recruited as active complexes to the spindle via CRM1. CRM1, which has originally been defined as a chromosome region maintenance in fission yeast (Fornerod, 1997), can thereby function as a major nuclear export receptor during interphase and as a regulator during mitosis.

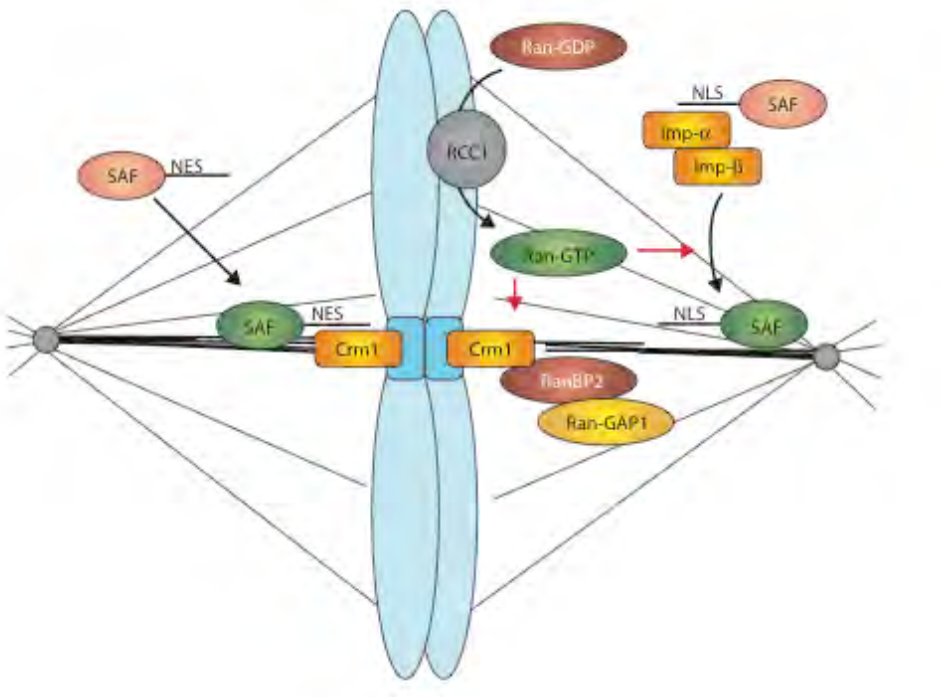

Figure 3.7.4.2. **Regulation of multiprotein complexes by Ran-GTP during mitosis.** Figure taken from (Clarke, 2005). For further explanations see text.

3.7.5 Cancer

Cancer is a complex disease generated by multiple genetic alterations (for review see Hanahan & Weinberg, 2000; Vogelstein & Kinzler, 2004). Malignant, invasive tumours are characterized by self-sufficiency in growth signals, insensitivity to growth-inhibitory signals, block of cellular differentiation, evasion of apoptosis, genetic instability, limitless replicative potential, sustained angiogenesis, tissue invasion and metastatic potential. As nucleo-cytoplasmic transport is an important aspect of normal cell function, defects in this process can lead to disturbances of the cellular homeostasis, and thereby also contribute to cancer formation (reviewed in Ferrando-May, 2005; Kau *et al.*, 2004; Poon & Jans, 2005). On the other hand, the detailed molecular knowledge of how nucleo-cytoplasmic transport contributes to disease conditions might also be exploited for the formulation of novel therapeutic strategies specifically targeting transport processes.

There are different ways how nucleo-cytoplasmic transport can be deregulated contributing also to malignant transformation.

First, modification of the cargo can in turn affect its ability to interact with its cognate transporter. Regulated modifications that affect nuclear transport include phosphorylation, acetylation and ubiquitylation (see also 3.6.), mostly inducing conformational changes (see Xu & Massague, 2004). Constitutive activation of signaling cascades leading to increased phosphorylation and nuclear transport of downstream target molecules, such as the STAT proteins, is observed in a variety of cancers.

On the other hand, dysregulation at the level of the transporters might also lead to cellular transformation. Some karyopherins are expressed only in certain tissues and might transport cargoes only during specific stages of development, or function in a particular cell type (Görlich & Kutay, 1999). Components of the nuclear transport machinery also appear to be differentially expressed in transformed cells, with strong proliferative signals leading to the alteration of nuclear import (Sherr, 2004). For example, overexpression of CAS has been reported in several different tumors and cancer cells (Kau *et al.*, 2004). In this case, excess CAS may lead to enhanced nuclear accumulation of nuclear acting factors that facilitate cell proliferation or prevent apoptosis, through accelerated importin-α recycling.

Further examples of an altered nuclear transport machinery in cancer are observed in patients with acute myelogenous leukemia, where chromosomal rearrangements can lead to the fusion of NUPs such as NUP98 or NUP214 with HOXA9 or DEK, respectively. Although these fusion proteins do not assemble into the NPC, their hydrophobic FG-repeat sequences

may enable them to bind to transport receptors and modify transport of certain cargos since overexpression of FG-repeats has been shown to interfere with transport (Kau *et al.*, 2004).
Finally, the nuclear pore itself can offer an added level of regulation. The number of functional and/or specific pores may vary depending on the growth state of the cell, which in turn affects the overall permeability of the nucleus.
Thus, modifications to cargo, changes in the nuclear transport machinery and alterations in the NPC itself could markedly alter cellular functions and potentially promote tumorigenesis.

3.8 Targeting nucleo-cytoplasmic transport as a potential therapeutic principle

Drugs that target nucleo-cytoplasmic transport can be envisaged to be active at the different levels described above. However, two important obstacles must be overcome - the problem of specificity for tumour cells versus normal cells, and the difficulty in creating drugs that interfere with protein-protein interactions (PPIs), in contrast to enzyme-substrate binding.
Drugs, which indirectly interfere with nuclear import/export by blocking posttranslational modification of the cargo and thereby inhibiting its ability to interact with its cognate transporter has been described for several proteins. Mostly, these consist of protein kinase inhibitors as exemplified by inhibitors of the PI3K/PTEN/Akt signal transduction pathway, which affected export of the Forkhead family of transcription factors (Kau *et al.*, 2003). Although these compounds interfere with nuclear transport of proteins they clearly lack specificity.
So far, no inhibitors have been described directed against components of the stationary nuclear transport machinery. In contrast, the karyopherin transport factors – the karyopherin-β proteins, in particular – represent a class of potential targets. Molecular structures of several different karyopherins have been solved, making these proteins potential therapeutic targets, since some of these factors might transport only a defined class of proteins (Kau *et al.*, 2004). For example Leptomycin B (LMB), which inhibits CRM1 export activity by covalent binding and prevention of the CRM1-NES interaction, was identified as a HIV-1 inhibitor (Wolff *et al.*, 1997) and had also been suggested as a potential anti-cancer drug (Komiyama *et al.*, 1985; Vigneri & Wang, 2001). However, although LMB clearly inhibits export of the HIV-1 Rev protein or the leukemia inducing Bcr-Abl kinase (Vigneri & Wang, 2001), LMB blocks all NES mediated export in the cell, and thus its cellular toxicity will not allow therapeutic applications.

Therefore, protein specific transport inhibitors are urgently needed. Since transport signals can be grouped into specific categories according to their activity *in vivo* (Heger *et al.*, 2001; Rosorius *et al.*, 1999), these differences may represent an attractive opportunity to selectively interfere with export and the biological functions of proteins by the generation of NES/NLS-specific inhibitors.

Targeting the proteins that are involved in nuclear transport, in addition to the nuclear transport of factors that have been associated with disease, could prove to be a promising approach for controlling cancer-cell growth as well as infectious diseases. In order to efficiently identify nuclear transport and protein-protein interaction small-molecule inhibitors, high-content, cell-based screening assays are urgently required.

4 Cell-based assay systems

As any biochemical data or potential drug therapies must be effective at the cellular level, isolated proteins cannot be regarded as representatives of complex biological systems, and cell-based assays have to be employed to complement *in vitro* data. Traditional small-molecule drug discovery focuses primarily on the activity of compounds against purified targets, such as binding to cell-surface receptors or inhibition of the catalytic activity of enzymes. While these approaches have led to the development of a large number of drugs, they clearly have limitations. Because of the complex network environment, in which intracellular signaling occurs, it is advantageous to screen compounds in living cells to reproduce the pathway and network context, in which the drug will eventually have to act. In addition, unwanted cellular toxicity can thereby be recognized very early in the expensive drug discovery process, and biosensors will help to ease the bottlenecks in the drug discovery process. High-content screening (HCS) has been created as a platform for measuring the temporal and spatial responses of cells to drug and biological treatments. Subcellular localization of mislocalized proteins in cancer cells have been suggested as a read-out to identify small molecules that redirect the proteins to the correct compartments (Kau *et al.*, 2003). Such screening approaches could lead to the discovery of novel compounds that provide new insights into the mechanisms of nucleo-cytoplasmic trafficking and disease-regulatory pathways. However, any realistic application of high-content and high-throughput CBAs critically depends on robust and reliable biological readout systems with a high signal to noise ratio. Quantification of the translocations of molecules between cellular compartments, including organelles, is considered an important parameter of HCS (Giuliano *et al.*, 2003b). Quantification can be performed in either a fixed end-point mode or a kinetic mode, using novel computer-driven, automated image acquisition and pattern-recognition from the cellular images (Liebel *et al.*, 2003). Cell-based assays that measure translocation of green fluorescent protein tagged targets as the primary read-out have been applied to identify inhibitors in the p38-MAP kinase (Almholt *et al.*, 2004) or the PI3K/Akt kinase pathway (Kau *et al.*, 2003).

Live cell assays have also been applied to monitor protease activity and to screen for protease inhibitors (Laxman *et al.*, 2002; Lindsten *et al.*, 2001). Site-specific proteases, which catalyze cleavage of peptide bonds in specific amino acid sequences of target proteins, play important roles in various biological events, and dysregulation of these site-specific proteases can also lead to pathological consequences (reviewed in Patel *et al.*, 2001). These

include, e.g., the prostate specific antigen (PSA), a serine protease in prostate cancer patients, an Alzheimer-specific aspartic protease, matrix metalloproteinases (MMP), involved in tumor invasion, metastasis, and angiogenesis as well as site-specific proteases involved in blood clotting, such as Factor Xa and Thrombin. Dysregulation of apoptosis also contributes to a variety of pathologic conditions, including cancer, with the main effectors, the caspases, also being proteases. For several viruses including HIV, viral proteases are essential for replication, and thus are crucial drug targets (Brik & Wong, 2003). Since nucleo-cytoplasmic translocation depends on the activity of defined linear signals, it can be envisaged to develop also translocation sensors into protease biosensors for the *in vivo* screening for protease inhibitors.

The proper biological functions of cells are controlled by interacting proteins in metabolic and signaling pathways, and in complexes such as the molecular machineries for transcription, translation, intracellular transport and apoptosis. Much of modern biological research is concerned with identifying proteins involved in these cellular processes. Because many of the properties of complex systems seem to be more closely determined by their interactions than by the characteristics of their individual components, identification and characterization of specific protein interactions is one of the main goals of current research. In addition, abolishing or inducing specific PPIs by molecular decoys may offer new opportunities for the treatment of human diseases (see Berg, 2003; Pagliaro *et al.*, 2004, and references within).

In cancer, cellular transformation and maintenance of the transformed phenotype often depend upon the formation of specific complexes, and thus, inhibitors that prevent Jun-Fos, Myc-Max or p53-Mdm2 interaction are currently under intense investigation as potential anti-cancer drugs (Berg *et al.*, 2002; Hermeking, 2003; Vassilev *et al.*, 2004). Consequently, many methods have been described to analyze PPIs, including numerous sophisticated biochemical techniques or the yeast two-hybrid (YTH) system. Methods to study protein interactions in living cells or even whole animals involve inter- and intramolecular FRET, bimolecular fluorescence complementation (BiFC) (Hu & Kerppola, 2003), as well as protein complementation assays, in which a signal is generated only when two interacting proteins come together (referenced in Day & Schaufele, 2005; Pagliaro *et al.*, 2004). Although these approaches shows great promise, they still await successful adaption to and application in high-throughput screening.

In conclusion, the living cell, with its amazing integrative abilities of environmental detection, molecular signal amplification and processing, and repertoire of genome-level responses to perturbation, represents a powerful test tube (Giuliano *et al.*, 2003a). As proteins have evolved to mediate intracellular chemical reactions, they are ideal candidates not only to sense the dynamic distribution of specific reactions in cells, but also to act as reporters of their own activities. An improved molecular understanding of protein-protein interactions as well as of nucleo-cytoplasmic transport is required to learn more about biological processes and their contributions to disease conditions. Exploitation of this knowledge in the context of living cells will lead to chemical genetic assay systems for elucidating complex pathways in biological systems and to the development of novel pharmaceuticals.

5 Summary of publications

The following section presents a brief summary of the publications achieved and specifies my contributions to the individual reports.
The overall topic of the thesis was to investigate the significance of nucleo-cytoplasmic transport for the biological fuctions of cellular proteins.

It could be shown that regulated nucleo-cytoplasmic transport of a subfamily of the homeobox transcription factors could fine-tune their transcriptional activity (Knauer *et al.*, 2005a). Experimental procedures and data analysis in this work were predominantly carried out by myself.

The work performed by Krämer *et al.* (Krämer *et al.*, 2005) showed that acetylation of the transcription factor Stat1 enhanced its interaction with NF-κB p65, which in turn influenced subcellular localization, DNA-binding and transcriptional activation of apoptosis-inducing NF-κB target genes. The main contributor, Oliver Krämer, performed most of the biochemical assays, and I confirmed the results on the cellular level.

In the case of the anti-apoptotic protein survivin, it could be demonstrated that the evolutionary conservation of an export signal plays an important role for ist dual function, apoptosis inhibition and ordered cell division (Knauer *et al.*, 2005b). This work was performed in collaboration with Oliver Krämer, who performed the caspase-3 activity assays. Thomas Knösel, Knut Engels, Franz Rödel, Hartmut Walendzik, Adoriàn Kovács, Jürgen Brieger, Wolf Mann and Iver Petersen provided the patient material and performed immunohistology stainings as well as the Kaplan-Meier survival analysis. RT-qPCR analysis was performed by Negusse Habtemichael.

These findings indicated that the intervention with nucleo-cytoplasmic transport of disease-relevant could be a potential therapeutic principle. To follow this approach, novel cell-based assay systems were developed that allow the identification of transport inhibitors (Knauer *et al.*, 2005c). The work was performed in collaboration with Thorsten Berg, who provided plasmids and chemical substance for screening procedures. Urban Liebel performed the automated image acquisition and analysis on a fully automated high-throughput screening microscope. In addition, the principle of nuclear translocation was exploited to establish protease- and protein-interaction biosensors (Knauer & Stauber, 2005). Experimental procedures, data analysis and interpretation presented in this work were carried out predominantly by myself.

5.1 Nuclear export is evolutionary conserved in CVC paired-like homeobox proteins and influences protein stability, transcriptional activation and extracellular secretion

Shirley K. Knauer, Gert Carra and Roland H. Stauber

Ordered development depends on the activity of transcription factors in a controlled manner. Among other mechanisms, regulated subcellular localization provides an attractive way to control the activity of transcription factors, which has been, demonstrated for several key players of signal transduction cascades (Cartwright & Helin, 2000, and references therein). Homeodomain transcription factors control a variety of essential cell fate decisions during development. To understand the developmental regulation by these transcription factors, we investigated the intracellular trafficking of the paired-like CVC Homeodomain proteins (PLC-HDPs) and analyzed its consequences for PLC-HDP function as transcriptional regulators. The PLC-HDPs are characterized by a conserved CVC domain, can be grouped into the *Vsx-1* (visual system homeobox) and *Vsx-2* family, and play a particular role in ocular development (Ohtoshi *et al.*, 2004, and references therein).

As representatives of the Vsx-1 and Vsx-2 group, we studied the zebrafish Vsx1 and the murine Chx10 (Ceh-10 homologous homeobox) protein in detail (Knauer *et al.*, 2005a). Nucleocytoplasmic transport was investigated by interspecies heterokaryon assays, microinjection of recombinant transport substrates, and the use of chemical transport inhibitors. We could demonstrate that PLC-HDPs contain an evolutionary conserved CRM1-dependent NES, previously described as the “octapeptide”.

Interestingly, preventing nuclear export by mutation of the NES resulted in a significantly increased half-life for the export deficient Vsx-1 and Chx10 mutant proteins, indicating that nuclear export is continuously supplying substrate for the proteasomal degradation machinery. Thus, by regulating the intracellular steady-state concentration, nuclear export indirectly influenced PLC-HDP transcriptional activation, since the export deficient Vsx-1 and Chx10 mutant proteins showed an increased stimulation of gene expression. In addition, we found that the export-mediated continuous supply of cytoplasmic PLC-HDPs facilitated their unconventional secretion required for the intercellular trafficking of PLC-HDP.

The predominant nuclear steady-state localization of PLC-HDPs was found to be mediated by the presence of a 100% conserved active nuclear import signal. The high homology of this

signal to known protein transduction domains (PTD) could be verified also functional, explaining the evolutionary conservation of this signal.

Based on our findings, we propose a model, in which the continuous nucleo-cytoplasmic shuttling of PLC-HDPs contributes to the optimal and flexible execution of their transcriptional activities (figure 5.1.). The evolutionarily conserved combination of a PTD, together with active nuclear export and import signals, may allow the fine-tuning of intracellular protein levels by the proteasome pathway and, in addition, also permits intercellular transfer.

The overlapping complex patterns of homeobox gene expression in the embryonic retina require a complex regulatory network of transcription factors. Although transcriptional regulation of PLC-HDPs is an important control mechanism, PLC-HDPs may have additional unexpected paracrine activity, thereby influencing and maintaining the complex expression pattern during development.

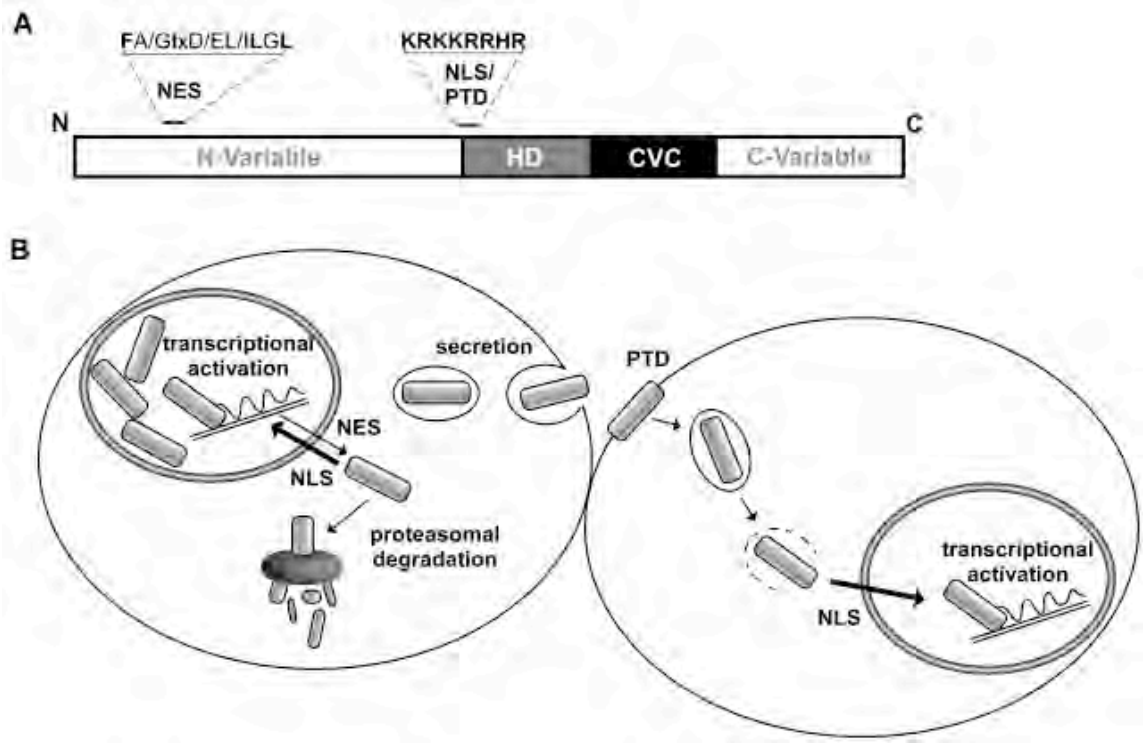

Figure 5.1. (A) **Organization of evolutionary conserved domains in PLC-HD proteins regulating cellular transport.** (B) **Model linking nucleo-cytoplasmic transport with PLC-HDP activity.** The predominantly nuclear localization of PLC-HD proteins is the net result of import exceeding the rate of export due to the different activities of NES and NLS. Nuclear export allows PLC-HD protein levels to be regulated by the proteasomal degradation pathway and continuously supplies cargo for extracellular unconventional secretion. Intercellular transport and trans-activation could be mediated by the protein transduction domain/NLS.

5.2 Acetylation of STAT1 modulates NF-κB signaling

Oliver H. Krämer, Daniela Baus, Shirley Knauer, Stefan Stein, Elke Jäger, Roland Stauber, Manuel Grez, Edith Pfitzner and Thorsten Heinzel

The modulation of signaling events by histone deacetylase inhibitors (HDACi) can lead to the induction of apoptosis or differentiation of carcinoma cells. The molecular mechanisms underlying these processes are still under investigation but their understanding is crucial for the efficient therapeutic application of HDACi. We found that sensitivity to HDACi correlated with STAT1 expression in human melanoma cell lines (Krämer *et al.*, 2005). Ectopic expression of STAT1 in resistant cells restored HDACi mediated induction of apoptosis. In STAT1-positive cells, HDACi increased expression and acetylation of STAT1 and promoted its interaction with NF-κB p65. As a consequence, NF-κB p65 DNA-binding, nuclear localization and ultimately expression of anti-apoptotic NF-κB target genes decreased (figure 5.2.). We identified lysines 410 and 413 of STAT1 as acetylation sites. Mutation of these residues to glutamine mimicked acetylation and rendered the interaction of STAT1 and NF-κB p65 constitutive, whereas mutation to arginine precluded this interaction as well as HDACi-induced apoptosis. Our study not only provides an additional example how posttranslational modifications can influence protein localization, but also shows that the crosstalk between STAT1 and NF-κB signaling pathways can be regulated by changes in the acetylation status of STAT1.

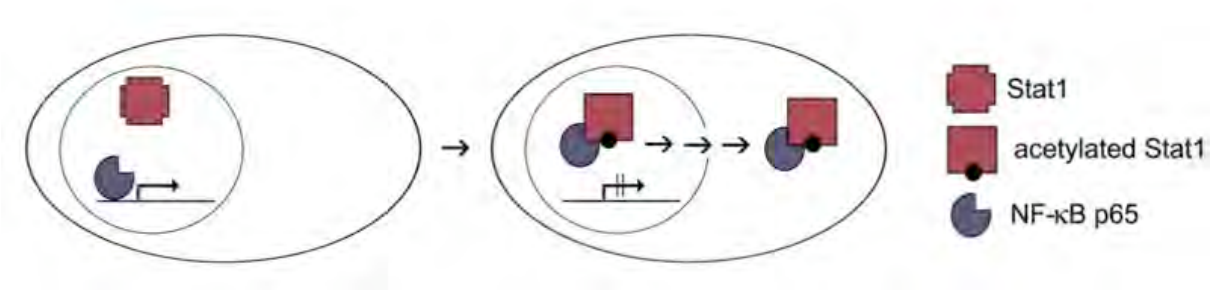

Figure 5.2. **Model for acetylation-dependent STAT1-NF-κB crosstalk.**

5.3 Nuclear export is essential for the biological activity of survivin - Novel aspects to target the survivin pathway in cancer

Shirley K. Knauer, Oliver H. Krämer, Thomas Knösel, Knut Engels, Franz Rödel, Hartmut Walendzik, Adoriàn F. Kovács, Negusse Habtemichael, Jürgen Brieger, Wolf Mann, Thorsten Heinzel, Iver Petersen and Roland H. Stauber

Evasion from apoptosis as well as enhanced proliferation are invariant molecular characteristics of human cancer (Hanahan & Weinberg, 2000). Among several mechanisms, escape from apoptosis can be the result of a deregulated overexpression of apoptosis inhibitors (IAPs). A major therapeutic and prognostic interest has been focused on the IAP survivin (Altieri, 2003a; Altieri, 2003d), which is expressed in most human tumors and correlates with reduced tumor cell apoptosis, abbreviated patient survival, accelerated rates of recurrences, and increased resistance to chemo- and radiotherapy (see Altieri, 2003c; Altieri, 2003d; Li, 2003, and references within).

Since survivin was reported to function as an apoptosis inhibitor and a regulator of cell division, i.e., functions executed in distinct intracellular compartments, we dissected the molecular mechanism regulating the dynamic cellular localization of survivin and investigated their functional consequences (Knauer *et al.*, 2005b).

We found that survivin was overexpressed in head and neck tumors and colorectal carcinomas and could be detected in both the cytoplasm and the nucleus. Nucleocytoplasmic transport was investigated in cell culture systems by deletion mutagenesis, microinjection of recombinant transport substrates, as well as biochemical assays resulting in the identification of an evolutionary conserved CRM1 dependent leucine-rich NES in survivin, present also in the splice variants 2B and 3B, but absent in the splice variants ΔExon3 and 2α. In contrast, neither survivin nor survivin splice variants harbor an active nuclear import signal, and thus appear to enter the nucleus by passive diffusion. Importantly, comparison of the anti-apoptotic activity of survivin and a NES-deficient survivin mutant revealed that nuclear export was required for survivin mediated protection against chemo- and radiotherapy induced apoptosis. Since the activity of IAPs is assumed to be mediated predominantly in the cytoplasm, the reduced colocalization of the NES-mutant with Caspase-3 and -9 could account for the diminished anti-apoptotic activity of the survivin NES-mutant.

Interfering with nuclear export of survivin also manifested in an increase in multinuclear cells, indicative for an impaired mitotic checkpoint control. We assume that survivin is tethered to the chromosomal passenger complex via the NES-mediated interaction with CRM1, which is an essential component of the mitotic machinery. Thus, nuclear export not only appears to play a role in protection against cancer therapy induced apoptosis but also seems to be required for proper cytokinesis.

The clinical relevance of our finding was supported by showing that preferential nuclear localization of survivin correlated with enhanced survival in a cohort of colorectal cancer patients. Cell culture experiments suggested interference with the nuclear export machinery as one potential mechanism promoting survivin's nuclear accumulation.

In conclusion, targeted interference with survivin's nuclear export can be regarded as a promising strategy for novel anti-cancer therapies.

5.4 Translocation biosensors to study signal specific nucleo-cytoplasmic transport, protease activity & protein interactions

Shirley K. Knauer, Sabrina Moodt, Thorsten Berg, Urban Liebel, Rainer Pepperkok and Roland H. Stauber

Nucleo-cytoplasmic transport is crucial to control the activity and stability of regulatory proteins and RNAs, and thus interfering with nucleo-cytoplasmic transport in general as a novel therapeutic principle has recently attracted major interest by academia and industry (reviewed in Kau *et al.*, 2004; Pagliaro *et al.*, 2004). In addition, regulated intracellular localization is also essential for the controlled activity of site-specific proteases, which play crucial roles in a variety of cellular functions, e.g. Thus, a great deal of interest has recently focused on caspases as therapeutic targets for various disease processes (Los *et al.*, 2003). Besides for nucleo-cytoplasmic transport, protein interaction networks are critical for all cellular events (Fahrenkrog & Aebi, 2003). In addition, modulating specific protein-protein interactions by chemical compounds offers tremendous potential for the treatment of human diseases.

As drug therapies must be effective at the cellular level, isolated proteins cannot be regarded as representatives of complex biological systems, and cell-based assays (CBAs) have to be employed. Recently, several methods have been developed to facilitate the implementation of high-throughput CBAs (Hemmila & Hurskainen, 2002). However, any realistic applications of high-throughput CBAs critically depend on robust and reliable biological readout systems with a high signal to noise ratio. In this context, the spatial and functional division into the nucleus and the cytoplasm marks two dynamic intracellular compartments that can easily be distinguished by microscopy. Facing the clear need for improved CBAs, we exploited our knowledge of regulated nucleo-cytoplasmic transport resulting in the development and application of modular biosensors tailored to investigate signal specific nuclear export and import, protease activity and specific protein-protein interactions in living cells (Knauer *et al.*, 2005c).

The cellular biosensors were composed of the SV40 nuclear import signal, glutathione S-transferase (GST), mutants of GFP and combinations of nuclear export signals. The fusion proteins met essential requirements prerequisite to function as screening systems to identify signal specific nucleo-cytoplasmic translocation inhibitors: The biosensors 1. localized predominantly to the cytoplasm. 2. were efficiently shuttling between the nucleus and the

cytoplasm. 3. accumulated in the nucleus following inhibition of nuclear export. 4. allowed the modular exchange of transport signals. 4. were neither toxic nor affected by passive diffusion or post-translational modifications in their intracellular localization.

We incorporated the NESs from PKI, from the HIV-1 Rev protein, from STAT1 and from Bcr-Abl into the translocation sensors. The performance of the biosensors were systematically investigated demonstrating that the designed transport sensors allowed to directly investigate the effects of drug treatment or of over-expression/conditional knock-down of proteins on general and signal-specific nucleo-cytoplasmic transport. Importantly, cytoplasmic to nuclear translocation of the sensors could be accurately and reproducibly quantitated also on an automated platform for high-throughput cell screening microscopy, which is an essential requirement for their practical use in screening assays.

The principle of the translocation sensors was further exploited by the development into protease biosensors. We incorporated the PARP (poly-(ADP-Ribose) polymerase) cleavage site for Caspase-3 N-terminal to the RevNES. The Casp3-sensor localized predominantly to the cytoplasm, and induction of apoptosis resulted in the cleavage of the RevNES and the subsequent nuclear accumulation of the Casp3-sensor.

Subsequently, we further developed the transport biosensor system into a “two-hybrid” protein interaction assay to visualize specific protein-protein interaction *in vivo.* W e engineered a cassette that allows the expression of any ORF (open reading frame) X as a NLS-GFP/GST-X-RevNES fusion protein (GFP-prey). Our previous work (Stauber *et al.*, 1998) demonstrated that a NES deficient HIV-1 Rev BFP fusion (RevM10-BFP) localized to the nucleolus, and thus represented an ideal frame to express nucleolar anchored Y-BFP fusion proteins (BFP-bait).

Having tested the leucine zipper protein interaction domains (ID) of Jun/Fos and Myc/Max as well as for the ID of p53/Mdm2 in our assay, we finally concluded that the protein interaction assay fulfills the following criteria: 1. The GFP-prey molecule containing ID1, although continuously shuttling between the nucleus and the cytoplasm, localizes predominantly to the cytoplasm. 2. The BFP-bait protein harboring ID2 is confined to the nucleolus. 3. Upon specific protein interaction between ID1 and ID2, the GFP-prey redistributes to the nucleus and colocalizes with the BFP-bait at the nucleolus. 4. The system is reversible and allows the modular exchange of interaction domains. 5. Inhibitors of protein interactions can significantly diminish the cytoplasmic to nuclear translocation.

In summary, the developed assays proved flexible, robust, facile and highly amenable to academic scale screens with the potential to be employed also in drug-screening

applications. Efficient nuclear accumulation served as the common reliable indicator for all biosensors (see figure 5.4.) and thus will facilitate fully automated image acquisition and data analysis using microscopy based assay platforms. The modular composition of the biosensors guarantees their flexible adoption and applications in numerous biological systems.

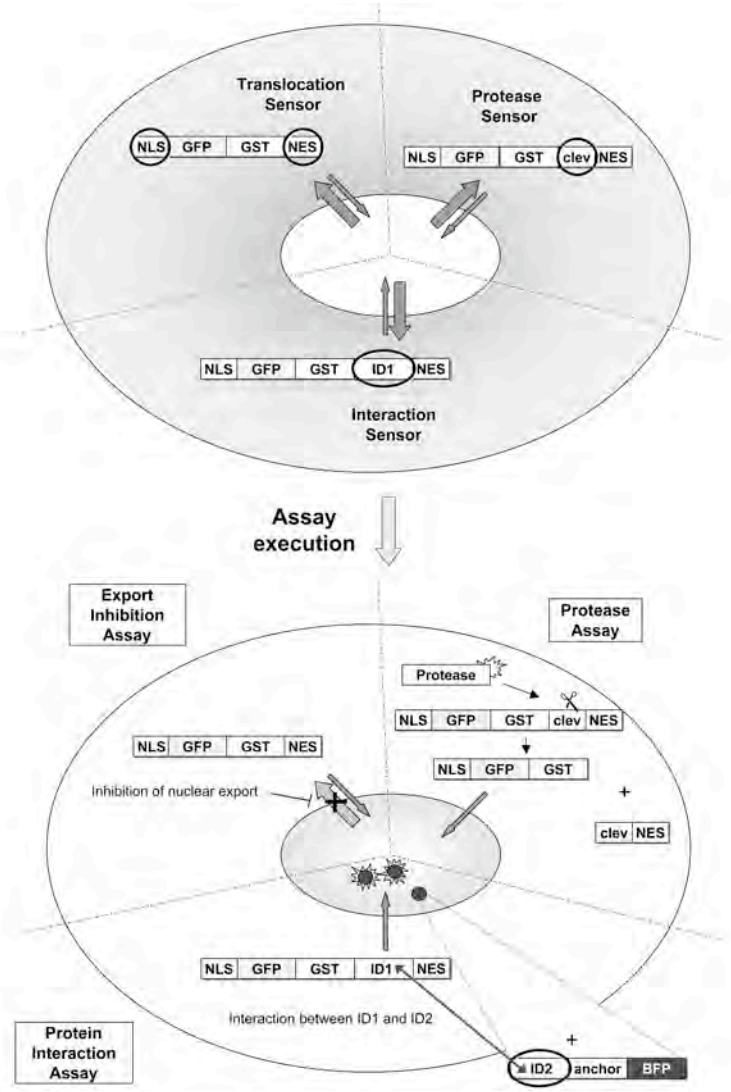

Figure 5.4. **Nuclear translocation of the biosensors as the principle for cell-based screening applications.** The cellular biosensors are composed of GST, GFP and rational combinations of nuclear import and export signals. (A) Addition of regulatory sequences resulted in three classes of biosensors applicable for the identification of signal specific nuclear transport inhibitors, small molecules that interfere with protease activity and compounds that modulate protein-protein interactions in living cells. (B) Nuclear accumulation of the cytoplasmic biosensors serves as the indicator, which can be induced by interference with nuclear export, induction of protease activity or formation of highly specific protein complexes.

5.5 Development of an Autofluorescent Translocation Biosensor System to Investigate Protein-Protein-Interactions in Living Cells

Shirley K. Knauer and Roland H. Stauber

Cellular homeostasis and communication strictly require regulated protein-protein interaction networks. Identification of these interactions and characterization of their physiological significance is one of the main goals in a wide range of biological fields (Mendelsohn & Brent, 1999; Ozawa *et al.*, 2001). In cancer, cellular transformation and maintenance of the transformed phenotype often strictly depend upon the formation of high molecular weight complexes (HMWC). Thus, it has become clear that molecules, which inhibit specific protein-protein interactions, have great potential as therapeutics with new modes of action (Arkin & Wells, 2004). Consequently, numerous methods have been described to analyze protein-protein interactions *in vitro*, in cell culture and *in vivo* including the yeast two-hybrid (YTH) system, several split-enzyme complementation/reconstitution assays (Paulmurugan *et al.*, 2002, and references therein), fluorescence resonance energy-transfer (FRET) (Ozawa *et al.*, 2001; Wehrman *et al.*, 2002) as well as bimolecular fluorescence complementation (BiFC) (see (Hu & Kerppola, 2003; Yu *et al.*, 2003). Although the various methods have been valuable tools in analyzing protein interactions, several intrinsic limitations apply (see (Ozawa *et al.*, 2001, and references within).

To analyze protein-protein interactions in live mammalian cells, we applied protein translocation biosensors (PTBs) composed of glutathione S-transferase, mutants of GFP and combinations of nuclear import and export signals (Knauer & Stauber, 2005). Nuclear accumulation of the cytoplasmic biosensors served as the reliable indicator, which was induced by the formation of protein complexes and could easily be detected by fluorescence microscopy. Efficacy of the system was systematically investigated by mapping the p53/Mdm2 protein interaction interface. Specificity and general applicability of the biosensors were confirmed by studying not only protein interaction domains (IDs), which function as heterodimers (e.g., the leucine-zipper IDs of Jun/Fos) but also of IDs, which form homodimers (e.g., the coiled-coil IDs of Bcr-Abl). Importantly, we found that, in comparison to protein complementation assays (e.g., BiFC), our system proved highly efficient and reversible, and thus suited for the identification of molecular decoys to prevent specific protein-protein interactions in living cells. Reversibility was demonstrated in competition

experiments by overexpressing the specific IDs or by the application of a chemical p53/Mdm2 protein interaction inhibitor.

Thus, in contrast to existing protein interaction assays, the presented strategy proved highly efficient, flexible and reversible. Since the majority of GFP-prey fusions are not expected to intrinsically localize to the nucleolus, our system is applicable to map the IDs of many proteins. Moreover, the modular translocation system has great potential to be employed in numerous cell-based assays for the identification of small molecule protein interaction inhibitors as potential novel therapeutics.

6 Achievements of this work and outlook

The thesis entitled "Investigations on the significance of nucleo-cytoplasmic transport for the biological function of cellular proteins" aimed to unreveal molecular mechanism in order to improve our understanding of the impact of nucleo-cytoplasmic transport on cellular functions.

Within the scope of this work, it could be shown that regulated nucleo-cytoplasmic transport of a subfamily of homeobox transcription factors also controls their intercellular transport, thereby influencing their transcriptional activity (Knauer *et al.*, 2005a). This study described a novel regulatory mechanism, which could in general play an important role for the ordered differentiation of complex organisms. Future work will focus on the analysis of the *in vivo* role of PLC-HDPs' nucleo-cytoplasmic shuttling for ordered development by the generation of transgenic mouse knock-in models, in which the nuclear export/import signals of PLC-HDPs are selectively abolished.

Besides *cis*-active transport signals, also post-translational modifications can influence the localization and biological activity of proteins *in trans*. In addition to the known impact of phosphorylation on the transport and activity of STAT1, experimental evidence was provided demonstrating that acetylation affected the interaction of STAT1 with NF-κB p65, and subsequently modulated the expression of apoptosis-inducing NF-κB target genes (Krämer *et al.*, 2005). Future work will be engaged in analyzing whether this mechanism is also relevant for other members of the STAT family.

The impact of nucleo-cytoplasmic transport on the regulation of apoptosis was underlined by showing that the evolutionary conservation of a NES within the anti-apoptotic protein survivin plays an essential role for its dual function in the inhibition of apoptosis and ordered cell division (Knauer *et al.*, 2005b). Since survivin is considered a bona fide cancer therapy target, these results strongly encourage future work to identify molecular decoys that specifically inhibit the nuclear export of survivin as novel therapeutics.

In order to further dissect the regulation of nuclear transport and to efficiently identify transport inhibitors, cell-based assays are urgently required. Therefore, the cellular assay systems developed in this work (Knauer *et al.*, 2005c) may not only serve to identify synthetic

nuclear export and import inhibitors, but may also be applied in systematic RNAi-screening approaches to identify novel components of the transport machinery. In addition, the translocation based protease and protein interaction biosensors can be applied in various biological systems, in particular to identify protein-protein interaction inhibitors of cancer relevant proteins (Knauer *et al.*, 2005c; Knauer & Stauber, 2005).

In summary, this work does not only underline the general significance of nucleo-cytoplasmic transport on cell biology, but also demonstrates its potential for the development of novel therapies against diseases like cancer and viral infections.

7 References

Adam S. A. (1999). Transport pathways of macromolecules between the nucleus and the cytoplasm. *Curr Opin Cell Biol* **11**, 3, p. 402-6.

Affolter M., Marty T. & Vigano M. A. (1999). Balancing import and export in development. *Genes Dev* **13**, 8, p. 913-5.

Almholt D. L., Loechel F., Nielsen S. J., Krog-Jensen C., Terry R., Bjorn S. P., Pedersen H. C., Praestegaard M., Moller S., Heide M., Pagliaro L., Mason A. J., Butcher S. & Dahl S. W. (2004). Nuclear export inhibitors and kinase inhibitors identified using a MAPK-activated protein kinase 2 redistribution screen. *Assay Drug Dev Technol* **2**, 1, p. 7-20.

Alt J. R., Cleveland J. L., Hannink M. & Diehl J. A. (2000). Phosphorylation-dependent regulation of cyclin D1 nuclear export and cyclin D1-dependent cellular transformation. *Genes Dev* **14**, 24, p. 3102-14.

Alt J. R., Gladden A. B. & Diehl J. A. (2002). p21(Cip1) Promotes cyclin D1 nuclear accumulation via direct inhibition of nuclear export. *J Biol Chem* **277**, 10, p. 8517-23.

Altieri D. C. (2003a). Blocking survivin to kill cancer cells. *Methods Mol Biol* **223**, p. 533-42.

Altieri D. C. (2003b). Survivin and apoptosis control. *Adv Cancer Res* **88**, p. 31-52.

Altieri D. C. (2003c). Survivin in apoptosis control and cell cycle regulation in cancer. *Prog Cell Cycle Res* **5**, p. 447-52.

Altieri D. C. (2003d). Validating survivin as a cancer therapeutic target. *Nat Rev Cancer* **3**, 1, p. 46-54.

Altieri D. C. (2004). Molecular circuits of apoptosis regulation and cell division control: The survivin paradigm. *J Cell Biochem* **92**, 4, p. 656-63.

Ambros V. (2001). microRNAs: tiny regulators with great potential. *Cell* **107**, 7, p. 823-6.

Arkin M. R. & Wells J. A. (2004). Small-molecule inhibitors of protein-protein interactions: progressing towards the dream. *Nat Rev Drug Discov* **3**, 4, p. 301-17.

Arnaoutov A., Azuma Y., Ribbeck K., Joseph J., Boyarchuk Y., Karpova T., McNally J. & Dasso M. (2005). Crm1 is a mitotic effector of Ran-GTP in somatic cells. *Nat Cell Biol* **7**, 6, p. 626-32.

Arnaoutov A. & Dasso M. (2003). The Ran GTPase regulates kinetochore function. *Dev Cell* **5**, 1, p. 99-111.

Azuma Y. & Dasso M. (2000). The role of Ran in nuclear function. *Curr Opin Cell Biol* **12**, 3, p. 302-7.

Bednenko J., Cingolani G. & Gerace L. (2003). Nucleocytoplasmic transport: navigating the channel. *Traffic* **4**, 3, p. 127-35.

Ben-Efraim I. & Gerace L. (2001). Gradient of increasing affinity of importin beta for nucleoporins along the pathway of nuclear import. *J Cell Biol* **152**, 2, p. 411-7.

Berg T. (2003). Modulation of protein-protein interactions with small organic molecules. *Angew Chem Int Ed Engl* **42**, 22, p. 2462-81.

Berg T., Cohen S. B., Desharnais J., Sonderegger C., Maslyar D. J., Goldberg J., Boger D. L. & Vogt P. K. (2002). Small-molecule antagonists of Myc/Max dimerization inhibit Myc-induced transformation of chicken embryo fibroblasts. *Proc Natl Acad Sci U S A* **99**, 6, p. 3830-5.

Briggs L. J., Stein D., Goltz J., Corrigan V. C., Efthymiadis A., Hubner S. & Jans D. A. (1998). The cAMP-dependent protein kinase site (Ser312) enhances dorsal nuclear import through facilitating nuclear localization sequence/importin interaction. *J Biol Chem* **273**, 35, p. 22745-52.

Brik A. & Wong C. H. (2003). HIV-1 protease: mechanism and drug discovery. *Org Biomol Chem* **1**, 1, p. 5-14.

Brooks C. L., Li M. & Gu W. (2004). Monoubiquitination: the signal for p53 nuclear export? *Cell Cycle* **3**, 4, p. 436-8.

Caldas H., Honsey L. E. & Altura R. A. (2005). Survivin 2alpha: a novel Survivin splice variant expressed in human malignancies. *Mol Cancer* **4**, 1, p. 11.

Cartwright P. & Helin K. (2000). Nucleocytoplasmic shuttling of transcription factors. *Cell Mol Life Sci* **57**, 8-9, p. 1193-206.

Clarke P. R. (2005). The Crm de la creme of mitosis. *Nat Cell Biol* **7**, 6, p. 551-2.

Connor M. K., Kotchetkov R., Cariou S., Resch A., Lupetti R., Beniston R. G., Melchior F., Hengst L. & Slingerland J. M. (2003). CRM1/Ran-mediated nuclear export of p27(Kip1) involves a nuclear export signal and links p27 export and proteolysis. *Mol Biol Cell* **14**, 1, p. 201-13.

Cory S. & Adams J. M. (2002). The Bcl2 family: regulators of the cellular life-or-death switch. *Nat Rev Cancer* **2**, 9, p. 647-56.

Cullen B. R. (2003a). Nuclear mRNA export: insights from virology. *Trends Biochem Sci* **28**, 8, p. 419-24.

Cullen B. R. (2003b). Nuclear RNA export. *J Cell Sci* **116**, Pt 4, p. 587-97.

Dasso M. (2001). Running on Ran: nuclear transport and the mitotic spindle. *Cell* **104**, 3, p. 321-4.

Dasso M. (2002). The Ran GTPase: theme and variations. *Curr Biol* **12**, 14, p. R502-8.

Day R. N. & Schaufele F. (2005). Imaging molecular interactions in living cells. *Mol Endocrinol*.

Denning D. P., Patel S. S., Uversky V., Fink A. L. & Rexach M. (2003). Disorder in the nuclear pore complex: the FG repeat regions of nucleoporins are natively unfolded. *Proc Natl Acad Sci U S A* **100**, 5, p. 2450-5.

Deveraux Q. L. & Reed J. C. (1999). IAP family proteins--suppressors of apoptosis. *Genes Dev* **13**, 3, p. 239-52.

Doye V. & Hurt E. (1997). From nucleoporins to nuclear pore complexes. *Curr. Opin. Cell Biol.* **9**, p. 401-11.

Endter C., Kzhyshkowska J., Stauber R. & Dobner T. (2001). SUMO-1 modification required for transformation by adenovirus type 5 early region 1B 55-kDa oncoprotein. *Proc Natl Acad Sci U S A* **98**, 20, p. 11312-7.

Englmeier L., Fornerod M., Bischoff F. R., Petosa C., Mattaj I. W. & Kutay U. (2001). RanBP3 influences interactions between CRM1 and its nuclear protein export substrates. *EMBO Rep* **2**, 10, p. 926-32.

Englmeier L., Olivo J. C. & Mattaj I. W. (1999). Receptor-mediated substrate translocation through the nuclear pore complex without nucleotide triphosphate hydrolysis. *Curr Biol* **9**, 1, p. 30-41.

Fahrenkrog B. & Aebi U. (2003). The nuclear pore complex: nucleocytoplasmic transport and beyond. *Nat Rev Mol Cell Biol* **4**, 10, p. 757-66.

Fahrenkrog B., Aris J. P., Hurt E. C., Pante N. & Aebi U. (2000). Comparative spatial localization of protein-A-tagged and authentic yeast nuclear pore complex proteins by immunogold electron microscopy. *J Struct Biol* **129**, 2-3, p. 295-305.

Fahrenkrog B., Koser J. & Aebi U. (2004). The nuclear pore complex: a jack of all trades? *Trends Biochem Sci* **29**, 4, p. 175-82.

Ferrando-May E. (2005). Nucleocytoplasmic transport in apoptosis. *Cell Death Differ*.

Fischer U., Huber J., Boelens W. C., Mattaj I. W. & Lührmann R. (1995). The HIV-1 Rev activation domain is a nuclear export signal that accesses an export pathway used by specific cellular RNAs. *Cell* **82**, 3, p. 475-83.

Fornerod M. (1997). Chromosomal localization of genes encoding CAN/Nup214-interacting proteins-human CRM1 localizes to 2p16, whereas Nup88 localizes to 17p13 and is physically linked to SF2p32. *Genomics* **42**, p. 538-40.

Fornerod M. & Ohno M. (2002). Exportin-mediated nuclear export of proteins and ribonucleoproteins. *Results Probl Cell Differ* **35**, p. 67-91.

Forwood J. K., Lam M. H. & Jans D. A. (2001). Nuclear import of creb and ap-1 transcription factors requires importin-beta1 and ran but is independent of importin-alpha. *Biochemistry* **40**, 17, p. 5208-17.

Fukuda M., Asano S., Nakamura T., Adachi M., Yoshida M., Yanagida M. & Nishida E. (1997). CRM1 is responsible for intracellular transport mediated by the nuclear export signal. *Nature* **390**, 6657, p. 308-11.

Gadde S. & Heald R. (2004). Mechanisms and molecules of the mitotic spindle. *Curr Biol* **14**, 18, p. R797-805.

Galliot B., de Vargas C. & Miller D. (1999). Evolution of homeobox genes: Q50 Paired-like genes founded the Paired class. *Dev Genes Evol* **209**, 3, p. 186-97.

Gerl R. & Vaux D. L. (2005). Apoptosis in the development and treatment of cancer. *Carcinogenesis* **26**, 2, p. 263-70.

Giuliano K. A., Chen Y. & Haskins J. R. (2003a). Fluorescent prorein biosensors - A new screening tool moves drug targets out of the test tube and into the cell. *Mod Drug Discovery* **6**, 8, p. 33-37.

Giuliano K. A., Haskins J. R. & Taylor D. L. (2003b). Advances in high content screening for drug discovery. *Assay Drug Dev Technol* **1**, 4, p. 565-77.

Goldberg M. (2004). Import and export at the nuclear envelope. *Symp Soc Exp Biol*, 56, p. 115-33.

Görlich D., Kostka S., Kraft R., Dingwall C., Laskey R. A., Hartmann E. & Prehn S. (1995). Two different subunits of importin cooperate to recognize nuclear localization signals and bind them to the nuclear envelope. *Curr Biol* **5**, 4, p. 383-92.

Görlich D. & Kutay U. (1999). Transport between the cell nucleus and the cytoplasm. *Annu. Rev. Cell Dev. Biol.* **15**, p. 607-60.

Görlich D. & Mattaj I. W. (1996). Nucleocytoplasmic transport. *Science* **271**, 5255, p. 1513-8.

Grinberg A. V., Hu C. D. & Kerppola T. K. (2004). Visualization of Myc/Max/Mad family dimers and the competition for dimerization in living cells. *Mol Cell Biol* **24**, 10, p. 4294-308.

Gu J., Nie L., Wiederschain D. & Yuan Z. M. (2001). Identification of p53 sequence elements that are required for MDM2-mediated nuclear export. *Mol Cell Biol* **21**, 24, p. 8533-46.

Hanahan D. & Weinberg R. A. (2000). The hallmarks of cancer. *Cell* **100**, 1, p. 57-70.

Harel A. & Forbes D. J. (2004). Importin beta: conducting a much larger cellular symphony. *Mol Cell* **16**, 3, p. 319-30.

Harley V. R., Layfield S., Mitchell C. L., Forwood J. K., John A. P., Briggs L. J., McDowall S. G. & Jans D. A. (2003). Defective importin beta recognition and nuclear import of the sex-determining factor SRY are associated with XY sex-reversing mutations. *Proc Natl Acad Sci U S A* **100**, 12, p. 7045-50.

Harper J. V. & Brooks G. (2005). The mammalian cell cycle: an overview. *Methods Mol Biol* **296**, p. 113-53.

Heger P., Lohmaier J., Schneider G., Schweimer K. & Stauber R. H. (2001). Qualitative highly divergent nuclear export signals can regulate export by the competition for transport cofactors in vivo. *Traffic* **2**, 8, p. 544-55.

Heger P., Rosorius O., Hauber J. & Stauber R. H. (1999). Titration of cellular export factors, but not heteromultimerization, is the molecular mechanism of *trans*-dominant HTLV-1 Rex mutants. *Oncogene* **18**, p. 4080-90.

Hemmila I. A. & Hurskainen P. (2002). Novel detection strategies for drug discovery. *Drug Discov Today* **7**, 18 Suppl, p. S150-6.

Hermeking H. (2003). The MYC oncogene as a cancer drug target. *Curr Cancer Drug Targets* **3**, 3, p. 163-75.

Hu C. D. & Kerppola T. K. (2003). Simultaneous visualization of multiple protein interactions in living cells using multicolor fluorescence complementation analysis. *Nat Biotechnol* **21**, 5, p. 539-45.

Hurlin P. J. & Dezfouli S. (2004). Functions of myc:max in the control of cell proliferation and tumorigenesis. *Int Rev Cytol* **238**, p. 183-226.

Igney F. H. & Krammer P. H. (2002). Death and anti-death: tumour resistance to apoptosis. *Nat Rev Cancer* **2**, 4, p. 277-88.

Izaurralde E. (2004). Directing mRNA export. *Nat Struct Mol Biol* **11**, 3, p. 210-2.

Izaurralde E., Kutay U., von Kobbe C., Mattaj I. W. & Görlich D. (1997). The asymmetric distribution of the constituents of the Ran system is essential for transport into and out of the nucleus. *Embo J* **16**, 21, p. 6535-47.

Jesenberger V. & Jentsch S. (2002). Deadly encounter: ubiquitin meets apoptosis. *Nat Rev Mol Cell Biol* **3**, 2, p. 112-21.

Kalderon D., Roberts B. L., Richardson W. D. & Smith A. E. (1984). A short amino acid sequence able to specify nuclear location. *Cell* **39**, p. 499-509.

Kau T. R., Schroeder F., Ramaswamy S., Wojciechowski C. L., Zhao J. J., Roberts T. M., Clardy J., Sellers W. R. & Silver P. A. (2003). A chemical genetic screen identifies inhibitors of regulated nuclear export of a Forkhead transcription factor in PTEN-deficient tumor cells. *Cancer Cell* **4**, 6, p. 463-76.

Kau T. R., Way J. C. & Silver P. A. (2004). Nuclear transport and cancer: from mechanism to intervention. *Nat Rev Cancer* **4**, 2, p. 106-17.

Kiernan R., Bres V., Ng R. W., Coudart M. P., El Messaoudi S., Sardet C., Jin D. Y., Emiliani S. & Benkirane M. (2003). Post-activation turn-off of NF-kappa B-dependent transcription is regulated by acetylation of p65. *J Biol Chem* **278**, 4, p. 2758-66.

Kim V. N. (2004). MicroRNA precursors in motion: exportin-5 mediates their nuclear export. *Trends Cell Biol* **14**, 4, p. 156-9.

Knauer S. K., Carra G. & Stauber R. H. (2005a). Nuclear export is evolutionarily conserved in CVC paired-like homeobox proteins and influences protein stability, transcriptional activation, and extracellular secretion. *Mol Cell Biol* **25**, 7, p. 2573-82.

Knauer S. K., Krämer O. H., Knösel T., Engels K., Rödel F., Walendzik H., Kovács A. F., Habtemichael N., Brieger J., Mann W., Heinzel T., Petersen I. & Stauber R. H. (2005b). Nuclear export is essential for the biological activity of survivin - Novel aspects to target the survivin pathway in cancer. *Cancer Res*, submitted.

Knauer S. K., Moodt S., Berg T., Liebel U., Pepperkok R. & Stauber R. H. (2005c). Translocation Biosensors To Study Signal Specific Nucleo-Cytoplasmic Transport, Protease Activity & Protein Interactions. *Traffic* **6**, p. 1-13.

Knauer S. K. & Stauber R. H. (2005). Development of an Autofluorescent Translocation Biosensor System To Investigate Protein-Protein Interactions in Living Cells. *Anal Chem*, published online.

Komiyama K., Okada K., Tomisaka S., Umezawa I., Hamamoto T. & Beppu T. (1985). Antitumor activity of leptomycin B. *J Antibiot (Tokyo)* **38**, 3, p. 427-9.

Kouzarides T. (1999). Histone acetylases and deacetylases in cell proliferation. *Curr Opin Genet Dev* **9**, 1, p. 40-8.

Krämer O. H., Baus D., Knauer S. K., Stein S., Jäger E., Stauber R. H., Grez M., Pfitzner E. & Heinzel T. (2005). Acetylation of Stat1 modulates NF-kB signaling *Genes Dev*, submitted.

Krammer P. H. (2000). CD95's deadly mission in the immune system. *Nature* **407**, 6805, p. 789-95.

Krätzer F., Rosorius O., Heger P., Hirschmann N., Dobner T., Hauber J. & Stauber R. H. (2000). The adenovirus type 5 E1B-55K oncoprotein is a highly active shuttle protein and shuttling is independent of E4orf6, p53 and Mdm2. *Oncogene* **19**, p. 850-57.

Kudo N., Matsumori N., Taoka H., Fujiwara D., Schreiner E. P., Wolff B., Yoshida M. & Horinouchi S. (1999). Leptomycin B inactivates CRM1/exportin 1 by covalent modification at a cysteine residue in the central conserved region. *Proc Natl Acad Sci U S A* **96**, 16, p. 9112-7.

Kuersten S., Ohno M. & Mattaj I. W. (2001). Nucleocytoplasmic transport: Ran, beta and beyond. *Trends Cell Biol* **11**, 12, p. 497-503.

Künzler M., Gerstberger T., Stutz F., Bischoff F. R. & Hurt E. (2000). Yeast Ran-binding protein 1 (Yrb1) shuttles between the nucleus and cytoplasm and is exported from the nucleus via a CRM1 (XPO1)-dependent pathway. *Mol Cell Biol* **20**, 12, p. 4295-308.

Kutay U. & Guttinger S. (2005). Leucine-rich nuclear-export signals: born to be weak. *Trends Cell Biol* **15**, 3, p. 121-4.

La Cour T., Kiemer L., Molgaard A., Gupta R., Skriver K. & Brunak S. (2004). Analysis and prediction of leucine-rich nuclear export signals. *Protein Eng Des Sel* **17**, 6, p. 527-36.

Laxman B., Hall D. E., Bhojani M. S., Hamstra D. A., Chenevert T. L., Ross B. D. & Rehemtulla A. (2002). Noninvasive real-time imaging of apoptosis. *Proc Natl Acad Sci U S A* **99**, 26, p. 16551-5.

Lens S. M., Wolthuis R. M., Klompmaker R., Kauw J., Agami R., Brummelkamp T., Kops G. & Medema R. H. (2003). Survivin is required for a sustained spindle checkpoint arrest in response to lack of tension. *Embo J* **22**, 12, p. 2934-47.

Levy D. E. & Darnell J. E., Jr. (2002). Stats: transcriptional control and biological impact. *Nat Rev Mol Cell Biol* **3**, 9, p. 651-62.

Li F. (2003). Survivin study: what is the next wave? *J Cell Physiol* **197**, 1, p. 8-29.

Li F., Ackermann E. J., Bennett C. F., Rothermel A. L., Plescia J., Tognin S., Villa A., Marchisio P. C. & Altieri D. C. (1999). Pleiotropic cell-division defects and apoptosis induced by interference with survivin function. *Nat Cell Biol* **1**, 8, p. 461-6.

Li F., Ambrosini G., Chu E. Y., Plescia J., Tognin S., Marchisio P. C. & Altieri D. C. (1998). Control of apoptosis and mitotic spindle checkpoint by survivin. *Nature* **396**, 6711, p. 580-4.

Liebel U., Starkuviene V., Erfle H., Simpson J. C., Poustka A., Wiemann S. & Pepperkok R. (2003). A microscope-based screening platform for large-scale functional protein analysis in intact cells. *FEBS Lett* **554**, 3, p. 394-8.

Lindsay M. E., Holaska J. M., Welch K., Paschal B. M. & Macara I. G. (2001). Ran-binding protein 3 is a cofactor for Crm1-mediated nuclear protein export. *J Cell Biol* **153**, 7, p. 1391-402.

Lindsten K., Uhlikova T., Konvalinka J., Masucci M. G. & Dantuma N. P. (2001). Cell-based fluorescence assay for human immunodeficiency virus type 1 protease activity. *Antimicrob Agents Chemother* **45**, 9, p. 2616-22.

Los M., Burek C. J., Stroh C., Benedyk K., Hug H. & Mackiewicz A. (2003). Anticancer drugs of tomorrow: apoptotic pathways as targets for drug design. *Drug Discov Today* **8**, 2, p. 67-77.

Maizel A., Tassetto M., Filhol O., Cochet C., Prochiantz A. & Joliot A. (2002). Engrailed homeoprotein secretion is a regulated process. *Development* **129**, 15, p. 3545-53.

McBride K. M. & Reich N. C. (2003). The ins and outs of STAT1 nuclear transport. *Sci STKE* **2003**, 195, p. RE13.

McManus M. T. (2003). MicroRNAs and cancer. *Semin Cancer Biol* **13**, 4, p. 253-8.

Meier P., Finch A. & Evan G. (2000). Apoptosis in development. *Nature* **407**, 6805, p. 796-801.

Mendelsohn A. R. & Brent R. (1999). Protein interaction methods - toward an endgame. *Science* **284**, 5422, p. 1948-50.

Miele L. (2004). The biology of cyclins and cyclin-dependent protein kinases: an introduction. *Methods Mol Biol* **285**, p. 3-21.

Mingot J. M., Kostka S., Kraft R., Hartmann E. & Gorlich D. (2001). Importin 13: a novel mediator of nuclear import and export. *Embo J* **20**, 14, p. 3685-94.

Nachury M. V., Ryder U. W., Lamond A. I. & Weis K. (1998). Cloning and characterization of hSRP1 gamma, a tissue-specific nuclear transport factor. *Proc Natl Acad Sci U S A* **95**, 2, p. 582-7.

Nachury M. V. & Weis K. (1999). The direction of transport through the nuclear pore can be inverted. *Proc Natl Acad Sci U S A* **96**, 17, p. 9622-7.

O'Brate A. & Giannakakou P. (2003). The importance of p53 location: nuclear or cytoplasmic zip code? *Drug Resist Updat* **6**, 6, p. 313-22.

Ohtoshi A., Wang S. W., Maeda H., Saszik S. M., Frishman L. J., Klein W. H. & Behringer R. R. (2004). Regulation of retinal cone bipolar cell differentiation and photopic vision by the CVC homeobox gene Vsx1. *Curr Biol* **14**, 6, p. 530-6.

Ozawa T., Kaihara A., Sato M., Tachihara K. & Umezawa Y. (2001). Split luciferase as an optical probe for detecting protein-protein interactions in mammalian cells based on protein splicing. *Anal Chem* **73**, 11, p. 2516-21.

Pagliaro L., Felding J., Audouze K., Nielsen S. J., Terry R. B., Krog-Jensen C. & Butcher S. (2004). Emerging classes of protein-protein interaction inhibitors and new tools for their development. *Curr Opin Chem Biol* **8**, 4, p. 442-9.

Palacios I., Hetzer M., Adam S. A. & Mattaj I. W. (1997). Nuclear import of U snRNPs requires importin beta. *Embo J* **16**, 22, p. 6783-92.

Palmeri D. & Malim M. H. (1999). Importin beta can mediate the nuclear import of an arginine-rich nuclear localization signal in the absence of importin alpha. *Mol Cell Biol* **19**, 2, p. 1218-25.

Pante N. (2004). Nuclear pore complex structure: unplugged and dynamic pores. *Dev Cell* **7**, 6, p. 780-1.

Pante N. & Kann M. (2002). Nuclear pore complex is able to transport macromolecules with diameters of about 39 nm. *Mol Biol Cell* **13**, 2, p. 425-34.

Paraskeva E., Izaurralde E., Bischoff F. R., Huber J., Kutay U., Hartmann E., Luhrmann R. & Görlich D. (1999). CRM1-mediated recycling of snurportin 1 to the cytoplasm. *J Cell Biol* **145**, 2, p. 255-64.

Patel D., Frelinger J., Goudsmit J. & Kim B. (2001). In vitro assay for site-specific proteases using bead-attached GFP substrate. *Biotechniques* **31**, 5, p. 1194-98.

Paulmurugan R., Umezawa Y. & Gambhir S. S. (2002). Noninvasive imaging of protein-protein interactions in living subjects by using reporter protein complementation and reconstitution strategies. *Proc Natl Acad Sci U S A* **99**, 24, p. 15608-13.

Pavlakis G. N. & Stauber R. H. (1998). Regulatory Proteins of HIV-1. In: *N. Saksenas*, N. Saksenas. Human Immunodeficiency Viruses: Biology, Immunology and Molecular Biology. Genova: Medical Systems SpA; p. 103-22.

Pemberton L. F. & Paschal B. M. (2005). Mechanisms of receptor-mediated nuclear import and nuclear export. *Traffic* **6**, 3, p. 187-98.

Perkins N. D. (2004). NF-kappaB: tumor promoter or suppressor? *Trends Cell Biol* **14**, 2, p. 64-9.

Phippard D. & Manning A. M. (2003). Screening for inhibitors of transcription factors using luciferase reporter gene expression in transfected cells. *Methods Mol Biol* **225**, p. 19-23.

Pollard V. W., Michael W. M., Nakielny S., Siomi M. C., Wang F. & Dreyfuss G. (1996). A novel receptor-mediated nuclear protein import pathway. *Cell* **86**, 6, p. 985-94.

Poon I. K. & Jans D. A. (2005). Regulation of nuclear transport: central role in development and transformation? *Traffic* **6**, 3, p. 173-86.

Porter L. A. & Donoghue D. J. (2003). Cyclin B1 and CDK1: nuclear localization and upstream regulators. *Prog Cell Cycle Res* **5**, p. 335-47.

Reichelt R., Holzenburg A., Buhle E. L., Jr., Jarnik M., Engel A. & Aebi U. (1990). Correlation between structure and mass distribution of the nuclear pore complex and of distinct pore complex components. *J Cell Biol* **110**, 4, p. 883-94.

Ribbeck K. & Görlich D. (2001). Kinetic analysis of translocation through nuclear pore complexes. *Embo J* **20**, 6, p. 1320-30.

Ribbeck K. & Görlich D. (2002). The permeability barrier of nuclear pore complexes appears to operate via hydrophobic exclusion. *Embo J* **21**, 11, p. 2664-71.

Robbins J., Dilworth S. M., Laskey R. A. & Dingwall C. (1991). Two interdependent basic domains in nucleoplasmin nuclear targeting sequence: identification of a class of bipartite nuclear targeting sequence. *Cell* **64**, 3, p. 615-23.

Rosorius O., Fries B., Stauber R. H., Hirschmann N., Bevec D. & Hauber J. (2000). Human ribosomal protein L5 contains defined nuclear localization and export signals. *J Biol Chem* **275**, 16, p. 12061-8.

Rosorius O., Heger P., Stelz G., Hirschmann N., Hauber J. & Stauber R. H. (1999). Direct observation of nucleo-cytoplasmic transport by microinjection of GFP-tagged proteins in living cells. *BioTechniques* **27**, p. 350-55.

Rout M. P. & Aitchison J. D. (2001). The nuclear pore complex as a transport machine. *J Biol Chem* **276**, 20, p. 16593-6.

Rout M. P., Aitchison J. D., Suprapto A., Hjertaas K., Zhao Y. & Chait B. T. (2000). The yeast nuclear pore complex: composition, architecture, and transport mechanism. *J Cell Biol* **148**, 4, p. 635-51.

Salvesen G. S. & Duckett C. S. (2002). IAP proteins: blocking the road to death's door. *Nat Rev Mol Cell Biol* **3**, 6, p. 401-10.

Schwoebel E. D., Talcott B., Cushman I. & Moore M. S. (1998). Ran-dependent signal-mediated nuclear import does not require GTP hydrolysis by Ran. *J Biol Chem* **273**, 52, p. 35170-5.

Sherr C. J. (2004). Principles of tumor suppression. *Cell* **116**, 2, p. 235-46.

Sherr C. J. & Roberts J. M. (2004). Living with or without cyclins and cyclin-dependent kinases. *Genes Dev* **18**, 22, p. 2699-711.

Siomi H. & Dreyfuss G. (1995). A nuclear localization domain in the hnRNP A1 protein. *J Cell Biol* **129**, 3, p. 551-60.

Stauber R. H., Afonina E., Gulnik S., Erickson J. & Pavlakis G. N. (1998). Analysis of intracellular trafficking and interactions of cytoplasmic HIV-1 Rev mutants in living cells. *Virology* **251**, p. 38-48.

Stoffler D., Fahrenkrog B. & Aebi U. (1999). The nuclear pore complex: from molecular architecture to functional dynamics. *Curr Opin Cell Biol* **11**, 3, p. 391-401.

Strom A. C. & Weis K. (2001). Importin-beta-like nuclear transport receptors. *Genome Biol* **2**, 6, p. REVIEWS3008.

Sun C., Nettesheim D., Liu Z. & Olejniczak E. T. (2005). Solution structure of human survivin and its binding interface with smac/diablo. *Biochemistry* **44**, 1, p. 11-7.

Suntharalingam M. & Wente S. R. (2003). Peering through the pore: nuclear pore complex structure, assembly, and function. *Dev Cell* **4**, 6, p. 775-89.

Tam W. F., Lee L. H., Davis L. & Sen R. (2000). Cytoplasmic sequestration of rel proteins by IkappaBalpha requires CRM1-dependent nuclear export. *Mol Cell Biol* **20**, 6, p. 2269-84.

van Dam H. & Castellazzi M. (2001). Distinct roles of Jun : Fos and Jun : ATF dimers in oncogenesis. *Oncogene* **20**, 19, p. 2453-64.

Vassilev L. T., Vu B. T., Graves B., Carvajal D., Podlaski F., Filipovic Z., Kong N., Kammlott U., Lukacs C., Klein C., Fotouhi N. & Liu E. A. (2004). In vivo activation of the p53 pathway by small-molecule antagonists of MDM2. *Science* **303**, 5659, p. 844-8.

Vasu S. K. & Forbes D. J. (2001). Nuclear pores and nuclear assembly. *Curr Opin Cell Biol* **13**, p. 363-75.

Vigneri P. & Wang J. Y. (2001). Induction of apoptosis in chronic myelogenous leukemia cells through nuclear entrapment of BCR-ABL tyrosine kinase. *Nat Med* **7**, 2, p. 228-34.

Vogelstein B. & Kinzler K. W. (2004). Cancer genes and the pathways they control. *Nat Med* **10**, 8, p. 789-99.

Vogelstein B., Lane D. & Levine A. J. (2000). Surfing the p53 network. *Nature* **408**, 6810, p. 307-10.

Vogt P. K. (2002). Fortuitous convergences: the beginnings of JUN. *Nat Rev Cancer* **2**, 6, p. 465-9.

Vousden K. H. & Prives C. (2005). P53 and prognosis: new insights and further complexity. *Cell* **120**, 1, p. 7-10.

Wehrman T., Kleaveland B., Her J. H., Balint R. F. & Blau H. M. (2002). Protein-protein interactions monitored in mammalian cells via complementation of beta -lactamase enzyme fragments. *Proc Natl Acad Sci U S A* **99**, 6, p. 3469-74.

Weis K. (2003). Regulating access to the genome: nucleocytoplasmic transport throughout the cell cycle. *Cell* **112**, 4, p. 441-51.

Wolff B., Sanglier J. J. & Wang Y. (1997). Leptomycin B is an inhibitor of nuclear export: inhibition of nucleo-cytoplasmic translocation of the human immunodeficiency virus type 1 (HIV-1) Rev protein and Rev-dependent mRNA. *Chem Biol* **4**, 2, p. 139-47.

Xu L. & Massague J. (2004). Nucleocytoplasmic shuttling of signal transducers. *Nat Rev Mol Cell Biol* **5**, 3, p. 209-19.

Yu H., West M., Keon B. H., Bilter G. K., Owens S., Lamerdin J. & Westwick J. K. (2003). Measuring drug action in the cellular context using protein-fragment complementation assays. *Assay Drug Dev Technol* **1**, 6, p. 811-22.

Yuan Z. L., Guan Y. J., Chatterjee D. & Chin Y. E. (2005). Stat3 dimerization regulated by reversible acetylation of a single lysine residue. *Science* **307**, 5707, p. 269-73.

Zhao Y. & Westphal H. (2002). Homeobox genes and human genetic disorders. *Curr Mol Med* **2**, 1, p. 13-23.

Zhong H., May M. J., Jimi E. & Ghosh S. (2002). The phosphorylation status of nuclear NF-kappa B determines its association with CBP/p300 or HDAC-1. *Mol Cell* **9**, 3, p. 625-36.

8 Appendix

8.1 List of figures and tables

8.2 Abbreviations and units

Abbreviations

40S	small ribosomal subunit
60S	large ribosomal subunit
aa	amino acids
Abl	Abelson murine leukemia
AIF	apoptosis inducing factor
Apaf	apoptotic protease activating factor
APRIL	A proliferation-inducing ligand
ATP	adenosine triphosphate
Bcl	B-cell lymphoma
Bcr	breakpoint cluster region
BFP	blue fluorescent protein
bHLH	basic helix-loop-helix
bHLH-ZIP	basic helix-loop-helix-leucine-zipper
BiFc	bimolecular fluorescence complementation
bZIP	basic leucine zipper
bzw.	beziehungsweise
Ca	calcium
CAS	cellular apoptosis susceptibility
caspase	cysteine aspartate-specific protease
CBA	cell-based assay
CBC	cap-binding complex
CBP	cap-binding protein
CBP/p300	CREB-binding protein and its homologue p300
CDK	cyclin dependent kinase
CDKI	CDK inhibitor
Chx10	Ceh-10 homologous homeobox
CRM	chromosome region maintenance
CTEM	conventional transmission electron microscopy
DNA	deoxyribonucleic acid
e.g.	for example
EM	electron microscopy
FADD	Fas-associated via death domain
FG repeats	phenylalanine-glycine repeats
FRET	fluorescence resonance energy transfer
G	gap phase
GAP	GTPase activating protein
GAS	IFN-gamma activated sequence
GDP	guanosine diphosphate
GEF	guanine nucleotide exchange factor

GFP	green fluorescent protein
GR	glucocorticoid receptor
GST	glutathione-S-transferase
GTP	guanosine triphosphate
GTPase	guanosine-5'-triphosphatase
HAT	histone acetyl transferase
HC	high-content
HCS	high-content screening
HD	homeodomain
HDAC	histone deacetylase
HDACi	HDAC inhibitor
HDP	homeodomain protein
HIV	human immunodeficiency virus
HMWC	high molecular weight complexes
hnRNP	heterogenous nuclear ribonucleoprotein particle
HOX	homeobox protein
Hsp	heat shock protein
HTLV	human T-cell leukemia virus
IAP	inhibitors of apoptosis
IBB domain	importin-β binding domain
ID	interaction domain
i.e.	*lat.*, id est
I-κB	inhibitor of NF-κB
Imp	importin
Jak	Janus kinase
LMB	leptomycin B
M	M-phase, mitosis
m7G	7-methylguanosine
MAPKK	Map kinase
Mdm2	Double minute 2 protein
MMP	matrix metalloproteinase
mRNA	messenger RNA
mRNP	mRNA containing ribonucleoprotein
NES	nuclear export signal (Kernexportsignal)
NF-κB	nuclear factor κB
NLS	nuclear localization signal (Kernimportsignal)
NPC	nuclear pore complex (Kernporenkomplex)
NTF	nuclear transport factor
NUP	nucleoporin
NXT	NTF2-related export protein
ORF	open reading frame
p55	55kDa NF-κB subunit
p65	65kDa NF-κB subunit

PARC	p53-associated Parkin-like cytoplasmic protein
PARP	poly-(ADP-Ribose) polymerase
PHAX	phosphorylated adapter for RNA export
PI3K	phosphoinositide-3 kinase
PKI	protein kinase inhibitor
PLC-HDP	paired-like CVC homeodomain protein
PPI	protein-protein interaction
pre	precursor
PSA	prostate specific antigen
PTB	protein translocation biosensor
PTD	protein transduction domain
PTEN	phosphatase and tensin homologue
Ran	Ras-related nuclear protein
RanBP	Ran binding protein
RCC	Regulator of chromosome condensation
Rev	regulator of expression of virion proteins
RNA	ribonucleic acid
RNP	ribonucleoprotein
RRE	Rev response element
rRNA	ribosomal RNA
S	S-phase, synthesis phase
SAF	spindle assembly factor
SH2	src homology 2
snRNA	small nuclear RNA
snRNP	small nuclear RNP
SV40	Simian Virus 40
SRY	sex determing factor
STAT	signal transducer and activator of transcription
TAD	transactivation domain
T-Ag	T-antigen
TAP	tip associating protein
TFIIIA	transcription factor IIIA
TRADD	TNF receptor-associated via death domain
tRNA	transfer RNA
UsnRNA	uridine-rich small nuclear RNA
UsnRNP	uridine-rich small nuclear RNP
Vsx	visual system homeobox
XPO-t	exportin-t
YTH	yeast two-hybrid
z.B.	zum Beispiel

Units and measures

Da	Dalton	M	Mega (10^6)
m	meter	k	kilo (10^3)
		n	nano (10^{-9})

Amino acids

A	Ala	alanine	**M**	Met	methionine
C	Cys	cysteine	**N**	Asn	asparagine
D	Asp	aspartic acid	**P**	Pro	proline
E	Glu	glutamic acid	**Q**	Gln	glutamine
F	Phe	phenylalanine	**R**	Arg	arginine
G	Gly	glycine	**S**	Ser	serine
H	His	histidine	**T**	Thr	threonine
I	Ile	isoleucine	**V**	Val	valine
K	Lys	lysine	**W**	Trp	tryptophan
L	Leu	leucine	**Y**	Tyr	tyrosine

9 Publications

1. **Knauer, S.K.**, Carra, G. and Stauber, R.H. (2005) Nuclear export is evolutionary conserved in CVC paired-like homeobox proteins and influences protein stability, transcriptional activation and extracellular secretion. ***Mol Cell Biol**, 25*: 2573–2582.

2. Krämer, O., Baus, D., **Knauer, S.K.**, Stein, S., Jäger, D., Stauber, R.H., Grez, M., Pfitzner, E. and Heinzel, T. (2005) Acetylation of STAT1 modulates NF-κB signaling. ***Genes Dev***, *submitted.*

3. **Knauer, S.K.**, Krämer, O., Knösel, T., Engels, K., Rödel, F., Walendzik, H., Kovács, A.F., Habtemichael, N., Brieger, J., Mann, W., Heinzel, T., Petersen, I. and Stauber, R.H. (2005) Nuclear export is essential for the biological activity of survivin - Novel aspects to target the survivin pathway in cancer. ***Cancer Res**, submitted*.

4. **Knauer, S.K.**, Moodt, S., Berg, T., Liebel, U., Pepperkok, R. and Stauber, R.H. (2005) Translocation biosensors to study signal specific nucleo-cytoplasmic transport, protease activity & protein interactions. ***Traffic**, 6*: 594-606.

5. **Knauer, S.K.** and Stauber R.H. (2005) Application of Autofluorescent Translocation Biosensors to Investigate Protein-Protein Interactions in Living Cells. ***Anal Chem**, DOI 10.1021/ac050413o*.

1

MOLECULAR AND CELLULAR BIOLOGY, Apr. 2005, p. 2573–2582 Vol. 25, No. 7
0270-7306/05/$08.00+0 doi:10.1128/MCB.25.7.2573–2582.2005

Nuclear Export Is Evolutionarily Conserved in CVC Paired-Like Homeobox Proteins and Influences Protein Stability, Transcriptional Activation, and Extracellular Secretion

Shirley K. Knauer, Gert Carra, and Roland H. Stauber*

Georg-Speyer-Haus, Institute for Biomedical Research, Frankfurt, Germany

Received 27 October 2004/Returned for modification 9 December 2004/Accepted 15 December 2004

Homeodomain transcription factors control a variety of essential cell fate decisions during development. To understand the developmental regulation by these transcription factors, we describe here the molecular analysis of paired-like CVC homeodomain protein (PLC-HDP) trafficking. Complementary experimental approaches demonstrated that PLC-HDP family members are exported by the Crm1 pathway and contain an evolutionary conserved leucine-rich nuclear export signal. Importantly, inactivation of the nuclear export signal enhanced protein stability, resulting in increased transactivation of transfected reporters and decreased extracellular secretion. In addition, PLC-HDPs harbor a conserved active nuclear import signal that could also function as a protein transduction domain. In our study, we characterized PLC-HDPs as mobile nucleocytoplasmic shuttle proteins with the potential for unconventional secretion and intercellular transfer. Nucleocytoplasmic transport may thus represent a conserved control mechanism to fine-tune the transcriptional activity of PLC-HDPs prerequisite for regulating and maintaining the complex expression pattern during development.

Ordered development depends on the activity of transcription factors in a controlled manner. One defining feature of eukaryotic cells is their spatial and functional division into the nucleus and the cytoplasm by the nuclear envelope. Thus, among other mechanisms, regulated subcellular localization provides an attractive way to control the activity of transcription factors which has been demonstrated for several key players of signal transduction cascades (reference 6 and references therein). This type of regulation requires a specific and selective transport machinery for the controlled transport of macromolecules between both compartments. Nucleocytoplasmic transport takes place through the nuclear pore (29) and is regulated by specific signals and transport receptors. In general, active nuclear import requires energy and is mediated by short stretches of basic amino acids, termed nuclear localization signals (NLS), which interact with specific import receptors (reviewed in references 3 and 13). In contrast, signal-mediated nuclear export pathways (31) are less understood. The best-characterized nuclear export signals (NES) consist of a short leucine-rich stretch of amino acids, interact with the export receptor Crm1 (references 3 and 13 and references therein), and depend on the RanGTP/GDP axis. Leucine-rich NES have been identified in an increasing number of cellular and viral proteins executing heterogeneous biological functions. These include transcription control (6, 35), cell cycle control (43), and RNA transport (8). Proteins containing both NLS and NES have the capacity for continuous shuttling between the cytoplasm and the nucleus.

Homeodomain proteins (HDPs) have been shown to exert key developmental functions throughout the metazoa since defects in the evolutionary conserved homeobox genes were shown to cause many human disorders and aberrant animal phenotypes (reference 57 and references therein). Homeobox-containing genes encode transcription factors and are characterized by the homeodomain (HD), a motif that directs specific DNA binding to regulate the expression of target genes. Homeobox genes are grouped into several subclasses according to the primary structure of their homeodomain and its flanking sequences (reference 12 and references therein). Among the paired-like subclass, the paired-like CVC (PLC)-HDPs are characterized by a conserved CVC domain and can be grouped into the *Vsx-1* and *Vsx-2* family (32, 40), containing orthologs from several species. PLC-HDPs appear to play a particular role in ocular development (references 7, 21, 38, and 41 and references therein) and execute their functions by binding to the conserved locus control region (LCR), located upstream of the transcription initiation site of the red opsin gene, and thus specify the development and differentiation of cone photoreceptors and a subset of retinal inner nuclear layer bipolar cells (references 16 and 49 and references therein). The observation that null mutations in *Chx10* cause congenital microphthalmia, including small eyes, cataracts, iris coloboma, and blindness in humans (42), mice (5), and zebra fish (2), underscores the importance of the PLC-HDP gene family for retinogenesis. Thus, a precise control of PLC-HDP functions is clearly critical for ordered development and homeostasis.

In concordance with their role as transcriptional regulators, homeoproteins localize predominantly to the nucleus, although several reports characterize them also as nucleocytoplasmic shuttle proteins, e.g., Extradenticle (1), Otx1 (56), and Engrailed (34). Since regulated subcellular localization has been reported for several transcription factors (e.g., p53, STATs, NF-κB, etc.) (6), we investigated the intracellular traf-

* Corresponding author. Mailing address: Georg-Speyer-Haus, Institute for Biomedical Research, Paul-Ehrlich-Str. 42-44, D-60596 Frankfurt, Germany. Phone: (49) 69-63395-222. Fax: (49) 69-63395-145. E-mail: stauber@em.uni-frankfurt.de.

ficking of PLC-HDPs and analyzed its consequences for PLC-HDP function as transcriptional regulators. As representatives of the *Vsx-1* and *Vsx-2* group, we studied the zebra fish Vsx1 and the murine Chx10 protein in detail. Nucleocytoplasmic transport was investigated by interspecies heterokaryon assays, microinjection of recombinant transport substrates, and the use of chemical transport inhibitors. We could demonstrate that PLC-HDPs contain a Crm1-dependent NES, previously described as the "octapeptide." Nuclear export influenced PLC-HDP transcriptional activation by enhancing proteasomal protein degradation and by facilitating extracellular secretion. The predominant nuclear steady-state localization of PLC-HDPs is mediated by the presence of an active nuclear import signal. This NLS can function also as a protein transduction domain (PTD), explaining the evolutionary conservation of this signal. The integrity of both NES and NLS/PTD appears to be prerequisite for PLC-HDPs to function as mobile nucleocytoplasmic shuttle proteins with the potential for intercellular transfer.

MATERIALS AND METHODS

Plasmids. Plasmids pc3-DrVsx1-green fluorescent protein (GFP) and pc3-MmChx10-GFP encode a zebra fish Vsx1-GFP or a mouse Chx10-GFP fusion protein, respectively. The coding regions of the genes were amplified by PCR with pSTT91zVsx-1 (27) and pT7tagNChx10 (42) as templates and appropriate primers containing BamHI and NheI restriction sites. The PCR products were subsequently cloned into the vector pc3-GFP as described previously (25). Likewise, truncated forms of various GFP fusion proteins were constructed by the same cloning strategy. To generate NES-deficient GFP fusion proteins critical residues were changed into alanines by mutagenesis as described previously (25). The MmChx10-responsive luciferase reporter pLCR-R-luc was constructed by PCR amplification of the luciferase gene with pHH-luc as the template (23), and appropriate primers containing SpeI/NotI-restriction sites and subsequent cloning into pcDNA3 (Invitrogen). Subsequently, the LCR, together with the red pigment promoter (48), was inserted into this construct by PCR amplification and subsequent cloning by SpeI restriction digest, thereby replacing the cytomegalovirus promoter. Potential nuclear export or import signals were cloned into the bacterial expression vector pGEX-GFP as described previously (45). pGEX-MmChx10 encodes a glutathione *S*-transferase (GST)–mouse Chx10 fusion protein. Plasmid p3-Crm1-HA, pGEX-RanQ69L, and pSV40-Gal were already described (18, 23).

Cells, transfection, microscopy, and microinjection. Vero cells, the microglia cell line CRL-2540, 293 cells, NIH 3T3 cells, and HeLa cells were maintained under conditions recommended by the American Type Culture Collection and were prepared for microinjection or transfected as described previously (18). Microinjection, observation, and image analysis in living or fixed cells were performed as described previously (18). Cells were observed and analyzed by using the appropriate fluorescence filters as described previously (19), and 12-bit black and white images were captured by using a digital Axiocam CCD camera (Zeiss). Quantitation, image analysis, and presentation was performed by using IPLab Spectrum (Scanalytics) and Axiovision software (Zeiss). The total cellular GFP signal was measured by calculating the integrated pixel intensity in the imaged cell multiplied by the area of the cell. The nuclear signal was similarly obtained by measuring the pixel intensity in the nucleus. The cytoplasmic signal was calculated by subtracting the nuclear signal from the total cellular signal. All pixel values were measured below the saturation limits, and the background signal in an area with no cells was subtracted from all values. To determine the average intracellular localizations of the respective proteins, at least 200 fluorescent cells in three independent experiments were examined, and the standard deviations were determined.

Transactivation assays. For transactivation assays, HeLa cells were transfected with 0.5 μg of the pLCR-R-luc reporter plasmid and the indicated amounts of the MmChx10 expression constructs, together with 0.1 μg of pSV40-Gal, and the cells were assayed for luciferase and β-galactosidase (β-Gal) activity as described previously (23). To analyze intercellular transactivation, 5×10^5 293 cells were transfected with either 3 μg of the indicated MmChx10 expression construct or with 1 μg of pLCR-R-luc and 0.1 μg of pSV40-Gal. At 12 h later MmChx10 transfected and pLCR-R-luciferase transfected cells were mixed at a ratio of 2:1 and assayed for luciferase and β-Gal activity 36 h later. Luciferase activity was normalized to β-Gal expression, and all measurements were conducted in duplicates in three independent experiments.

Purification of recombinant GST fusion proteins. GST-GFP hybrid proteins were expressed and purified as described previously (45). Removal of GST by proteolytic cleavage using factor Xa protease (Roche) was performed according to the manufacturer's recommendations.

Immunoblotting, immunofluorescence, and antibodies. Immunoblotting and immunofluorescence were carried out according to standard procedures, as previously described (18). Purified mouse Chx10 fused to GST was used for immunization of rabbits by using standard protocols (10). The immunoglobulin G fraction was purified by protein A chromatography and used at a 1:500 dilution for immunofluorescence.

Protein transduction assay. Exponentially growing Vero cells were incubated with 1 μM concentrations of the corresponding recombinant GFP fusion proteins in phosphate-buffered saline (PBS) for 2 h. Subsequently, cells were extensively washed with PBS before incubation with trypsin (1 mg/ml) for 2 min to remove unspecifically bound protein from the cell surface. After removal of trypsin cells were cultured in medium for 3 h, washed with PBS, fixed with ice-cold methanol for 15 min and rehydrated in PBS prior to analysis by fluorescence microscopy.

Heterokaryon assay. HeLa cells were transfected with the indicated plasmids and 12 h later seeded with untransfected mouse NIH 3T3 cells at a ratio of 1:3. Cells were cultured and fused 8 h later by using polyethylene glycol (Gibco) in the presence of cycloheximide as described previously (50). To discriminate between human donor and mouse acceptor nuclei, staining with Hoechst 33258 was performed as described previously (50). A total of 50 heterokaryons were chosen at random, and the percentage of fusion events positive for internuclear transfer was calculated in three independent experiments, and the standard deviations were determined.

Treatment with chemical export inhibitors. Cells transfected with the indicated plasmids were treated with 10 nM leptomycin B (LMB; Sigma-Aldrich) or 5 nM Ratjadone A (Alexis Biochemicals) as described previously (25).

Crm1 pull-down assays and in vitro translation. Coupled transcription-translation was performed by using the TNT reticulocyte lysate system (Promega) supplemented with [^{35}S]methionine (Amersham) and the plasmid p3-Crm1-HA as a template. Crm1 pull-down assays with the specific recombinant GST-GFP substrates, Ran-GTP and nuclear extracts were performed as described previously (18). Care was taken to ensure equal input levels of labeled Crm1 protein into the binding reactions.

Secretion assay. A total of 2×10^6 293 cells were transfected with the indicated plasmids and incubated for 8 h. Subsequently, cells were cultured in methionine-free medium supplemented with [^{35}S] methionine (50 μCi) for additional 12 h. To block classical protein secretion, brefeldin A (BFA; Sigma-Aldrich) at 10 μg/ml was added to the cultures. Culture supernatants were collected and cleared by centrifugation (10,000 × *g*, 1 h, 4°C). Analysis of whole-cell lysates and immunoprecipitation of GFP fusion proteins from culture supernatants and cellular lysates by using a polyclonal anti-GFP antibody (BD Biosciences), as well as analysis of the complexes by sodium dodecyl sulfate-polyacrylamide gel electrophoresis (SDS-PAGE) and autoradiography, were performed as described previously (18, 28).

Pulse-chase experiments. A total of 5×10^5 HeLa cells were transfected with pc3DrVsx1-GFP or pc3DrVsx1_NESmut-GFP, followed by incubation for 16 h. Subsequently, cells were incubated for 2 h in Dulbecco's modified Eagle medium lacking methionine and pulse-labeled with 50 μCi of [^{35}S]methionine (Amersham) for 2 h. Unlabeled methionine was then added to a final concentration of 100 mM. At the indicated time points, cells were washed with cold PBS, and whole-cell lysates were prepared as described previously (28). To prevent proteasomal degradation, cells were treated with the proteasome inhibitors MG-132 and hemin (Sigma-Aldrich; 50 μM final concentration). The total radioactivity in each sample was determined by trichloroacetic acid precipitation, and sample volumes were adjusted to represent equal amounts of radioactivity. Immunoprecipitation was done by using a polyclonal anti-GFP antibody (Clontech), and the complexes were resolved by SDS-PAGE as described previously (18). Band intensities were quantified by using a phosphorimager (Bio-Rad).

RESULTS

PLC-HDPs are active shuttle proteins and nuclear export is mediated by the Crm1 pathway. To study PLC-HDPs localization and trafficking in live cells, we expressed the complete zebra fish (Dr) Vsx1 (amino acids [aa] 1 to 344) and murine

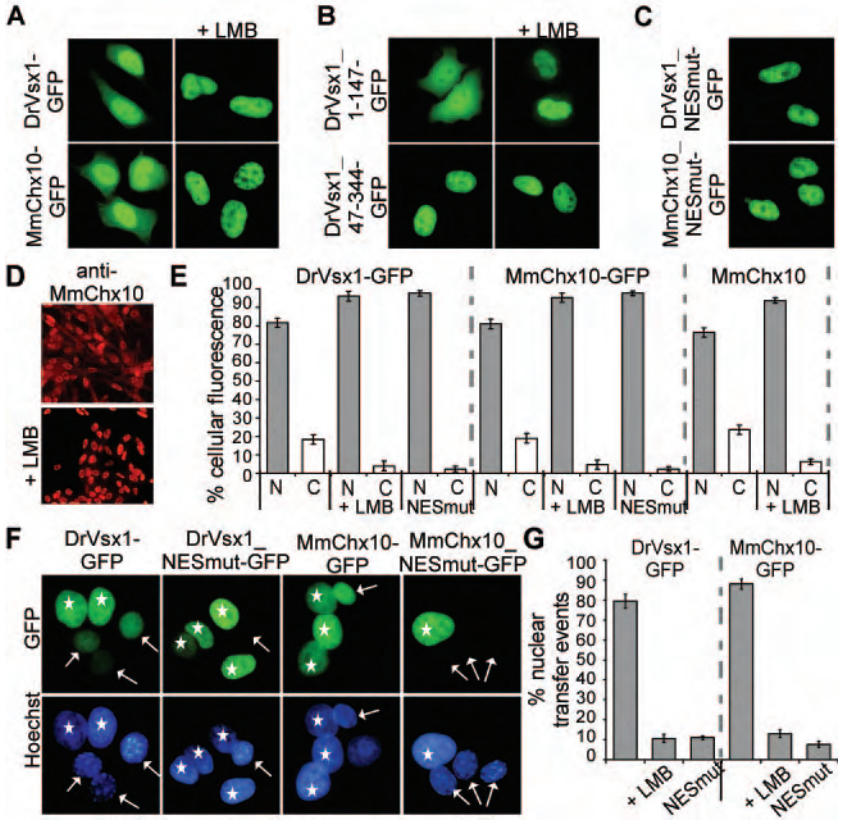

FIG. 1. PLC-HD proteins are nucleocytoplasmic shuttle proteins. (A) HeLa cells were transfected with the indicated plasmids and analyzed by fluorescence microscopy. In living cells, DrVsx1-GFP and MmChx10-GFP localized predominantly to the nucleus. Significant amounts of the proteins were also detectable in the cytoplasm and accumulated completely in the nucleus after LMB treatment. (B) DrVsx1_1-147-GFP still responded to LMB treatment, whereas the construct lacking the first 47 aa (DrVsx1_47-344-GFP) displayed an exclusively nuclear localization. (C) Inactivation of the NES by mutating critical residues into alanines (DrVsx1_NESmut-GFP, aa^{37}**F**AITDLL**GL**^{45} → ^{37}**A**AITDL**A**G**A**^{45}; MmChx10_NESmut-GFP, aa^{32}**F**GIQEI**L**G**L**^{40} → ^{32}**A**GIQEI**A**G**A**^{40}) resulted in complete nuclear localization. (D) Endogenous MmChx10 protein in the microglia cell line CRL-2540 displayed a similar intracellular localization and LMB responsiveness as observed for the MmChx10-GFP protein. MmChx10 was visualized by indirect immunofluorescence with a polyclonal anti-MmChx10 antiserum. (E) To determine the average intracellular localizations of the respective proteins, at least 200 fluorescent cells in three independent experiments were examined, and the standard deviations were determined. (F) DrVsx1- and MmChx10-GFP are capable of nucleocytoplasmic trafficking in a heterokaryon assay. Upon polyethylene glycol fusion of DrVsx1-GFP- and MmChx10-GFP-expressing HeLa donor cells with untransfected NIH 3T3 acceptor cells, DrVsx1-GFP and MmChx10-GFP were exported from the donor (marked by asterisks) and imported into the mouse acceptor nuclei (marked by arrows) 60 min after fusion. In contrast, NES-deficient mutants (DrVsx1_NESmut-GFP and MmChx10_NESmut-GFP) were not exported. (G) To quantify the number of transfer events, 50 heterokaryons were chosen at random, and the percentage of fusion events positive for internuclear transfer was calculated in three independent experiments with standard deviations. Scale bars: 10 μm (A, B, C, and F) and 100 μm (D).

(Mm) Chx10 (aa 1 to 380) as GFP fusion proteins. Fluorescence microscopy revealed that DrVsx1-GFP and MmChx10-GFP were predominantly nuclear. However, a significant amount of the respective protein was detectable also in the cytoplasm following transient expression in human (HeLa and 293) and rodent (NIH 3T3) cell lines (Fig. 1A and E and data not shown), indicating their potential for nucleocytoplasmic transport. Indirect immunofluorescence revealed a similar intracellular localization for the endogenous MmChx10 in the microglia cell line CRL-2540 (Fig. 1D) thereby excluding the possibility that the observed localization was due to the ectopic expression of GFP-tagged fusion proteins. Antiserum specificity was confirmed by staining MmChx10-GFP expressing HeLa cells (data not shown).

To examine whether nuclear export was mediated via the Crm1 pathway, we used the export inhibitors LMB and Ratjadone A. These substances bind to Crm1, thereby preventing the interaction with leucine-rich NES (24, 55). LMB or Ratjadone A treatment not only resulted in exclusive nuclear accumulation of DrVsx1- and MmChx10-GFP in transfected HeLa and 293 cells but also blocked export of the endogenous MmChx10 protein (Fig. 1A/D/E and data not shown).

To further address whether DrVsx1-GFP and MmChx10-GFP were capable of nucleocytoplasmic trafficking, we performed heterokaryon assays in the presence of cycloheximide to prevent de novo protein synthesis. Upon fusion of DrVsx1-GFP and MmChx10-GFP expressing HeLa donor cells with untransfected NIH 3T3 acceptor cells, both PLC-HDPs were exported from the donor and imported into the mouse acceptor nuclei 60 min after fusion (Fig. 1F and G). As a control, incubation of the fused cells at 4°C (data not shown) or in the presence of LMB did not result in detectable accumulation of GFP fusion proteins in the acceptor nuclei, indicative for active transport (Fig. 1G). Since the cytoplasm of donor and acceptor

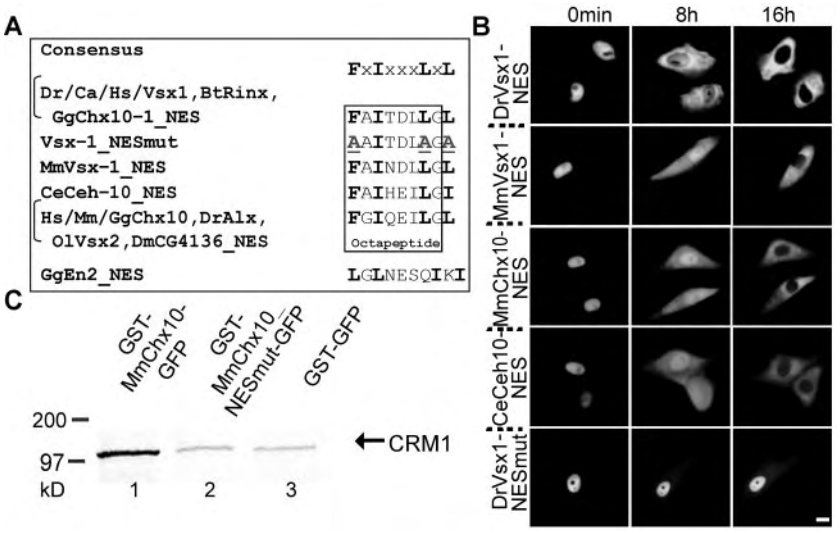

FIG. 2. PLC-HDPs contain evolutionarily conserved active NES and interact with Crm1 in vitro. (A) Alignment of the tested PLC-HDPs export signals from different species with the NES consensus motif (18) and the inactive Engrailed "NES." (B) Indicated GST-NES-GFP substrates were microinjected into the nuclei of Vero cells, and nuclear export was recorded in living cells by fluorescence microscopy after various time points. Approximately 100 cells were injected and representative examples are shown. Panels: left, $t = 0$ min; middle, $t = 8$ h; right, $t = 16$ h. Nuclear export was completed after 16 h. Inactivation of the NES by mutating critical residues into alanines (DrVsx1_NESmut) completely blocked export. (C) MmChx10 interacts with Crm1 in a GST pull-down assay. In vitro-translated ^{35}S-labeled Crm1 protein was incubated with equal amounts of immobilized full-length GST-MmChx10-GFP, GST-MmChx10_NESmut-GFP, or GST-GFP in the presence of GST-RanQ69L and nuclear extracts. The specific binding of Crm1 to GST-MmChx10-GFP (lane 1) was abolished by mutating the NES (lane 2). GST-GFP served to control for unspecific binding (lane 3). *Homo sapiens* (Hs), *Mus musculus* (Mm), *Bos taurus* (Bt), *Danio rerio* (Dr), *Carassius auratus* (Ca), *Oryzias latipes* (Ol), *Gallus gallus* (Gg), *Caenorhabditis elegans* (Ce), *Drosophila melanogaster* (Dm). Scale bar, 10 μm.

cells are fused in the heterokaryon assay the low amount of cytoplasmic DrVsx1-GFP or MmChx10-GFP protein, respectively, initially present in the donor cells was diluted and not detectable postfusion. Of note, the level of nuclear fluorescence in the acceptor nuclei increased, and the fluorescence signal in the donor nuclei decreased over time, excluding the formal possibility that the observed nuclear transfer events resulted from the import of the cytoplasmic GFP fusion proteins present prior to fusion.

PLC-HDPs contain a highly conserved NES previously described as the "octapeptide." To identify domains directing nuclear export, we first expressed N- and C-terminal deletion mutants of DrVsx1 and MmChx10 as GFP hybrids. As indicated in Fig. 1B, only fusion proteins containing the first 47 aa responded to LMB treatment, indicating the presence of an active NES. Database searches identified potential NES in the PLC-HDPs, matching the still loosely defined consensus sequence for leucine-rich NES (18, 20). Because predicted signals need to be verified experimentally, we tested the activity of the potential NES in a highly stringent system that allows the observation and quantification of nuclear export in living cells, independent of drug treatment, nuclear import, and passive diffusion (45). Signals (Fig. 2A) were expressed as fusions with GST and GFP (GST-NES-GFP) and tested by microinjection. Due to the size of the fusion proteins (54 kDa, as a monomer) the localization of the microinjected autofluorescent transport substrate is not flawed by passive diffusion, and the protein remains at the site of injection for up to 24 h (45). We observed that only substrates containing active PLC-HDP NES were quantitatively exported into the cytoplasm within 16 h after microinjection into the nucleus of Vero (Fig. 2B) and microglia CRL-2540 cells (data not shown). As a stringent control, a signal in which essential residues were replaced by alanines was inactive under identical experimental conditions (Fig. 2A and B). Likewise, treatment with LMB completely prevented export (data not shown). Interestingly, analysis of NES representative for all known PLC-HDP family members revealed that these NES mediated export with comparable kinetics (Fig. 2A and B). Approximately 100 cells were injected and analyzed, and representative examples are shown. These results were confirmed in two independent experiments (data not shown). The evolutionary conservation of the NES strongly argues that nuclear export is critical for the biological function of PLC-HDPs. Since nuclear export had been proposed also for other members of the homeoprotein family (34), we included the proposed NES of the Engrailed homeoprotein (Fig. 2A; GgEn2 NES) in our study. In contrast to the PLC-HDP NES, the GgEn2 NES was not active in our assay (data not shown).

NES inactivation prevents export of PLC-HDPs. To verify the functionality of the export signals also in the context of the full-length proteins in vivo, we mutated critical residues of the NES into alanines (DrVsx1_NESmut-GFP, aa^{37}**F**AITDL**LGL**^{45} → ^{37}**A**AITDL**AGA**^{45}; MmChx10_NESmut-GFP, aa^{32}**F**GIQEI**LGL**^{40} → ^{32}**A**GIQEI**AGA**^{40}). In contrast to the wild-type proteins DrVsx1_NESmut-GFP and MmChx10_NESmut-GFP displayed a complete nuclear localization after transient transfection (Fig. 1C). Likewise, the NES-deficient mutants were not exported in the heterokaryon assays (Fig. 1F and G), excluding the presence of additional NES or the possibility that export was mediated by shuttling interaction partners in *trans*.

PLC-HDP export signals interact with Crm1 in vitro. If the defined PLC-HDPs are exported via the Crm1 pathway, these

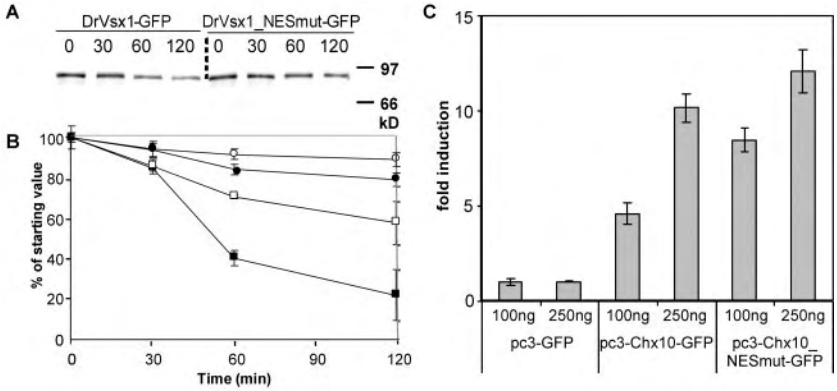

FIG. 3. Nuclear export affects PLC-HD protein stability and transcriptional activation. (A) Preventing nuclear export increases the intracellular stability of DrVsx1-GFP. HeLa cells were transiently transfected with expression plasmids encoding DrVsx1-GFP (2 μg) or DrVsx1-NESmut-GFP (2 μg). After 16 h, methionine-starved cells were pulsed with [^{35}S]methionine for 2 h and chased with excess methionine for the indicated times. Proteins were immunoprecipitated with anti-GFP antibody, resolved by SDS-PAGE and detected by fluorography. Whereas DrVsx1-GFP and DrVsx1-NESmut-GFP were degraded over time, inactivation of the NES resulted in a significantly increased half live of DrVsx1-NESmut-GFP. (B) Band intensities from two independent experiments (including the gel in panel A) were quantified by using a phosphorimager and graphed with standard errors for DrVsx1-GFP (■), DrVsx1-GFP + proteasomal inhibitors (PI) (●), DrVsx-1_NESmut-GFP (□), and DrVsx-1_NESmut-GFP + PI (○). (C) Luciferase assays after cotransfection of HeLa cells with pSV40-Gal, an MmChx10-responsive luciferase reporter and different amounts of expression plasmids for GFP, MmChx10-GFP, and MmChx10_NESmut. Expression of wild-type MmChx10-GFP resulted in higher transcriptional activation compared to the export-deficient mutant. Luciferase activity was normalized to β-Gal expression. Error bars indicate the standard deviations.

proteins should interact with the export receptor also in a cell-free system. We therefore performed in vitro interaction assays to biochemically verify the Crm1 interaction. Figure 2C demonstrates that recombinant GST-MmChx10-GFP significantly bound to Crm1 in the presence of Ran-GTP and nuclear extracts in contrast to inactive GST-MmChx10_NESmut-GFP or GST-GFP alone. Similar results were obtained for GST-DrVsx1-GFP or the other GST-NES-GFP fusion proteins, respectively (data not shown).

Nuclear export facilitates intracellular degradation of DrVsx1-GFP. Kurtzman et al. (26) reported the polyubiquitination and degradation of DrVsx1 by the ubiquitin/proteasome pathway. Because the proteasome degradative pathway appears to operate predominantly in the cytoplasm (51), we investigated whether nuclear export influences indirectly the intracellular stability of DrVsx1. HeLa cells transiently expressing DrVsx1-GFP or DrVsx1_NESmut-GFP, respectively, were metabolically pulse-labeled, followed by a chase with cold methionine for 0, 30, 60, and 120 min. Subsequently, GFP fusion proteins were immunoprecipitated with anti-GFP antiserum and resolved by SDS-PAGE (Fig. 3A). Band intensities from two independent experiments were quantified by using a phosphorimager; this showed that both DrVsx1-GFP and DrVsx1_NESmut-GFP were degraded over time and that degradation could be reduced by treatment with proteasomal inhibitors. Interestingly, preventing nuclear export resulted in a significantly increased half-live for DrVsx1_NESmut-GFP (Fig. 3A and B), suggesting that nuclear export is continuously supplying substrate for the proteasomal degradation machinery. Similar results were obtained for MmChx10 (data not shown).

Nuclear export influences MmChx10-mediated transactivation. To investigate the effect of export-enhanced degradation on the transcriptional activity of MmChx10, we tested the ability of the export-defective MmChx10 to transactivate a MmChx10-responsive luciferase reporter plasmid in transient transfections. These experiments revealed a good correlation between dose-dependent MmChx10 mediated transactivation and protein stability since expression of MmChx10_NESmut resulted in increased stimulation of gene expression (Fig. 3C).

Nuclear export facilitates unconventional secretion of PLC-HD proteins. Having demonstrated that PLC-HDPs are nucleocytoplasmic shuttle proteins, we investigated their potential for intercellular trafficking. In general, intercellular transfer requires both internalization and secretion. To analyze secretion of DrVsx1-GFP and to investigate the influence of nuclear export on secretion, we attempted to recover metabolically labeled DrVsx1-GFP or DrVsx1_NESmut-GFP protein, respectively, from the culture supernatant of transfected 293 cells. Figure 4A illustrates that DrVsx1-GFP, but not DrVsx1_NESmut-GFP could be immunoprecipitated by anti-GFP antibodies from the supernatant. Transfected cells were controlled by microscopic observation for cytotoxic effects caused by the expression of the respective GFP fusion proteins prior to lysate preparation to minimize unspecific protein release due to cell death. To also exclude the possibility that the observed result reflects differences in protein expression, equal expression levels of the GFP fusion proteins were verified by Western blot analysis of cellular extracts (Fig. 4B). Similar results were obtained for the MmChx10-GFP or MmChx10_NESmut-GFP protein, respectively (data not shown). Of note, we could not recover a NES-GFP fusion protein (DrVsx1 NES-GFP) from the supernatant of transfected 293 cells (data not shown). Thus, the continuous supply of cytoplasmic DrVsx1 from the nuclear pool by active nuclear export appears to facilitate secretion, but the NES itself does not represent an unconventional secretion signal. To determine whether protein secretion was mediated via the classical endoplasmic reticulum/Golgi-dependent pathway or by unconventional secretion, we attempted to inhibit secretion by treatment of the trans-

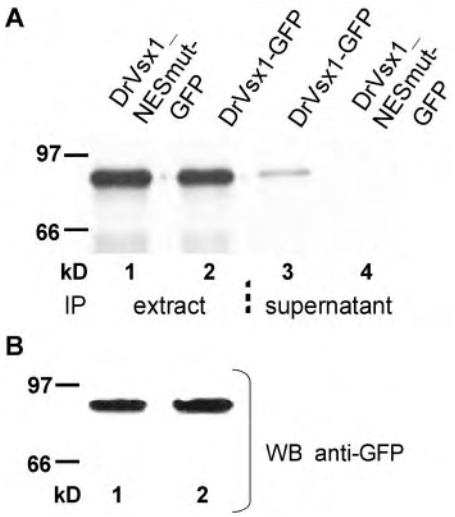

FIG. 4. Nuclear export affects DrVsx1-GFP protein secretion. (A) 293 cells were transfected with the indicated plasmids (4 μg) and cultured in methionine-free medium supplemented with [^{35}S]methionine. GFP fusion proteins were immunoprecipitated from the culture supernatants and from whole-cell lysates with an anti-GFP antibody. Although DrVsx1_NESmut-GFP and DrVsx1-GFP could be immunoprecipitated equally from cellular lysates (lanes 1 and 2), only DrVsx1-GFP could be recovered from the supernatants (lanes 3 and 4). (B) Equal expression levels of the GFP fusion proteins were verified by Western blot analysis of cellular lysates using a polyclonal anti-GFP antiserum.

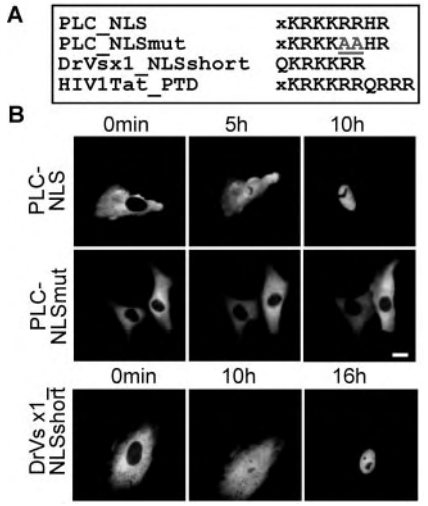

FIG. 5. PLC-HD proteins contain a highly conserved active nuclear import signal. (A) Sequence alignment of the NLS conserved in all PLC-HDP members, the inactive NLS mutant, Vsx1_short, and the HIV1Tat_PTD. (B) GST-NLS-GFP fusion protein were microinjected into the cytoplasm of Vero cells, and nuclear import was observed directly by fluorescence microscopy. Approximately 100 cells were injected, and representative examples are shown. Nuclear import of GST-PLC_NLS-GFP was completed after 10 h (upper panel). Import activity was lost by replacing two conserved arginines by alanines (GST-PLC_NLSmut-GFP, middle panel). In contrast, Vsx1_short was less active in mediating import (GST-Vsx1_NLSshort-GFP, lower panel). Scale bars, 10 μm.

fected cells with BFA. However, BFA treatment did not interfere with MmChx10-GFP release in support of secretion by the unconventional pathway, as also reported for several other proteins (39; data not shown).

PLC-HDPs contain a highly conserved active nuclear import signal which can function as a PTD. For continuous signal-mediated shuttling between the cytoplasm and the nucleus proteins require both NES and NLS. Thus, we next sought to determine whether the predominant nuclear steady-state localization of PLC-HDPs is the result of active nuclear import or is mediated by nuclear retention. The database comparisons revealed that the motif KRKKRRHR located at the beginning of the homeodomain is 100% conserved in all known PLC-HDPs (Fig. 5A). In contrast to GFP alone, a KRKK RRHR-GFP fusion protein localized to the nucleus (data not shown). However, because even a GFP-GFP fusion protein (54 kDa) can enter the nucleus by passive diffusion (45), we investigated whether this motif can function not only as nuclear retention but also as an active nuclear import signal. Microinjection experiments with recombinant GST-GFP fusion proteins (Fig. 5B) demonstrated that the tested signal mediated nuclear import and can therefore be considered as a bona fide nuclear import signal for PLC-HDs (PLC_NLS). Import activity was lost by replacing two conserved arginines by alanines (Fig. 5A and B, PLC_NLSmut). Approximately 100 cells were injected and analyzed, and representative examples are shown. These results were confirmed in two independent experiments (data not shown). Our observations are supported by the report of Kurtzman and Schechter (27), who demonstrated that a DrVsx1 mutant lacking the sequence QKRKKRR no longer accumulated in the nucleus. Of note, GST-QKRKKRR-GFP (Vsx1_short) was less active in mediating import (Fig. 5B).

Interestingly, the KRKKRRHR motif displayed a high homology to the widely used PTD KRKKRRQRRR of the human immunodeficiency virus type 1 (HIV-1) Tat protein (Fig. 5A) (52). To test the potential of the PLC-HD_NLS to also traverse intact cellular membranes, human cells were incubated with recombinant GFP fusion proteins, followed by treatment with trypsin to remove unspecifically bound protein. Fluorescence microscopy revealed that PLC-HD_NLS-GFP displayed a similar protein transduction activity as the positive control, HIV1Tat_PTD-GFP, and localized to the cytoplasm and nucleus of the treated cells (Fig. 6A). In contrast, GFP fusion proteins containing the QKRKKRR motif (Vsx1-short-GFP), the mutated NLS, or GFP alone could not mediate protein transduction under identical experimental conditions, arguing against PTD-independent cellular entry (Fig. 6A). These results provide a rational for the evolutionary conservation of the bifunctional KRKKRRHR motif. Importantly, recombinant full-length DrVsx1-GFP protein was also able to enter cells, although less efficiently, most likely due to its larger size since GST-HIV1Tat_PTD-GFP or GST-PLC-HD_NLS-GFP, respectively, also displayed a diminished transduction activity (data not shown).

PLC-HD proteins have the potential for intercellular transport. Having demonstrated that PLC-HDPs are nucleocytoplasmic shuttle proteins, can be secreted, and contain a PTD, we investigated their potential for intercellular trafficking. Although described for the Engrailed protein (22), we could not visually detect the spread of DrVsx1-GFP or MmChx10-GFP

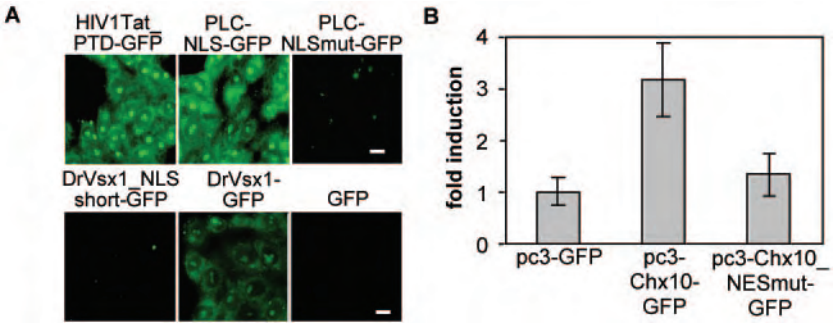

FIG. 6. PLC-HDPs have the capacity for intercellular transport. (A) The PLC-HD NLS can function as a PTD. Vero cells were incubated with 1 μM concentrations of the indicated GFP fusion proteins for 2 h and treated as described in Materials and Methods. Fluorescence microscopy indicated that DrVsx1_NLS-GFP, HIV1Tat_PTD-GFP and, to a lesser extent, DrVsx1-GFP were able to enter the cells. In contrast, DrVsx1_NLSmut-GFP, DrVsx1_short-GFP or GFP could not mediate cellular entry. Scale bars, 10 μm. (B) Inhibition of nuclear export interferes with intercellular transactivation. Luciferase assays after cocultivation of 293 cells expressing MmChx10-GFP, MmChx10_NESmut-GFP, or GFP, together with 293 cells transfected with the MmChx10-responsive luciferase reporter and pSV40-Gal. Luciferase activity was normalized to β-Gal expression. Error bars indicate the standard deviations.

from transfected to untransfected HeLa cells by fluorescence microscopy upon cocultivation for up to 72 h (data not shown). This might be due to the low amount of secreted and internalized protein which could be below the detection level. However, since even low concentrations of transcription factors are sufficient to trigger biological relevant responses in vivo, we used an intercellular transactivation assay to investigate intercellular trafficking. 293 cells transfected with MmChx10-GFP, MmChx10_NESmut-GFP, or GFP alone were cocultivated with 293 cells transfected with the MmChx10 responsive pLCR-R-luc reporter plasmid. Intercellular transport of MmChx10 should result in enhanced luciferase activity that should be abolished by NES inactivation. Figure 6B indicates that the wild-type but not the export-deficient MmChx10 protein was able to activate reporter gene expression, supporting the potential of CVC-HDPs for intercellular trafficking.

DISCUSSION

Transcriptional networks ensure the ordered development of complex multifunctional organs as exemplified by the spinal cord (17) or the retina (9). In particular, homeodomain proteins represent transcription factors exerting key developmental functions. The paired-like CVC-HDPs play an essential role in ocular development and, therefore, a precise control of PLC-HDPs functions is critical for ordered development and homeostasis. In eukaryotic cells, the nuclear envelope generates two distinct cellular compartments that separate transcription and DNA replication from protein biosynthesis. Among other mechanisms, regulated subcellular localization provides an attractive way to control the activity of PLC-HDPs. We demonstrated for two representatives of the PLC-HDP family that endogenous MmChx10, as well as ectopically expressed MmChx10-GFP and DrVsx1-GFP proteins, did not exclusively localize to the nucleus. A similar, nonexclusive nuclear localization was recently reported for the MmChx10 protein (46). This could either be due to the retention of newly synthesized protein in the cytoplasm or to its continuous nucleocytoplasmic transport. We showed that PLC-HDs can shuttle between the nucleus and the cytoplasm by using the heterokaryon assay. Furthermore, we characterized the previously described "octapeptide" as part of an evolutionary conserved active leucine-rich NES present in all members of the PLC-HDP family. Nuclear export of PLC-HDPs was mediated by the Crm1 pathway, as supported by several lines of evidence. First, Crm1 antagonists caused nuclear accumulation of DrVsx1 and MmChx10, were able to block nuclear export in the heterokaryon assay, and prevented export of recombinant PLC-HDP-NES transport substrates. Second, DrVsx1-GFP, MmChx10-GFP, and PLC-HDP-NES bound to Crm1 in vitro, and these interactions could be prevented by mutating critical residues in the NES which also blocked export of the full-length proteins in vivo. The NES of PLC-HDPs fit the still loosely defined consensus sequence for leucine-rich export signals and are evolutionary conserved in all known PLC-HDPs from human, mouse, rat, chicken, and zebra fish (see Fig. 3A). Interestingly, the tested PLC-HDP NES were equally active in microinjection experiments and displayed a similar activity, as observed for the NES from other transcriptional regulators such as p53 or Mdm2 (19). As demonstrated in our previous work (18) and by others (20), it appears that the distance between the critical **LxL** motif and the next hydrophobic residue should not exceed 3 aa in the proposed NES consensus sequence (see Fig. 3). We are not aware of any functional NES breaking this rule. The 4-aa spacer in the suggested Engrailed export signal (34) marks this sequence as nonfunctional explaining the lack of activity observed in our study. To date, nuclear export has been proposed for a growing list of proteins, including also several homeodomain proteins, e.g., Extradenticle (1), Otx1 (56), and Engrailed (34). However, the numerous reports on nuclear export sometimes lead to conflicting results. To standardize the definition for active, Crm1-mediated nuclear export mediated by a "classical" leucine-rich NES, we propose the following quality criteria. (i) Nuclear export of a protein, as assayed by transfection and heterokaryon assay, should be blocked by Crm1 inhibitors. (ii) The export signal should be active also in the context of a heterologous system in *trans* and should interact with Crm1 in vitro. (iii) Mutation of critical residues in the NES should inactivate its export activity also in the context of the full-length protein. According to our knowledge, the

present study is the first to demonstrate the nuclear export of homeodomain proteins fulfilling all of these criteria.

As transcription factors, PLC-HDPs have to access the nucleus to execute their function. Theoretically, the size of ca. 34 kDa allows PLC-HDPs to enter the nucleus also by passive diffusion. However, even smaller proteins are transported by active, signal-mediated mechanisms, most likely because active transport is more efficient and amendable to specific control mechanisms (3, 13). The transfection and/or microinjection experiments indicated that the conserved KRKKRRHR motif can not only function as a nuclear retention signal but also represents a bona fide monopartite nuclear import signal for PLC-HDPs in which the underlined arginines are critical for function and efficiency. Although Ubc9 has been suggested to mediate the nuclear localization of Vsx1 (27), we are currently investigating in detail whether Vsx1 is directly imported via the transportin 13/Ubc9 axis (37) or can also use alternative import pathways. Although the PLC-HDPs NLS is less active compared to the classical SV40 NLS (45), the rate of import still exceeds the rate of export, resulting in the observed dynamic but predominantly nuclear steady-state localization of PLC-HDPs.

The activity of transcriptional regulators can be modulated at various levels. As shown for other transcription factors (6, 44), these include posttranscriptional modifications in the nucleus or the cytoplasm, e.g., phosphorylation (35), sumoylation (10), and interactions with other proteins (14). The detailed molecular pathways regulating the activity of PLC-HDPs are currently under intense investigation. Here, we provided evidence that PLC-HDPs are dynamic transcription factors that have the capability to shuttle between the nucleus and the cytoplasm. Consequently, PLC-HDPs might be subjected to regulatory control mechanism homing in these specific compartments. Degradation by the ubiquitin/proteasome pathway is crucial to control protein homeostasis and was described for several transcription factors, including the DrVsx1 protein (26). In the present study, we found that inactivation of the nuclear export activity of DrVsx1 and MmChx10 resulted in increased protein stability and thus in increased transcriptional activation. Since the ubiquitin/proteasome pathway appears to act predominantly in the cytoplasm (47), our transactivation result indicate that regulating nucleocytoplasmic transport can indirectly influence the intracellular protein levels and the biological activity of PLC-HDPs by the proteasome pathway. A similar model was proposed for the IκB/NF-κB axis in which the nuclear export activity of IκB regulates the intracellular localization, degradation, and transcriptional activity of NF-κB (see references 30 and 33 and references therein). In contrast, Rehberg et al. reported that the inactivation of the NES in the Sox10 protein resulted in decreased transactivation by an unknown mechanism (44). Although it is less likely, we cannot formally rule out the possibility that the mutations introduced to generate the export deficient DrVsx1 protein directly resulted in enhanced degradation resistance. The increased stability observed would thus be due to conformational changes and not caused by blocking export.

We found that the continuous supply of cytoplasmic DrVsx1 or MmChx10 from the nuclear pool by active export facilitated also extracellular release of the proteins. PLC-HDPs in general

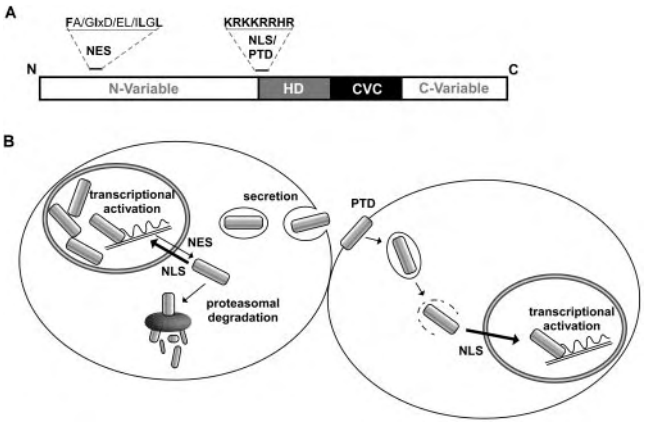

FIG. 7. (A) Organization of evolutionary conserved domains in PLC-HD proteins regulating cellular transport. (B) Model linking nucleocytoplasmic transport with PLC-HDP activity. The predominantly nuclear localization of PLC-HD proteins is the net result of import exceeding the rate of export due to the different activities of NES and NLS. Nuclear export allows PLC-HD protein levels to be regulated by the proteasomal degradation pathway and continuously supplies cargo for extracellular unconventional secretion. Intercellular transport and transactivation could be mediated by the protein transduction domain/NLS.

lack a canonical secretion signal and appear not to be targeted into the endoplasmic reticulum by a cotranslational mechanism. In addition, secretion could not be inhibited by treatment with BFA, an inhibitor of the classical endoplasmic reticulum/Golgi-dependent secretion pathway. Thus, extracellular release appears to be mediated by the unconventional secretion pathway reported also for several viral and cellular proteins (see reference 39 and references therein). In this context, Julian Huxley's term "growth gradient" may be relevant for the biological function of PLC-HDPs. In the morphogen gradient model, the local concentration of a diffusible molecule can determine cells' rates of proliferation and differentiation as a continuous function of concentration (4, 11, 36). This model is made particularly attractive by our finding that PLC-HDPs also harbor a highly conserved PTD with a similar activity as the widely used HIV-1 Tat PTD (52). The mechanism of transduction has been studied extensively for a variety of proteins, including the Antennapedia and PDX-1 homeodomain transcription factors (15). Recent evidence suggests that transduction occurs via a multistep mechanism involving endocytosis and macropinocytosis (54). Although we could not visually monitor the spread of DrVsx1-GFP or MmChx10-GFP from expressing donor to untransfected acceptor cells as described for the Engrailed protein (22), the results of our intercellular transactivation assays support the intercellular trafficking of PLC-HDPs, as demonstrated for other PTD-containing transcription factors (53). However, to fully understand the biological relevance of transduction in vivo, the activity of PTD-deficient PLC-HDP mutants has to be investigated in adequate animal models.

In summary, our report provides novel insights into the functional domain organization of PLC-HDPs (Fig. 7A). Based on our findings, we propose a model in which the continuous nucleocytoplasmic shuttling of PLC-HDPs contributes to the optimal and flexible execution of their transcriptional

activities (Fig. 7B). The evolutionarily conserved combination of a PTD, together with active nuclear export and import signals, may allow the fine-tuning of intracellular protein levels by the proteasome pathway and, in addition, also permits intercellular transfer. The overlapping complex patterns of homeobox gene expression in the embryonic retina requires a complex regulatory network of transcription factors that specifies differentiation of competent retinal progenitors. Although transcriptional regulation of PLC-HDPs is an important control mechanism, PLC-HDPs may have additional unexpected paracrine activity, thereby influencing and maintaining the complex expression pattern during development. To ultimately gain profound insight into the detailed role of PLC-HDPs' nucleocytoplasmic shuttling for ordered development has to await transgenic mouse knock-in models in which nucleocytoplasmic transport of Chx10 is selectively abolished. Currently, we are pursuing this strategy in our laboratory.

ACKNOWLEDGMENTS

We thank B. Groner for support and N. Schechter, J. Nathans, and E. F. Percin for materials.

This study was supported by the Deutsche Forschungsgemeinschaft (Sta 598/1-2) and the Studienstiftung des Deutschen Volkes (S.K.K.).

REFERENCES

1. **Affolter, M., T. Marty, and M. A. Vigano.** 1999. Balancing import and export in development. Genes Dev. **13:**913–915.
2. **Barabino, S. M., F. Spada, F. Cotelli, and E. Boncinelli.** 1997. Inactivation of the zebrafish homologue of Chx10 by antisense oligonucleotides causes eye malformations similar to the ocular retardation phenotype. Mech. Dev. **63:** 133–143.
3. **Bednenko, J., G. Cingolani, and L. Gerace.** 2003. Nucleocytoplasmic transport: navigating the channel. Traffic **4:**127–135.
4. **Briscoe, J., Y. Chen, T. M. Jessell, and G. Struhl.** 2001. A hedgehog-insensitive form of patched provides evidence for direct long-range morphogen activity of sonic hedgehog in the neural tube. Mol. Cell **7:**1279–1291.
5. **Burmeister, M., J. Novak, M. Y. Liang, S. Basu, L. Ploder, N. L. Hawes, D. Vidgen, F. Hoover, D. Goldman, V. I. Kalnins, T. H. Roderick, B. A. Taylor, M. H. Hankin, and R. R. McInnes.** 1996. Ocular retardation mouse caused by Chx10 homeobox null allele: impaired retinal progenitor proliferation and bipolar cell differentiation. Nat. Genet. **12:**376–384.
6. **Cartwright, P., and K. Helin.** 2000. Nucleocytoplasmic shuttling of transcription factors. Cell Mol. Life Sci. **57:**1193–1206.
7. **Chow, R. L., B. Volgyi, R. K. Szilard, D. Ng, C. McKerlie, S. A. Bloomfield, D. G. Birch, and R. R. McInnes.** 2004. Control of late off-center cone bipolar cell differentiation and visual signaling by the homeobox gene Vsx1. Proc. Natl. Acad. Sci. USA **101:**1754–1759.
8. **Cullen, B. R.** 2003. Nuclear RNA export. J. Cell Sci. **116:**587–597.
9. **Dyer, M. A.** 2003. Regulation of proliferation, cell fate specification and differentiation by the homeodomain proteins Prox1, Six3, and Chx10 in the developing retina. Cell Cycle **2:**350–357.
10. **Endter, C., J. Kzhyshkowska, R. H. Stauber, H. Wolf, and T. Dobner.** 2001. SUMO-1 modification required for transformation by adenovirus type 5 early 1B 55-kDa oncoprotein. Proc. Natl. Acad. Sci. USA **98:**11312–11317.
11. **Franceschi, R. T.** 1999. The developmental control of osteoblast-specific gene expression: role of specific transcription factors and the extracellular matrix environment. Crit. Rev. Oral Biol. Med. **10:**40–57.
12. **Galliot, B., C. de Vargas, and D. Miller.** 1999. Evolution of homeobox genes: Q50 paired-like genes founded the Paired class. Dev. Genes Evol. **209:**186–197.
13. **Görlich, D., and U. Kutay.** 1999. Transport between the cell nucleus and the cytoplasm. Annu. Rev. Cell Dev. Biol. **15:**607–660.
14. **Green, E. S., J. L. Stubbs, and E. M. Levine.** 2003. Genetic rescue of cell number in a mouse model of microphthalmia: interactions between Chx10 and G1-phase cell cycle regulators. Development **130:**539–552.
15. **Green, I., R. Christison, C. J. Voyce, K. R. Bundell, and M. A. Lindsay.** 2003. Protein transduction domains: are they delivering? Trends Pharmacol. Sci. **24:**213–215.
16. **Hayashi, T., J. Huang, and S. S. Deeb.** 2000. RINX(VSX1), a novel homeobox gene expressed in the inner nuclear layer of the adult retina. Genomics **67:**128–139.
17. **Hedlund, E., S. L. Karsten, L. Kudo, D. H. Geschwind, and E. M. Carpenter.** 2004. Identification of a Hoxd10-regulated transcriptional network and combinatorial interactions with Hoxa10 during spinal cord development. J. Neurosci. Res. **75:**307–319.
18. **Heger, P., J. Lohmaier, G. Schneider, K. Schweimer, and R. H. Stauber.** 2001. Qualitative highly divergent nuclear export signals can regulate export by the competition for transport cofactors in vivo. Traffic **555:**544–555.
19. **Heger, P., O. Rosorius, J. Hauber, and R. H. Stauber.** 1999. Titration of cellular export factors, but not heteromultimerization, is the molecular mechanism of *trans*-dominant HTLV-1 Rex mutants. Oncogene **18:**4080–4090.
20. **Henderson, B. R., and A. Eleftheriou.** 2000. A comparison of the activity, sequence specificity, and CRM1 dependence of different nuclear export signals. Exp. Cell Res. **256:**213–224.
21. **Heon, E., A. Greenberg, K. K. Kopp, D. Rootman, A. L. Vincent, G. Billingsley, M. Priston, K. M. Dorval, R. L. Chow, R. R. McInnes, G. Heathcote, C. Westall, J. E. Sutphin, E. Semina, R. Bremner, and E. M. Stone.** 2002. VSX1: a gene for posterior polymorphous dystrophy and keratoconus. Hum. Mol. Genet. **11:**1029–1036.
22. **Joliot, A., A. Maizel, D. Rosenberg, A. Trembleau, S. Dupas, M. Volovitch, and A. Prochiantz.** 1998. Identification of a signal sequence necessary for the unconventional secretion of Engrailed homeoprotein. Curr. Biol. **8:**856–863.
23. **Kino, T., A. Gragerov, J. B. Kopp, R. H. Stauber, G. N. Pavlakis, and G. P. Chrousos.** 1999. The HIV-1 virion-associated protein Vpr is a coactivator of the human glucocorticoid receptor. J. Exp. Med. **189:**51–61.
24. **Koster, M., S. Lykke-Andersen, Y. A. Elnakady, K. Gerth, P. Washausen, G. Hofle, F. Sasse, J. Kjems, and H. Hauser.** 2003. Ratjadones inhibit nuclear export by blocking CRM1/exportin 1. Exp. Cell Res. **286:**321–331.
25. **Krätzer, F., O. Rosorius, P. Heger, N. Hirschmann, T. Dobner, J. Hauber, and R. H. Stauber.** 2000. The adenovirus type 5 E1B-55K oncoprotein is a highly active shuttle protein and shuttling is independent of E4orf6, p53, and Mdm2. Oncogene **19:**850–857.
26. **Kurtzman, A. L., L. Gregori, A. L. Haas, and N. Schechter.** 2000. Ubiquitination and degradation of the zebra fish paired-like homeobox protein VSX-1. J. Neurochem. **75:**48–55.
27. **Kurtzman, A. L., and N. Schechter.** 2001. Ubc9 interacts with a nuclear localization signal and mediates nuclear localization of the paired-like homeobox protein Vsx-1 independent of SUMO-1 modification. Proc. Natl. Acad. Sci. USA **98:**5602–5607.
28. **Kzhyshkowska, J., H. Schutt, M. Liss, E. Kremmer, R. Stauber, H. Wolf, and T. Dobner.** 2001. Heterogeneous nuclear ribonucleoprotein E1B-AP5 is methylated in its Arg-Gly-Gly (RGG) box and interacts with human arginine methyltransferase HRMT1L1. Biochem. J. **358:**305–314.
29. **Lamond, A. I., and J. E. Sleeman.** 2003. Nuclear substructure and dynamics. Curr. Biol. **13:**R825–R828.
30. **Lee, S. H., and M. Hannink.** 2001. The N-terminal nuclear export sequence of IκBalpha is required for RanGTP-dependent binding to CRM1. J. Biol. Chem. **23:**23.
31. **Lei, E. P., and P. A. Silver.** 2002. Protein and RNA export from the nucleus. Dev. Cell **2:**261–272.
32. **Levine, E. M., M. Passini, P. F. Hitchcock, E. Glasgow, and N. Schechter.** 1997. Vsx-1 and Vsx-2: two Chx10-like homeobox genes expressed in overlapping domains in the adult goldfish retina. J. Comp. Neurol. **387:**439–448.
33. **Magnani, M., R. Crinelli, M. Bianchi, and A. Antonelli.** 2000. The ubiquitin-dependent proteolytic system and other potential targets for the modulation of nuclear factor-κB (NF-κB). Curr. Drug Targets **1:**387–399.
34. **Maizel, A., O. Bensaude, A. Prochiantz, and A. Joliot.** 1999. A short region of its homeodomain is necessary for engrailed nuclear export and secretion. Development **126:**3183–3190.
35. **McBride, K. M., and N. C. Reich.** 2003. The ins and outs of STAT1 nuclear transport. Sci. STKE **195:**RE13.
36. **Megason, S. G., and A. P. McMahon.** 2002. A mitogen gradient of dorsal midline Wnts organizes growth in the CNS. Development **129:**2087–2098.
37. **Mingot, J. M., S. Kostka, R. Kraft, E. Hartmann, and D. Gorlich.** 2001. Importin 13: a novel mediator of nuclear import and export. EMBO J. **20:**3685–3694.
38. **Mintz-Hittner, H. A., E. V. Semina, L. J. Frishman, T. C. Prager, and J. C. Murray.** 2004. VSX1 (RINX) mutation with craniofacial anomalies, empty sella, corneal endothelial changes, and abnormal retinal and auditory bipolar cells. Ophthalmology **111:**828–836.
39. **Nickel, W.** 2003. The mystery of nonclassical protein secretion: a current view on cargo proteins and potential export routes. Eur. J. Biochem. **270:** 2109–2119.
40. **Ohtoshi, A., M. J. Justice, and R. R. Behringer.** 2001. Isolation and characterization of Vsx1, a novel mouse CVC paired-like homeobox gene expressed during embryogenesis and in the retina. Biochem. Biophys. Res. Commun. **286:**133–140.
41. **Ohtoshi, A., S. W. Wang, H. Maeda, S. M. Saszik, L. J. Frishman, W. H. Klein, and R. R. Behringer.** 2004. Regulation of retinal cone bipolar cell differentiation and photopic vision by the CVC homeobox gene Vsx1. Curr. Biol. **14:**530–536.
42. **Percin, E. F., L. A. Ploder, Y. J. J., K. Arici, D. J. Horsford, A. Rutherford, B. Bapat, D. W. Cox, A. M. V. Duncan, V. I. Kalnins, A. Kocak-Altintas, J. C. Sowden, E. Trabousli, M. Sarfarazi, and R. R. McInnes.** 2000. Human

microphthalmia associated with mutations in the retinal homeobox gene CHX10. Nat. Genet. **25:**397–401.
43. **Porter, L. A., and D. J. Donoghue.** 2003. Cyclin B1 and CDK1: nuclear localization and upstream regulators. Prog. Cell Cycle Res. **5:**335–347.
44. **Rehberg, S., P. Lischka, G. Glaser, T. Stamminger, M. Wegner, and O. Rosorius.** 2002. Sox10 is an active nucleocytoplasmic shuttle protein, and shuttling is crucial for Sox10-mediated transactivation. Mol. Cell. Biol. **22:** 5826–5834.
45. **Rosorius, O., P. Heger, G. Stelz, N. Hirschmann, J. Hauber, and R. H. Stauber.** 1999. Direct observation of nucleo-cytoplasmic transport by microinjection of GFP-tagged proteins in living cells. BioTechniques **27:**350–355.
46. **Rowan, S., and C. L. Cepko.** 2004. Genetic analysis of the homeodomain transcription factor Chx10 in the retina using a novel multifunctional BAC transgenic mouse reporter. Dev. Biol. **271:**388–402.
47. **Sakamoto, K. M.** 2002. Ubiquitin-dependent proteolysis: its role in human diseases and the design of therapeutic strategies. Mol. Genet. Metab. **77:**44–56.
48. **Smallwood, P. M., B. P. Olveczky, G. L. Williams, G. H. Jacobs, B. E. Reese, M. Meister, and J. Nathans.** 2003. Genetically engineered mice with an additional class of cone photoreceptors: implications for the evolution of color vision. Proc. Natl. Acad. Sci. USA **100:**11706–11711.
49. **Smallwood, P. M., Y. Wang, and J. Nathans.** 2002. Role of a locus control region in the mutually exclusive expression of human red and green cone pigment genes. Proc. Natl. Acad. Sci. USA **99:**1008–1011.
50. **Stauber, R. H., and G. N. Pavlakis.** 1998. Intracellular trafficking and interactions of the HIV-1 Tat protein. Virology **252:**126–132.
51. **Ulrich, H. D.** 2002. Natural substrates of the proteasome and their recognition by the ubiquitin system. Curr. Top. Microbiol. Immunol. **268:**137–174.
52. **Vives, E., J. P. Richard, C. Rispal, and B. Lebleu.** 2003. TAT peptide internalization: seeking the mechanism of entry. Curr. Protein Pept. Sci. **4:**125–132.
53. **Wadia, J. S., and S. F. Dowdy.** 2003. Modulation of cellular function by TAT mediated transduction of full length proteins. Curr. Protein Pept. Sci. **4:**97–104.
54. **Wadia, J. S., R. V. Stan, and S. F. Dowdy.** 2004. Transducible TAT-HA fusogenic peptide enhances escape of TAT-fusion proteins after lipid raft macropinocytosis. Nat. Med. **10:**310–315.
55. **Yashiroda, Y., and M. Yoshida.** 2003. Nucleo-cytoplasmic transport of proteins as a target for therapeutic drugs. Curr. Med. Chem. **10:**741–748.
56. **Zhang, Y. A., A. Okada, C. H. Lew, and S. K. McConnell.** 2002. Regulated nuclear trafficking of the homeodomain protein otx1 in cortical neurons. Mol. Cell Neurosci. **19:**430–446.
57. **Zhao, Y., and H. Westphal.** 2002. Homeobox genes and human genetic disorders. Curr. Mol. Med. **2:**13–23.

2

Acetylation of Stat1 modulates NF-κB signaling

Oliver H. Krämer[1, 2], Daniela Baus[1], Shirley Knauer[1], Stefan Stein[1], Elke Jäger[3], Roland Stauber[1], Manuel Grez[1], Edith Pfitzner[1] and Thorsten Heinzel[1, 2, 4]

[1] Georg-Speyer-Haus, Paul-Ehrlich-Straße 42-44, D-60596 Frankfurt, Germany

[2] Present address: Institute of Biochemistry and Biophysics, University of Jena, Philosophenweg 12, D-07743 Jena

[3] Medizinische Klinik II – Onkologie, Krankenhaus Nordwest, Steinbacher Hohl 2-26, D-60488 Frankfurt, Germany

[4] Corresponding author e-mail: heinzel@em.uni-frankfurt.de

Running title: **Acetylation of Stat1**

Key words: Stat1, NF-κB, acetylation, histone deacetylase, HDAC inhibitor

Total character count: 54869

Summary

The modulation of signaling events by histone deacetylase inhibitors has been shown to lead to the induction of apoptosis or differentiation of carcinoma cells. Nevertheless, the molecular mechanisms underlying these processes are still under intense investigation. Our study shows that Stat1 and NF-κB, two key regulators of signal transduction, gene expression and apoptosis are linked via acetylation of Stat1 lysine residues. Stat1 expression levels correlate with sensitivity of cells to HDAC inhibitors and introduction of Stat1 into resistant cells permits induction of apoptosis. Although acetylation of Stat1 does not change its transcriptional activity, it is a prerequisite for the interaction with NF-κB p65. As a consequence, p65 DNA-binding, nuclear localization and expression of anti-apoptotic NF-κB target genes decrease. The analysis of Stat1 mutants revealed lysines 410 and 413 as acetylation sites. Mutations of these residues mimicking either constitutively acetylated or non-acetylated states demonstrate that the crosstalk between Stat1 and NF-κB signaling pathways is modulated by changes in the acetylation status of Stat1.

Introduction

Many signal transduction pathways ultimately result in the posttranslational modification of histones, which determines the expression of genes important for cell growth, differentiation and apoptosis (Wolffe and Hayes 1999; Schreiber and Bernstein 2002). Acetylation of the N-terminal tails of histones correlates with gene activation, whilst histone deacetylation mediates transcriptional repression (Strahl and Allis 2000). It has also become clear that regulated acetylation of non-histone proteins determines cellular fate and survival (Blobel 2000; Kouzarides 2000; Cohen et al. 2004). The fine-tuned equilibrium of protein acetylation and deacetylation is maintained by histone acetyltransferases (HATs) and histone deacetylases (HDACs) (Kouzarides 1999). HDAC-inhibitors (HDACi) have been shown to change the expression pattern of genes involved in differentiation, cell cycle arrest and apoptosis. Intriguingly, repression of gene expression after HDAC-inhibition has been demonstrated (Van Lint et al. 1996; Nusinzon and Horvath 2003; Mitsiades et al. 2004) and HDACi were also shown to affect several signal transduction pathways (Blaheta and Cinatl 2002; Gurvich et al. 2004).

Despite the fact that HDACi are considered as candidate drugs for cancer therapy (Krämer et al. 2001; Kelly et al. 2002; Melnick and Licht 2002), it often remains to be elucidated why they may induce either apoptosis, necrosis, differentiation or have no effect in different cell types. Consequently, the molecular mechanisms underlying cell-specific modulation of signaling pathways by HDACi and factors determining sensitivity towards these compounds are still subject to intense investigation (Mayo et al. 2003). Several recent reports suggest that HDACi-induced apoptosis depends on the expression of Jun, Bcl-2-proteins, $p21^{WAF/CIP1}$, p53, NF-κB and Akt (Vrana et al. 1999; Henderson et al. 2003; Mayo et al. 2003). For some of these proteins association with HDACs and/or acetylation of lysine residues has been shown (Kouzarides 2000; Chen and Greene 2003; Kiernan et al. 2003; Weiss et al. 2003).

In the case of NF-κB, which contributes significantly to anti-apoptotic signaling (Perkins 2004), HDACi were shown to up-regulate NF-κB transcriptional activity in certain cell lines (Mayo et al. 2003). On the other hand, there is strong evidence that NF-κB signaling and expression of several NF-κB target genes are repressed by compounds inhibiting HDACs (Huang et al. 1997; Inan et al. 2000; Krämer et al. 2001). Given the critical role of NF-κB in tumorigenesis, several studies were undertaken to identify factors influencing this tumor promoter (Perkins 2004). It became clear that NF-κB signaling is controlled at several levels by regulatory proteins, such as the I-κB protein family. Besides the I-κBs, Stat1 has been suggested to repress signaling mediated by NF-κB (Wang et al. 2000; Suk et al. 2001; Shen and Lentsch 2004). Moreover, several stimuli induce apoptosis to a significantly greater extent in a Stat1-positive cellular background (Kumar et al. 1997; Meyer et al. 2002). Similar to NF-κB, Stat1 associates with histone acetyltransferases (HATs) and HDACs (Korzus et al. 1998; Nusinzon and Horvath 2003). Stat1 regulates the expression of gene products mediating apoptosis, growth and other cellular processes constitutively or inducibly in a phosphorylation-dependent manner (Chatterjee-Kishore et al. 2000; Ihle 2001). Remarkably, tyrosine phosphorylation and transcriptional activity of Stat1 appear dispensable for the inhibition of NF-κB and apoptosis induction in response to certain stimuli (Wang et al. 2000; Meyer et al. 2002). However, it is still unclear which other posttranslational modifications are involved in this process and whether conditions exist in which Stat1 and NF-κB can interact with each other.

We investigated the molecular mechanisms underlying the induction of apoptosis and the modulation of signaling pathways by HDACi in human melanoma cells. Our results show that in sensitive cells HDACi increase expression and induce acetylation of Stat1. Experiments conducted in both, HDACi-sensitive and -resistant cell lines, indicate that acetylated Stat1 interacts with NF-κB and reduces NF-κB signaling. These molecular changes are critical for the induction of cell death by these substances.

Results

Response of human melanoma cells to HDAC-inhibitors

HDAC-inhibitors (HDACi) can induce growth arrest and apoptosis in tumor cells of different origin (Krämer et al. 2001; Kelly et al. 2002). We found significant differences in the sensitivity of various melanoma cell lines towards these compounds. SK-37 cells show strong growth reduction in the MTT-assay upon HDACi-treatment, whereas NW-1539 cells are not affected significantly (Figure 1A). These cell lines are prototypical examples and have characteristics similar to other melanoma cell lines which are either HDACi-sensitve (e. g. MZ-19) or -resistant (e. g. NW-450).

In order to investigate the molecular mechanisms underlying this differential response, we first had to evaluate whether the reduced proliferation due to HDACi relies on pro-apoptotic properties and effects on caspases (Thornberry and Lazebnik 1998). In the HDACi-sensitive SK-37 cell line, we detected activation of the initiator caspases 8 and 9 after treatment (Figure 1B). Furthermore, we measured Caspase 3 activity in extracts from these cells by colorimetric assay. Conversion of the proenzyme form of the excutioner Caspase 3 (p32) to the catalytically active proteases p17 and p19 was detectable in SK-37 but not in HDACi-resistant NW-450 cells (Figure 1B).

Activation of Caspase 3 during HDACi-mediated apoptosis of SK-37 cells was also verified by examining the cleavage of PARP (116 kDa) into 85-kDa and 28-kDa fragments (Thornberry and Lazebnik 1998) (Figure 1C). The pan-caspase-inhibitor Z-VAD-FMK inhibits PARP cleavage as well as occurence of a hypodiploid (sub G1) fraction resulting from DNA fragmentation in SK-37 cells (Figure 1C). Analysis of nuclei stained with Hoechst 33258 gave similar results (data not shown). These results confirm that HDACi trigger apoptotic, caspase-dependent pathways in SK-37 melanoma cells (Figure 1C). Furthermore, no signs of nonspecific cell permeabilization and necrotic cell death were found in a PI/Hoechst staining assay (data not shown).

Alteration of Stat1 gene expression after HDAC-inhibition

We employed microarray and Western blot analyses to define alterations in gene expression patterns after incubation with HDACi. These assays revealed a time- and dose-dependent increase in Stat1 expression at the mRNA and protein level in SK-37 (Figure 2A) and several other HDACi-sensitive cell lines (data not shown). Treatment of SK-37 cells with HDACi and cycloheximide showed that the HDACi-induced increase in Stat1 expression depends on *de novo* protein synthesis (data not shown). Hence, an increase in Stat1 stability due to reduced HDAC-activity cannot account for higher Stat1 expression levels. Intriguingly, HDACi-resistant cell lines, such as NW-450 and NW-1539 do not undergo HDACi-induced Caspase 3 cleavage and apoptosis (Figures 1A, B) and express very low levels of Stat1, which are not induced by HDACi (Figure 2B, C). Since no significant difference in HDACi-induced histone hyperacetylation was detected between NW-1539 and SK-37 cells, HDACi were equally effective in blocking HDAC activity in both cell lines (Figure 2C). This result shows that not only inhibition of HDACs but also the presence of Stat1 appears to be crucial for HDACi-mediated apoptosis in melanoma cells. Consistent with previous reports (Wong et al. 2002), we detected a strong increase in Stat1 expression in the Stat1-positive SK-37 cell line, but not in NW-1539 cells treated with interferon α. Moreover, co-treatment with HDACi further increased Stat1 expression in SK-37 cells. (data not shown). This correlates with enhanced induction of apoptosis as assessed by MTT and FACS analysis (Figure 2D).

These results prompted us to investigate whether Stat1α is required for HDACi-induced apoptosis in NW-1539 cells. We transduced these cells with a lentiviral vector expressing Stat1α. Indeed, sensitivity towards VPA was confered to Stat1α-transduced NW-1539 cells but not to cells which received only the vector encoding GFP (Figures 3A, B). Hence, Stat1 expression levels appear to determine the response of this cell line to HDACi. Furthermore, introduction of Stat1α renders these cells susceptible to enhanced apoptosis induction by VPA and interferon α (Figure 3B), whereas interferon α alone did not induce apoptosis (data not

shown). Similar results were obtained with the Stat1-negative cell line U3A (Müller et al. 1993) reconstituted with Stat1α, albeit with less pronounced apoptosis induction (data not shown).

Our results clearly show that HDACi induce Stat1 in a cell-type specific manner. However, microarray analyses gave no evidence for increased expression of Stat1 target genes as a result of HDAC inhibition in SK-37 cells. Therefore, the activity of Stat1 in HDACi-induced apoptosis is likely to involve non-genomic effects of Stat1, such as cross-talk with other signaling pathways.

HDACi modulate NF-κB activity

In order to identify such signaling pathways, gene expression analyses can provide valuable information. Since a critical role of NF-κB for HDACi-induced apoptosis has been described, we analyzed the expression of NF-κB-dependent genes in the HDACi-sensitive cell line SK-37. Our data indicate HDACi-dependent repression of NF-κB target genes such as bcl-X_L, survivin and Stat5 (Figure 4A, left). These results confirm several reports describing effects of HDACi on these genes (Krämer et al. 2001; Hinz et al. 2002; De Schepper et al. 2003). On the other hand, expression of NF-κB-regulated genes remained unaltered in HDACi-resistant NW-1539 cells, which express hardly any Stat1 (Figure 4A, right).

Data shown in Figure 4A indicate that Stat1α expression inversely correlates with the activity of NF-κB after HDACi-treatment. Therefore, we investigated whether DNA binding of NF-κB might be affected. EMSAs displayed functional impairment of NF-κB p65/p50 heterodimer binding to its cognate DNA-sequence in extracts from HDACi-treated SK-37 cells (Figure 4B, compare lanes 1 and 4). The same observation was made with Stat1α-transduced NW-1539 cells, but not in parental or vector-transduced NW-1539 cells (Figure 4B, compare lanes 13 and 16 with lanes 5 and 8, 9 and 12). Hence, DNA-binding of NF-κB after treatment with HDACi is only reduced if Stat1α is expressed, suggesting a link of both signaling pathways.

The localization of nuclear p65 is modulated by Stat1 and HDACi

Immunoblotting and fluorescence microscopy were employed to gain further insights into the mechanism underlying inhibition of NF-κB in HDACi-treated SK-37 cells. *In situ* immunofluorescence analysis shows a shift of NF-κB p65 from the nucleus to the cytosol and increased co-localization with Stat1α. Treatment of cells with the nuclear export inhibitor LMB prevents basal and HDACi-induced export of NF-κB p65 and causes nuclear accumulation of Stat1α and p65. Again, co-localization of these proteins was enhanced if HDACs were inhibited by VPA (Figure 5A). The analysis of cytosolic and nuclear fractions of SK-37 cells indicates that Stat1 expression increases both, in the cytosol and in the nucleus (Figure 5B). For NF-κB p65 a clear reduction in the nuclear compartment is evident after treatment with HDACi, which confirms our microscopy results. These data suggest that removal of p65 from the nucleus and interaction with Stat1 might be a key step in HDACi-induced repression of NF-κB target genes and apoptosis induction. Another possible explanation, changes in NF-κB p65 expression, can be ruled out, since p65 levels are not altered significantly (Figure 5B). Western blot analysis of 2fTGH cells and their derived Stat1-negative cell line U3A confirmed dependence on Stat1 for nuclear export of p65 upon HDAC-inhibition (Figure 5C). Hence, it appears plausible that HDACi inhibit nuclear localization of p65 only in cells expressing Stat1.

HDACi induce the interaction of Stat1α and NF-κB

Having established a role of Stat1α in NF-κB signaling, we investigated whether these transcription factors could interact physically. First, we tested if this interaction is mediated by TRADD, which was shown to associate with Stat1α under certain conditions (Wang et al. 2000). However, in several immunoprecipitation experiments, we could not detect an HDACi-dependent interaction of Stat1α with TRADD in SK-37 cells (data not shown). On the other hand, precipitation of Stat1α or NF-κB p65 with monoclonal antibodies revealed robust association of these proteins under conditions in which HDACs were inhibited (Figure 5D).

Next, we analyzed Stat1 complexes by Superose 6 column fractionation of SK-37 cell extracts and found that in high molecular weight complexes the amount of Stat1 increases together with NF-κB p65 after VPA treatment (Figure 5E). Notably, this complex accumulates in a time-dependent manner and parallels apoptosis induction after HDAC-inhibition. Immunoprecipitation of Stat1α out of these fractions followed by Western blotting against p65 showed that a weak basal interaction of these proteins is increased upon HDAC-inhibition (Figure 5E).

We also analyzed the composition of the Stat1 complex before and after HDAC-inhibition by specific immunoprecipitation and Western blot. Addition of HDACi to SK-37 cells leads to reduced association of Stat1 with HDACs 1 and 3 (Figure 5F). However, no binding of Stat1 to other class I HDACs (2 and 8) was observed (data not shown). Superose 6 fractionation substantiates these results and revealed decreased co-migration of Stat1α complexes with the corepressor mSin3 (Figure 5E). Our observations not only confirm that Stat1 can interact with negative cofactors but also indicate that HDACs dissociate upon HDACi treatment.

Acetylation of Stat1

Stat1 can undergo multiple posttranslational modifications (Darnell 1997). Since recent publications show that acetylation of proteins mediates multiple cellular processes (Kouzarides 2000; Cohen et al. 2004), we tested whether Stat1 undergoes acetylation. Stat1α was immunoprecipitated from SK-37 whole cell extracts with a monoclonal antibody under stringent lysis conditions in RIPA-buffer. A pan-acetyl-lysine antibody recognized a band corresponding to the molecular weight of Stat1α (Figure 6A). Reprobing with the monoclonal Stat1α antibody confirmed the acetylation signal as Stat1α. As expected, the basal acetylation level of endogenous Stat1α is increased after HDAC-inhibition (Figure 6A). To obtain further evidence for acetylation of Stat1, an anti-acetyl-lysine antibody was used for immunoprecipitation and Western blots were probed with an antibody against Stat1. In this direction, the pan-acetyl-lysine antibody precipitated Stat1. Again, the acetylation level of Stat1 increased after HDAC-inhibition and allowed recovery of increasing amounts of Stat1 from treated cells (Figure 6A,

right panel). These findings indicate that endogenous Stat1 is acetylated *in vivo* and that this modification can be increased by HDACi (Figure 6A) and/or decreased association with corepressors and HDACs (Figure 5E). No acetylation of endogenous NF-κB p65 was detectable under these conditions. Furthermore, p65 could not be precipitated with the pan-acetyl-lysine antibody (Figure 6A). This is consistent with reports stating the need for overexpression of a histone acetyltransferase (HAT) to detect NF-κB acetylation (Chen and Greene 2003).

Transfection experiments with 293T cells revealed that increased expression of CBP enhances Stat1 acetylation (Figure 6B). Moreover, we were able to acetylate Stat1α *in vitro* using immunoprecipitated CBP (Figure 6B, right panel). Ectopically expressed Stat1 was also found to be acetylated upon co-transfection of CBP (Figure 6C). Presumably, CBP levels became limiting under conditions of Stat1 overexpression. A deletion mutant of Stat1 (ΔXbaI) lacking the Ser^{727} phosphorylation site retained acetylation, as indicated by a corresponding smaller band detected with an anti-acetyl-lysine antibody (Figure 6C). Hence, stress-induced serine phosphorylation of Stat1 (Ihle 2001), which has been described as a response to VPA treatment (Gurvich et al. 2004), should not be critical for Stat1 acetylation. Considering that the Stat1 ΔXbaI mutant resembles Stat1β, it is likely that this Stat1 splice variant can also be acetylated.

To identify lysine residues in Stat1α that are subject to acetylation, several Stat1 lysine mutants (Horvath et al. 1996; Yang et al. 1999; Meyer et al. 2002; Yang et al. 2002) were overexpressed in 293T cells and immunoprecipitated. Western blot analysis with an antibody against acetylated lysine showed that only the Stat1 $410,413^{K\rightarrow E}$ mutant (Meyer et al. 2002) was not acetylated under conditions in which wild-type Stat1 became strongly acetylated (Figure 6D). Since this was not due to decreased interaction of this mutant with CBP (data not shown), our experimental data suggest that lysines located in the Stat1 DNA-binding domain (DBD) are the major sites of acetylation.

Acetylation of Stat1α mediates p65-binding and confers susceptibility to apoptosis

Given that the acetylation of Stat1 correlates with the induction of apoptosis, interaction with p65 and repression of NF-κB signaling, we tested whether p65-associated Stat1α is acetylated *in vivo*. Indeed, an acetylated protein corresponding in size to Stat1α co-precipitated with NF-κB p65 from 2fTGH cell lysates after VPA treatment (Figure 6E). We confirmed that this acetylated protein is indeed Stat1 by reprobing the membrane with Stat1 antibody. Additionally, both, the acetylation signal and the signal for Stat1 were not detectable in the Stat1-negative U3A cell line. Thus, we conclude that at least a fraction of p65-associated Stat1α is acetylated *in vivo*.

We hypothesized that acetylation of Stat1α might render cells sensitive to HDACi-induced apoptosis. Therefore, we tested whether induction of apoptosis is specifically due to the acetylation of lysines within the DBD of Stat1α. Lysines K410 and K413 were replaced either with glutamine (K→Q) or arginine (K→R) resembling constitutively acetylated or non-acetylated states, respectively (Figure 6F). NW-1539 cells transfected with wild-type and corresponding mutant Stat1α expression vectors were either incubated with VPA or left untreated. Proliferation and apoptosis were scored by MTT and FACS analysis (Figure 7A). Equal expression was verified by Western blot (Figure 7B). Consistent with Figure 3A, overexpression of Stat1 together with VPA treatment led to reduced proliferation and apoptosis induction (Figure 6A). Transfection of the Stat1 mutant, in which K410 and K413 were replaced by glutamine ($410,413^{K\rightarrow Q}$) even enhanced the ability of Stat1α to confer HDACi sensitivity to NW-1539 cells and reduced proliferation. In contrast, substitution of K410 and K413 with arginine ($410,413^{K\rightarrow R}$) could not render cells sensitive to HDACi as measured by the ability of VPA to induce apoptosis (Figure 7A). In order to test whether these results are due to differential interactions of Stat1α mutants and NF-κB p65, we examined the association of endogenous p65 with ectopically expressed wild-type and mutant Stat1 proteins in U3A cells. Immunoprecipitates of p65 were analyzed for the presence of Stat1 by Western blotting. Results shown in Figure 7B confirm that treatment with VPA significantly enhances the association of wild-type Stat1α and p65.

Furthermore, the pseudo-acetylated Stat1α mutant 410,413$^{K\rightarrow Q}$ constitutively bound p65 *in vivo*, whereas Stat1α 410,413$^{K\rightarrow R}$ did not associate with p65 even after treatment with VPA (Figure 7B). We found that Stat1α 410,413$^{K\rightarrow Q}$ significantly reduced expression of the NF-κB target gene survivin independent of HDAC-inhibition. In contrast, Stat1α 410,413$^{K\rightarrow R}$ failed to reduce Survivin expression under identical conditions (Figure 7C). Furthermore, immunofluorescence analysis showed that nuclear p65 is reduced in NW-1539 cells only if wild-type Stat1 is expressed ectopically and cells are treated with HDACi. Stat1α 410,413$^{K\rightarrow Q}$ mimicked these effects, whereas expression of Stat1α 410,413$^{K\rightarrow R}$ did not increase cytoplasmic localization of p65 (Figure 7D; compare transfected and untransfected cells within each field). Moreover, expression of Stat1α 410,413$^{K\rightarrow Q}$ in NW-1539 cells reduced DNA-binding of NF-κB similar to overexpressed wild-type Stat1 in cells treated with VPA, whereas expression of Stat1α 410,413$^{K\rightarrow R}$ did not (Figure 7E). Based on these results, we propose a model in which acetylated Stat1α binds and sequesters NF-κB p65 in the cytoplasm, which interferes with NF-κB function (Figure 7F). As a consequence, cells become susceptible to apoptosis induction.

Discussion

A number of recent publications have shown that HDAC inhibitors (HDACi) can induce apoptosis in many tumor cell lines (Krämer et al. 2001; Kelly et al. 2002). However, the molecular mechanisms determining whether a particular cell line responds to HDACi treatment are not well understood. In this study we show that in melanoma cell lines resistance towards HDACi inversely correlates with Stat1 expression levels. HDACi-induced acetylation of lysines 410 and 413 within the DNA-binding domain of Stat1 promotes strong interaction with NF-κB p65. As a consequence, the level of nuclear p65 decreases significantly and DNA-binding of NF-κB is inhibited. This leads to the down-regulation of anti-apoptotic NF-κB target genes, thus shifting the balance towards cell death. This mechanism of altered cross-talk of signal transduction pathways provides an explanation how HDACi could down-regulate target gene expression.

HDACi-resistant and -sensitive melanoma cell lines

When we started to study the effects of HDACi on melanoma cell lines, we realized that they can be divided into resistant and sensitive sub-classes. This allowed us to investigate the underlying molecular mechanisms in a set of cell lines derived from the same type of tumor. Our data indicate that sensitive cell lines (e. g. SK-37) undergo programmed cell death via both, the extrinsic and the intrinsic apoptotic pathways (Figure 1). In sensitive cell lines HDACi treatment significantly decreases the expression of anti-apoptotic genes such as bcl-X_L, survivin and Stat5 which are bona fide target genes of NF-κB (Krämer et al. 2001; Hinz et al. 2002; De Schepper et al. 2003). In resistant cell lines, on the other hand, neither changes in expression levels of these genes nor apoptosis induction are detectable, although hyperacetylation of histones is readily apparent (Figures 2C and 4A).

A microarray analysis revealed that Stat1 is among those genes which are significantly up-regulated in sensitive melanoma cell lines in response to the HDACi VPA and TSA. These

findings were confirmed at the protein level (Figure 2A, B). Interestingly, Stat1 expression was very low (close to the detection limit) and not inducible in the HDACi-resistant cell lines NW-450 and NW-1539. Furthermore these cell lines, in contrast to HDACi-sensitive cells, did not respond to interferon α, which induces Stat1 signaling (Darnell 1997; Ihle 2001). In order to investigate whether these findings are merely correlative or whether Stat1 plays indeed a causative role in the induction of apoptosis in response to HDACi we introduced Stat1α into NW-1539 cells by lentiviral transduction. Our results show that expression of Stat1 in NW-1539 restored sensitivity of this cell line towards HDACi and interferon α (Figure 3A, B). The introduction of wild-type and mutant Stat1 into melanoma cells which initially had very low expression levels of Stat1 (Figures 3, 7) indicates that Stat1 is required but not sufficient to enter apoptosis. Additional actions of HDACi such as modulation of other signaling pathways and altered cell cycle regulation appear to be necessary.

The HDACi-resistant cell lines were originally established from patients who had undergone immunotherapy including interferon α treatment. We speculate that during this process interferon α resistant cells with defects in Stat1 signaling were selected. In principle both, mutations within the Stat1 gene as well as epigenetic silencing could shut down Stat1 expression. Our observation that the resistant cell lines NW-450 and NW-1539 re-express Stat1 when treated with 5-aza-cytidine highlights the relevance of DNA methylation in this context (O.H.K. and T.H. unpublished results). HDACi are being considered as candidate drugs for cancer therapy (Krämer et al. 2001; Kelly et al. 2002). According to our data, the combination of HDACi and interferon α or demethylating agents could be particularly effective in the treatment of melanomas. If this would turn out to be the case, Stat1 expression might serve as a useful marker for the prediction of clinical response.

Stat1 - NF-κB cross-talk

The finding that the expression of a subset of NF-κB target genes inversely correlates with Stat1 expression levels prompted us to analyze the DNA-binding activity of NF-κB using lysates from

cells with different Stat1 expression levels. A reduction of NF-κB DNA binding was only observed with VPA-treated Stat1-positive but not with Stat1-negative cell extracts (Figure 4). Remarkably, the amount of p65 in the nucleus drops significantly in response to HDACi treatment, and this effect can be inhibited by the nuclear export inhibitor LMB (Figure 5A). Since these results could be due to an interaction of both proteins we performed co-IP experiments. Indeed, we detected formation of a Stat1 - NF-κB complex upon HDACi treatment. Gel filtration experiments indicate that the molecular weight of this complex is in the mega-dalton range. Therefore, several additional proteins have to be involved (Figure 5). Although a potential cross-talk of Stat1 and NF-κB signaling pathways has been discussed in several reports (Chatterjee-Kishore et al. 2000; Suk et al. 2001; Shen and Lentsch 2004; Sizemore et al. 2004), unequivocal evidence for the physical association of these factors has not been published. This is most likely due to the fact that we observed a robust interaction only upon treatment of cells with HDACi. Additional experiments are required to establish whether the Stat1-dependent mechanism determining resistance or sensitivity towards HDACi represents a general principle relevant to many different types of tumor cells.

Acetylated Stat1 mediates suppression of anti-apoptotic NF-κB target genes

Acetylation is considered as a covalent modification which could, similar to phosphorylation affect the activity of a wide range of proteins by altering intermolecular interactions. However, a relatively limited number of acetylated regulatory proteins including p53, Ku70, NF-κB p65 and Stat3 is known (Kouzarides 2000; Chan et al. 2001; Chen and Greene 2003; Kiernan et al. 2003; Cohen et al. 2004; Yuan et al. 2005). In this report, we show that CBP can serve as an acetyltransferase for Stat1 and that acetylation of Stat1 lysine residues 410 and 413 regulates the interaction with NF-κB p65. Inhibition of HDAC-activity exerts negative effects on Stat1 signal transduction (Nusinzon and Horvath 2003). This finding provides a possible explanation why the transcriptional activity of Stat1 is reduced after HDAC-inhibition (Nusinzon and Horvath 2003; Sakamoto et al. 2004). In contrast to Stat1, Stat3 acetylation occurs on a C-terminal

residue and exerts positive effects on Stat3 signal transduction (Wang et al. 2005; Yuan et al. 2005). Based on interactions of endogenous proteins in Co-IP experiments, HDACs 1 and 3, but not HDACs 2 and 8, are likely candidates for enzymes which could deacetylate Stat1. It is conceivable that cell type-specific differences in expression or activity of HATs and HDACs could alter Stat1 acetylation levels and thereby modulate NF-κB signaling. Consistent with this hypothesis, HDACi can shift the dynamic equilibrium of Stat1 acetylation towards the fully acetylated state which in turn promotes complex formation with p65. The resulting down-regulation of anti-apoptotic NF-κB target genes could be a prototypical example for the HDACi-mediated inhibition of gene expression.

Interestingly, microarray experiments revealed that in cells exposed to HDACi about one third of significant changes in gene expression reflect repression instead of activation events (Van Lint et al. 1996; Mitsiades et al. 2004). This initially unexpected observation could be due to the induction of transcriptional repressors that do not require HDAC activity to function. Such an indirect mechanism would be rather slow as it requires *de novo* protein synthesis. On the other hand, the modulation of cross-talk between Stat1 and NF-κB signaling pathways we discovered is independent of protein synthesis and provides a plausible explanation for the rapid suppression of genes upon inhibition of HDAC activity.

Materials and methods

Drugs and Chemicals

Valproic acid, trichostatin A, prodidium iodide, LMB, Hoechst 33258, trypan blue and 4,5 dimethyl-2-yl 2,5-diphenyl tetrazolium bromide (MTT) were purchased from Sigma. Interferon-α was from Roche and Z-VAD-FMK and Ac-DEVD-pNA were supplied by Alexis.

Cell Lines, transfections and microscopy

SK-Mel-37, Mz-Mel-19, NW-Mel-1539, NW-Mel-450 (Jäger et al. 2002) (abbreviated as SK-37, Mz-19, NW-1539 or NW-450), Mz-Mel-5, Mz-Mel-7, NW-Mel-726, NW-Mel-745, 293T, 2fTGH and U3A cells were maintained in DMEM (Invitrogen) supplemented with 10% FCS (Gibco/Sigma), 1% penicillin/streptomycin and 5% L-glutamine (BioWhittaker) at 37 °C in a 5% CO_2 atmosphere. SK-Mel-28 and Malme-3-M cell lines were grown in RPMI containing the same additives. Cells were transfected using PEI (Sigma) for 293T or Lipofectamine (Invitrogen). Preparation and image analysis of cells were performed as described (Heger et al. 2001).

Preparation of cell lysates and immunoblotting

Lysate preparation and Western blot procedures were carried out as described (Standke et al. 1994; Krämer et al. 2003). Antibodies were obtained from Santa Cruz Biotechnology (Stat1, sc346/sc417; p65, sc8008; p50, sc7178; HDAC1, sc6298; HDAC3, sc8138/sc11417; Survivin, sc17779; Caspase 3, sc7272/sc7148; Tradd, sc1163; TBP, sc204; HA, sc7392/805; GFP, sc9996; mSin3, sc994), Sigma (Actin, A2066), Pharmingen (Bcl-X_L, 66461A; PARP, 556362), Transduction labs (Stat5, S21520) and NEB (Caspase 8, 9746; Caspase 9, 9501S; AcK, 9441/9681). The AcH4 antibody has been described (Göttlicher et al. 2001). Western blots were probed for Actin to ensure equal sample loading. Co-immunoprecipitation experiments were performed as described (Heinzel et al. 1997). For direct immunoprecipitations of Stat1α and NF-κB cells were lysed in RIPA-buffer. To detect interactions NETN buffer containing 0.1% NP-40 was used. TSA (1 µM) was added to preserve acetylation.

Measurement of proliferation and apoptosis

MTT assays were performed as described (Denizot and Lang 1986). The cellular DNA content was determined by PI flow cytometry (Göttlicher et al. 2001). Cell viability was also determined by trypan blue exclusion and a PI/Hoechst staining assay (Suk et al. 2001). Caspase 3 assays were performed with 200 µl of caspase 3 cleavage buffer (100 mM Tris pH 8.0, 10% sucrose, 150 mM NaCl, 0.1% CHAPS, 10 mM DTT), 2.5 µl of 2 mM Ac-DEVD-pNA and 50 µg protein.

Production of lentiviral particles

HA-Stat1α was cloned into the SacII site of the pHR'cPPT SIEW Sin vector (kindly provided by M. Scherr, Hannover) to yield pS-Stat1α-IEW. Lentiviral vector stocks were produced from 293T cells cotransfected with the pCMVΔR9.81 packaging construct (Zufferey et al. 1997) and the pMD.G envelope construct (Naldini et al. 1996). Effective transduction was confirmed by fluorescence microscopy, FACS and Western blot.

EMSA (gel retardation assay)

Radioactive DNA-binding assays were performed as described (Garcia et al. 1997). The NF-κB oligonucleotide (sc-2505) and supershift antibodies were purchased from Santa Cruz.

Plasmids

Untagged Stat1α was mutagenized by overlap extension PCR (Ho et al. 1989) using HA-Stat1 as template. The primers (Thermo Electron) used are:

KK: 5'AAAAGATCTATGTCTCAGTGGTACGAACTTCAGCAGC 3';
5'AAAGAATTCGTACTGTGTTCATCATACTGTCGAACTCTAC 3'

QQ: 5'GCAATTGCAAGAACAGCAAAATGCTGG 3';
5'CCAGCATTTTGCTGTTCTTGCAATTGC 3'

RR: 5'GCAATTGCGAGAACAGCGAAATGCTGG 3';
5'CCAGCATTTCGCTGTTCTCGCAATTGC 3'.

PCR products were cloned into pc3.1 TOPO (Invitrogen).

Acknowledgements

We thank A. Schimpf, G. Carra and H. Kunkel for excellent technical assistance, D. Zimmermann, I. Oehme and B. Dälken for help with this project and M. Göttlicher for critical reading of the manuscript. M. Zörnig and S. Hövelmann were invaluable discussion partners throughout the entire project. G. Stark, M. Müller and P. Heinrich generously provided cell lines. M. Scherr kindly provided the lentiviral expression vector, C. Glass, J. Darnell and U. Vinkemeier Stat1 expression vectors. This work was supported by a grant of the NGFN to T.H.

References

Blaheta, R.A. and Cinatl, J., Jr. 2002. Anti-tumor mechanisms of valproate: a novel role for an old drug. *Med Res Rev* **22**: 492-511.

Blobel, G.A. 2000. CREB-binding protein and p300: molecular integrators of hematopoietic transcription. *Blood* **95**: 745-55.

Chan, H.M., Krstic-Demonacos, M., Smith, L., Demonacos, C., and La Thangue, N.B. 2001. Acetylation control of the retinoblastoma tumour-suppressor protein. *Nat Cell Biol* **3**: 667-74.

Chatterjee-Kishore, M., Wright, K.L., Ting, J.P., and Stark, G.R. 2000. How Stat1 mediates constitutive gene expression: a complex of unphosphorylated Stat1 and IRF1 supports transcription of the LMP2 gene. *Embo J* **19**: 4111-22.

Chen, L.F. and Greene, W.C. 2003. Regulation of distinct biological activities of the NF-kappaB transcription factor complex by acetylation. *J Mol Med* **81**: 549-57.

Cohen, H.Y., Lavu, S., Bitterman, K.J., Hekking, B., Imahiyerobo, T.A., Miller, C., Frye, R., Ploegh, H., Kessler, B.M., and Sinclair, D.A. 2004. Acetylation of the C terminus of Ku70 by CBP and PCAF controls Bax-mediated apoptosis. *Mol Cell* **13**: 627-38.

Darnell, J.E., Jr. 1997. STATs and gene regulation. *Science* **277**: 1630-5.

De Schepper, S., Bruwiere, H., Verhulst, T., Steller, U., Andries, L., Wouters, W., Janicot, M., Arts, J., and Van Heusden, J. 2003. Inhibition of histone deacetylases by chlamydocin induces apoptosis and proteasome-mediated degradation of survivin. *J Pharmacol Exp Ther* **304**: 881-8.

Denizot, F. and Lang, R. 1986. Rapid colorimetric assay for cell growth and survival. Modifications to the tetrazolium dye procedure giving improved sensitivity and reliability. *J Immunol Methods* **89**: 271-7.

Garcia, R., Yu, C.L., Hudnall, A., Catlett, R., Nelson, K.L., Smithgall, T., Fujita, D.J., Ethier, S.P., and Jove, R. 1997. Constitutive activation of Stat3 in fibroblasts transformed by diverse oncoproteins and in breast carcinoma cells. *Cell Growth Differ* **8**: 1267-76.

Göttlicher, M., Minucci, S., Zhu, P., Krämer, O.H., Schimpf, A., Giavara, S., Sleeman, J.P., Lo, C.F., Nervi, C., Pelicci, P.G., and Heinzel, T. 2001. Valproic acid defines a novel class of HDAC inhibitors inducing differentiation of transformed cells. *Embo J* **20**: 6969-6978.

Gu, W. and Roeder, R.G. 1997. Activation of p53 sequence-specific DNA binding by acetylation of the p53 C-terminal domain. *Cell* **90**: 595-606.

Gurvich, N., Tsygankova, O.M., Meinkoth, J.L., and Klein, P.S. 2004. Histone deacetylase is a target of valproic acid-mediated cellular differentiation. *Cancer Res* **64**: 1079-86.

Heger, P., Lohmaier, J., Schneider, G., Schweimer, K., and Stauber, R.H. 2001. Qualitative highly divergent nuclear export signals can regulate export by the competition for transport cofactors in vivo. *Traffic* **2**: 544-55.

Heinzel, T., Lavinsky, R.M., Mullen, T.M., Söderström, M., Laherty, C.D., Torchia, J., Yang, W.M., Brard, G., Ngo, S.D., Davie, J.R., Seto, E., Eisenman, R.N., Rose, D.W., Glass, C.K., and Rosenfeld, M.G. 1997. A complex containing N-CoR, mSin3 and histone deacetylase mediates transcriptional repression. *Nature* **387**: 43-8.

Henderson, C., Mizzau, M., Paroni, G., Maestro, R., Schneider, C., and Brancolini, C. 2003. Role of caspases, Bid, and p53 in the apoptotic response triggered by histone deacetylase inhibitors trichostatin-A (TSA) and suberoylanilide hydroxamic acid (SAHA). *J Biol Chem* **278**: 12579-89.

Hinz, M., Lemke, P., Anagnostopoulos, I., Hacker, C., Krappmann, D., Mathas, S., Dorken, B., Zenke, M., Stein, H., and Scheidereit, C. 2002. Nuclear factor kappaB-dependent gene expression profiling of Hodgkin's disease tumor cells, pathogenetic significance, and link to constitutive signal transducer and activator of transcription 5a activity. *J Exp Med* **196**: 605-17.

Ho, S.N., Hunt, H.D., Horton, R.M., Pullen, J.K., and Pease, L.R. 1989. Site-directed mutagenesis by overlap extension using the polymerase chain reaction. *Gene* **77**: 51-9.

Horvath, C.M., Stark, G.R., Kerr, I.M., and Darnell, J.E., Jr. 1996. Interactions between STAT and non-STAT proteins in the interferon-stimulated gene factor 3 transcription complex. *Mol Cell Biol* **16**: 6957-64.

Huang, N., Katz, J.P., Martin, D.R., and Wu, G.D. 1997. Inhibition of IL-8 gene expression in Caco-2 cells by compounds which induce histone hyperacetylation. *Cytokine* **9**: 27-36.

Ihle, J.N. 2001. The Stat family in cytokine signaling. *Curr Opin Cell Biol* **13**: 211-7.

Inan, M.S., Rasoulpour, R.J., Yin, L., Hubbard, A.K., Rosenberg, D.W., and Giardina, C. 2000. The luminal short-chain fatty acid butyrate modulates NF-kappaB activity in a human colonic epithelial cell line. *Gastroenterology* **118**: 724-34.

Jäger, E., Karbach, J., Gnjatic, S., Jäger, D., Maeurer, M., Atmaca, A., Arand, M., Skipper, J., Stockert, E., Chen, Y.T., Old, L.J., and Knuth, A. 2002. Identification of a naturally processed NY-ESO-1 peptide recognized by CD8+ T cells in the context of HLA-B51. *Cancer Immun* **2**: 12.

Kelly, W.K., O'Connor, O.A., and Marks, P.A. 2002. Histone deacetylase inhibitors: from target to clinical trials. *Expert Opin Investig Drugs* **11**: 1695-713.

Kiernan, R., Bres, V., Ng, R.W., Coudart, M.P., El Messaoudi, S., Sardet, C., Jin, D.Y., Emiliani, S., and Benkirane, M. 2003. Post-activation turn-off of NF-kappa B-dependent transcription is regulated by acetylation of p65. *J Biol Chem* **278**: 2758-66.

Korzus, E., Torchia, J., Rose, D.W., Xu, L., Kurokawa, R., McInerney, E.M., Mullen, T.M., Glass, C.K., and Rosenfeld, M.G. 1998. Transcription factor-specific requirements for coactivators and their acetyltransferase functions. *Science* **279**: 703-7.

Kouzarides, T. 1999. Histone acetylases and deacetylases in cell proliferation. *Curr Opin Genet Dev* **9**: 40-8.

-. 2000. Acetylation: a regulatory modification to rival phosphorylation? *Embo J* **19**: 1176-9.

Krämer, O.H., Göttlicher, M., and Heinzel, T. 2001. Histone deacetylase as a therapeutic target. *Trends in Endocrinology and Metabolism* **12**: 294-300.

Krämer, O.H., Zhu, P., Ostendorff, H.P., Golebiewski, M., Tiefenbach, J., Peters, M.A., Brill, B., Groner, B., Bach, I., Heinzel, T., and Göttlicher, M. 2003. The histone deacetylase inhibitor valproic acid selectively induces proteasomal degradation of HDAC2. *Embo J* **22**: 3411-20.

Kumar, A., Commane, M., Flickinger, T.W., Horvath, C.M., and Stark, G.R. 1997. Defective TNF-alpha-induced apoptosis in STAT1-null cells due to low constitutive levels of caspases. *Science* **278**: 1630-2.

Mayo, M.W., Denlinger, C.E., Broad, R.M., Yeung, F., Reilly, E.T., Shi, Y., and Jones, D.R. 2003. Ineffectiveness of histone deacetylase inhibitors to induce apoptosis involves the transcriptional activation of NF-kappa B through the Akt pathway. *J Biol Chem* **278**: 18980-9.

Melnick, A. and Licht, J.D. 2002. Histone deacetylases as therapeutic targets in hematologic malignancies. *Curr Opin Hematol* **9**: 322-32.

Meyer, T., Begitt, A., Lodige, I., van Rossum, M., and Vinkemeier, U. 2002. Constitutive and IFN-gamma-induced nuclear import of STAT1 proceed through independent pathways. *Embo J* **21**: 344-54.

Mitsiades, C.S., Mitsiades, N.S., McMullan, C.J., Poulaki, V., Shringarpure, R., Hideshima, T., Akiyama, M., Chauhan, D., Munshi, N., Gu, X., Bailey, C., Joseph, M., Libermann, T.A., Richon, V.M., Marks, P.A., and Anderson, K.C. 2004. Transcriptional signature of histone deacetylase inhibition in multiple myeloma: biological and clinical implications. *Proc Natl Acad Sci U S A* **101**: 540-5.

Müller, M., Laxton, C., Briscoe, J., Schindler, C., Improta, T., Darnell, J.E., Jr., Stark, G.R., and Kerr, I.M. 1993. Complementation of a mutant cell line: central role of the 91 kDa polypeptide of ISGF3 in the interferon-alpha and -gamma signal transduction pathways. *Embo J* **12**: 4221-8.

Naldini, L., Blomer, U., Gallay, P., Ory, D., Mulligan, R., Gage, F.H., Verma, I.M., and Trono, D. 1996. In vivo gene delivery and stable transduction of nondividing cells by a lentiviral vector. *Science* **272**: 263-7.

Nusinzon, I. and Horvath, C.M. 2003. Interferon-stimulated transcription and innate antiviral immunity require deacetylase activity and histone deacetylase 1. *Proc Natl Acad Sci U S A* **100**: 14742-7.

Perkins, N.D. 2004. NF-kappaB: tumor promoter or suppressor? *Trends Cell Biol* **14**: 64-9.

Sakamoto, S., Potla, R., and Larner, A.C. 2004. Histone deacetylase activity is required to recruit RNA polymerase II to the promoters of selected interferon-stimulated early response genes. *J Biol Chem* **279**: 40362-7.

Schreiber, S.L. and Bernstein, B.E. 2002. Signaling network model of chromatin. *Cell* **111**: 771-8.

Shen, H. and Lentsch, A.B. 2004. Progressive dysregulation of transcription factors NF-kappa B and STAT1 in prostate cancer cells causes proangiogenic production of CXC chemokines. *Am J Physiol Cell Physiol* **286**: C840-7.

Sizemore, N., Agarwal, A., Das, K., Lerner, N., Sulak, M., Rani, S., Ransohoff, R., Shultz, D., and Stark, G.R. 2004. Inhibitor of kappaB kinase is required to activate a subset of interferon gamma-stimulated genes. *Proc Natl Acad Sci U S A* **101**: 7994-8.

Standke, G.J., Meier, V.S., and Groner, B. 1994. Mammary gland factor activated by prolactin on mammary epithelial cells and acute-phase response factor activated by interleukin-6 in liver cells share DNA binding and transactivation potential. *Mol Endocrinol* **8**: 469-77.

Strahl, B.D. and Allis, C.D. 2000. The language of covalent histone modifications. *Nature* **403**: 41-5.

Suk, K., Chang, I., Kim, Y.H., Kim, S., Kim, J.Y., Kim, H., and Lee, M.S. 2001. Interferon gamma (IFNgamma) and tumor necrosis factor alpha synergism in ME-180 cervical cancer cell apoptosis and necrosis. IFNgamma inhibits cytoprotective NF-kappa B through STAT1/IRF-1 pathways. *J Biol Chem* **276**: 13153-9.

Thornberry, N.A. and Lazebnik, Y. 1998. Caspases: enemies within. *Science* **281**: 1312-6.

Van Lint, C., Emiliani, S., and Verdin, E. 1996. The expression of a small fraction of cellular genes is changed in response to histone hyperacetylation. *Gene Expr* **5**: 245-53.

Vrana, J.A., Decker, R.H., Johnson, C.R., Wang, Z., Jarvis, W.D., Richon, V.M., Ehinger, M., Fisher, P.B., and Grant, S. 1999. Induction of apoptosis in U937 human leukemia cells by suberoylanilide hydroxamic acid (SAHA) proceeds through pathways that are regulated by Bcl-2/Bcl-XL, c-Jun, and p21CIP1, but independent of p53. *Oncogene* **18**: 7016-25.

Wang, R., Cherukuri, P., and Luo, J. 2005. Activation of Stat3 sequence-specific DNA binding and transcription by p300/CBP mediated acetylation. *J Biol Chem*.

Wang, Y., Wu, T.R., Cai, S., Welte, T., and Chin, Y.E. 2000. Stat1 as a component of tumor necrosis factor alpha receptor 1-TRADD signaling complex to inhibit NF-kappaB activation. *Mol Cell Biol* **20**: 4505-12.

Weiss, C., Schneider, S., Wagner, E.F., Zhang, X., Seto, E., and Bohmann, D. 2003. JNK phosphorylation relieves HDAC3-dependent suppression of the transcriptional activity of c-Jun. *Embo J* **22**: 3686-95.

Wolffe, A.P. and Hayes, J.J. 1999. Chromatin disruption and modification. *Nucleic Acids Res* **27**: 711-20.

Wong, L.H., Sim, H., Chatterjee-Kishore, M., Hatzinisiriou, I., Devenish, R.J., Stark, G., and Ralph, S.J. 2002. Isolation and characterization of a human STAT1 gene regulatory element. Inducibility by interferon (IFN) types I and II and role of IFN regulatory factor-1. *J Biol Chem* **277**: 19408-17.

Yang, E., Henriksen, M.A., Schaefer, O., Zakharova, N., and Darnell, J.E., Jr. 2002. Dissociation time from DNA determines transcriptional function in a STAT1 linker mutant. *J Biol Chem* **277**: 13455-62.

Yang, E., Wen, Z., Haspel, R.L., Zhang, J.J., and Darnell, J.E., Jr. 1999. The linker domain of Stat1 is required for gamma interferon-driven transcription. *Mol Cell Biol* **19**: 5106-12.

Yuan, Z.L., Guan, Y.J., Chatterjee, D., and Chin, Y.E. 2005. Stat3 dimerization regulated by reversible acetylation of a single lysine residue. *Science* **307**: 269-73.

Zufferey, R., Nagy, D., Mandel, R.J., Naldini, L., and Trono, D. 1997. Multiply attenuated lentiviral vector achieves efficient gene delivery in vivo. *Nat Biotechnol* **15**: 871-5.

Legends

Figure 1. HDACi induce apoptosis in SK-37 cells.

(A) The proliferation of SK-37 and NW-1539 melanoma cells was determined by MTT test after exposure to VPA (0.5 - 5 mM) or TSA (100 nM) for 48 h (SK-37) or 72 h (NW-1539); 0, untreated cells.

(B) Induction of activated Caspase 9 (Casp 9, activation denoted by an asterisk) and cleavage of Caspase 8 (Casp 8 fl) into the active subunits p43/41/18 were detected by Western blot after treatment of SK-37 cells with VPA (V, 1.5 mM) or TSA (T, 100 nM) for 48 h. Caspase 3 activity was measured by conversion of Ac-DEVD-pNA to pNA, which has an absorption peak at 405 nm. This increase is given relative to the activity of lysates from untreated cells (Ctl). HDACi-induced conversion of Caspase 3 (Casp 3 fl) to the active p17/19 subunits was analyzed in SK-37 and NW-450 cells.

(C) Proteolytic cleavage of PARP and apoptotic chromatin fragmentation induced by VPA (1.5 mM) or TSA (100 nM) after 48 h were detected by Western blot and PI FACS analysis. Co-treatment of SK-37 cells with Z-VAD-FMK (Z, 100 µM) blocks HDACi-induced apoptosis.

Figure 2. Correlation of Stat1 expression and apoptosis induction.

(A) The time- and dose-dependent increase of Stat1 expression was investigated by Western blot. SK-37 cells were exposed to 1.5 mM VPA or 100 nM TSA for the indicated periods of time. Alternatively, cells were treated for 24 h with different concentrations of VPA (0.1-1.5 mM) or TSA (10-300 nM) as indicated or left untreated (0).

(B) Expression of Stat1α in SK-37 and NW-450 melanoma cells treated with 1.5 mM VPA (V), 100 nM TSA (T) or left untreated (C) or for 24 h was analyzed by Western blot.

(C) Expression of Stat1 and accumulation of hyperacetylated histone H4 (AcH4) in SK-37 and NW-1539 cells after 24 h were analyzed by Western blot. Cells were treated with VPA (V, 1.5 mM), TSA (T, 30 nM) or left untreated (C)

(D) Sensitivity of melanoma cell lines to VPA (V, 1.5 mM) and interferon α (α, 10^3 U/ml) was determined by MTT assay. Enhanced induction of apoptosis after treatment of SK-37 cells with VPA and interferon α (α/V) was detected by PI FACS analysis.

Figure 3. Stat1 sensitizes resistant melanoma cells to HDACi-induced apoptosis.

(A) Western blot analysis was employed to detect Stat1 expression and induction of apoptosis in NW-1539 cells transduced with SIEW (vector) or S-Stat1α-IEW (Stat1) and treated with VPA (1.5 mM) for 48 h. Asterisks denote activated forms of Caspase 3 or Caspase 8.

(B) DNA fragmentation was analyzed by PI FACS analysis after treatment with VPA (1.5 mM) or VPA and IFN-α (10^3 U/ml) for 60 h; Ctl, untreated cells.

Figure 4. Expression of Stat1 interferes with NF-κB DNA-binding in cells exposed to HDACi.

(A) Expression of NF-κB target genes after HDAC-inhibition was investigated by Western blot analysis of SK-37 and NW-1539 cell lysates. Cells were incubated with 1.5 mM VPA (V), 30 nM TSA (T) or left untreated (C) for 24 h.

(B) NF-κB was analyzed by EMSA of lysates from SK-37, NW-1539 and transduced NW-1539 cells (vector or Stat1), which were either untreated or treated with VPA (1.5 mM) for 48 h. Identity of the NF-κB-DNA complex was verified by p65 and p50 antibody supershifts (SS-AB).

Figure 5. HDCAi-induced complex formation of Stat1α and NF-κB p65.

(A) Interaction and co-localization of Stat1α and NF-κB p65 in SK-37 cells treated with VPA (1.5 mM, 24 h) and/or LMB (10 nM) were analyzed by immunofluorescence microscopy (Ctl, untreated). Cy3- and FITC-labeled secondary antibodies were used for detection of Stat1 and NF-κB .

(B) Exclusion of p65 from the nuclear compartment after treatment of SK-37 cells with VPA (1.5 mM) or TSA (100 nM) for 24 h was confirmed by cellular fractionation and p65 Western blot. Reprobing was done with antibodies against Stat1. The affinity of the Stat1α antibody is not

sufficient to detect nuclear Stat1. All other proteins detected serve as loading and fractionation controls.

(C) U3A and 2fTGH cells were analyzed for cytoplasmic retention of p65 after incubation with 1.5 mM VPA (V) for 24 h by Western blot of cytosolic and nuclear fractions.

(D) Interaction of Stat1α and NF-κB p65 in SK-37 cell lysates was investigated by Western blot of specific immunoprecipitations (IP; Ctl, untreated; V, 1.5 mM VPA, 24 h; Pre, pre-immune serum). Input lanes and IP-efficiencies are shown to allow comparison of protein amounts used.

(E) The composition of Stat1 complexes in SK-37 cells after treatment with VPA (1.5 mM, 48 h) was investigated by Western blot analysis of Superose 6 column fractions. IP was used to verify the interaction of Stat1α with NF-κB.

(F) HDAC1 and HDAC3 were precipitated from whole cell extracts (IP). Western blot analysis was performed with an antibody against Stat1α/β.

Figure 6. Acetylation of Stat1.

(A) SK-37 cells were either treated with VPA (1.5 mM) or left untreated for 24 h. Endogenous Stat1α or NF-κB p65 were immunoprecipitated from RIPA lysates and analyzed by Western blot with an antibody recognizing acetylated lysines (anti-AcLys, left). Reprobing of the same membrane confirms that the acetylation signal corresponds to Stat1α and shows efficiency and specificity of the immunoprecipitation (IP). Anti-AcLys immunoprecipitates from RIPA lysates were probed with antibodies recognizing Stat1α/β or NF-κB p65. Pre-immune serum was used as a control. Input lanes show 2% of the extract used for IP.

(B) Increasing amounts of a CBP expression vector (1; 5; 10 µg) were transfected into 293T cells. Stat1α was precipitated from RIPA lysates and probed with anti-AcLys. IPs with pre-immune serum and IPs from cells transfected with the empty vector pc3.1 (10 µg) are controls. TNT-translated HA-Stat1 was acetylated *in vitro* as described (Gu and Roeder 1997) using immunoprecipitated CBP.

(C) Acetylation levels of HA-Stat1ΔXbaI compared to full-length HA-Stat1α were determined by IP from 293T cell lysates as described in *(A)*. Cells were transfected with recombinant Stat1 and CBP vectors at a ratio of 5:1.

(D) The experiment was performed as in *(C)*, except that HA-Stat1α or GFP-Stat1 410,413$^{K\rightarrow E}$ were transfected.

(E) NF-κB p65 was immunoprecipitated from 2fTGH or U3A cell extracts. Presence and acetylation of Stat1α were detected by Western blot as described in *(A)*. Cells were treated with 1.5 mM VPA for 24 h or left untreated.

(F) Schematic representation of Stat1α showing positions of acetylated lysines and mutants generated. NTD, N-terminal domain; CC, coiled coil, DBD, DNA-binding domain; LD, linker domain; TAD, transcriptional activation domain. Mutants are designated QQ (mutation of both, K410 and K413 to Q) and RR (mutation of both, K410 and K413 to R).

Figure 7. Identification of Stat1α acetylation as critical regulator of HDACi-induced apoptosis.

(A) NW-1539 cells were transfected with Stat1α (WT), lysine mutants or equal amounts of empty vector (pc3.1). Proliferation and apoptosis were scored 72 h later by MTT and PI FACS-analysis, respectively. WT, wild type; QQ, 410,413$^{K\rightarrow Q}$; RR, 410,413$^{K\rightarrow R}$; -, untreated; V, 1.5 mM VPA.

(B) Interaction of overexpressed WT and mutant Stat1α (QQ, RR) with NF-κB p65 in U3A cells was analyzed by immunoprecipitation and Western blot. Cells were incubated with 1.5 mM VPA for 48 h or left untreated. Input lanes are 2% of the lysate used for IP and are shown at expositons allowing signal comparison.

(C) U3A cells were transfected and treated as described in *(B)*. Survivin expression was analyzed by Western blot. Detection of Actin and AcH4 serve as loading and treatment controls, respectively.

(D) p65 localization was analyzed by immunofluorescence microscopy of NW-1539 cells transfected and treated as described in *(B)*. Note: Compare transfected and non-transfected cells within each field.

(E) DNA-binding of NF–κB was investigated by EMSA with cell lysates of NW-1539 cells transfected and treated as described in *(B)*.

(F) Model for acetylation-dependent Stat1 - NF-κB cross-talk.

Krämer *et al.*, Figure 1

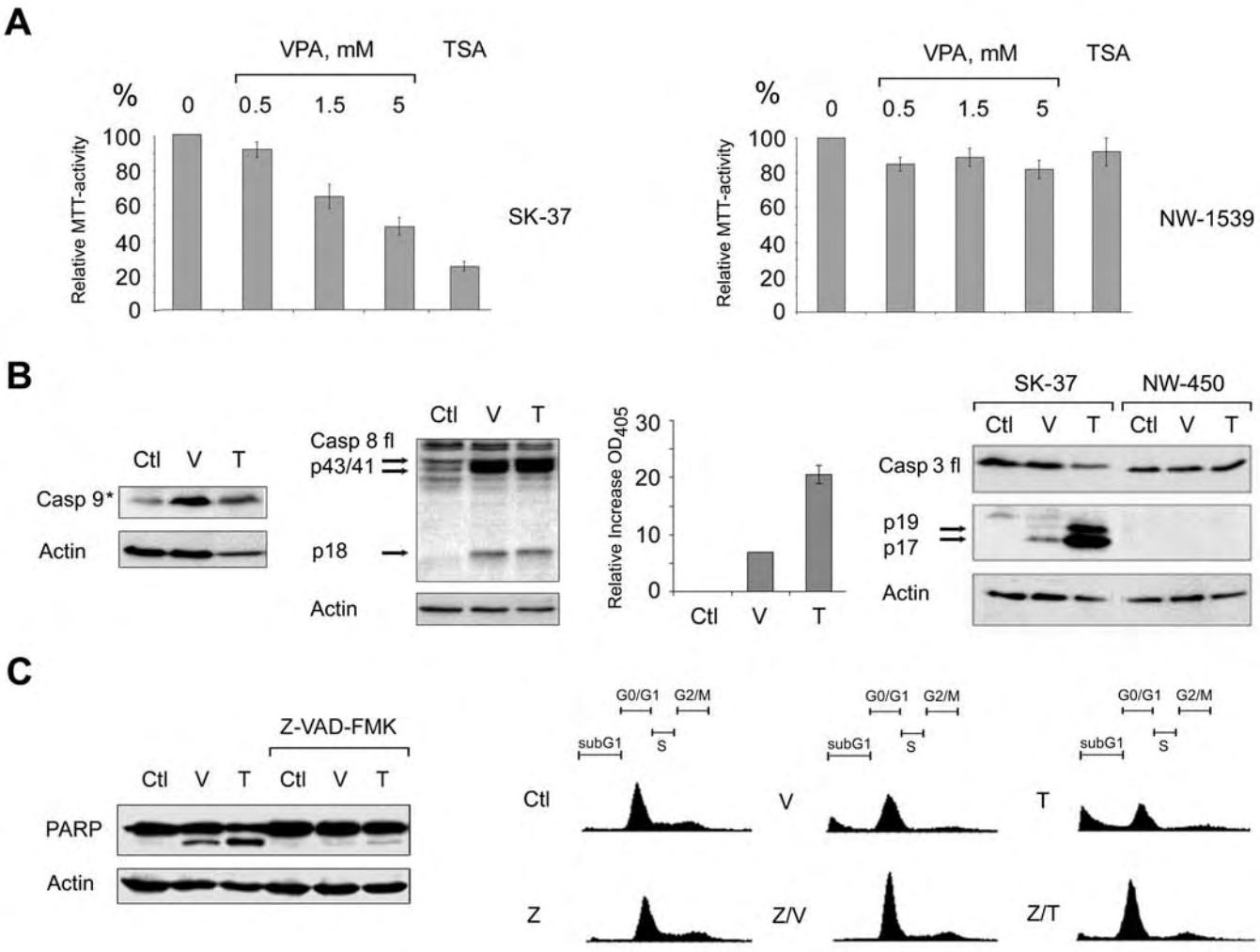

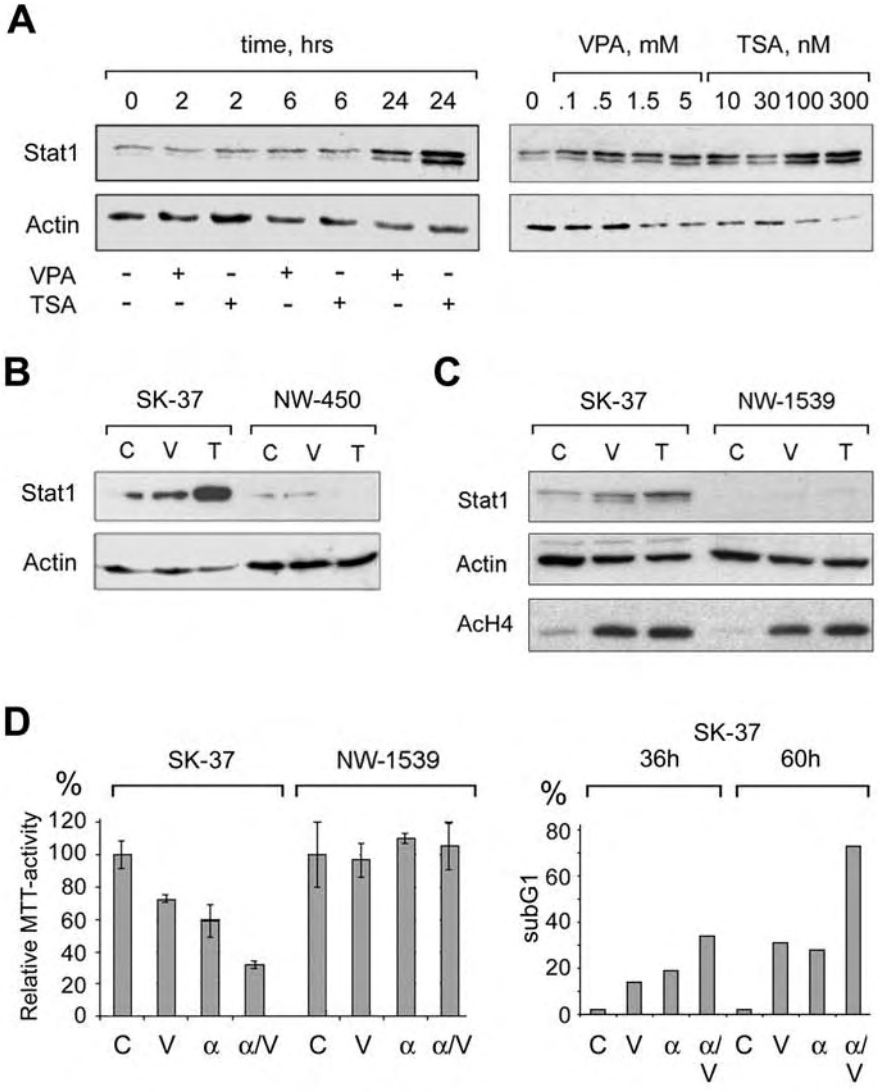
A
time, hrs
0 2 2 6 6 24 24
VPA, mM
TSA, nM
0 .1 .5 1.5 5 10 30 100 300
Stat1
Actin
VPA - + - + - + -
TSA - - + - + - +
B
SK-37
NW-450
C V T C V T
Stat1
Actin
C
SK-37
NW-1539
C V T C V T
Stat1
Actin
AcH4
D
SK-37
NW-1539
%
Relative MTT-activity
120
100
80
60
40
20
0
C V α α/V C V α α/V
SK-37
36h
60h
%
subG1
80
60
40
20
0
C V α α/V C V α α/V

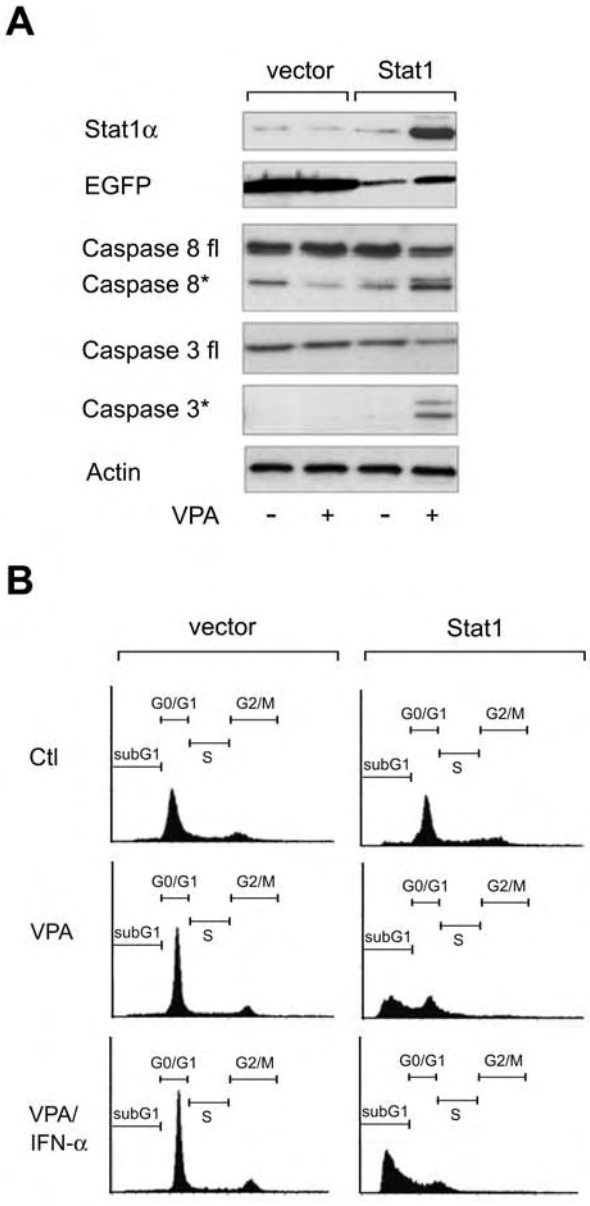
A
vector
Stat1
Stat1α
EGFP
Caspase 8 fl
Caspase 8*
Caspase 3 fl
Caspase 3*
Actin
VPA - + - +
B
vector
Stat1
Ctl
VPA
VPA/
IFN-α
G0/G1
G2/M
subG1
S

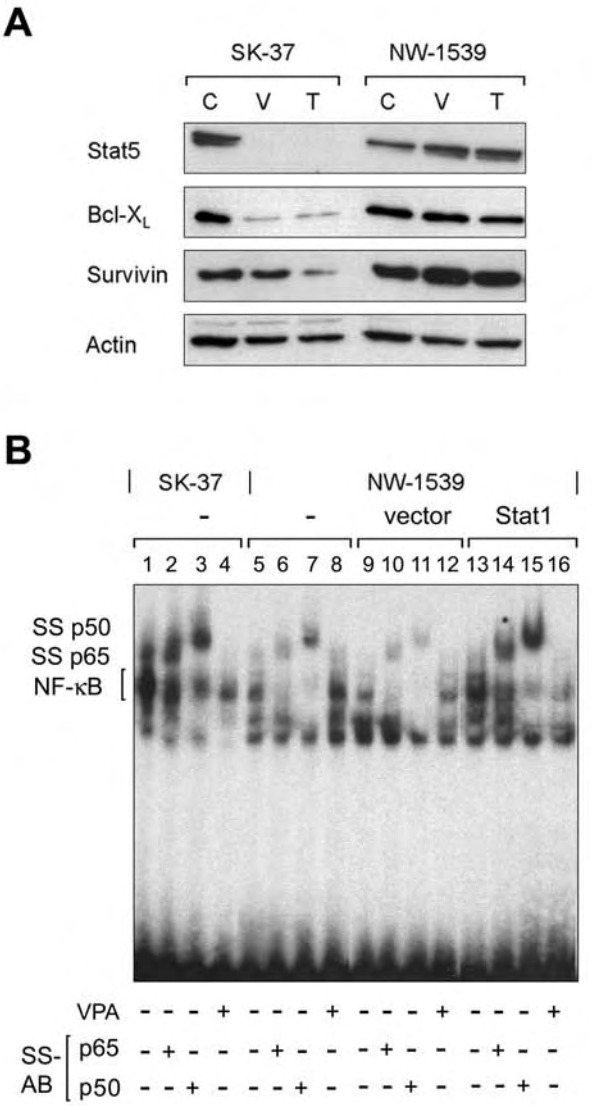
A
SK-37
NW-1539
C V T C V T
Stat5
Bcl-X$_L$
Survivin
Actin
B
SK-37
NW-1539
-
-
vector
Stat1
1 2 3 4 5 6 7 8 9 10 11 12 13 14 15 16
SS p50
SS p65
NF-κB
VPA - - - + - - - + - - - + - - - +
SS-AB p65 - + - - - + - - - + - - - + - -
SS-AB p50 - - + - - - + - - - + - - - + -

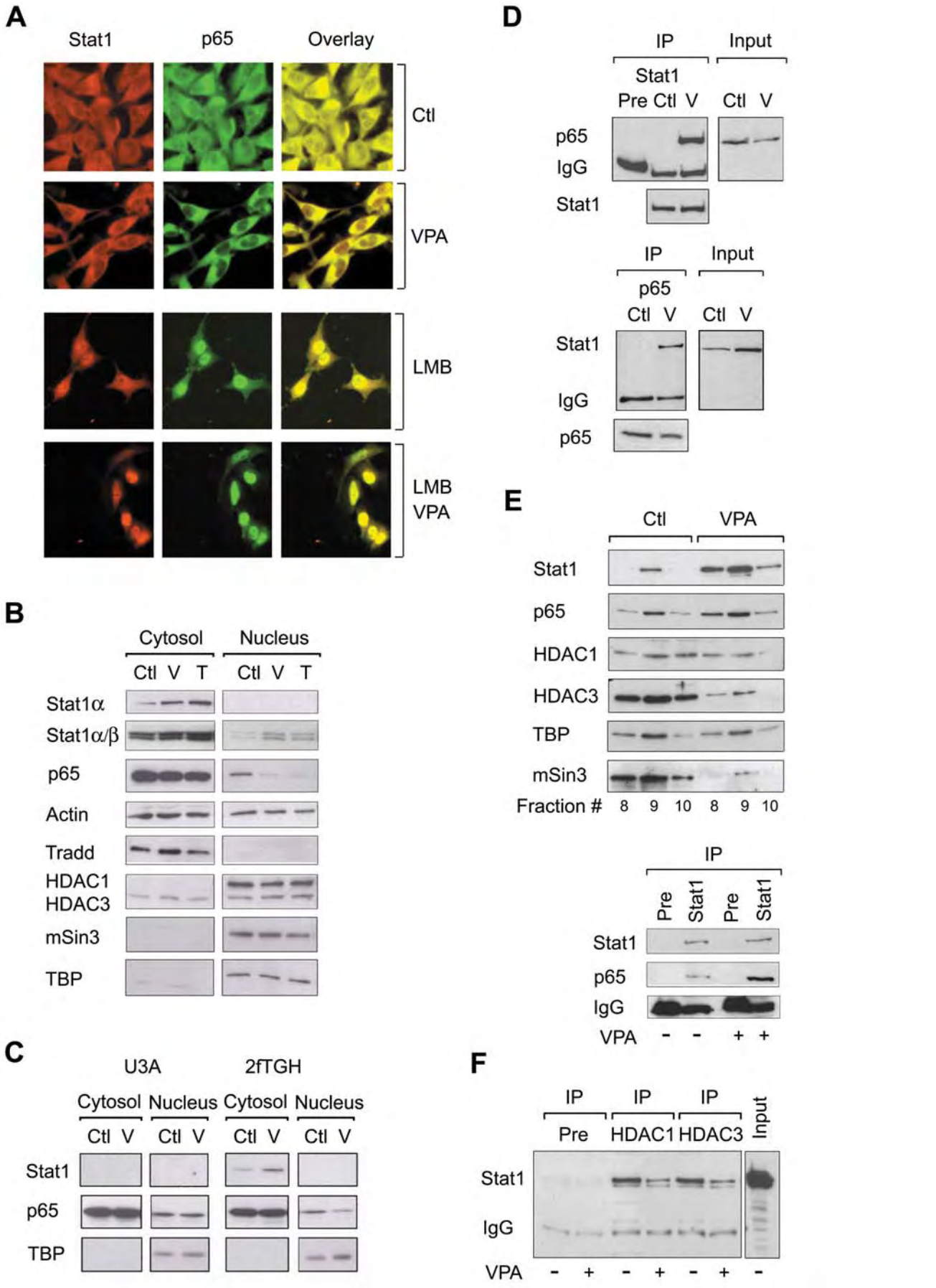
A
Stat1
p65
Overlay
Ctl
VPA
LMB
LMB
VPA
B
Cytosol
Nucleus
Ctl V T
Ctl V T
Stat1α
Stat1α/β
p65
Actin
Tradd
HDAC1
HDAC3
mSin3
TBP
C
U3A
2fTGH
Cytosol
Nucleus
Cytosol
Nucleus
Ctl V
Ctl V
Ctl V
Ctl V
Stat1
p65
TBP
D
IP
Input
Stat1
Pre Ctl V
Ctl V
p65
IgG
Stat1
IP
Input
p65
Ctl V
Ctl V
Stat1
IgG
p65
E
Ctl
VPA
Stat1
p65
HDAC1
HDAC3
TBP
mSin3
Fraction # 8 9 10 8 9 10
IP
Pre
Stat1
Pre
Stat1
Stat1
p65
IgG
VPA - - + +
F
IP
IP
IP
Input
Pre
HDAC1
HDAC3
Stat1
IgG
VPA - + - + - + -

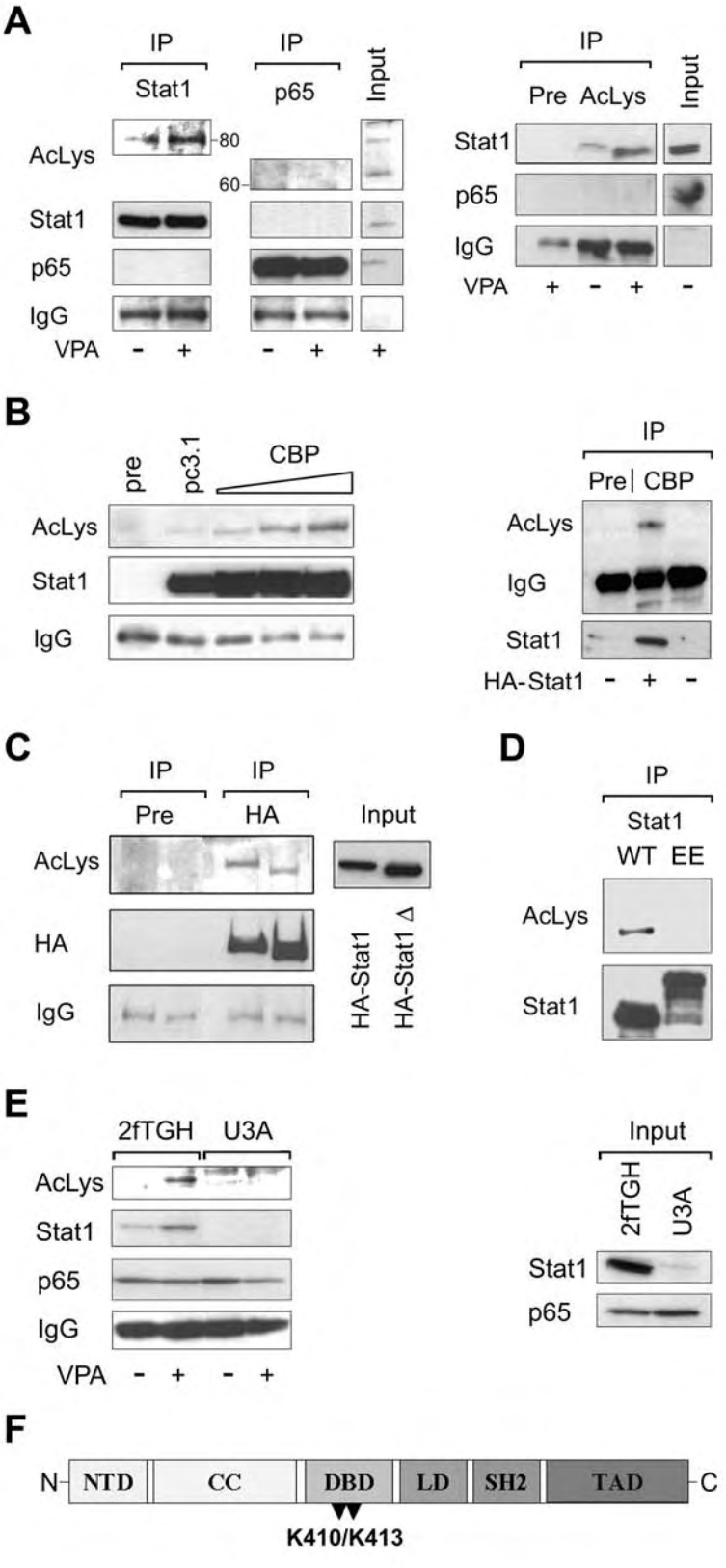
A
IP
Stat1
IP
p65
Input
AcLys
80
60
Stat1
p65
IgG
VPA - + - + +
IP
Pre AcLys
Input
Stat1
p65
IgG
VPA + - + -
B
pre
pc3.1
CBP
AcLys
Stat1
IgG
IP
Pre CBP
AcLys
IgG
Stat1
HA-Stat1 - + -
C
IP
Pre
IP
HA
Input
AcLys
HA
IgG
HA-Stat1
HA-Stat1 Δ
D
IP
Stat1
WT EE
AcLys
Stat1
E
2fTGH
U3A
AcLys
Stat1
p65
IgG
VPA - + - +
Input
2fTGH
U3A
Stat1
p65
F
N
NTD
CC
DBD
LD
SH2
TAD
C
K410/K413

Krämer *et al.*, Figure 7

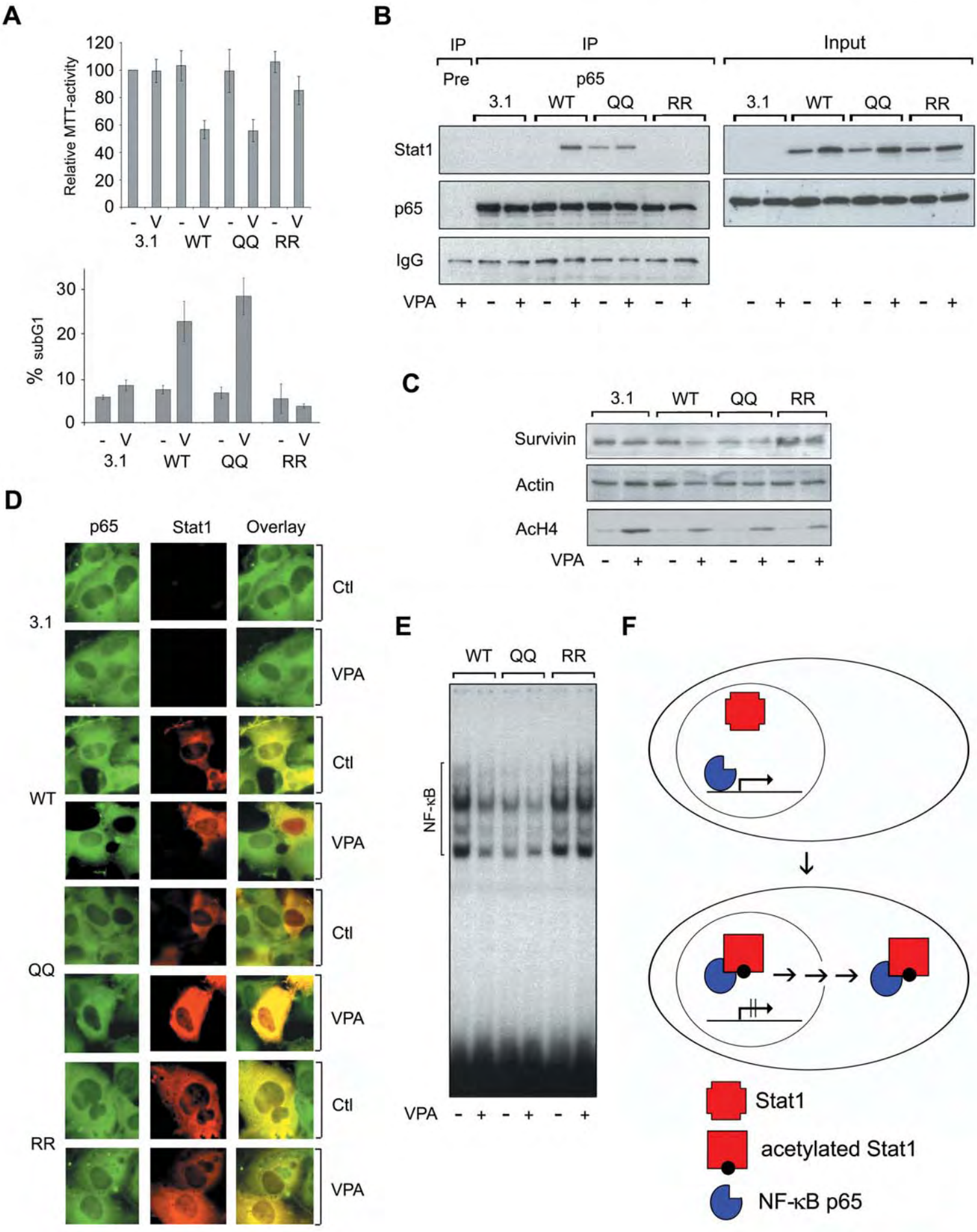

3

Nuclear export is essential for the biological activity of survivin - Novel aspects to target the survivin pathway in cancer

Shirley K. Knauer, Oliver Krämer[1], Thomas Knösel[2], Knut Engels[3], Franz Rödel[4], Hartmut Walendzik[5], Adoriàn F. Kovács[5], Negusse Habtemichael, Jürgen Brieger[6], Wolf Mann[6], Thorsten Heinzel[1], Iver Petersen[2] and Roland H. Stauber‡

Georg-Speyer-Haus, Institute for Biomedical Research, Paul-Ehrlich-Str. 42–44, D-60596 Frankfurt, Germany

[1]Institute for Cell biology, University of Jena, Germany

[2]Institute of pathology, Charité – CCM, Medical Faculty of the Humboldt-University Berlin

[3]Department of Pathology, University of Frankfurt, D-60596 Frankfurt, Germany

[4]Department of Radiation Oncology, University of Erlangen-Nuremberg, Germany

[5]Maxillofacial Plastic Surgery, Johann Wolfgang Goethe-Universität Frankfurt, D-60596 Frankfurt, Germany

[6]Department of Otorhinolaryngology, University Hospital of Mainz, Germany
Langenbeckstr. 1, 55101 Mainz, Germany

‡To whom correspondence should be addressed:
Roland H. Stauber, Ph.D.
Georg-Speyer-Haus
Institute for Biomedical Research
Paul-Ehrlich-Str. 42–44
D-60596 Frankfurt, Germany
Phone: (+49) 69 63395-222
Fax: (+49) 69 63395-145
E-mail: stauber@em.uni-frankfurt.de

Running title: survivin nuclear export

Key words: survivin, nucleocytoplasmic transport; Crm1; apoptosis; colorectal cancer; head and neck cancer; caspase-3; LMB; radiotherapy; cisplatin; valproic acid, cancer therapy

Abstract

Survivin functions as an apoptosis inhibitor and a regulator of cell division during development and tumorigenesis, and is thus regarded an attractive target for tumor therapy. We found survivin overexpressed in head and neck as well as in colorectal cancers and identified an evolutionary conserved Crm1 dependent nuclear export signal (NES) in survivin, present also in the splice variants 2B and 3B, but absent in the splice variants ΔExon3 and 2α. Although, survivin was detectable in both, the cytoplasm and the nucleus in tumors, survivin does not contain an active nuclear import signal and appears to enter the nucleus by passive diffusion. Importantly, nuclear export was required for survivin mediated protection against chemo- and radiotherapy-induced apoptosis and also for its function as a chromosomal passenger. In dividing cells, the NES mediated tethering of survivin to the mitotic machinery and thus, was required for proper execution of cytokinesis. Export mediated cytoplasmic localization in interphase cells secured efficient direct or indirect interference with caspases. The clinical relevance of our finding was supported by showing that preferential nuclear localization of survivin correlated with enhanced survival in colorectal cancer patients. Cell culture experiments suggested interference with the nuclear export machinery as one mechanism to promote survivin's nuclear accumulation. In conclusion, nuclear export is essential for the pivotal biological activity of survivin, and thus, interfering specifically with survivin's nuclear export will be a promising strategy for anti-cancer therapies.

Introduction

Evasion from apoptosis as well as enhanced proliferation are invariant molecular characteristics of human cancer (1), which facilitate the acquisition of additional cancer traits promoting resistance to therapy and disseminated disease. Among various mechanisms, escape from apoptosis can be the result of deregulated overexpression of apoptosis inhibitors (2, 3). A major therapeutic and prognostic interest is focused on survivin (3, 4), which at 16.5 kDa, is the smallest mammalian member of the inhibitor of apoptosis (IAP) gene family (5). Survivin contains a single Baculovirus IAP Repeat (BIR) and exists as a stable homodimer in solution (6). A single-copy survivin gene located on chromosome 17q25 gives rise also to the four alternatively spliced survivin transcripts survivin-2B, -3B, -ΔEx-3 and -2α (7-9) and references within). Survivin is largely undetectable in differentiated tissues, but is expressed in most human tumors and correlates with reduced tumor cell apoptosis, abbreviated patient survival, accelerated rates of recurrences, and increased resistance to chemo- and radiotherapy (see 3, 10, 11, and references within). The molecular mechanisms, by which survivin and in particular survivin splice variants counteract apoptosis and facilitate cell division, have been extensively explored, but are not yet understood. The large amount of data reported so far provide considerable evidence that survivin acts as a link between the apoptotic process and the checkpoints that control mitotic progression (see 12, 13). This assumption is also supported by the dynamic intracellular localizations of survivin reported, which range from predominantly cytoplasmic, nuclear, mitochondrial, to components of the mitotic apparatus (reviewed in 8, 13, 14).

Although, the low molecular weight would allow survivin to access intracellular compartments by passive diffusion, regulated subcellular localization in general provides an attractive way to control the activity of proteins (15), which has been proposed also for key players of apoptosis (referenced in (16). Nucleocytoplasmic transport for instance is regulated by specific signals and transport receptors, and takes place through the nuclear pore complex (17). Active nuclear import requires energy and is mediated by short stretches of basic amino acids, termed nuclear localization signals (NLS), which interact with import receptors (reviewed in 15). The best characterized nuclear export signals (NESs) consist of a short leucine-rich stretch of amino acids, interact with the export receptor Crm1 and depend on the RanGTP/GDP axis (18 and references therein). Active transport signals have been identified in an increasing number of cellular proteins executing crucial heterogeneous biological functions (15), and have been suggested also for survivin (reviewed in 12).

Interfering specifically with regulated nucleocytoplasmic transport of proteins as a novel therapeutic principle has recently attracted major interest by academia and industry (reviewed in 19). Consequently, to conclusively credential the survivin pathway for novel cancer therapeutics we thoroughly characterized the molecular regulation of survivin's

dynamic localization and analyzed its consequences for the tumor promoting functions of survivin.

Complementary experimental approaches demonstrated that all mammalian survivin homologs are actively exported via the Crm1 pathway and contain a conserved leucine-rich nuclear export signal. Importantly, active nuclear export of survivin was essential for its protection against apoptosis and for tethering survivin to the mitotic machinery. Our data provide a molecular rational why cancer patients displaying predominantly nuclear survivin showed improved survival. In addition, our study suggests that targeting survivin's nuclear export but not import pathway by molecular decoys may represent a novel therapeutic strategy.

Materials and Methods

Patient Characteristics and Biopsy Samples. Tissue samples were obtained from patients undergoing surgical resection between 1998 and 2004 at the Charité University Medical Center Berlin, the Department of Radiation Oncology of the University Erlangen-Nuremberg, the Department of Otolaryngology of the University Mainz, and the Department of Maxillofacial Plastic Surgery of the University Frankfurt. The study protocols were approved by the local ethics committee after obtaining the patients' informed consent to participate in the study and processed anonymously. All cases were diagnosed histopathologically as colorectal carcinoma (CRC) or head and neck squamous carcinoma (HNSCC), respectively, and staged according to the TNM classification. The biopsy of macroscopically normal mucosa (NOM) was taken at a distance of >3 cm surrounding the tumor location. Tissue specimens were flash frozen in liquid nitrogen and stored until extraction of mRNA.

RNA extraction, reverse transcription and quantitative real-time PCR analysis (RT-qPCR). Total RNA was purified from patient material or cells using TRIzol® reagent (Invitrogen Life Technologies, Karlsruhe, Germany) and quality controlled as described (20). Changes in mRNA levels were compared by reverse transcription (RT) and subsequent quantitative real-time PCR analysis as described (20). To define the relative gene expression, the PCR product from each tumor sample was compared with NOM from the same patient. The relative expression ratio (R) of target gene was calculated using the equation:

$$R = \frac{(E_{\text{target}})^{\Delta CP_{\text{target (control-sample)}}}}{(E_{\text{ref}})^{\Delta CP_{\text{ref (control-sample)}}}}$$, based on its real-time PCR efficiencies E, the crossing point (CP) difference of the tumor sample versus NOM in comparison to the expression of the reference gene glyceraldehyde-3-phosphate dehydrogenase (GAPDH) (20). Primers were*:* *Hu survivin WT*, 5'-ATGGCCGAGGCTGGCTTCATC-3' (sense) and 5'-GCGCAACCGGACGAATGCT-3' (antisense); *Hu survivinΔExon3,* 5'-ATGGCCGAGGCTGGCTTCATC-3' (sense) and 5'-GCACTTTCTCCGCAGTTTCCTC-3' (antisense).

Statistical analysis. Survival analysis was applied to all patients and was performed with SPSS software (SPSS, Munich, Germany) as described (21). The differences of the Kaplan-Meier survival curves were tested for statistical significance with the log-rank test, and the 95 percent confidence intervals were calculated. Differences were considered to be significant for $p<0.05$. No multivariate analysis was conducted.

Irradiation procedure. Cells were irradiated at room temperature from a cesium 137 (^{137}Cs) source using a CIS IBL437 irradiation device (CIS, France) at a dose rate of 5,2 Gy/min with a single dose of 8 Gy. Sham-irradiated cultures were kept at room temperature in the X-ray control room while the other samples were irradiated. After irradiation, the cells were kept in culture medium up to 48 h.

Plasmids. Eukaryotic and bacterial expression constructs for GFP-tagged and untagged versions of survivin wild type (WT), splice forms and deletion mutants were constructed by PCR amplification using appropriate primers containing *BamHI/NheI*-restriction sites and cloned into the vector pc3-GFP or pGEX-GFP, respectively, as described (22). To generate NES deficient survivin mutants, critical aa were changed by mutagenesis (^{89}**V**KKQ**F**EE**L**T**L**^{98} → ^{89}**V**KKQPEEATA^{98}, essential residues underlined) as described (22). siRNA-resistant human survivin mutants were generated by introducing silent mutations at positions essential for siRNA-binding (nucleotides ^{1229}C→T and ^{1235}A→C) by mutagenesis as described (22). Plasmids p3-Crm1-HA, pc3-PKI-BFP, encoding a PKI-BFP fusion, p3CANc/VSV-G, encoding the carboxy terminus of CAN/Nup214, and pDS-RED-N1, encoding the red-fluorescent protein (RFP) were already described (23).

Cells, transfection, microscopy and microinjection. The CRC cell line RKO, the HNSCC cell line 1624, HeLa, Vero and 293 cells were maintained under conditions recommended by the American Type Culture Collection and were prepared for microinjection or transfected as described (22). Microinjection, observation and image analysis in living or fixed cells were performed as described in detail (24). Briefly, to determine the average intracellular protein localization at least 200 fluorescent cells from three separate images were examined. The number of cells exhibiting cytoplasmic (C; cytoplasmic signal > 70% of the total cellular signal), cytoplasmic and nuclear (C/N), or nuclear (N; nuclear signal > 70% of the total cellular signal) fluorescence was counted, and the percentages of C, N/C and N cells were calculated. DNA/cell nuclei were visualized by staining with Hoechst 33258 (Sigma Aldrich, Munich, Germany) as described (22). Cell lines stable expressing survivin-GFP fusion proteins were selected with G418 as described (24).

Immunoprecipitation, immunoblotting, immunofluorescence and immuno-histochemistry. Immunoblotting and immunofluorescence were carried out according to standard procedures as described (22). Immunoprecipitation of survivin-GFP/survivin-complexes from co-transfected cell lysates using polyclonal anti-GFP antibodies (BD Biosciences, San Jose, CA, USA) as well as analysis of the complexes by immunoblotting

using polyclonal anti-survivin antibodies was performed according to standard procedures (22).

Immunohistochemical staining of survivin was performed according to standard procedures using the polyclonal anti-survivin antibodies (1:2000) and the FastRed Chromogen® detection system (Immunotech, Hamburg, Germany) as described (21). The slides were finally counterstained with 50% hematoxylin and examined by light microscopy on a Leica microscope at 100x magnification. The overall intracellular localization of survivin in the tumors was evaluated independently by two pathologists and scored semiquantitatively as: •, negative; +C, predominantly cytoplasmic (>70% of tumor cells display cytoplasmic staining); +N, predominantly nuclear (>70% of tumor cells display nuclear staining).

The following antibodies were used in the study: polyclonal anti-survivin (Novus NB 500-201; Novus Biologicals, Littleton, CO, USA), anti-ß-actin (A2066; polyclonal antibody; Sigma-Aldrich, St. Louis, MO, USA), anti-α-tubulin (T5168; monoclonal antibody; Sigma-Aldrich, St. Louis, MO, USA), anti-CRM1 (goat polyclonal antibody, Santa Cruz), anti-caspase-3 (C8487; polyclonal antibody; Sigma-Aldrich, St. Louis, MO, USA), and anti-caspase-9 (C7729; polyclonal antibody; Sigma-Aldrich, St. Louis, MO, USA).

Drug treatment. Cells were treated with the export inhibitor leptomycin B (LMB) (Sigma Aldrich, Munich, Germany) (10 nM) as described (22). Treatment with 1.5 mM valproic acid, 1.5 mM sodium butyrate or 3 mM cisplatin (Sigma Aldrich, Munich, Germany) was performed as described (25).

Purification of recombinant GST-fusion proteins. GST-GFP hybrid proteins were expressed and purified as described (22).

Crm1 pull-down assays and *in vitro* translation. Coupled transcription/translation was performed using the plasmid p3-Crm1-HA as the template, the specific recombinant GST-GFP substrates, Ran-GTP and nuclear extracts as described (22).

RNAi. The sequence and activity of the survivin double-stranded siRNA (Eurogenetec, Searing, Belgium) (sense: 5´-CUGGACAGAGAAAGAGCCATT-3´, residues mutated in the siRNA-resistant survivin mutants are underlined; antisense: 5´-UGG-CUCUUUCUCUGUCCAGTT-3´) has been described (26). Cells were treated in parallel with a scrambled siRNA duplex (sense: 5´-GGUGUGCUGUUUGGAGGUCTT-3´, antisense: 5´-GAACUCCAAACAGCACACCTT-3´) as a non-specific control. The siRNA duplexes (each 50 nM) were transfected together with 0.5 µg of the RFP expression plasmid using the

Lipofectamine2000® reagent (Invitrogen, Carlsbad, CA, USA) according to the manufacturer's recommendations.

Quantification of apoptosis. Apoptosis was assessed by labeling free 3'OH ends in genomic DNA with rhodamine-dUTP (TUNEL-staining) using the *in situ* cell death detection kit (Roche Diagnostics) as described (24). Briefly, 200 GFP-positive cells from three separate images were inspected, the number of TUNEL-positive cells was counted, and the percentages were calculated.

Cell extracts were assayed for caspase-3-dependent hydrolysis of the fluorogenic substrate N-acetyl-Asp-Glu-Val-Asp-p-nitroanilide (Axxora, Grunberg, Germany) and enzyme-catalyzed release of p-nitroanilide was monitored at 405nm as described (27).

Results

Survivin is overexpressed in colorectal and head and neck cancer, and localized to the nucleus and the cytoplasm of tumor cells. We examined the levels of survivin gene expression in colorectal (CC) as well as in head and neck squamous cell carcinomas (HNSCC) and in the corresponding normal mucosa (NOM) of the same patient by RT-qPCR analysis. As summarized in Figure 1*A*, survivin was found to be overexpressed in the tumors of almost all patients examined (see Supplementary Table S1 and S2 for patient characteristics and for values of the RT-qPCR analysis). Gene expression data could be confirmed on the protein level by IHC (Fig. 1*B*). Whereas survivin expression was almost absent in NOM, we observed tumors, in which survivin was predominantly cytoplasmic (Fig. 1*B*, left panel), but also tumors showing predominantly nuclear survivin staining (Fig. 1*B*, right panel).

Survivin contains an evolutionary conserved leucine-rich nuclear export signal. The results of the IHC analysis as well as the pivotal role of survivin as an apoptosis inhibitor and a regulator of cell division were indicative for a regulated nucleocytoplasmic localization of survivin. To systematically investigate the nucleocytoplasmic transport of survivin in live cells, we expressed human survivin, all known splice variants as well as the rat (Rn) survivin as C-terminal GFP fusion proteins (see Supplementary Table S3). Fluorescence microscopy revealed that survivin-GFP and Rn_survivin-GFP were predominantly cytoplasmic following transient or stable expression in several cell lines including the HNSCC cell line 1624, the human CRC cell line RKO, and HeLa cells (Fig. 2*A*, upper panel, and data not shown). Treatment with the nuclear export inhibitor LMB resulted in enhanced nuclear localization (Fig. 2*A*, lower panel). Indirect immunofluorescence revealed a similar intracellular localization and LMB sensitivity for the endogenous survivin in 1624, RKO and HeLa cells (Fig. 2*B*, and data not shown). Survivin splice variants 2B- and 3B-GFP fusions also localized to the cytoplasm (Fig. 2*C*), and were sensitive to LMB treatment. In contrast, survivinΔEx3-GFP was predominantly nuclear and survivin2α-GFP distributed equally between the nucleus and the cytoplasm, and both did not respond to LMB as analyzed in several cell lines (Fig. 2*C*, and data not shown). To further map the nuclear export signal (NES), we expressed survivin deletion mutants aa1-119 and aa1-88 as GFP-fusions and tested their localization and LMB-sensitivity. These results located the NES between aa 88 to 119 (Fig. 2*D*; and Supplementary Table S3).

We next examined the nucleocytoplasmic transport of survivin in a highly stringent system that allows the observation and quantification of transport in living cells (22). Survivin was expressed as a fusion with glutathione S-transferase (GST) and GFP (GST-survivin-GFP), and tested by microinjection. Due to the size of the GST-GFP fusion protein (54 kDa),

the localization of the recombinant autofluorescent transport substrate is not flawed by passive diffusion, and the protein remains at the site of injection (22). Following nuclear injection in 1624, Vero and RKO cells, GST-survivin-GFP was quantitatively exported into the cytoplasm (Fig. 3*A*/*B*, upper panel; Supplementary Fig. *S1*, and data not shown). Export was abrogated by treatment with LMB (data not shown). In contrast, no nuclear import was observed upon cytoplasmic injection, even in the presence of LMB, arguing against the presence of an active nuclear import signal (Fig. 3*A*/*B*). Similar results were observed for GST-Rn_survivin-GFP (data not shown).

Database searches identified motifs within aa 88 to 119 of survivin, matching the loosely defined consensus sequence for leucine-rich NESs (28). To verify the predicted signals, we tested the activity of the potential NESs by microinjection. Microinjection experiments revealed that only a recombinant GST-GFP protein containing the survivin aa 89-99 was quantitatively exported (Fig. 3*B* and Supplementary Fig. *S1*). As a stringent control, a signal in which essential residues were mutated (NESmut) was inactive under identical experimental conditions (Fig. 3*B*/*D* and Supplementary Fig. *S1*). The evolutionary conservation of the NES (Fig. 3*D*) was verified by the analysis of the respective survivin NESs from several species (data not shown). To confirm the functionality of the export signal also in the context of the full-length protein *in vivo*, we mutated critical residues of the NES (Fig. 3*D*). In contrast to the wild type protein, survivinΔNES-GFP was equally distributed between the nucleus and the cytoplasm, and did not respond to LMB treatment (Fig. 3*E*, and data not shown). In addition, recombinant GST-survivinΔN*E*S-GFP was neither exported nor imported in microinjection experiments (Fig. 3*A*, lower panel). These data exclude additional NESs as well as an active nuclear import signal in survivin.

Survivin interacts with Crm1. Inhibition of export by treatment with LMB indicated that survivin was exported via the Crm1 pathway. This assumption was supported by demonstrating that overexpression of Crm1 resulted in colocalization with survivin-GFP at the nuclear membrane in contrast to survivinΔNES-GFP (Fig. 3*E*). The direct Crm1-survivin interaction was biochemically verified in a cell free system. Figure 3*C* illustrates that recombinant GST-survivin-GFP bound to Crm1 in contrast to inactive GST-survivinΔNES-GFP or GST-GFP alone. Similar results were obtained for GST-survivinNES-GFP and GST-survivinNESmut-GFP fusion proteins, respectively (Fig. 3*C*).

Nuclear export of survivin is required for proper cytokinesis. Various reports demonstrated defects in cell cycle progression following downregulation of survivin levels resulting in mitotic arrest and polyploidy. To investigate the role of nuclear export for proper cytokinesis, we analyzed whether survivinΔNES-GFP was able to counteract the formation of

multinucleated cells upon ablation of endogenous survivin by RNAi. Transfection of HeLa cells stably expressing GFP with survivin siRNA resulted in an increased number of multinuclear cells, which was significantly reduced in survivin-GFP but not in survivinΔNES-GFP expressing cell lines (Fig. 4*A*/*B*). Since RNAi affected endogenous as well as ectopically expressed survivin, we generated HeLa cell lines stably expressing siRNA resistant survivin-GFP fusion proteins (survivin_sim-GFP and survivinΔNES_sim-GFP), by introducing two silent mutations within the survivin siRNA target sequence. Upon RNAi-mediated transient ablation of endogenous survivin, the inability of export deficient survivin to rescue cytokinesis became more prominent (Fig. 4*A*/*B*; right panel, and Supplementary Fig. *S2*). Of note, prolonged treatment with LMB also resulted in multinuclear cells (data not shown).

The integrity of the NES is required for tethering survivin to the mitotic machinery. To provide a molecular rationale why NES-deficient survivin-GFP was unable to promote proper cytokinesis, we examined the localization of survivin-GFP and survivinΔNES-GFP in stable cell lines. In contrast to wild type survivin-GFP, which localized correctly to the metaphase plate, the kinetochores and the midbody during cytokinesis, survivinΔNES-GFP failed to associate with the mitotic machinery (Fig. 4*C*, and data not shown). Similar results were observed in the RKO cell line, for untagged survivin and survivinΔNES, respectively, as well as for the rat survivin (data not shown). Thus, the integrity of the NES is required for survivin to function as a chromosomal passenger and explains, why the survivin NES is evolutionary conserved and required for proper cytokinesis.

Survivin mediated protection against chemo- or radiotherapy-induced apoptosis depends on active nuclear export. Survivin expression in tumors has been correlated with resistance against and chemo- and radiotherapy induced apoptosis. To investigate whether nuclear export was required for the clinical relevant protective activity of survivin, HeLa and RKO cells stably expressing survivin-GFP or survivinΔNES-GFP, respectively, were treated with apoptosis inducing chemotherapeutic compounds or irradiated. Figure 5*A*/*B* demonstrates that WT survivin-GFP could counteract induction of apoptosis by treatment with butyrate, VPA and cisplatin, whereas treatment of survivinΔNES-GFP expressing cells resulted in an increased apoptotic rate as analyzed by TUNEL staining (Fig. 5*A*, and Supplementary Fig. *S3*; and data not shown) and measurement of caspase-3 activity (Fig. 5*B*). Importantly, export deficient survivin-GFP also displayed a significantly reduced protective activity against irradiation-induced apoptosis (Fig. 5*A*/*B*). Of note, blocking the nuclear export of survivin by treatment with LMB for 24 h enhanced irradiation induced apoptosis analyzed by measurement of caspase-3 activity. Similar expression levels of

survivin-GFP and survivinΔNES-GFP were controlled by immunoblot analysis (data not shown).

The activity of IAPs is assumed to be mediated predominantly in the cytoplasm. Although for survivin the types of caspases and exact molecular mechanisms involved are still disputed. Our co-localization studies demonstrate that the amount of cytoplasmic survivin, capable to directly or indirectly inhibit cytoplasmic localized pro-caspase-3 and -9, was significantly higher for survivin-GFP compared to survivinΔNES-GFP (Fig. 5*C*/*D*, and data not shown). These results provide an explanation for the observed reduced anti-apoptotic effect of the NES-mutant and nuclear export appears not only to be required for proper cytokinesis but also plays a role in protection against cancer therapy induced apoptosis.

To exclude the formal possibility that the observed inhibition of the biological activity of survivin was not primarily mediated by blocking nuclear export but by affecting survivin dimerization due to the introduced NES-inactivating mutations, we performed immunoprecipitation experiments. Survivin could be immunoprecipitated as a complex with survivin-GFP as well as with survivinΔNES-GFP from the lysates of HeLa cells co-transfected with the respective expression constructs with equal efficiencies (data not shown).

Preferential nuclear localization of survivin correlated with enhanced survival. Our results argued that nuclear export is important for the biological activity of survivin. Consequently, interference with the nuclear export of survivin should result in increased nuclear survivin in tumor cells, and thereby impair the tumor promoting activity of survivin. Thus, we would expect that patients with predominantly nuclear survivin in their tumors should show increased overall survival. To test this hypothesis, the intracellular localization of survivin was analyzed by immunohistologic staining (IHC) in colorectal cancer specimens (for patients characteristics see Supplementary Table S4). Predominantly nuclear survivin staining of tumor cells (Fig. 1*B* shows an example in a representative tumor) was evident in 24 out of 263 cases (9,2%), and Kaplan-Meier curves of overall and recurrence-free survival showed a statistically significant association (p=0.005) with improved survival as calculated by the log-rank test (Fig. 6*A*).

The possibility that the detected nuclear survivin represented the survivinΔExon3 splice variant instead of WT survivin was excluded by analyzing the expression levels of the respective proteins in several tumors with enhanced nuclear survivin staining by RT-qPCR. In contrast to WT survivin, survivinΔExon3 levels were almost undetectable (data not shown), consistent with previous reports (referenced in 9).

Nuclear localization of survivin can be induced by interference with nuclear export.

To provide a molecular mechanism causing enhanced nuclear localization of survivin as also observed in the patient specimens, we investigated whether nuclear accumulation of survivin could be induced by overexpressing proteins competing for export factors or interfering with the nuclear transport machinery. Figure 6*B* shows that co-expression of survivin-GFP together with PKI-BFP or together with the FG-repeat containing C-terminal part of Nup214 affected nuclear export and caused nuclear accumulation of survivin-GFP. Similar results were obtained for endogenous survivin (data not shown).

Discussion

We have identified the evolutionary conserved Crm1 mediated nuclear export signal in survivin. The integrity of the NES was not only important for the anti-apoptotic activity of survivin but also for its function as a chromosomal passenger. Thereby, we annotated survivin as another essential regulatory protein the activity of which is regulated by active nucleocytoplasmic transport.

We demonstrated that endogenous as well as ectopically expressed survivin localized predominantly to the cytoplasm during interphase. This could either be due to the retention of newly synthesized protein in the cytoplasm or to its continuous nuclear export. Rodriguez et al. (29) assigned the export activity of survivin to its carboxy-terminal domain, but could not map the NES, and proposed that export is mediated in *trans* by a NES-containing protein binding to the carboxy-terminal domain. In contrast, we identified the NES, which was present in WT survivin, the splice variants 2B and 3B, but absent in the splice variants ΔExon3 and 2α. Absence or presence of the NES also correlated with the cytoplasmic localization of the splice variants (Supplementary Fig. *S4A*). Nuclear export of survivin was mediated by the Crm1 pathway as supported by several lines of evidence presented in our report. For one, Crm1 antagonists caused nuclear accumulation of survivin and prevented export of recombinant full-length survivin as well as survivinNES transport substrates. Secondly, survivin-GFP and survivinNES-GFP bound to Crm1 *in vitro* and *in vivo,* and these interactions could be prevented by mutating critical residues in the NES, which also blocked export of the full length protein *in vivo*. The NES of survivin is evolutionary conserved in all known mammalian survivin proteins (**V**xxx**F/M/V**xx**L**x**L/V**) and fits the consensus sequence for leucine-rich export signals (28). Although suggested in previous reports (referenced in 14), our data do not support the presence of an active nuclear import signal. First, Crm1 antagonists did not result in complete nuclear accumulation of survivin. Secondly, recombinant full-length GST-survivin-GFP as well as GST-survivinΔNES-GFP were not imported into the nucleus upon microinjection into the cytoplasm. Thus, the low molecular weight of survivin even as a dimer, allows survivin to enter the nucleus by passive diffusion, and if active nuclear export is inhibited may attach to nuclear binding sites in interphase cells. This assumption is supported in dividing cells, where we and others found survivin attached to components of the mitotic machinery and to localize to the metaphase plate, the kinetochores and the midbodies (30, 31). It is tempting to speculate that among other components of the chromosomal passenger complex (CPC) like Aurora B and INCENP, Crm1 is critically involved in tethering survivin to the mitotic machinery. First, Crm1 has clearly been identified as an essential Ran-GTP effector for mitotic spindle assembly and function in yeast and mammalian cells (32 and references therein), besides its function as a

nuclear export receptor. Secondly, survivin but not NES-deficient survivin interacts with Crm1 *in vitro* and *in vivo,* which correlates with its localization to the mitotic machinery and its activity to promote proper cytokinesis. As reported by Yang et al. (13), survivin is essential for cellular proliferation by ensuring accurate sister chromatid segregation and assembly/stabilization of microtubules in late mitosis.

Although the notion that survivin inhibits apoptosis is established, the mechanis by which this occurs has not been conclusively determined (2, 3). Several reports suggest that survivin directly interacts with Smac/DIABLO (6, 33), can form complexes with other IAP members (34) or binds to pro-caspase-3 (35) and -9 (36). Clearly, a predominantly cytoplasmic localization of survivin mediated by active nuclear export would enable survivin to function effectively an inhibitor of apoptosis. This molecular mechanism could be supported by our findings that survivin but not export deficient survivin was able to counteract chemo- and radiotherapy induced apoptosis.

As survivin appears to play a dual role as an apoptosis inhibitor and a regulator of cell division, it is intriguing how the concept of active nuclear export is exploited to efficiently function in both pathways. First, during cell division, the NES is used to target survivin to the chromosomal passenger complex in order to promote proper cytokinesis. During interphase, nuclear export serves to ensure a high cytoplasmic concentration of survivin to counteract pro-apoptotic signals. Since survivin is not only expressed in somatic cancer cells but also in stem cells (37), the same molecular mechanism may control stem cell survival and proliferation, and might also be important for the development and maintenance of cancer stem cells (38).

Thus, besides other mechanism like phosphorylation or interaction with other proteins, nuclear export is clearly important not only for the biological function of survivin in normal cells, but also for its cancer promoting activity. Is this finding also of clinical relevance? Others and we could show that preferential nuclear localization of survivin in tumors was linked with a favorable prognosis in colorectal cancer patients (this study), breast cancers (39), non-small-cell lung cancers (40), gastric cancers (41), ovary tumors (42, 43), pancreatic cancer patients (44) and osteosarcomas (45). Some reports however consider nuclear survivin to be associated with poor survival (46-48). This discrepancy may be due to different IHC staining protocols, the tumor entity examined or caused by additional unknown factors (14). Applying defined standardized procedures for analyzing nuclear/cytoplasmic localization of survivin by IHC is clearly required to clarify the predictive value of nuclear survivin.

The molecular reasons why survivin accumulated in some tumors in contrast to others is not known. Our previous studies (23, 49) and the cell culture experiments in this report indicate that nuclear localization of shuttle proteins can be induced by competing for export

factors or by interfering with the nuclear transport machinery. Although this mechanism needs to be verified in tumors, it is known that shuttling proteins like cyclin D1, p21, p27, p53, mdm2, STATs are overexpressed in various types of cancers (19) and can influence nucleocytoplasmic transport of other proteins (50). Likewise, overexpression of full length or truncated FG-repeat containing proteins has been described (19, 51).

Recently, interfering specifically with regulated nucleocytoplasmic transport of proteins as a novel therapeutic principle has attracted major interest by academia and industry (reviewed in 19). Although our data indicate that the inhibition of the nuclear export of survivin by LMB increased irradiation induced apoptosis, Crm1-directed inhibitors will not be used in therapeutic applications due to their toxic side effects by blocking all cellular Crm1-mediated transport pathways. Therefore, protein specific transport inhibitors are urgently needed. Since NESs can be grouped into specific categories according to their activity *in vivo* (23), these differences represent an attractive opportunity to selectively interfere with export and the biological functions of proteins by the generation of NES-specific inhibitors. The NMR structure of survivin (6) indicates that the hydrophobic NES is exposed at the surface of the survivin dimer (Supplementary Fig. *S4B*). This knowledge may now allow to *in silico* design molecules specifically binding to the NES. Application of our recently developed cell based translocation assays (24) will allow the systematic identification and validation of NES-specific inhibitors. Thus, besides known molecular antagonists of the survivin pathway, including siRNAs or dominant negative mutants, survivin-specific nuclear export inhibitors will be promising candidates for a novel class of cancer therapeutics.

Acknowledgment

We thank J. Sleeman for the rat cDNA and C. Mahotka for survivinΔexon3 expression plasmid, B. Groner for support, and Gert Carra and Silke Deckert for technical assistance. Grant support: Supported by the Deutsche Forschungsgemeinschaft (Sta 598/1-2), the Deutsche Krebshilfe, the EU-FP6 (BRECOSM) and the Studienstiftung des Deutschen Volkes (S.K.).

References

1. Hanahan D Weinberg RA The hallmarks of cancer. Cell 2000;100:57-70.
2. Altieri DC Survivin and apoptosis control. Adv Cancer Res 2003;88:31-52.
3. Altieri DC Validating survivin as a cancer therapeutic target. Nat Rev Cancer 2003;3:46-54.
4. Altieri DC Blocking survivin to kill cancer cells. Methods Mol Biol 2003;223:533-42.
5. Salvesen GS Duckett CS IAP proteins: blocking the road to death's door. Nat Rev Mol Cell Biol 2002;3:401-10.
6. Sun C, Nettesheim D, Liu Z, et al. Solution structure of human survivin and its binding interface with smac/diablo. Biochemistry 2005;44:11-7.
7. Caldas H, Honsey LE Altura RA Survivin 2alpha: a novel Survivin splice variant expressed in human malignancies. Mol Cancer 2005;4:11.
8. Altieri DC Survivin, versatile modulation of cell division and apoptosis in cancer. Oncogene 2003;22:8581-9.
9. Li F Role of survivin and its splice variants in tumorigenesis. Br J Cancer 2005;92:212-6.
10. Altieri DC Survivin in apoptosis control and cell cycle regulation in cancer. Prog Cell Cycle Res 2003;5:447-52.
11. Li F Survivin study: what is the next wave? J Cell Physiol 2003;197:8-29.
12. Altieri DC Molecular circuits of apoptosis regulation and cell division control: The survivin paradigm. J Cell Biochem 2004;92:656-63.
13. Yang D, Welm A Bishop JM Cell division and cell survival in the absence of survivin. Proc Natl Acad Sci U S A 2004;101:15100-5.
14. Li F, Yang J, Ramnath N, et al. Nuclear or cytoplasmic expression of survivin: what is the significance? Int J Cancer 2005;114:509-12.
15. Pemberton LF Paschal BM Mechanisms of receptor-mediated nuclear import and nuclear export. Traffic 2005;6:187-98.
16. Ferrando-May E Nucleocytoplasmic transport in apoptosis. Cell Death Differ 2005;
17. Lamond AI Sleeman JE Nuclear substructure and dynamics. Curr Biol 2003;13:R825-8.
18. Bednenko J, Cingolani G Gerace L Nucleocytoplasmic transport: navigating the channel. Traffic 2003;4:127-35.
19. Kau TR, Way JC Silver PA Nuclear transport and cancer: from mechanism to intervention. Nat Rev Cancer 2004;4:106-17.
20. Schlingemann J, Habtemichael N, Ittrich C, et al. Patient-based cross-platform comparison of oligonucleotide microarray expression profiles. Lab. Investigation (in press) 2005;
21. Knosel T, Yu Y, Stein U, et al. Overexpression of cyclooxygenase-2 correlates with chromosomal gain at the cyclooxygenase-2 locus and decreased patient survival in advanced colorectal carcinomas. Dis Colon Rectum 2004;47:70-7.
22. Knauer SK, Carra G Stauber RH Nuclear export is evolutionarily conserved in CVC paired-like homeobox proteins and influences protein stability, transcriptional activation, and extracellular secretion. Mol. Cell. Biol. 2005;25:2573–82.
23. Heger P, Lohmaier J, Schneider G, et al. Qualitative highly divergent nuclear export signals can regulate export by the competition for transport cofactors *in vivo*. Traffic 2001;544-555:544-55.
24. Knauer SK, Moodt S, Berg T, et al. Translocation Biosensors To Study Signal Specific Nucleo-Cytoplasmic Transport, Protease Activity & Protein Interactions. Traffic 2005;6:1-13.
25. Zhu P, Martin E, Mengwasser J, et al. Induction of HDAC2 expression upon loss of APC in colorectal tumorigenesis. Cancer Cell 2004;5:455-63.

26. Rodel F, Hoffmann J, Distel L, et al. Survivin as a radioresistance factor, and prognostic and therapeutic target for radiotherapy in rectal cancer. Cancer Res 2005;65:4881-7.

27. Kwon KB, Kim EK, Shin BC, et al. Induction of apoptosis by takrisodokyeum through generation of hydrogen peroxide and activation of caspase-3 in HL-60 cells. Life Sci 2003;73:1895-906.

28. la Cour T, Kiemer L, Molgaard A, et al. Analysis and prediction of leucine-rich nuclear export signals. Protein Eng Des Sel 2004;17:527-36.

29. Rodriguez JA, Span SW, Ferreira CG, et al. CRM1-mediated nuclear export determines the cytoplasmic localization of the antiapoptotic protein Survivin. Exp Cell Res 2002;275:44-53.

30. Wheatley SP, Carvalho A, Vagnarelli P, et al. INCENP is required for proper targeting of Survivin to the centromeres and the anaphase spindle during mitosis. Curr Biol 2001;11:886-90.

31. Honda R, Korner R Nigg EA Exploring the functional interactions between Aurora B, INCENP, and survivin in mitosis. Mol Biol Cell 2003;14:3325-41.

32. Arnaoutov A, Azuma Y, Ribbeck K, et al. Crm1 is a mitotic effector of Ran-GTP in somatic cells. Nat Cell Biol 2005;7:626-32.

33. Song Z, Yao X Wu M Direct interaction between survivin and Smac/DIABLO is essential for the anti-apoptotic activity of survivin during taxol-induced apoptosis. J Biol Chem 2003;278:23130-40.

34. Dohi T, Okada K, Xia F, et al. An IAP-IAP complex inhibits apoptosis. J Biol Chem 2004;279:34087-90.

35. Shin S, Sung BJ, Cho YS, et al. An anti-apoptotic protein human survivin is a direct inhibitor of caspase-3 and -7. Biochemistry 2001;40:1117-23.

36. O'Connor DS, Grossman D, Plescia J, et al. Regulation of apoptosis at cell division by p34cdc2 phosphorylation of survivin. Proc Natl Acad Sci U S A 2000;97:13103-7.

37. Fukuda S Pelus LM Elevation of Survivin levels by hematopoietic growth factors occurs in quiescent CD34+ hematopoietic stem and progenitor cells before cell cycle entry. Cell Cycle 2002;1:322-6.

38. Kim PJ, Plescia J, Clevers H, et al. Survivin and molecular pathogenesis of colorectal cancer. Lancet 2003;362:205-9.

39. Kennedy SM, O'Driscoll L, Purcell R, et al. Prognostic importance of survivin in breast cancer. Br J Cancer 2003;88:1077-83.

40. Vischioni B, van der Valk P, Span SW, et al. Nuclear localization of survivin is a positive prognostic factor for survival in advanced non-small-cell lung cancer. Ann Oncol 2004;15:1654-60.

41. Okada E, Murai Y, Matsui K, et al. Survivin expression in tumor cell nuclei is predictive of a favorable prognosis in gastric cancer patients. Cancer Lett 2001;163:109-16.

42. Ferrandina G, Legge F, Martinelli E, et al. Survivin expression in ovarian cancer and its correlation with clinico-pathological, surgical and apoptosis-related parameters. Br J Cancer 2005;92:271-7.

43. Tringler B, Lehner R, Shroyer AL, et al. Immunohistochemical localization of survivin in serous tumors of the ovary. Appl Immunohistochem Mol Morphol 2004;12:40-3.

44. Tonini G, Vincenzi B, Santini D, et al. Nuclear and cytoplasmic expression of survivin in 67 surgically resected pancreatic cancer patients. Br J Cancer 2005;

45. Trieb K, Lehner R, Stulnig T, et al. Survivin expression in human osteosarcoma is a marker for survival. Eur J Surg Oncol 2003;29:379-82.

46. Shinohara ET, Gonzalez A, Massion PP, et al. Nuclear survivin predicts recurrence and poor survival in patients with resected nonsmall cell lung carcinoma. Cancer 2005;103:1685-92.

47. Lu B, Gonzalez A, Massion PP, et al. Nuclear survivin as a biomarker for non-small-cell lung cancer. Br J Cancer 2004;91:537-40.

48. Grabowski P, Gribeta S, Arnold CN, et al. Nuclear Survivin Is a Powerful Novel Prognostic Marker in Gastroenteropancreatic Neuroendocrine Tumor Disease. Neuroendocrinology 2005;81:1-9.

49. Heger P, Rosorius O, Hauber J, et al. Titration of cellular export factors, but not heteromultimerization, is the molecular mechanism of *trans*-dominant HTLV-1 Rex mutants. Oncogene 1999;18:4080-90.

50. Alt JR, Gladden AB Diehl JA p21(Cip1) Promotes cyclin D1 nuclear accumulation via direct inhibition of nuclear export. J Biol Chem 2002;277:8517-23.

51. Kasper LH, Brindle PK, Schnabel CA, et al. CREB binding protein interacts with nucleoporin-specific FG repeats that activate transcription and mediate NUP98-HOXA9 oncogenicity. Mol Cell Biol 1999;19:764-76.

Figure legends

Figure 1. Survivin is overexpressed in CRC and HNSCC, and could be detected in the cytoplasm and the nucleus. *A,* quantitative RT-PCR indicating the fold change in expression of survivin mRNA in tumor versus NOM. Bar, median. *B,* examples of nuclear (upper panel) and cytoplasmic staining of survivin in tumor sections. Scale bar, 20µm.

Figure 2. Localization and LMB sensitivity of survivin and survivin splice variants. Cells were transfected with the indicated plasmids and analyzed by fluorescence microscopy or indirect immunofluorescence using a polyclonal anti-survivin antiserum. *A,* human and rat (rat) survivin-GFP localized predominantly to the cytoplasm in RKO, 1624 or HeLa cells (upper panel). Significant amounts of the proteins accumulated in the nucleus following LMB-treatment (lower panel). *B,* endogenous survivin in RKO or 1624 cells also displayed a predominantly cytoplasmic localization and accumulated in the nucleus following LMB-treatment (lower panel). *C,* survivin splice variants 2B- and 3B-GFP fusions also localized to the cytoplasm and were sensitive to LMB treatment. In contrast, survivinΔEx3-GFP was predominantly nuclear and survivin2α-GFP distributed equally between the nucleus and the cytoplasm and both, did not respond to LMB. *D,* survivin aa1-119- but not aa1-88-GFP was cytoplasmic and LMB sensitive. Representative images are shown. Scale bars, 10 µm.

Figure 3. The survivin NES is evolutionary conserved and interacts with Crm1. Indicated GST-survivin-GFP substrates were microinjected into the nucleus or cytoplasm of 1624 cells, and transport was recorded in living cells by fluorescence microscopy after the indicated time points. Approximately 100 cells were injected, and representative examples are shown. Scale bars, 10 µm. *A,* GST-survivin-GFP was injected into the nuclei of 1624 cells and nuclear export was completed after 3 h (upper panel). In the multinucleated cell, no import activity into the non-injected nucleus (marked by the asterisk) was observed. In contrast, export deficient survivinΔNES was neither exported after nuclear injection nor imported after cytoplasmic injection (lower panel). *B,* nuclear injected GST-survivin aa89-99-GFP (NES) was efficiently exported (upper panel), whereas inactivation of the NES blocked export (lower panel). *C,* survivin interacts with Crm1 in GST-pulldown-assays. *In vitro* translated [^{35}S]-labeled Crm1 protein was incubated with equal amounts of immobilized GST-survivin-GFP, GST-survivinΔNES-GFP, GST-survivinNES-GFP, GST-survivinNESmut-GFP or GST-GFP in the presence of GST-RanQ69L and nuclear extracts. Binding of Crm1 to the NES containing substrates (lanes 1/3) was abolished by mutating the NES (lanes 2/4). GST-GFP served to control for unspecific binding (lane 5). *D,* inter-species alignment of the tested survivin export signals from different species and the inactive mutated NES. *Homo sapiens (*Hs*), Bos taurus*

*(*Bt*), Canis familiarias (*Cf*), Felis canis (*Fc*), Pan trophogloydes (*Pt*), Sus scrofa (*Ss*), Mus musculus (*Mm*), Rattus norvegicus (*Rn*). E,* survivin interacts with Crm1 *in vivo*. Overexpression of Crm1 resulted in colocalization with survivin-GFP at the nuclear membrane in contrast to survivinΔNES-GFP. HeLa cells were transfected with the indicated plasmids and Crm1 expression was visualized by indirect immunofluorescence using a monoclonal anti-Crm1 antibody. Scale bars, 10 μm.

Figure 4. Nuclear export of survivin is required for proper cytokinesis. Hela cells stably expressing GFP, survivin-GFP, survivinΔNES-GFP or the siRNA resistant survivin mutants (survivin_sim-GFP and survivinΔNES_sim-GFP), were transfected with survivin siRNA or a control siRNA together with an RFP expression plasmid as the transfection control. *A,* siRNA mediated silencing, and similar expression levels of the survivin-GFP fusion proteins were verified by Western-blot analysis of cellular lysates using a polyclonal anti-survivin antiserum (upper panel). Actin was used as a control. Exposition times were 30s for survivin-GFP and actin and 90s for endogenous survivin. *B,* in parallel cultures, the number of multinucleated cells was examined in 200 cells from three separate images and the percentages of GFP- and RFP-double-positive cells, in which two ore more nuclei could be detected, were determined. *Columns*, mean; *bars*, ± SD from two independent experiments. siRNA-mediated silencing of survivin resulted in an increased number of multinuclear cells (left panel), which could be partially rescued by coexpressing survivin-GFP, but not by survivinΔNES-GFP (middle panel). Since RNAi affected endogenous as well as ectopically expressed survivin, rescue by survivin-GFP but not by survivinΔNES-GFP became more prominent in the siRNA–resistant cell lines (right panel). *C,* the NES tethers survivin to the mitotic machinery. Cell-cycle distribution of survivin-GFP and survivinΔNES-GFP (green). DNA was marked by Hoechst dye (blue), and microtubules by a monoclonal anti-α-tubulin antibody (red). Whereas wild type survivin-GFP correctly localized to the metaphase plate (M) and the midbody during cytokinesis (left panel), survivinΔNES-GFP failed to associate with the mitotic machinery (right panel). Representative images are shown. Scale bars, 10 μm.

Figure 5. Nuclear export is required for survivin mediated protection against chemo- and radiotherapy induced apoptosis. HeLa cells stably expressing the indicated proteins were treated with valproic acid (VPA), butyrate, cisplatin (CPL) or irradiated (8 Gy). 48 h later, apoptosis was assessed by TUNEL staining *A*, or by measuring caspase-3 activity *B* (see material and methods for details). Columns*, mean;* bars*,* ± SD from two independent experiments. In contrast to WT survivin-GFP, overexpression of survivinΔNES-GFP could not counteract induction of apoptosis by drug treatment or irradiation. SurvivinΔNES-GFP or

GFP expressing cells showed similar levels of apoptosis, whereas survivin-GFP displayed significantly reduced rate of apoptotic cells. Blocking the nuclear export of survivin by treatment with LMB for 24 h enhanced irradiation induced apoptosis. *C*, nuclear export of survivin ensures efficient co-localization with pro-caspase-3. HeLa cells were transfected with the indicated plasmids, fixed and stained with an anti-caspase-3 antibody. The amount of survivin protein that co-localized with pro-caspase-3 in the cytoplasm (left panel) was significantly reduced for the NES mutant (right panel). Scale bar, 10µm. *D*, to quantify the degree of co-localization the percentage of total cellular survivin-GFP that co-localized with caspase-3 was quantitated in 100 cells. *Columns,* mean*; bars,* ± SD from two independent experiments.

Figure 7. Preferential nuclear localization of survivin is associated with enhanced survival of colorectal cancer patients, and can be induced by interference with nuclear export. *A,* Kaplan-Meier survival curves for positive (n=24) and negative (n=239) cases of CRC regarding nuclear survivin localization. The intracellular localization of survivin was analyzed by IHC staining. Predominantly nuclear survivin staining of tumors was evident in 24 cases (9,2%) and showed a statistically significantly association (p=0.005) with improved survival as calculated by the log-rank test. *B*, HeLa cells expressing survivin-GFP were transfected with the PKI-BFP or the CanC expression plasmids (3 µg each) together with 0.3 µg of the RFP expression plasmid and analyzed by fluorescence microscopy. Overexpression of PKI-BFP or CanC inhibited nuclear export and resulted in the nuclear accumulation of survivin-GFP in contrast to non-transfected cells (marked by the asterisk). Scale bar, 10 µm.

Supplementary Figure S1. The survivin NES is active also in Vero cells. Indicated GST-survivin-GFP substrates were microinjected into the nucleus or cytoplasm of Vero cells, and transport was recorded in living cells by fluorescence microscopy after the indicated time points. Approximately 100 cells were injected, and representative examples are shown. Whereas *A,* GST-survivin-GFP or *B*, GST-survivinNES-GFP was completed exported (upper panel), inactivation of the NES by mutating critical residues into alanines (aa^{89}VKKQ**F**EE**L**T**L**^{98} → ^{89}VKKQ**P**EE**A**T**A**^{98}) completely blocked export (lower panel). In contrast, no import was observed after cytoplasmic injection (*A*, lower panel). Scale bars, 10 µm.

Supplementary Figure S2. NES deficient survivin cannot support proper cytokinesis. Representative image of siRNA/RFP-transfected Hela cells expressing survivinΔNES_sim-GFP. Survivin silencing resulted in multinuclear RFP positive cells in contrast to untransfected control cells. Scale bar, 10 µm.

Supplementary Figure S3. The integrity of the nuclear export signal is crucial for the cytoprotective activity of survivin against apoptosis. Hela cells stably expressing the indicated proteins were treated with valproic acid (VPA) (middle panel) or cisplatin (CPL) (lower panel) to induce apoptosis. The amount of TUNEL-positive apoptotic cells (shown in red) was significantly reduced in cells expressing survivin-GFP (middle panel) compared to cells expressing GFP (left panel) or export deficient survivin (right panel). Scale bars, 100µm.

Supplementary Figure S4. *A,* domain organization of survivin and its alternatively spliced variants. The first two exons (aa1-73) are common to all splice forms. Survivin-2*B,* (165aa) contains an insertion of exon 2B (23 aa) between exon 2 and 3, disrupting the BIR domain. The survivin-DeltaEx3 variant (137aa) encodes a truncated BIR domain and a frameshift from exon 4 generates a novel C-terminal protein sequence with 64 amino acids. A frameshift in exon 3 of survivin-3B (120aa) results in a truncated protein with a distinct C-terminus. In the recently discovered variant 2α exon 1 and 2 are followed by an in frame stop codon within intron 2, generating a protein of 74aa. The NES (▸) is only encoded in survivin wild-type, 2B and 3B, but is absent in survivin DeltaEx3 and 2α. Boxes represent exons, with exon numbers and numbers of aa indicated below. *B*, position of the NES within the NMR structure of human survivin (PDB 1XOX). Ribbon representation of the backbone superposition (residues 1-117). Residues 89-98 encompassing the NES are shown in a cyan spacefill depiction. Critical amino acids for NES activity (89, 93, 96 and 98) are shown in red.

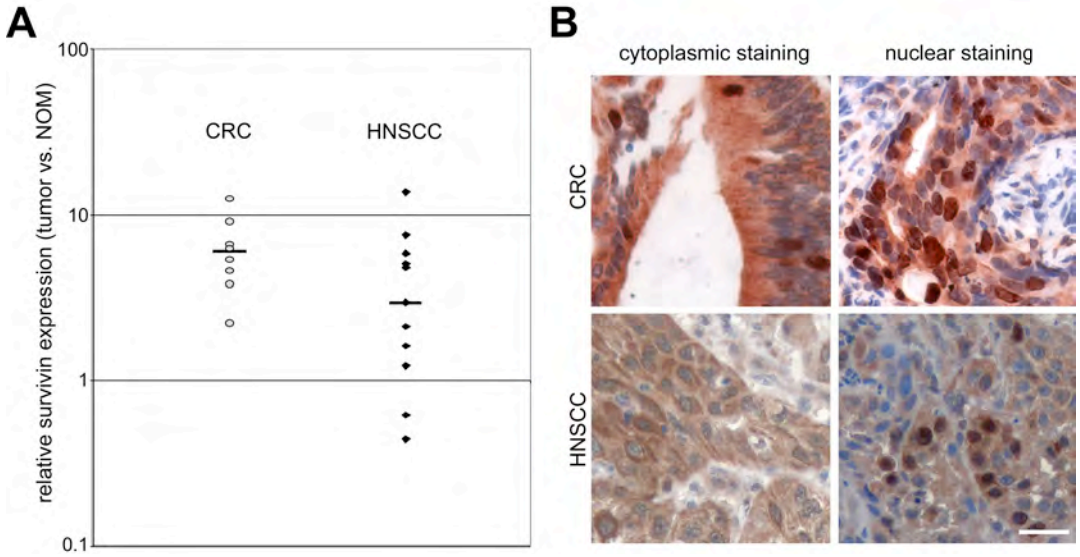
A
100
10
1
0.1
relative survivin expression (tumor vs. NOM)
CRC
HNSCC
B
cytoplasmic staining
nuclear staining
CRC
HNSCC

Figure 1

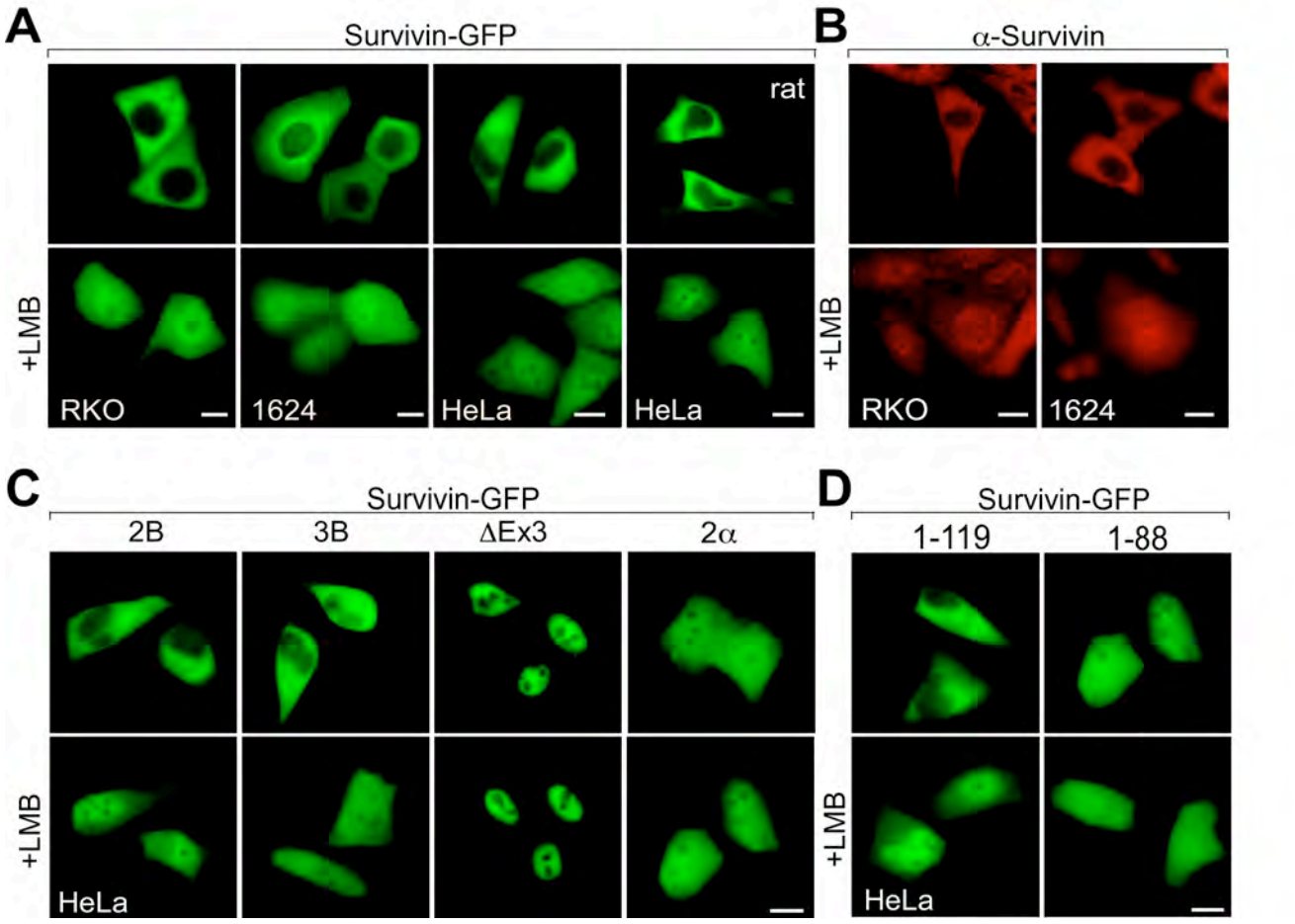
A
Survivin-GFP
rat
+LMB
RKO
1624
HeLa
HeLa
B
α-Survivin
+LMB
RKO
1624
C
Survivin-GFP
2B
3B
ΔEx3
2α
+LMB
HeLa
D
Survivin-GFP
1-119
1-88
+LMB
HeLa

Figure 2

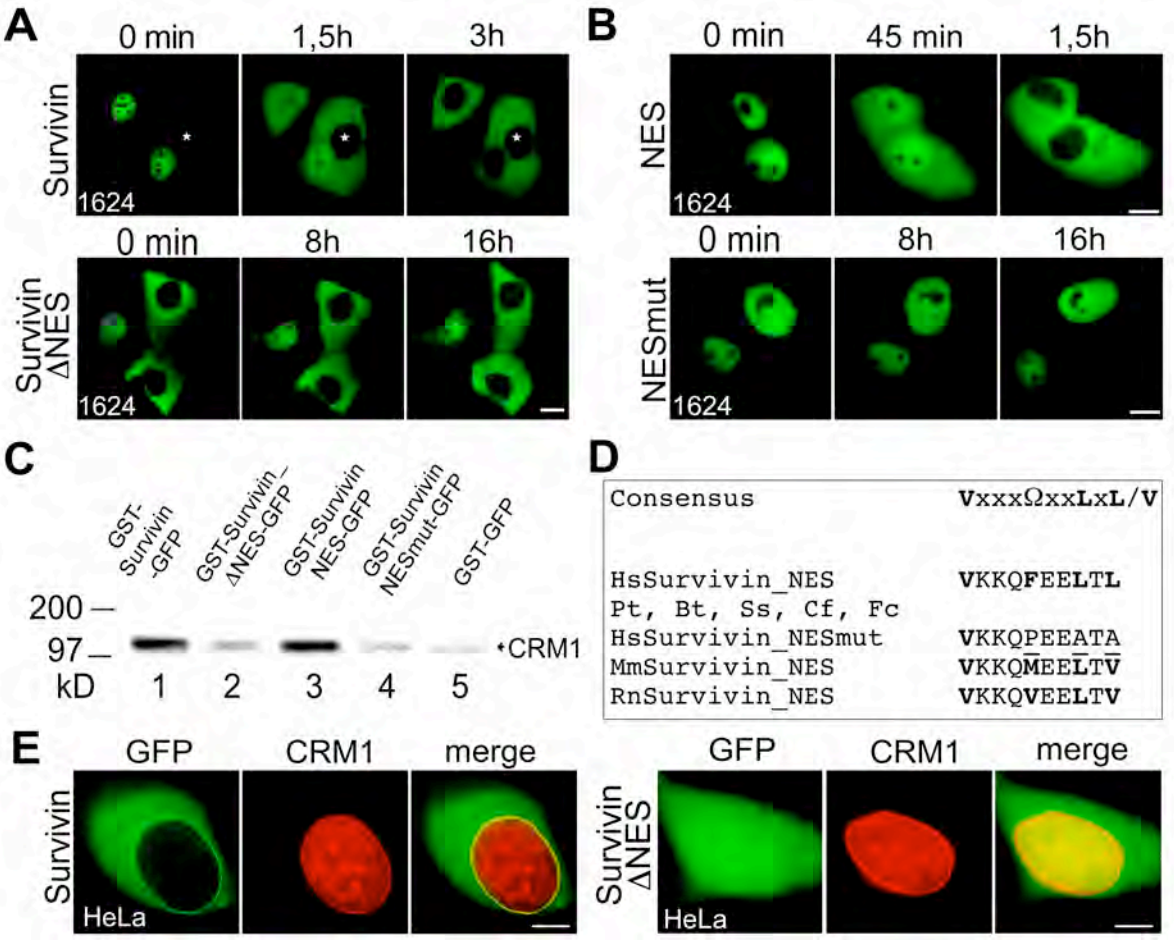
A
0 min
1,5h
3h
Survivin
1624
0 min
8h
16h
Survivin ΔNES
1624
B
0 min
45 min
1,5h
NES
1624
0 min
8h
16h
NESmut
1624
C
GST-Survivin -GFP
GST-Survivin_ ΔNES-GFP
GST-Survivin NES-GFP
GST-Survivin NESmut-GFP
GST-GFP
200
97
kD
1
2
3
4
5
CRM1
D
Consensus VxxxΩxxLxL/V
HsSurvivin_NES VKKQFEELTL
Pt, Bt, Ss, Cf, Fc
HsSurvivin_NESmut VKKQPEEATA
MmSurvivin_NES VKKQMEELTV
RnSurvivin_NES VKKQVEELTV
E
GFP
CRM1
merge
Survivin
HeLa
GFP
CRM1
merge
Survivin ΔNES
HeLa

Figure 3

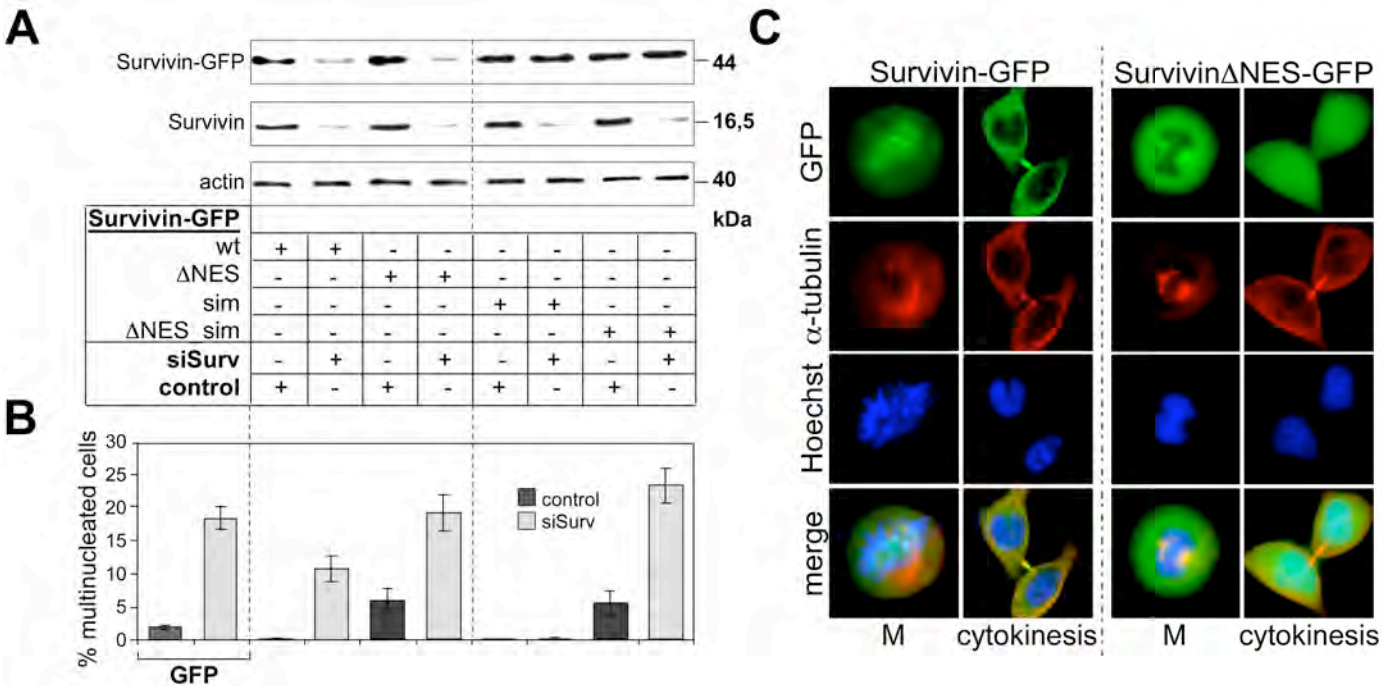
A
Survivin-GFP
Survivin
actin
44
16,5
40
kDa
Survivin-GFP
wt
ΔNES
sim
ΔNES_sim
siSurv
control
B
% multinucleated cells
30
25
20
15
10
5
0
control
siSurv
GFP
C
Survivin-GFP
SurvivinΔNES-GFP
GFP
α-tubulin
Hoechst
merge
M
cytokinesis
M
cytokinesis

Figure 4

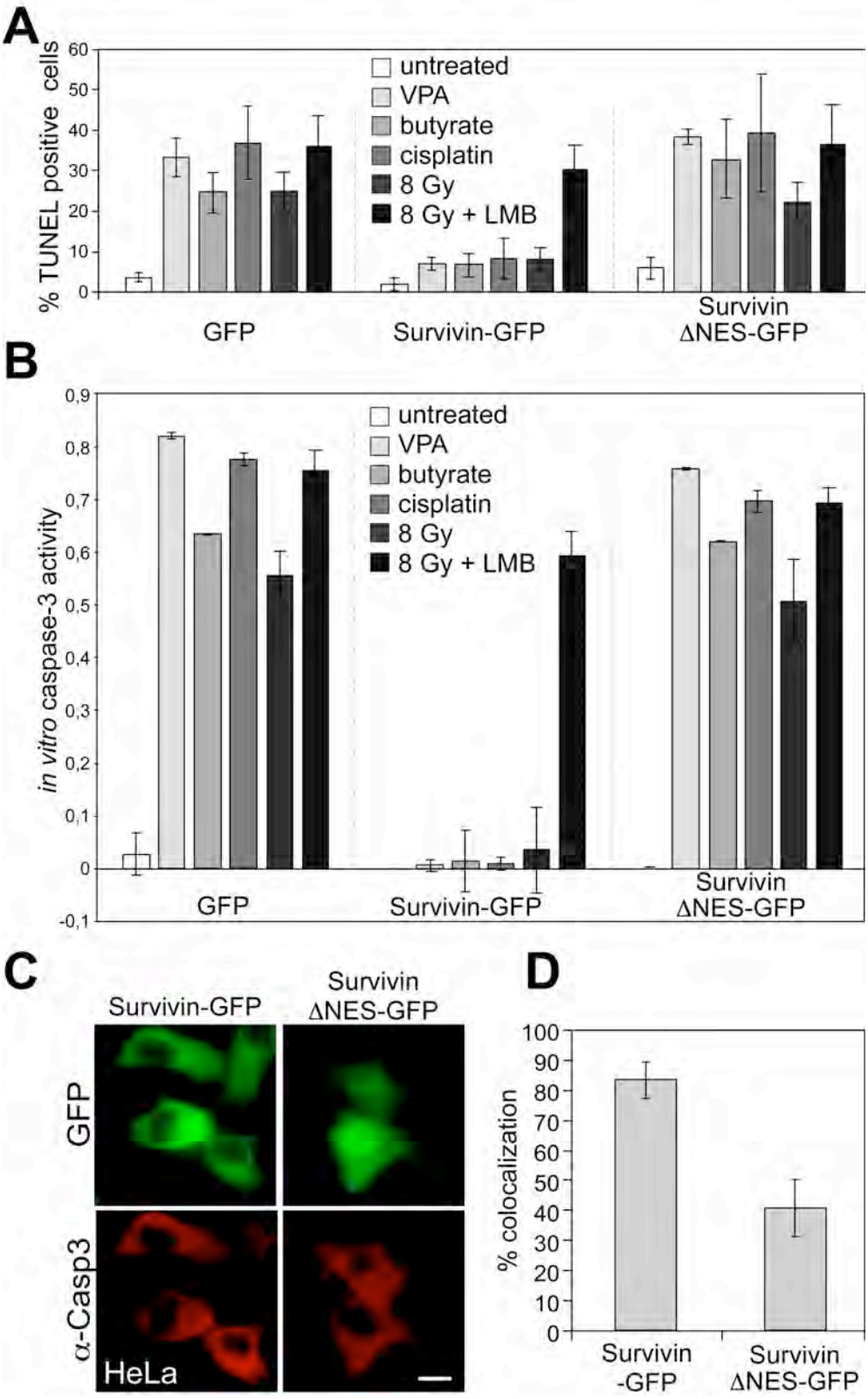
A
% TUNEL positive cells
60
50
40
30
20
10
0
untreated
VPA
butyrate
cisplatin
8 Gy
8 Gy + LMB
GFP
Survivin-GFP
Survivin ΔNES-GFP
B
in vitro caspase-3 activity
0,9
0,8
0,7
0,6
0,5
0,4
0,3
0,2
0,1
0
-0,1
untreated
VPA
butyrate
cisplatin
8 Gy
8 Gy + LMB
GFP
Survivin-GFP
Survivin ΔNES-GFP
C
Survivin-GFP
Survivin ΔNES-GFP
GFP
α-Casp3
HeLa
D
% colocalization
100
90
80
70
60
50
40
30
20
10
0
Survivin -GFP
Survivin ΔNES-GFP

Figure 5

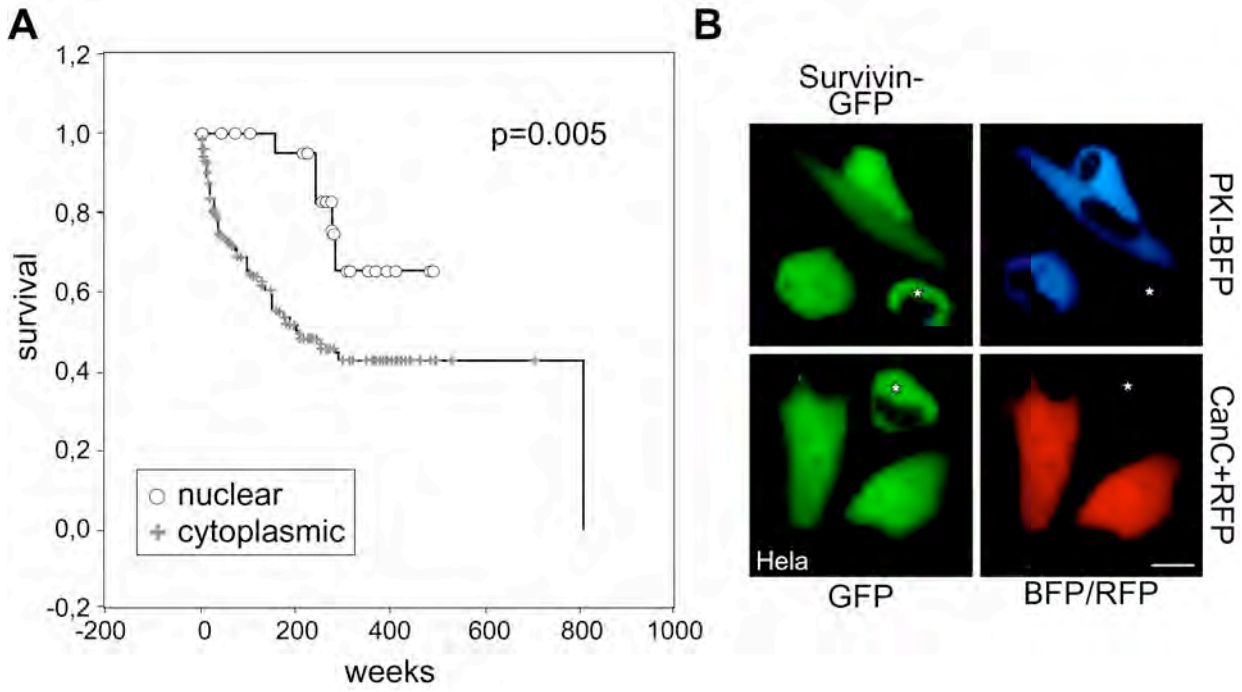
A
1,2
1,0
0,8
0,6
0,4
0,2
0,0
-0,2
survival
p=0.005
nuclear
cytoplasmic
-200
0
200
400
600
800
1000
weeks
B
Survivin-
GFP
PKI-BFP
CanC+RFP
Hela
GFP
BFP/RFP

Figure 6

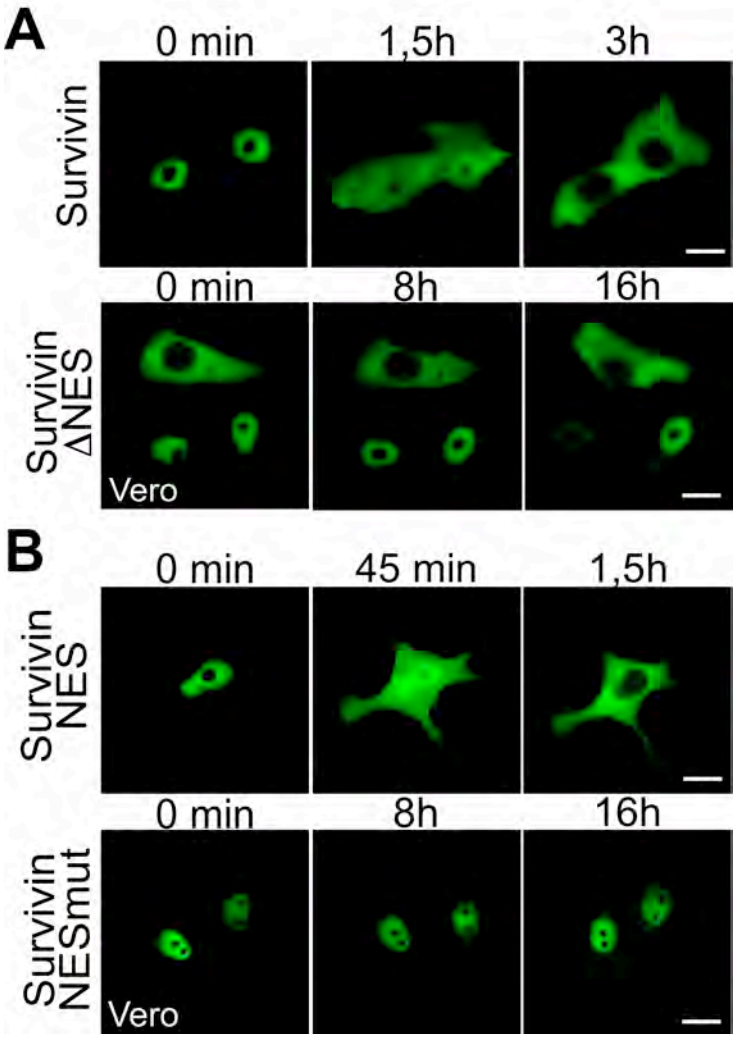

Supplementary Figure S1

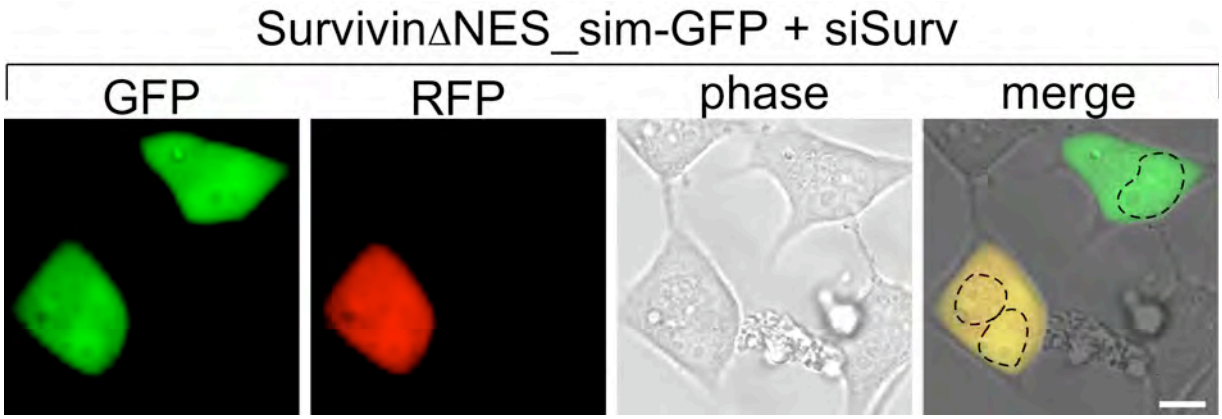

Supplementary Figure S2

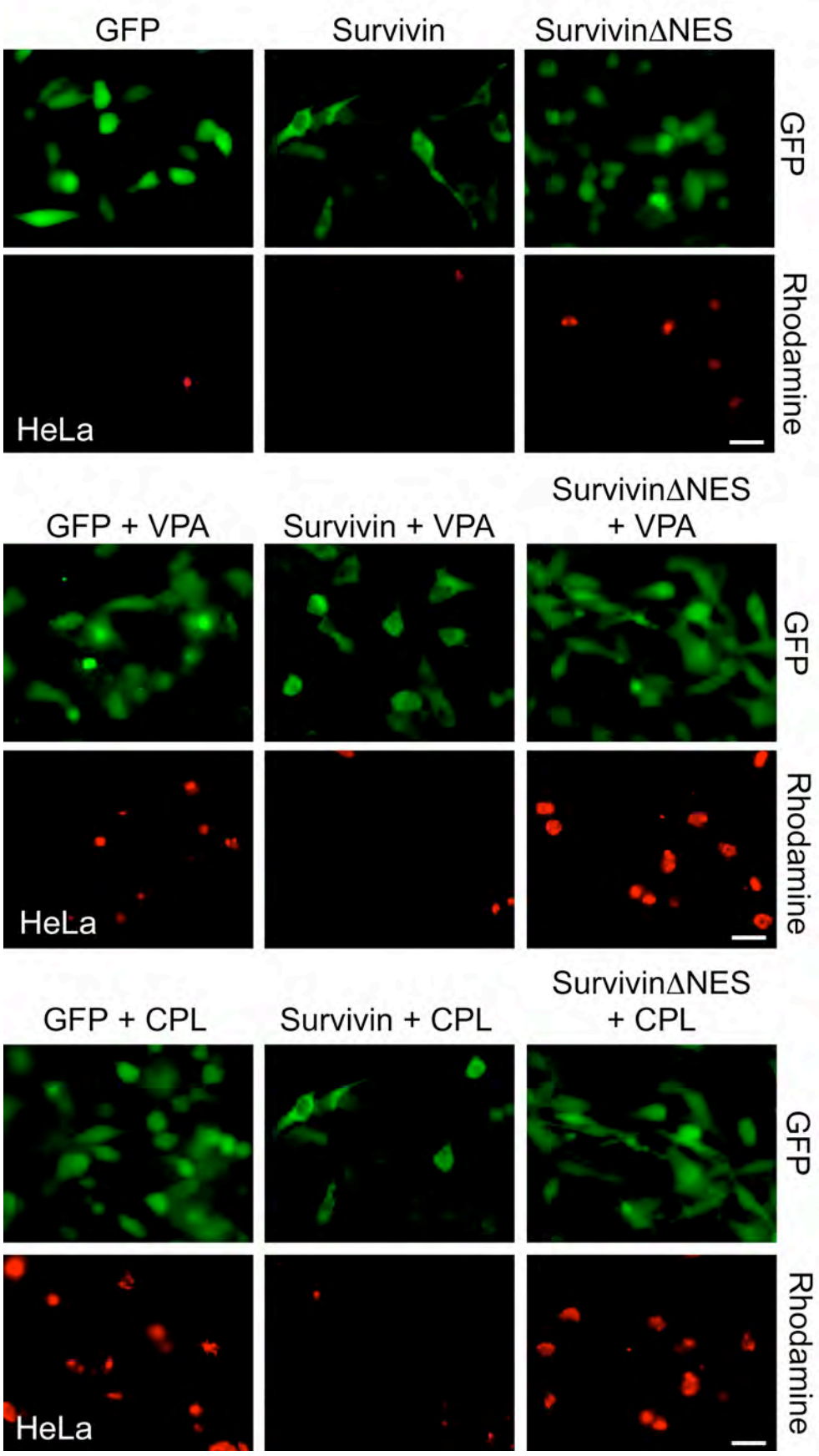

Supplementary Figure S3

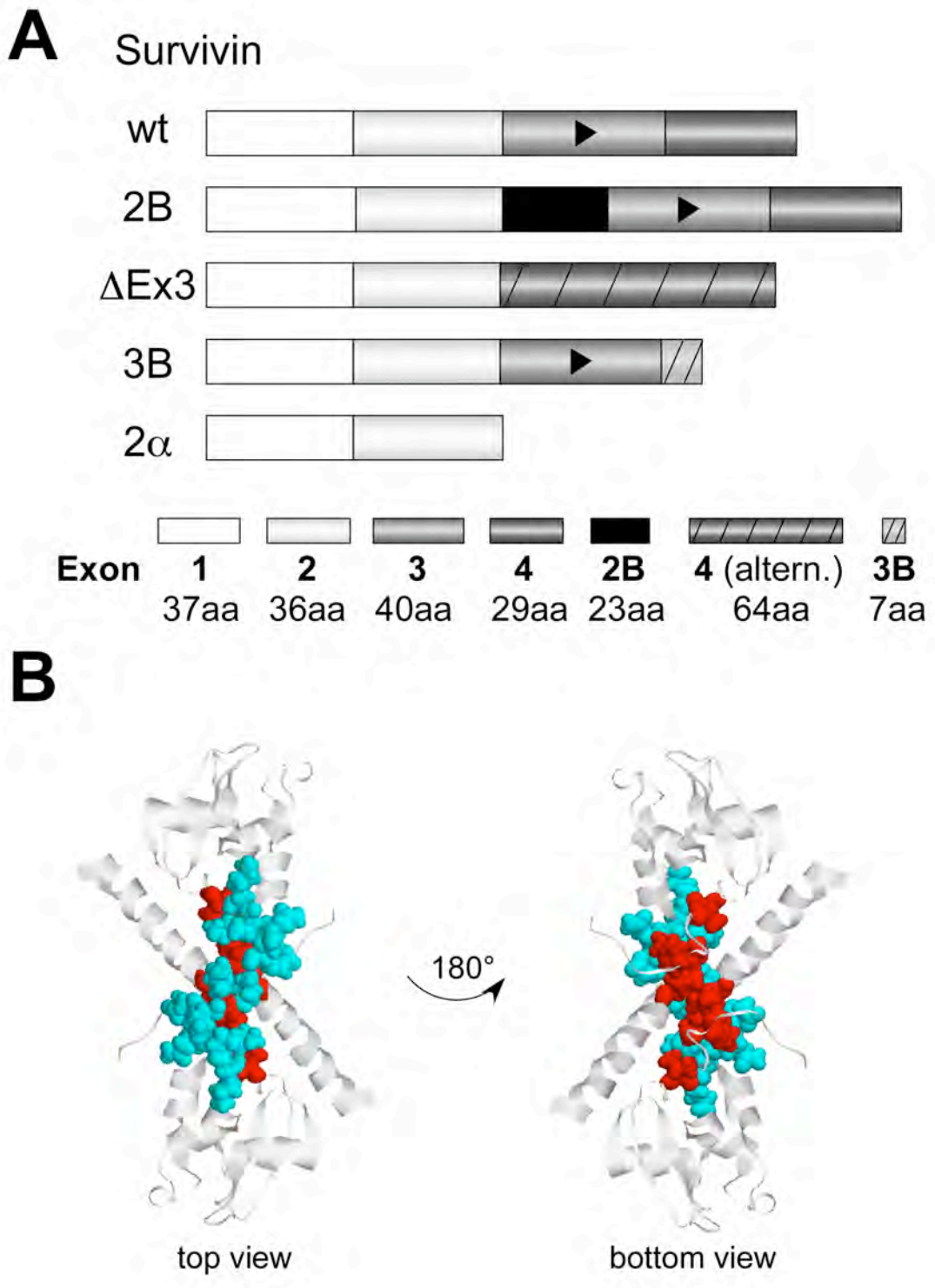

Supplementary Figure S4

Supplementary Tables:

***Table S1*:** Tumor stages and clinical characteristics of CRC patients examined by RT-qPCR analysis

Case	*Staging*			*Grading*	*Age*	*Sex*	*Ratio*
	pT	*pN*	*pM*				
1	T3	N1	M1	G2	67	M	6,24
2	T2	N0	M0	G1	58	M	3,83
3	T4	N1	M1	G3	64	M	2,23
4	T3	N2	M0	G2	65	M	5,40
5	T3	N0	M1	G2	76	M	6,69
6	T3	N1	M1	G2	56	F	9,09
7	T4	N2	M0	G3	76	M	4,60
8	T3	N1	M0	G2	77	M	12,48

Ratio: $R = \frac{\left(E_{\text{target}}\right)^{\Delta CP_{\text{target (control-sample)}}}}{\left(E_{\text{ref}}\right)^{\Delta CP_{\text{ref (control-sample)}}}}$

Table S2: Tumor stages and clinical characteristics of HNSCC patients examined by RT-qPCR analysis

Case	*Localization*	*Staging*		*Grading*	*Age*	*Sex*	*Ratio*
		pT	*pN*				
1	Oral cavity	T4	N2	G2	51	M	2,13
2	Oral cavity	T3	N1	G2	47	M	1,23
3	Oropharynx	T3	N2	G2	56	M	2,96
4	Oral cavity	T4	N1	G2	42	F	5,8
5	Larynx	T4	N3	G3	56	M	5,04
6	Hypopharynx	T3	N2	G2	49	M	0,62
7	Oropharynx	T3	N1	G2	58	M	1,63
8	Oral cavity	T1	N2	G3	57	M	0,45
9	Oral cavity	T2	N3	G2	57	M	7,53
10	Oral cavity	T2	N2	G2	47	M	4,81
11	Oral cavity	T4	N2	G2	80	M	13,68

Ratio: $R = \frac{\left(E_{\text{target}}\right)^{\Delta CP_{\text{target (control-sample)}}}}{\left(E_{\text{ref}}\right)^{\Delta CP_{\text{ref (control-sample)}}}}$

Table S3: Collective results of the transport activity of survivin, survivin splice mutants and survivin deletion mutants.

Protein	aa	Export activity		Import activity
		tf	mj	mj
HsSurvivin	1-142	**+** (2, H, HN, CC)	**+** (V, HN, CC)	**-** (V, HN, CC)
HsSurvivin_NESmut	1-142	**-** (2, H, HN, CC)	**-** (V, HN, CC)	**-** (V, HN, CC)
survivin_sim-GFP	1-142	**+** (2, H, HN, CC)	**+** (V, HN, CC)	**-** (V, HN, CC)
survivinΔNES_sim-GFP	1-142	**-** (2, H, HN, CC)	**-** (V, HN, CC)	**-** (V, HN, CC)
RnSurvivin	1-142	**+** (H, N)	**+** (V, N)	n.d.
HsSurvivin2B	1-165	**+** (H, HN, CC)	n.d.	n.d.
HsSurvivinDEx3	1-137	**-** (H, HN, CC)	n.d.	n.d.
HsSurvivin3B	1-120	**+** (H, HN, CC)	n.d.	n.d.
HsSurvivin2α	1-74	**-** (H, HN, CC)	n.d.	n.d.
HsSurvivin1-119	1-119	**+** (H, HN, CC)	n.d.	n.d.
HsSurvivin1-88	1-88	**-** (H, HN, CC)	n.d.	n.d.
HsSurvivinNES	89-98	n.d.	**+** (V, HN, CC)	n.d.
HsSurvivinNESmut	89-98	n.d.	**-** (V, HN, CC)	n.d.
HsSurvivin93-104	93-104	n.d.	**-** (V)	n.d.
RnSurvivinNES	89-98	n.d.	**+** (V, N)	n.d.

2: 293T; H: HeLa; HN: 1624; CC: RKO; V: Vero; N: NIH3T3; tf: transient expression; mj: microinjection; Hs: Homo sapiens; Rn: Rattus norvegicus; n.d., not done.

***Table S4**:* Overall clinical characteristics of CRC patients examined by ICH.

Survivin		***N/C***	***N***
	n	***n (%)***	***n (%)***
Number of specimens	263	239 (91)	24 (9)
Stage			
pT2	24	24	0
pT3	239	215	24
pN0	39	34	5
pN1	81	68	13
pN2	132	129	6
pNx*	11	8	0
pM0	107	100	7
pM1	125	113	12
pMx*	31	26	5
Grade			
G1	22	20	2
G2	218	198	20
G3	23	21	2

*status unknown in metastatic tumors

4

Traffic 2005; **6:** 1–13
Blackwell Munksgaard

doi: 10.1111/j.1600-0854.2005.00298.x

Toolbox

Translocation Biosensors to Study Signal-Specific Nucleo-Cytoplasmic Transport, Protease Activity and Protein–Protein Interactions

Shirley K. Knauer[1], Sabrina Moodt[2], Thorsten Berg[3], Urban Liebel[4], Rainer Pepperkok[4] and Roland H. Stauber[1,*]

[1]Georg-Speyer-Haus, Paul-Ehrlich-Str. 42–44, D-60596 Frankfurt, Germany
[2]ZMBH Heidelberg, Im Neuenheimer Feld 282, D-69120 Heidelberg, Germany
[3]Max Planck Institute of Biochemistry, Am Klopferspitz 18, D-82152 Martinsried, Germany
[4]EMBL Heidelberg, Meyerhofstrasse 1, D-69117 Heidelberg, Germany
**Corresponding author: Roland H. Stauber, stauber@em.uni-frankfurt.de*

Regulated nucleo-cytoplasmic transport is crucial for cellular homeostasis and relies on protein interaction networks. In addition, the spatial division into the nucleus and the cytoplasm marks two intracellular compartments that can easily be distinguished by microscopy. Consequently, combining the rules for regulated nucleo-cytoplasmic transport with autofluorescent proteins, we developed novel cellular biosensors composed of glutathione S-transferase, mutants of green fluorescent protein and rational combinations of nuclear import and export signals. Addition of regulatory sequences resulted in three classes of biosensors applicable for the identification of signal-specific nuclear export and import inhibitors, small molecules that interfere with protease activity and compounds that prevent specific protein–protein interactions in living cells. As a unique feature, our system exploits nuclear accumulation of the cytoplasmic biosensors as the reliable readout for all assays. Efficacy of the biosensors was systematically investigated and also demonstrated by using a fully automated platform for high throughput screening (HTS) microscopy and assay analysis. The introduced modular biosensors not only have the potential to further dissect nucleo-cytoplasmic transport pathways but also to be employed in numerous screening applications for the early stage evaluation of potential drug candidates.

Key words: apoptosis, cancer, export, Exportin 1/CRM1, HIV-1 Rev, import, Jun/Fos, Myc/Max, p53/mdm2, protein–protein interaction, Stat

Received 7 February 2005, revised and accepted for publication 5 April 2005, published on-line XXXX

Cellular communication strictly depends on regulated nucleo-cytoplasmic transport through the nuclear pore complex (NPC), which is controlled by specific signals and transport factors (1). Those include the proteins of the NPC (nucleoporins), the RanGTPase, transport receptors and specialized factors that promote the transport of specific protein/RNA complexes (2). In general, active nuclear import requires energy and is mediated by short stretches of basic amino acids, termed nuclear localization signals (NLSs), which interact with specific import receptors [(2) and references within]. The best characterized nuclear export signals (NESs) consist of a short leucine-rich stretch of amino acids and interact with the export receptor Exportin 1 [(3) and references therein]. Leucine-rich NESs have been identified in an increasing number of disease-relevant cellular and viral proteins implicated in transcription control (4), cell cycle control (5) and RNA transport (6). Although the orchestration of export is still unclear, NESs can be grouped into specific classes according to their activity *in vivo* (7). Because regulated subcellular localization provides an attractive way to control the activity and stability of regulatory proteins and RNAs, interfering with nucleo-cytoplasmic transport in general as a novel therapeutic principle has recently attracted major interest by academia and industry [reviewed in (8,9)].

Regulated intracellular localization is also essential for the controlled activity of site-specific proteases, which play crucial roles in a variety of cellular functions. Deregulation of key proteases is known to contribute to pathological consequences. For several viruses, such as HIV, viral proteases are essential for replication and thus are crucial drug targets (10). Among the key mediators of apoptosis are also proteolytic enzymes known as caspases. Given their central role as death effector molecules, a great deal of interest has recently focused on caspases as therapeutic targets for various disease processes (11).

Because protein interaction networks are critical for all cellular events including intracellular transport (1), identification of specific protein interactions and characterization of their physiological significance is one of the main goals of current research in a wide range of biological fields. In addition, abolishing or inducing specific protein–protein interactions by molecular decoys offers tremendous possibilities for the

treatment of human diseases. Consequently, numerous methods have been described to analyze protein–protein interactions *in vitro* and *in vivo* [(8,12–14) and references therein]. In cancer, cellular transformation and maintenance of the transformed phenotype often depend upon the formation of specific complexes. For example, the proto-oncogenes *jun* and *fos* encode basic leucine zipper (bZip) containing oncogenic transcription factors that bind DNA as dimers and can promote malignant transformation [see (15) and references therein]. Potential drug targets are also the basic helix–loop–helix leucine zipper (bHLHZip) transcription factors Myc and Max. Myc is associated with numerous types of human cancers and must dimerize with the Max protein for its oncogenic activity. Inhibitors that prevent Jun-Fos or Myc-Max dimerization are thus currently under intense investigation as potential anticancer drugs (16,17). Likewise, the tumor-suppressor protein p53 forms an autoregulatory feedback loop with mdm2, in which the latter inhibits p53 transcriptional activity and stimulates its degradation [(18) and references therein]. Inhibition of the p53–mdm2 interaction with synthetic molecules can lead to the nuclear accumulation and the activation of p53 followed by the death of the tumor cells from apoptosis (19).

As any biochemical data or potential drug therapies must be effective at the cellular level, isolated proteins cannot be regarded as representatives of complex biological systems, and cell-based assays (CBAs) have to be employed to complement *in vitro* data. Recently, several methods have been developed to facilitate the implementation of high-throughput CBAs (20). In particular, the advent of autofluorescent proteins (AFPs) [e.g. green fluorescent protein (GFP)] as imaging tools, combined with novel computer-driven automated image acquisition and pattern-recognition systems, will help to make high-throughput screening a rapid and facile process [referenced in (21)]. However, any realistic applications of high-content (HC) and high-throughput CBAs critically depend on robust and reliable biological readout systems with a high signal to noise ratio. In this context, the spatial and functional division into the nucleus and the cytoplasm marks two dynamic intracellular compartments that can easily be distinguished by microscopy. Facing the clear need for improved CBAs, we exploited our knowledge of regulated nucleo-cytoplasmic transport resulting in the development and application of modular protein translocation biosensors tailored to investigate signal-specific nuclear export and import, protease activity and specific protein–protein interactions in living cells.

Results

Rational design of biosensors to investigate signal-specific nucleo-cytoplasmic transport

Autofluorescent protein-based cellular assays for the identification of signal-specific nucleo-cytoplasmic translocation inhibitors should meet the following requirements: The AFP-biosensor (i) should localize predominantly to the cytoplasm, (ii) is efficiently shuttled between the nucleus and the cytoplasm, (iii) should accumulate in the nucleus following inhibition of nuclear export, (iv) should allow the modular exchange of transport signals and (v) is neither toxic nor affected by passive diffusion or post-translational modifications in its intracellular localization.

Previously, we showed that the intracellular localization of a glutathione S-transferase (GST)-GFP fusion strictly depends on the presence of transport signals and is not flawed by passive diffusion (22). In addition, GST-GFP is highly fluorescent, non-toxic and stable. To design a GFP-GST shuttle protein with a predominantly cytoplasmic steady-state localization, an appropriate combination of NLS and NES had to be used. On the basis of our kinetic classification studies (7), we choose the SV40 large T-antigen NLS (NLS) and the NESs from the HIV-1 Rev protein, protein kinase inhibitor (PKI), p53, the MAPKK, STAT1 and the Bcr-Abl oncoprotein and investigated their activities by microinjection of recombinant GST-GFP-NLS or -NES fusion proteins, respectively. The results (see Supplementary Table S1 available online at http://www.traffic.dk/suppmat/6_7a.asp) indicated that combining the SV40 NLS with the NESs from PKI (PKINES), the HIV-1 Rev protein, STAT1, Bcr-Abl and from MAPKK but not from p53 should result in predominantly cytoplasmic NLS-GFP/GST-NES shuttle proteins. We confirmed this prediction by the transient expression of selected fusion proteins (NLS-GFP/GST-PKINES = PKINES-sensor; NLS-GFP/GST-RevNES = RevNES-sensor; NLS-GFP/GST-AblNES =AblNES-sensor; NLS-GFP/GST-Stat1NES = StatNES-sensor and NLS-GFP/GST-p53NES = p53NES-sensor) in several cell lines (Figure 1A–D and Supplementary Table S2 online for detailed values, available online at http://www.traffic.dk/suppmat/6_7a.asp). With the exception of the p53-sensor, all sensor constructs displayed a predominantly cytoplasmic steady-state localization. Of note, exchanging the positions of the NLS with the RevNES or the PKINES-impaired NES activity (Figure 1C and data not shown) resulting in strictly nuclear fusion proteins, most likely due to sterical interference between the NES and the GFP.

The continuous shuttling of the transport sensors was confirmed by treatment with the export inhibitor leptomycin-B (LMB), resulting in their nuclear accumulation (Figure 1B,D and Supplementary Table S2 online for detailed values, available online at http://www.traffic.dk/suppmat/6_7a.asp). The activity of the biosensor appeared not to be cell-type specific, and translocation of the biosensors could also be detected in non-adherent K562 cells (Figure 1D). In addition, the localization was not affected by fixation and storage of the cells prior to analysis (see Supplementary Table S2 online for detailed values, available online at http://www.traffic.dk/suppmat/6_7a.asp).

For HCS (high content screening)/HTS assays, cell lines inducibly expressing the biosensor are essential. Thus,

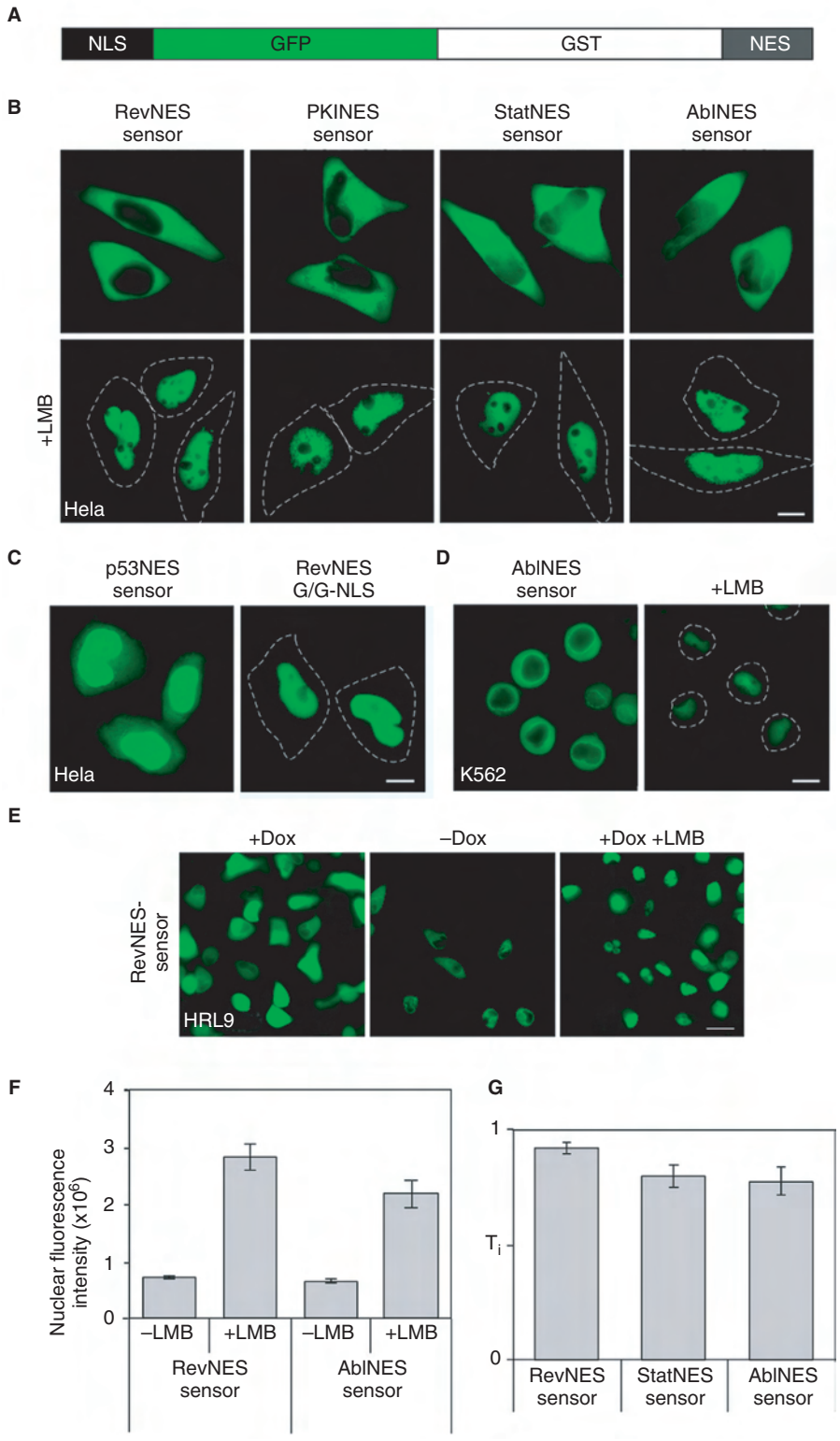

Figure 1: Transport biosensors to detect interference with nuclear export. A) Schematic representation of the transport sensors. B) In transfected cells, the indicated sensor proteins localized predominantly to the cytoplasm and accumulated in the nucleus following leptomycin-B (LMB) treatment. C) In contrast, the p53NES sensor or the RevNES-GFP/GST-NLS fusion (RevNES-G/G-NLS) localized predominantly in the nucleus. D) Cytoplasmic-nuclear translocation of the AblNES sensor was detectable also in non-adherent leukemia cells. Scale bars, 10 μm. Dashed lines mark the cell boundaries visualized from the corresponding phase-contrast images. E) Inducible expression of transport sensors in stable cell lines. Cells cultured in the presence or absence of doxycycline were recorded using identical camera settings. Upon LMB-treatment, the cytoplasmic RevNES sensor accumulated completely in the nucleus after 2 h. Scale bar, 100 μm. F) Translocation assay performed on an automated platform for high-throughput cell screening microscopy and assay analysis. The total nuclear fluorescence in at least 200 sensor-expressing cells from two independent experiments was recorded before and after the treatment with LMB for 2 h. Mean values ± SD from two independent experiments are shown. G) To quantify the cytoplasmic to nuclear translocation, the percentage of cytoplasmic and nuclear fluorescence of the indicated biosensors in inducible cell lines was determined before and after the treatment, and the mean translocation index T_i was calculated. Error bars, SD.

we generated cell lines, in which the expression of the transport sensors could be induced by the addition of doxycycline (Dox) (Tet-on system). The induced sensors retained the desired property of an efficient cytoplasmic to nuclear transition following LMB treatment (Figure 1E–G and Supplementary Table S2 online for detailed values, available online at http://www.traffic.dk/suppmat/6_7a.asp).

Next, we tested the inducible RevNES- and the AblNES-sensor on an automated platform for high-throughput cell screening microscopy and assay analysis. Figure 1F demonstrates that cytoplasmic to nuclear translocation of the sensors following LMB treatment could be accurately and reproducibly quantitated in an automated fashion.

To further investigate whether the biosensors are superior in analyzing signal-specific translocation compared with full-length GFP-fusions of the corresponding proteins from which the signals originated, we quantitated the translocation index T_i (difference of cytoplasmic signal before and after inhibition of export) for the respective proteins. As shown in Figure 2A, Rev14-GFP, PKI-BFP (blue fluorescent protein) and STAT1-GFP localized predominantly to the cytoplasm following transient expression in HeLa cells and accumulated to various degrees in the nucleus following LMB treatment. However, the translocation index for the corresponding biosensors was significantly higher and reached a maximum already 2 h after treatment in contrast to the full-length GFP-fusions (Figure 2B and Supplementary Table S2 online for detailed values, available online at http://www.traffic.dk/suppmat/6_7a.asp).

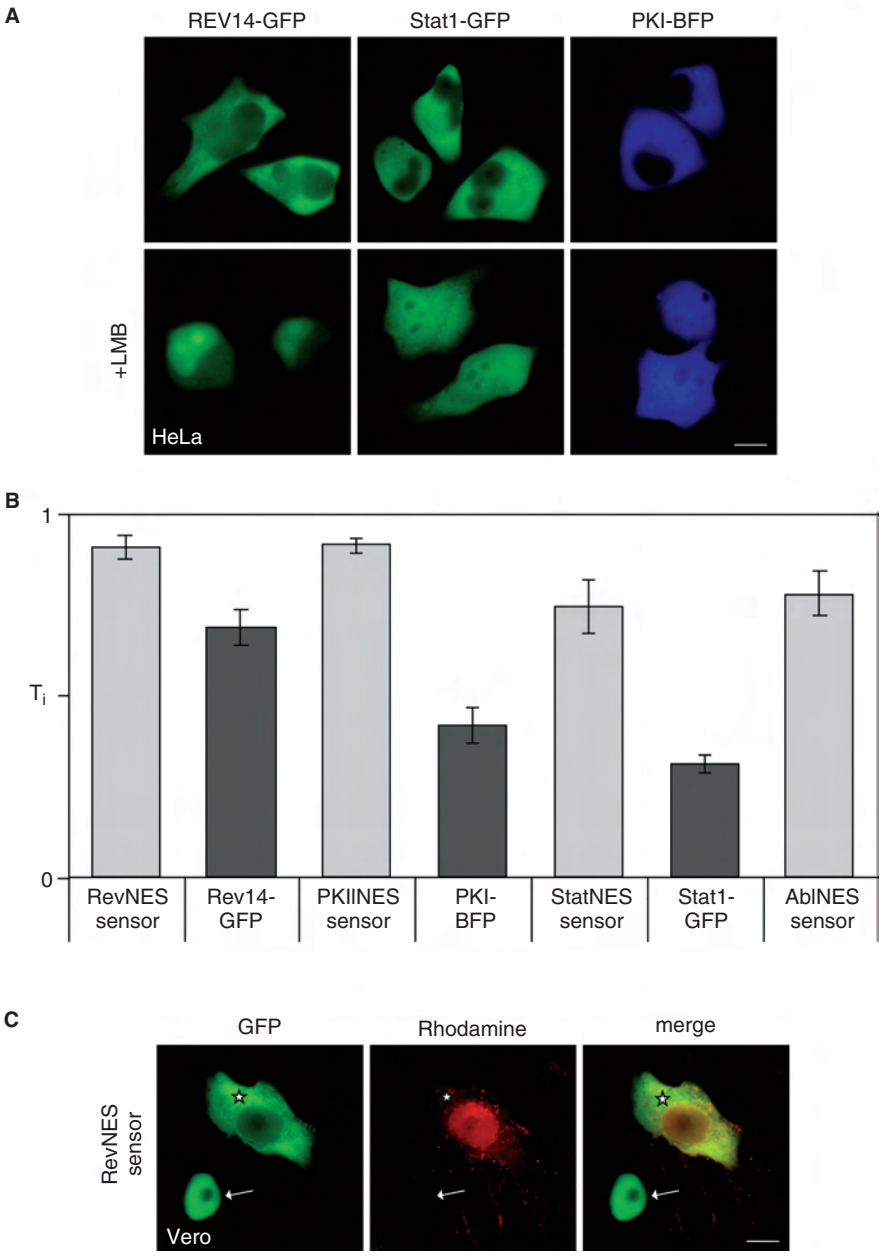

Figure 2: A) Transport biosensors are superior in studying signal-specific transport compared with full-length green fluorescent protein (GFP)-fusion. In transfected HeLa cells, Rev14-GFP, Stat1-GFP and PKI-BFP localized predominantly to the cytoplasm (upper panel) and accumulated to various degrees in the nucleus following treatment with leptomycin-B (LMB) for 6 h (lower panel). Scale bar, 10 μm. B) To quantify the cytoplasmic to nuclear translocation, the percentage of cytoplasmic and nuclear fluorescence was determined in several cell lines before and after treatment (see Supplementary Table S1 online for detailed values, available online at http://www.traffic.dk/suppmat/6_7a.asp), and the mean translocation index T_i was calculated. Error bars, SD. C) Transport biosensors to identify import inhibitors. Microinjection of Texas Red-conjugated WGA into a RevNES sensor-expressing cell (marked by the asterisk) inhibited nuclear import and prevented LMB-induced nuclear accumulation of the sensor protein, which was observed for a non-injected control cell (marked by the arrow). Scale bar, 10 μm.

To date, no specific small molecular weight nuclear import inhibitors are available. To test whether the biosensors can be used to also identify compounds interfering with nuclear import, wheat germ agglutinin (WGA) was microinjected into the nucleus of cells expressing the RevNES-sensor, and cells were subsequently treated with LMB. Wheat germ agglutinin interferes with nuclear import by binding to nucleoporins (7). As depicted in Figure 2C, nuclear import of the biosensor was inhibited in injected cells in contrast to control cells. Thus, compounds that preserve the cytoplasmic localization of the biosensors after the subsequent addition of nuclear export inhibitors can be annotated as nuclear import inhibitors.

96-well plate assays to screen for drugs or proteins that interfere with nucleo-cytoplasmic transport

To demonstrate the applicability of the transport sensors for HTS assays, we performed screening experiments in 96-well plates. Expression of the respective transport biosensors was induced by Dox, and cells were subsequently incubated with drugs, which previously have been reported to affect nucleo-cytoplasmic transport (see Supplementary Table S3 online for details, available online at http://www.traffic.dk/suppmat/6_7a.asp). Interestingly, of the tested substances, only the Exportin 1 targeting compounds LMB and RatA caused nuclear accumulation of all transport sensors. Although prolonged treatment with taxol or nocodazol for 16 h caused cell rounding and partial detachment, the transport sensors still remained cytoplasmic (Supplementary Figure S1A, available online at http://www.traffic.dk/suppmat/6_7a.asp). To investigate whether drug treatment affected nuclear import, compound treated cells were subsequently incubated with LMB. The resulting nuclear accumulation of the sensors indicated that the tested substances did not significantly interfere with import (Supplementary Figure S1A and Supplementary Table S3 online for details, available online at http://www.traffic.dk/suppmat/6_7a.asp).

The intracellular localization of a shuttle protein may also be influenced *in trans* by interacting proteins or by proteins interfering with the transport machinery. As an example for a genetic screen, we investigated whether translocation of the transport sensors was affected by overexpressing proteins *in trans*. Transfection of several expression constructs (see Supplementary Table S3 online for details, available online at http://www.traffic.dk/suppmat/6_7a.asp) revealed that the overexpression of PKI-BFP and the C-terminal part of Nup214 affected nuclear export as previously reported (7) and caused nuclear accumulation of all sensor constructs (see Supplementary Figure S1B and Supplementary Table S3, available online at http://www.traffic.dk/suppmat/6_7a.asp). Transfected cells were treated with LMB to investigate whether the overexpression of the indicated proteins *in trans* interfered with nuclear import. As summarized in Supplementary Table S3, all sensor proteins accumulated in the nucleus upon LMB treatment arguing against negative effects of the overexpressed proteins on nuclear import.

Biosensors for protease and apoptosis research

The robust performance of the translocation sensors was further exploited by the development into protease biosensors. We incorporated the poly (ADP-ribose)-polymerase (PARP) cleavage site for Caspase 3 (CS3) N-terminal to the Myc-epitope-RevNES resulting in an NLS-GFP/GST-CS3-RevNES fusion protein (Casp3-sensor) (Figure 3A). Upon transient expression, the Casp3-sensor localized predominantly to the cytoplasm in HeLa cells (see Supplementary Table S2 online for values, available online at http://www.traffic.dk/suppmat/6_7a.asp). Induction of apoptosis by treatment with staurosporin-induced caspase activity, which resulted in the cleavage of the Myc-epitope-RevNES and the subsequent nuclear accumulation of the Casp3-sensor in early apoptotic, TdT-mediated biotin – dUTP nick-end labelling (TUNEL)-positive cells (Figure 3B). In non-apoptotic, TUNEL-negative cells, no change in localization was observed (Figure 3B, cells marked by the arrow). As a control, a construct containing a non-functional Casp3 cleavage site (Casp3mut-sensor) remained cytoplasmic under identical experimental conditions, indicating that nuclear accumulation was not caused by unspecific interference with nuclear export (Figure 3B). Of note, in late apoptotic cells, the Casp3-sensor was equally distributed throughout the cell due to the loss of the integrity of the nuclear membrane (data not shown). Proteolytic cleavage was verified by staining with an anti-Myc antibody. The cytoplasmic Casp3-sensor was detectable by anti-Myc staining in non-apoptotic cells, whereas caspase activation resulted in the cleavage of the Myc-epitope-RevNES, and thus, the nuclear Casp3-sensor could no longer be detected by the anti-Myc antibody (Figure 3D). To underline the performance of the Casp3-sensor, we performed a comparison with a commercially available apoptosis indicator composed of the MAPKK NES, CS3, GFP and three copies of the SV40 NLS (MKNES-CS3-GFP-NLS). In contrast to the Casp3-sensor, a significant amount of the MKNES-CS3-GFP-NLS was already detectable in the nucleus prior to induction of apoptosis (see Supplementary Table S2 online for values, available online at http://www.traffic.dk/suppmat/6_7a.asp), and the indicator accumulated less efficiently in the nucleus after staurosporin treatment (Figure 3B). Consequently, the nuclear translocation index was significantly higher for the Casp3-sensor upon induction of apoptosis (Figure 3C). This difference was most likely caused by the passive diffusion of GFP in combination with the weaker activity of the MAPKK NES compared to the Rev NES (see Supplementary Table S1, available online at http://www.traffic.dk/suppmat/6_7a.asp) and the

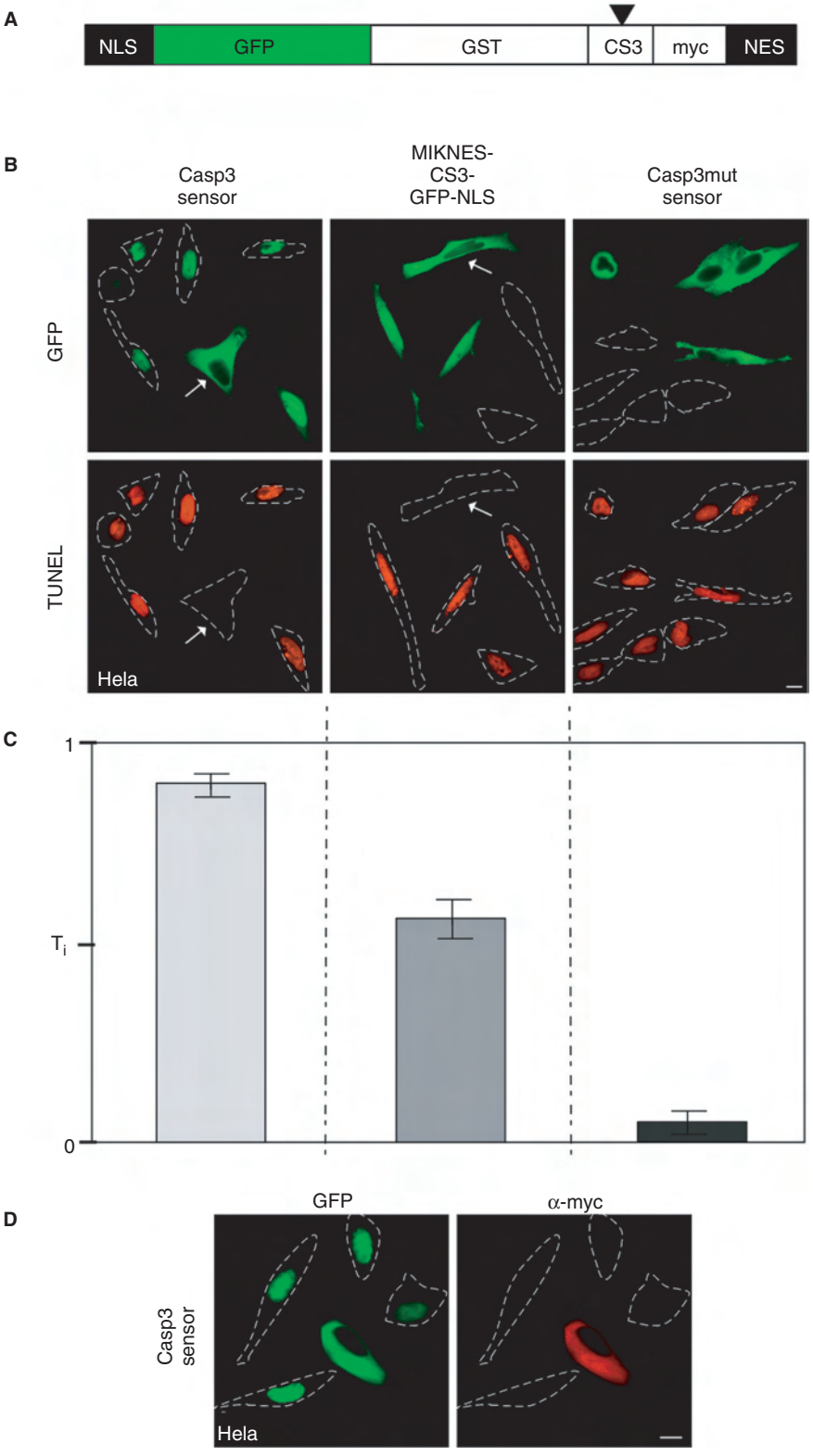

Figure 3: Induction of apoptosis resulted in proteolytic cleavage and nuclear accumulation of the Casp3-biosensor. A) Schematic representation of the Casp3-sensor. B) Cells expressing the indicated plasmids were treated with staurosporin to induce apoptosis. In TdT-mediated biotin–dUTP nick-end labelling-positive apoptotic cells (red, lower panel), the Casp3-sensor accumulated in the nucleus in contrast to non-apoptotic cells (marked by the arrow) (left panel). The MKNES-CS3-GFP-NLS protein accumulated less efficiently in the nucleus and displayed a detectable nuclear localization in non-apoptotic cells (middle panel). As a control, the Casp3mut sensor containing a non-functional Casp3-recognition site remained cytoplasmic (right panel). Scale bar, 10 μm. C) To quantify the cytoplasmic to nuclear translocation of the biosensors, the translocation index T_i was calculated. Mean values ± SD from two independent experiments. D) The cytoplasmic Casp3 sensor was detectable by staining with the anti-Myc antibody in non-apoptotic cells. Caspase activation resulted in the cleavage of the Myc-epitope-RevNES, and thus, the Casp3 sensor in the nucleus was no longer detectable.

presence of three copies of the SV40 NLS in the MKNES-CS3-GFP-NLS construct.

Facile cellular biosensors to visualize specific protein–protein interaction in vivo

A facile and reliable system that allows visualizing protein interactions in living cells applicable also for drug screening CBAs has to fulfill the following criteria: (i) the GFP-tagged molecule I (GFP-prey), although continuously shuttling between the nucleus and the cytoplasm, should localize predominantly to the cytoplasm, (ii) the BFP-tagged molecule II (BFP-bait) should be confined to the nucleus, (iii) upon specific protein interaction between molecule I and II, the GFP-prey should redistribute to the nucleus and colocalize with the BFP-bait, (iv) the system should be reversible and should allow the modular exchange of interaction domains (IDs) and (v) inhibitors/inductors of protein interactions should prevent/induce the cytoplasmic to nuclear translocation.

Because the RevNES translocation sensor fulfilled all the quality criteria of a GFP-prey, we engineered a cassette that allows the expression of any open reading frame (ORF) X as a NLS-GFP/GST-X-RevNES fusion protein (GFP-prey). Our previous work (23) demonstrated that a NES-deficient HIV-1 Rev BFP fusion (RevM10-BFP) localized to the nucleolus and thus represented an ideal frame to express nucleolar anchored Y-BFP fusion proteins (BFP-bait).

To demonstrate that our system was applicable for the analysis of protein IDs, we first tested the bZip IDs of Jun and Fos and the bHLHZip IDs of Myc and Max in our assay. We found that the NLS-GFP/GST-JunbZip-RevNES fusion (GFP-prey_Jun) localized predominantly to the cytoplasm in the presence of the empty BFP-bait (Figures 4A and 6C). In contrast, coexpression of the FosbZip-RevM10-BFP protein (Fos_BFP-bait) resulted in the colocalization of the GFP-prey_Jun fusion with the Fos_BFP-bait at the nucleolus (Figures 4B and 6C). Similar results were obtained for the Myc and Max bHLHZip IDs (Figures 4A,B and 6C) and could be confirmed in MCF7, 293 and non-adherent K562 cells (data not shown). As a control, we switched the Jun/Fos IDs in the prey and bait constructs which resulted in a similar prey-redistribution upon coexpression (Figure 4C, left panel). Importantly, we did not observe protein interaction upon coexpression of the GFP-prey_Jun together with the Max_BFP-bait (Figures 4C, middle panel, and 6C) or of the GFP-prey_Myc together with the Fos_BFP-bait (Figures 4C, right panel, and 6C), which underlined the specificity of the interaction assay. To further investigate whether our system was also applicable for non-leucine zipper mediated protein interactions, we tested the p53/mdm2 IDs. The GFP-prey_mdm2 fusion localized to the cytoplasm and colocalized with the p53_BFP-bait but not with the empty BFP-bait at the nucleolus upon coexpression (Figures 4A,B and 6C).

The routine use of live cell assays to analyze protein–protein interaction requires that the system is robust and does not depend on demanding technological assay platforms. We compared the translocation biosensors to bimolecular fluorescence complementation (BiFC) by cotransfecting equal amounts of the GFP-prey_Jun and Fos_BFP-bait or the FosGC and JunGN expression plasmids into HeLa cells together with a red fluorescent protein (RFP) expression construct as the transfection control. Quantitation of the number of RFP-positive cells also displaying nuclear GFP-fluorescence, indicative for active protein interaction (Figure 5A), revealed that not only the number of individual protein interaction events but also the average fluorescence signal was significantly higher for the translocation assay (TA) compared with that for the BiFC (Figure 5A,B). Equal transfection efficiencies and expression levels were confirmed by immunoblot analysis of the respective GFP-fusion proteins (data not shown).

The protein interaction assay is reversible and suited for the identification of small molecule protein interaction inhibitors (SMPIIs)

Besides efficacy and specificity, reversibility is an important criterion for cellular protein interaction assays. We confirmed the reversibility of our assay by overexpressing the untagged Fos leucine zipper (Fos bZip) in cells coexpressing GFP-prey_Jun and Fos_BFP-bait, which resulted in a significantly reduced nucleolar colocalization of the GFP-prey_Jun protein (Figure 6A,C). Similar results were obtained in competition experiments for the Myc and Max IDs using the untagged Max-bHLHZip (Figure 6C).

As a case study for the application of a SMPPII, we attempted to disrupt the p53/mdm2 interaction by microinjection of a synthetic peptide (comP) or an inactive scrambled control peptide (comPmut) into the nucleus of GFP-prey_mdm2 and p53_BFP-bait coexpressing cells. The comP peptide had been described as an inhibitor of p53/mdm2 interaction *in vitro* (18). Injection of comP interfered with p53/mdm2 ID interaction, resulting in a significantly cytoplasmic redistribution of the GFP-prey_mdm2, in contrast to non-injected cells or cells injected with comPmut (Figure 6B, lower panel, and 6C). Of note, comP injection had no effect on Jun/Fos complexes (data not shown), excluding the possibility that the GFP-prey_mdm2 redistribution was caused by comP-mediated inhibition of nuclear import.

Discussion

Despite intense investigation, the detailed molecular mechanism regulating the orchestration of nucleo-cytoplasmic transport is still not completely understood. Thus, in addition to biochemical studies, systematic cell-based chemical-genetic screens need to be applied to unravel novel regulatory mechanism and to clarify cargo specificity.

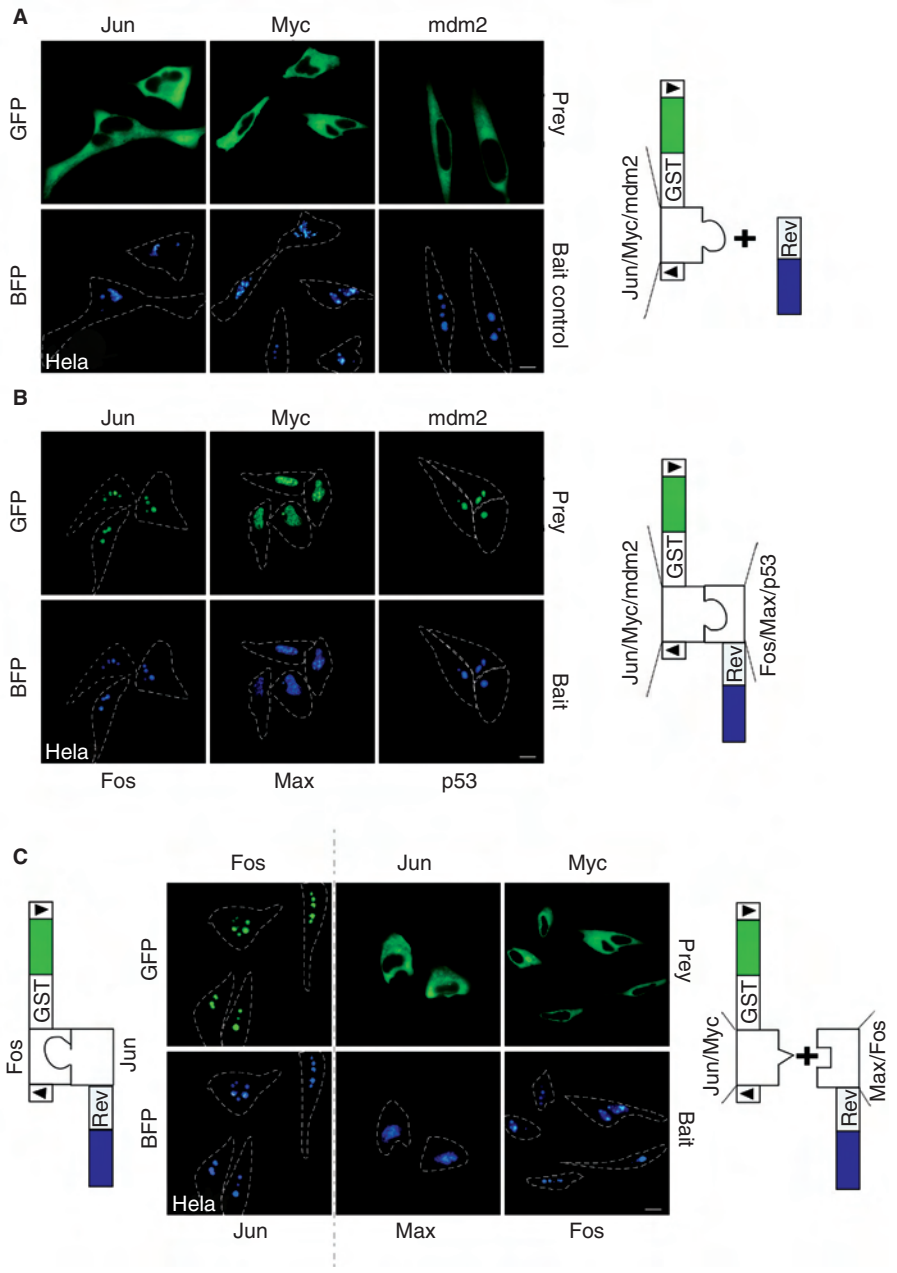

Figure 4: Application of the autofluorescent protein-based interaction biosensors to visualize specific protein–protein interaction *in vivo*. HeLa cells coexpressing the indicated prey/bait proteins were analyzed by fluorescence microscopy. A) The green fluorescent protein (GFP)-prey proteins localized predominantly to the cytoplasm (upper panel), and no colocalization was detectable by coexpression of the empty BFP-bait proteins (lower panel). B) In contrast, the GFP-prey proteins accumulated in the nucleus/nucleolus upon coexpression of the matching BFP-bait interaction partners. C) Domain swapping in the GFP-prey/BFP-bait constructs also resulted in efficient Fos/Jun protein interaction (left column). No significant colocalization was detectable by coexpression of GFP-prey_Jun and Max_BFP-bait or GFP-prey_Myc and Fos_BFP-bait fusion proteins (middle and right column). Scale bars, 10 μm4. ▶: nuclear localization signal, ◀: nuclear export signal.

Although nucleo-cytoplasmic TAs using GFP-fusions have been described (see (8), and references therein), this strategy is not generally applicable for every protein and often not suited for the development of systematic HCS/HTS assays. Firstly, applications are hampered by either the inability to generate cell lines stably overexpressing the particular GFP-fusion protein due to its toxicity and/or the inefficient cytoplasmic-nuclear redistribution, which makes fast and reliable automatic detection and analysis difficult. These limitations are exemplified by investigating the cytoplasmic nuclear translocation of the HIV-1 Rev-, the PKI- and the STAT1-GFP fusions. The lower T_is were caused by the lack/inaccessibility of an efficient nuclear import signal and/or interference by passive diffusion due to the small size of the fusion proteins. Secondly, the GFP TAs reported so far did not allow to discriminate whether export inhibition was caused by unspecific interference with the export machinery, by binding to the NES, by induction of intramolecular conformational changes or indirectly by affecting proteins that interact with the target protein *in trans*. Kau et al. (24) used a FOXO1a immunofluorescence translocation screen to identify compounds that caused FOXO1a nuclear accumulation. Additional assays were required to show that one class of compounds was indirectly interfering with FOXO1a transport by inhibiting PI3K/Akt signaling in general. The other class of compounds reacted with Exportin 1 and thus represents unspecific export inhibitors similar to other drugs

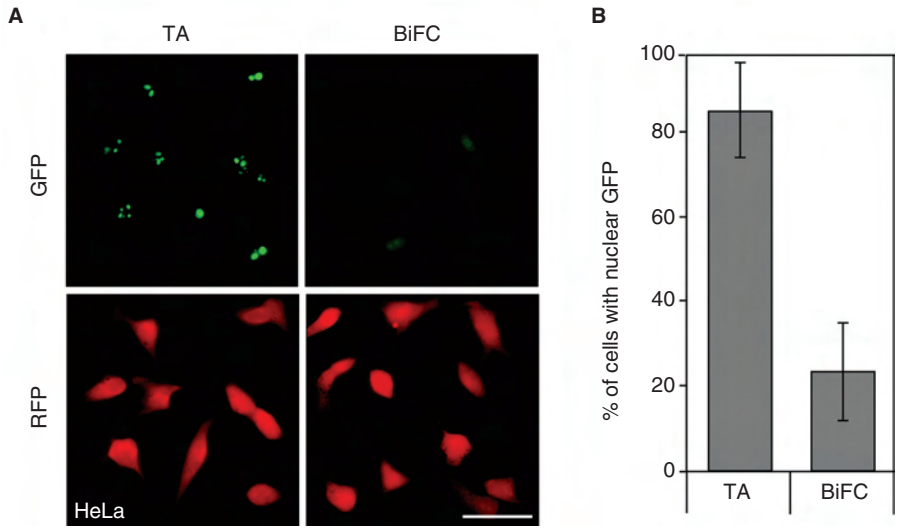

Figure 5: The autofluorescent protein-based protein–protein interaction assay is superior to bimolecular fluorescence complementation. HeLa cells were cotransfected with 1 μg of each of the green fluorescent protein (GFP)-prey_Jun and Fos_BFP-bait or the FosGC and JunGN expression plasmids, respectively, together with 1 μg of the red fluorescent protein (RFP)-expression plasmid and analyzed by fluorescence microscopy. Cells were recorded using identical camera settings. A significantly higher percentage of RFP-positive cells displaying also nuclear GFP-fluorescence was observed for the translocation assay (TA). A) Representative fields are shown. B) To quantify the number of protein interaction events, 200 cells from three separate images were inspected, and the number of RFP-positive cells, in which nuclear GFP fluorescence could be detected, was counted. Mean values ± SD from two independent experiments. Scale bars, 100 μm.

reported (25,26). Exportin 1 inhibitors can most likely not be used in target-specific therapeutic applications due to their toxic side-effects by blocking all cellular Exportin 1-mediated transport pathways. Therefore, protein-specific transport inhibitors are urgently needed. Because NESs can be grouped into specific categories according to their activity *in vivo*, these differences represent an attractive opportunity to selectively interfere with export and the biological functions of proteins by the generation of NES-specific inhibitors. The developed sensor system allows the modular integration of any specific transport signal into a constant protein backbone to now identify signal-specific inhibitors by a systematic screening of compound libraries. In contrast to other assays (24,27), the sensors were not restricted to a specific cell type, displayed a high translocation index and allowed the generation of inducible stable cell lines.

As a case study, we screened compounds that have been reported previously to affect nucleo-cytoplasmic transport including inhibitors of receptor signaling pathways (24,28,29), drugs, which affected the cytoskeleton (30,31), inhibitors of epigenetic regulators (32), transcription inhibitors (6) and inductors of apoptosis (see Supplementary Table S3, available online at http://www.traffic.dk/suppmat/6_7a.asp). In summary, we found that only drugs, which directly inactivated Exportin 1 inhibited nuclear export of all translocation sensors, indicating that the other compounds tested neither directly affected the transport machinery nor displayed any specificity for transport signals.

Because intracellular transport of proteins is not only regulated by specific signals but may also be influenced *in trans* by interacting proteins or by proteins interfering with the transport machinery, systematic genetic screens can be used to identify novel proteins engaged in intracellular transport networks. Of the randomly selected expression constructs, the overexpression of the C-terminal part of Nup214 affected nuclear export of all sensor constructs. Although it was reported that Nup214 is involved in the specific transport of the HIV-1 Rev protein (33) or of STAT1 (4), our data support the previous notion that overexpression of xFxFG-repeat containing nucleoporins unspecifically inhibits the nuclear export machinery (34). Thus, although suggested (9), components of the NPC appear not to represent pathway-specific drug targets.

In conclusion, the designed transport sensors will allow directly investigating the effects of drug treatment or of over-expression/conditional knock-down of proteins on general and signal-specific nucleo-cytoplasmic transport. The sensors were functional in chemical screens and could also be used on a fully automated platform for high-throughput cell screening microscopy and assay analysis, which is an essential requirement for their practical use in HTS assays.

To further exploit the common principle of cytoplasmic to nuclear translocation, the transport sensors were developed into protease biosensors. Because caspases are central players in several pathological states, we investigated the applicability of our principle by the generation of a caspase biosensor. Numerous *in vitro* and *in vivo* caspase assays have

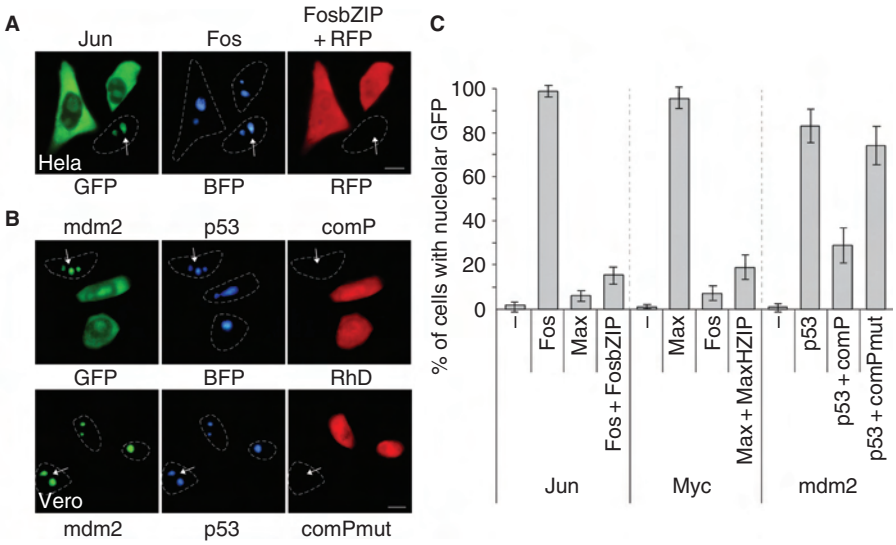

Figure 6: The interaction biosensors are reversible and suited for the identification of small molecule protein interaction inhibitors. A) Overexpression of the untagged Fos bZip domain in green fluorescent protein (GFP)-prey_Jun- and Fos_BFP-bait-coexpressing cells competes with Jun/Fos interaction. Red fluorescent protein (RFP) served as the transfection control. In RFP-positive cells, expression of the Fos bZip competitor relieved the nuclear accumulation of GFP-prey_Jun in contrast to non-transfected cells (marked by the arrow). B) Application of a synthetic peptide competitor (comP) to inhibit the p53/mdm2 interaction. GFP-prey_mdm2- and p53_BFP-bait-coexpressing cells were microinjected with the rhodamine-conjugated peptides and analyzed 4 h later. Injection of comP interfered with protein interaction resulting in a significant cytoplasmic redistribution of GFP-prey_mdm2 (upper panel) in contrast to non-injected cells (marked by the arrow) or cells injected with the control peptide comPmut (lower panel). Scale bars, 10 μm. C) To quantify the degree of protein interaction, 200 cells coexpressing the indicated GFP-prey and BFP-bait proteins together with the indicated competitors were inspected. The percentage of cells in which BFP and GFP colocalized in the nucleolus was determined. Mean values ± SD from two independent experiments.

been developed to date, including the application of fluorochrome-labeled inhibitors of caspases (35), fluorescence resonance energy transfer (FRET) (36) or even caspase-mediated activation of luciferase in whole animals (37). Analysis of caspase activity in intact cells, however, is often limited to the measurement of end-point apoptosis markers. In contrast, induction of apoptosis resulted in the cleavage of the RevNES and the nuclear accumulation of the Casp3-sensor already early in the cell death cascade. A commercially available indicator that is also based on the induction of nuclear accumulation upon proteolytic cleavage displayed a lower T_i and thus appears to be less applicable for CBAs. Our results suggest the use of the described protease biosensor to investigate caspase activity in real time and to study novel inhibitors or inductors of apoptosis in the context of an intact cellular environment. In addition, the modular composition of the translocation sensor implies that the system is readily adaptable for use with additional protease targets (e.g. HIV-1 protease).

A major emphasis of proteomic research and systems biology is the mapping and validation of protein interaction networks [(38,39) and references therein]. In addition, it has been acknowledged that molecules, which modulate protein–protein interactions may have great potential as therapeutics (40). Methods to study protein interactions in living cells or whole animals involve the yeast two hybrid (YTH) system, inter- and intramolecular FRET, BiFC as well as several split-enzyme complementation/reconstitution assays [(41) and references therein]. Although these various methods have been proven as valuable tools, several intrinsic limitations apply [see (42) and references within]. For example, the YTH detects only protein interactions in the nucleus of yeast cells, and potential interactions have to be verified assiduously in mammalian cellular systems. Although BiFC represents a powerful method, the efficiency and signal intensity are low, which was also demonstrated in our study. In addition, BiFC depends on the proper orientation of the two AFP fragments, and the likelihood of complementation is expected to decrease with protein size and distinct intracellular localization of the interaction partners, which will limit its application for the characterization of high molecular weight complexes. Moreover, BiFC as well as other reconstitution/complementation assays appear to be irreversible (12), which hampers the screening for inhibitory protein interaction decoys. Likewise, the efficiency of FRET in cellular assays is often inefficient, affected by background fluorescence and requires demanding technological assay and analysis platforms in order to perform HTS. All these limitations do not apply to the described AFP-based cellular "two hybrid" interaction system, which proved to be effective for different classes of protein IDs. The cytoplasmic to nucleolar redistribution of the sensors was easily

detectable, and in contrast to FRET, the IDs did not depend on specific linker sequences for functionality. Importantly, the distinct intranuclear colocalization patterns observed were characteristic for the IDs used, and in the case of the Myc-Max Ids, a similar granular pattern was exhibited as reported for full-length Myc-Max heterodimers (43). This suggests that the IDs displayed by the prey/bait backbone can mimic the conformation of the IDs in the full-length proteins *in vivo*. This assumption is supported by the report of Berg et al. (44), who used *in vitro* FRET assays to identify SMPPIIs interfering with Myc/Max ID dimerization. Importantly, the identified compounds also inhibited Myc-induced oncogenic transformation but were not entirely specific and also extended to Jun. Because we observe neither Myc/Fos nor Max/Jun interaction, our *in vivo* assay could discriminate between different classes of leucine zipper IDs and therefore represents an ideal screening tool to identify ID-specific inhibitors. Besides specificity, reversibility is an important issue in CBAs to identify potent SMPIIs. Overexpression of the untagged Fos or Max IDs was able to chase the respective prey fusion proteins of the Jun/Fos or Myc/Max complexes, and microinjection of an *in vitro* inhibitory peptide was able to successfully compete with the p53/mdm2 ID interaction *in vivo*.

In addition, because the majority of GFP-prey fusions are not expected to intrinsically localize to the nucleolus or nuclear structures, our system is applicable for a wide variety of proteins.

In summary, the assays presented proved flexible, robust, facile and highly amenable to academic scale screens with the potential to be employed in novel drug-screening applications, in particular, when combined with biochemical assays. Efficient nuclear accumulation served as the reliable indicator for all biosensors (see Supplementary Figure S2 online, available online at http://www.traffic.dk/suppmat/6_7a.asp) and thus facilitates fully automated image acquisition and data analysis using commercial and academic microscopy assay platforms. The modular composition of the biosensors guarantees their adoption and thus application in numerous biological systems.

Methods

Plasmids

To construct pc3GFP/GST, the coding region for GST was polymerase chain reaction (PCR) amplified using primers containing *KpnI*-restriction sites, pGEX-GFP (45) as the template and cloned into the vector pc3-GFP (45). Subsequently, complementary oligonucleotides encoding the SV40 NLS and the NES of the PKI, of the HIV-1 Rev, of the STAT1, of the Bcr-Abl or of the p53 protein (see Supplementary Table S1, available online at http://www.traffic.dk/suppmat/6_7a.asp) were cloned into the *HindIII-/BamHI*- or the *KpnI-/EcoRI*-restriction sites, respectively, to generate pNLS-GFP/GST-PKINES, pNLS-GFP/GST-RevNES, pNLS-GFP/GST-StatNES, pNLS-GFP/GST-AblNES, pNLS-GFP/GST-p53NES, pRevNES-GFP/GST-NLS and pPKINES-GFP/GST-NLS. Plasmids pTRE-NLS-GFP/GST-RevNES, pTRE-NLS-GFP/GST-Stat1NES and pTRE-NLS-GFP/GST-AblNES allow the inducible expression of the GFP-biosensors. The cytomegalovirus-promoter in the respective pc3 expression plasmids was therefore replaced by the tetracycline-regulated promoter using *HindIII/BamHI*-restriction sites and vector pTRE-d2EGFP.1 (BD Biosciences, San Jose, CA, USA) as the template for PCR amplification. The protease sensor expression vector, pNLS-GFP/GST-CS3-RevNES, was constructed by inserting the PARP Casp3 cleavage recognition site (CS3) (KRKG***D***EV***D***GVDE) N-terminal to the RevNES using complementary oligonucleotides containing *NotI*- and *XhoI*-restriction sites, and subsequently, the Myc-epitope was inserted into the *Xho*I-restriction site using complementary oligonucleotides. pNLS-GFP/GST-CS3m-RevNES encodes a fusion protein containing a non-functional CS3 (KRKG***A***EV***A***GVDE). Plasmids pNLS-GFP/GST-bZipJun-RevNES, pNLS-GFP/GST-bZipFos-RevNES, pNLS-GFP/GST-HZipMyc-RevNES, GFP/GST-HZipMax-RevNES, pNLS-GFP/GST-p53-RevNES and pNLS-GFP/GST-mdm2-RevNES encode NLS-GFP/GST-ID-RevNES fusions, containing the IDs of human Jun (aa 222–331), of human Fos (aa 118–209), of human Myc (aa 354–434), of the rat Max (aa 13–93), of the human p53 (aa 2–42) and of the human mdm2 protein (aa 1–118). The expression vectors were constructed by inserting the IDs N-terminal to the RevNES by PCR amplifying the respective domains (44,45) using oligonucleotides containing *NotI*- and *XhoI*-restriction sites. pRevM10-BFP encodes a NES-deficient HIV-1 Rev-blue fluorescent fusion protein (RevM10-BFP) (23). Plasmids pFos-RevM10-BFP, pJun-RevM10-BFP, pMyc-RevM10-BFP, pMax-RevM10-BFP, pp53-RevM10-BFP and pmdm2-RevM10-BFP encode N-terminal fusions of the respective protein IDs and RevM10-BFP. Plasmids were constructed by PCR amplification and cloning of the IDs 5′- to the Rev ORF by using oligonucleotides containing *KpnI*-restriction sites. pc3Fos-bZip and pc3Max-HZip encode the untagged Fos bZip or the Max bHLHZip IDs, respectively, and were constructed by PCR amplifying the IDs using oligonucleotides containing *HindIII-/BamHI*-restriction sites and cloning into pc3 (45). Nuclear export/import signals (Supplementary Table S1, available online at http://www.traffic.dk/suppmat/6_7a.asp) were cloned into the bacterial expression vector pGEX-GFP as described (7). For details on previously described expression plasmids, see Supplementary Online Methods, available online at http://www.traffic.dk/suppmat/6_7a.asp.

Cell culture, microinjection and fluorescence imaging of cells

Vero, 293, MCF7, HLR9, HeLa and K562 human chronic myelogenous leukemia lymphoblast cell lines were maintained under conditions recommended by the American Type Tissue Culture. Cells were transfected or microinjected and observed as described (46). Twelve-bit black and white images were captured using a digital Axiocam CCD camera (Carl Zeiss, Jena, Germany). Quantitation, image analysis and presentation were performed using IPLab Spectrum (Scanalytics, Fairfax, VA, USA) and Axiovision software (Carl Zeiss). The total cellular GFP signal was measured by calculating the integrated pixel intensity in the imaged cell multiplied by the area of the cell. The nuclear signal was similarly obtained by measuring the pixel intensity in the nucleus. Nuclei were marked by staining with Hoechst 33258 (Sigma Aldrich, Munich, Germany) as described (45) or stained with TO-PRO^{TM}-3-iodide (Molecular Probes, Eugene, OR, USA) according to the manufacturer's recommendations. The cytoplasmic signal was calculated by subtracting the nuclear signal from the total cellular signal. All pixel values were measured below the saturation limits and the background signal in an area with no cells was subtracted from all values. To determine the average intracellular protein localization, at least 200 fluorescent cells from three separate images were examined. The number of cells exhibiting cytoplasmic (C; cytoplasmic signal >80% of the total cellular signal), cytoplasmic and nuclear (C/N) or nuclear (N; nuclear signal >80% of the total cellular signal) fluorescence was counted, the percentages of C, N/C and N cells were calculated, and standard deviations were determined. To quantitate the efficiency of cytoplasmic to nuclear redistribution, the difference between the percentages of the cytoplasmic signal before (C_b) and after (C_a) the treatment was calculated in 100 cells resulting in the translocation index T_i. To quantify the degree of

protein interaction, the percentage of 200 BFP- and GFP-positive cells in which BFP and GFP colocalized to the nucleus from three separate images was determined with standard deviations.

To compare the protein translocation biosensors and BiFC, 200 cells from three separate images were inspected, and the number of RFP-positive cells in which nuclear GFP fluorescence could be detected using equal CCD-camera settings was counted.

Automated image acquisition and analysis

For automated image acquisition on a fully automated screening microscope, cells were seeded in Laboratory-Tek eight-well chamber slides (Nunc, Wiesbaden, Germany). Following treatment, cells were fixed, and nuclei were marked by staining with Hoechst 33258. Data acquisition and analysis were performed as described (47). Briefly, images were acquired with an Orca^{TM}-cooled CCD camera (Hamamatsu, Bridgewater, NJ, USA) OLYMPUS IX81 microscope (Olympus Biosystems, Munich, Germany). Camera and shutter were triggered via a real-time controller for fast data acquisition and ultra precise camera integration. The set-up was controlled by custom-made software (Olympus Biosystems). A cell detecting autofocus was used for every field of view. Cell detection during image acquisition was based on object intensity, size (min, max) and contrast (frequency analysis) information. The focal plane with the maximum number of "in focus objects" was imaged. Relative z-shifts were used between the different color channels to compensate focus differences. Images, containing also meta information (filter cubes, integration times and position), were stored as TIFF files in a hierarchical file structure. Image analysis was done with custom-made scripts written in Labview Vision^{TM} (National Instruments, Munich, Germany & Olympus Biosystems). Cell nuclei detection was performed using the Labview Vision^{TM} threshold-based particle feature. Cytosol was measured via symmetrical extension of the nucleus (dilation), and ratios were generated accordingly. Detailed information can also be found at www.embl.de/~liebel.

Generation of stable cell lines

To generate cell clones allowing the inducible expression of the GFP-biosensors, HLR9 cells (HeLa Tet-On) transfected with the respective pTRE expression vectors together with pBABE were grown in the presence of 500 μg/mL G418 and 2 μg/mL puromycin (Sigma Aldrich). Pooled G418/puromycin-resistant colonies were cultured in medium containing 1 μg/mL Dox (Sigma Aldrich) to induce expression of the GFP-fusion proteins. Fluorescent clones were isolated by fluorescence-activated cell sorting and cloned twice by limited dilution.

96-well plate assays

HLR9 cell lines expressing the indicated transport sensors were cultured in the absence of Dox and plated into black-walled 96-well clear-bottomed plates (Corning, Acton, MA, USA) at a density of 3000 cells/well in Dox-containing medium (1 μg/mL). After 16 h, cells were transfected or incubated in media containing the specified drugs (see Supplementary Table S3 online for details, available online at http://www.traffic.dk/suppmat/6_7a.asp) and inspected by fluorescence microscopy. For each experiment, two wells were drug treated, and each experiment was performed in duplicates.

Microinjection of synthetic peptides

The synthetic rhodamine B-conjugated fluorescent peptide comP (Ac-Met-Pro-Arg-Phe-Met-Asp-Tyr-Trp-Glu-Gly-Leu-Asn-NH_2) or a scrambled control peptide comPmut with the identical aa composition (Ac-Met-Tyr-Pro-Arg-Met-Phe-Asp-Trp-Glu-Leu-Gly-Asn-NH_2) (Thermo Electron, Waltham, MA, USA) were microinjected for competition experiments at a concentration of 2 mg/mL. Microinjection of the synthetic peptides, IgG or Texas Red-conjugated WGA (Molecular Probes) was performed as described (46).

Apoptosis assay

To induce apoptosis, cells were treated with staurosporin (1 μM) for 6 h. Apoptosis was assessed by labeling free 3′OH ends in genomic DNA with rhodamine-dUTP (TUNEL-staining) using the *in situ* cell death detection kit (Roche Diagnostics, Basel, Switzerland).

Immunoprecipitation, immunoblotting and immunofluorescence

5×10^5 HeLa cells were transfected with the indicated plasmids. Whole cell lysates and immunoprecipitation of GST fusion proteins from cellular lysates using a monoclonal anti-GST antibody (Abcam, Cambridge, UK) as well as analysis of the complexes by SDS-PAGE and immunoblotting using polyclonal anti-GFP antibodies (BD Biosciences) were performed as described (46). Immunofluorescence was carried out according to standard procedures as described previously (7). Myc-epitope-tagged proteins were detected using a monoclonal antibody (Cell Signaling Technology, Beverly, MA, USA).

Acknowledgments

We thank B. Groner for support, G. Carra and Y. Fernandez for technical assistance and D. Krüger (Olympus Biosystems) for data analysis. This work was supported by the Deutsche Forschungsgemeinschaft (Sta 598/1–2 to S.R), the BMBF (NGFN 01GS0451 to R.S and T.B.; NGFN 01GR1001 and 01KW0013 to R.P) and the Studienstiftung des Deutschen Volkes (S.K).

References

1. Fahrenkrog B, Aebi U. The nuclear pore complex: nucleocytoplasmic transport and beyond. Nat Rev Mol Cell Biol 2003;4:757–766.
2. Bednenko J, Cingolani G, Gerace L. Nucleocytoplasmic transport: navigating the channel. Traffic 2003;4:127–135.
3. Lei EP, Silver PA. Protein and RNA export from the nucleus. Dev Cell 2002;2:261–272.
4. Marg A, Shan Y, Meyer T, Meissner T, Brandenburg M, Vinkemeier U. Nucleocytoplasmic shuttling by nucleoporins Nup153 and Nup214 and CRM1-dependent nuclear export control the subcellular distribution of latent Stat1. J Cell Biol 2004;165:823–833.
5. Porter LA, Donoghue DJ. Cyclin B1 and CDK1: nuclear localization and upstream regulators. Prog Cell Cycle Res 2003;5:335–347.
6. Cullen BR. Nuclear RNA export. J Cell Sci 2003;116:587–597.
7. Heger P, Lohmaier J, Schneider G, Schweimer K, Stauber RH. Qualitative highly divergent nuclear export signals can regulate export by the competition for transport cofactors in vivo. Traffic 2001;2:544–555.
8. Pagliaro L, Felding J, Audouze K, Nielsen SJ, Terry RB, Krog-Jensen C, Butcher S. Emerging classes of protein–protein interaction inhibitors and new tools for their development. Curr Opin Chem Biol 2004;8:442–449.
9. Kau TR, Way JC, Silver PA. Nuclear transport and cancer: from mechanism to intervention. Nat Rev Cancer 2004;4:106–117.
10. Brik A, Wong CH. HIV-1 protease: mechanism and drug discovery. Org Biomol Chem 2003;1:5–14.
11. Los M, Burek CJ, Stroh C, Benedyk K, Hug H, Mackiewicz A. Anticancer drugs of tomorrow: apoptotic pathways as targets for drug design. Drug Discov Today 2003;8:67–77.
12. Hu CD, Kerppola TK. Simultaneous visualization of multiple protein interactions in living cells using multicolor fluorescence complementation analysis. Nat Biotechnol 2003;21:539–545.
13. Yu H, West M, Keon BH, Bilter GK, Owens S, Lamerdin J, Westwick JK. Measuring drug action in the cellular context using protein-fragment complementation assays. Assay Drug Dev Technol 2003;1:811–822.
14. Stagljar I. Finding partners: emerging protein interaction technologies applied to signaling networks. Sci STKE 2003;2003:pe56.
15. Vogt PK. Fortuitous convergences: the beginnings of JUN. Nat Rev Cancer 2002;2:465–469.

16. Berg T. Modulation of protein–protein interactions with small organic molecules. Angew Chem Int Ed Engl 2003;42:2462–2481.
17. Hermeking H. The MYC oncogene as a cancer drug target. Curr Cancer Drug Targets 2003;3:163–175.
18. Chene P. Inhibition of the p53–MDM2 interaction: targeting a protein–protein interface. Mol Cancer Res 2004;2:20–28.
19. Vassilev LT, Vu BT, Graves B, Carvajal D, Podlaski F, Filipovic Z, Kong N, Kammlott U, Lukacs C, Klein C, Fotouhi N, Liu EA. In vivo activation of the p53 pathway by small-molecule antagonists of MDM2. Science 2004;303:844–848.
20. Hemmila IA, Hurskainen P. Novel detection strategies for drug discovery. Drug Discov Today 2002;7:S150–S156.
21. Horrocks C, Halse R, Suzuki R, Shepherd PR. Human cell systems for drug discovery. Curr Opin Drug Discov Devel 2003;6:570–575.
22. Stauber RH, Kratzer F, Schneider G, Hirschmann N, Hauber J, Rosorius O. Investigation of nucleo-cytoplasmic transport using UV-guided microinjection. J Cell Biochem 2001;80:388–396.
23. Stauber RH, Afonina E, Gulnik S, Erickson J, Pavlakis GN. Analysis of intracellular trafficking and interactions of cytoplasmic HIV-1 Rev mutants in living cells. Virology 1998;251:38–48.
24. Kau TR, Schroeder F, Ramaswamy S, Wojciechowski CL, Zhao JJ, Roberts TM, Clardy J, Sellers WR, Silver PA. A chemical genetic screen identifies inhibitors of regulated nuclear export of a Forkhead transcription factor in PTEN-deficient tumor cells. Cancer Cell 2003;4:463–476.
25. Koster M, Lykke-Andersen S, Elnakady YA, Gerth K, Washausen P, Hofle G, Sasse F, Kjems J, Hauser H. Ratjadones inhibit nuclear export by blocking CRM1/exportin 1. Exp Cell Res 2003;286:321–331.
26. Fukuda M, Asano S, Nakamura T, Adachi M, Yoshida M, Yanagida M, Nishida E. CRM1 is responsible for intracellular transport mediated by the nuclear export signal. Nature 1997;390:308–311.
27. Almholt DL, Loechel F, Nielsen SJ, Krog-Jensen C, Terry R, Bjorn SP, Pedersen HC, Praestegaard M, Moller S, Heide M, Pagliaro L, Mason AJ, Butcher S, Dahl SW. Nuclear export inhibitors and kinase inhibitors identified using a MAPK-activated protein kinase 2 redistribution screen. Assay Drug Dev Technol 2004;2:7–20.
28. McBride KM, Reich NC. The ins and outs of STAT1 nuclear transport. Sci STKE 2003;2003:RE13.
29. Zhu J, McKeon F. Nucleocytoplasmic shuttling and the control of NF-AT signaling. Cell Mol Life Sci 2000;57:411–420.
30. Woodring PJ, Hunter T, Wang JY. Regulation of F-actin-dependent processes by the Abl family of tyrosine kinases. J Cell Sci 2003;116:2613–2626.
31. Theodoropoulos PA, Polioudaki H, Kostaki O, Derdas SP, Georgoulias V, Dargemont C, Georgatos SD. Taxol affects nuclear lamina and pore complex organization and inhibits import of karyophilic proteins into the cell nucleus. Cancer Res 1999;59:4625–4633.
32. Jang ER, Lim SJ, Lee ES, Jeong G, Kim TY, Bang YJ, Lee JS. The histone deacetylase inhibitor trichostatin A sensitizes estrogen receptor alpha-negative breast cancer cells to tamoxifen. Oncogene 2004;23:1724–1736.
33. Zolotukhin AS, Felber BK. Nucleoporins nup98 and nup214 participate in nuclear export of human immunodeficiency virus type 1 Rev. J Virol 1999;73:120–127.
34. Boer J, Bonten-Surtel J, Grosveld G. Overexpression of the nucleoporin CAN/NUP214 induces growth arrest, nucleocytoplasmic transport defects, and apoptosis. Mol Cell Biol 1998;18:1236–1247.
35. Smolewski P, Grabarek J, Halicka HD, Darzynkiewicz Z. Assay of caspase activation in situ combined with probing plasma membrane integrity to detect three distinct stages of apoptosis. J Immunol Methods 2002;265:111–121.
36. Tawa P, Tam J, Cassady R, Nicholson DW, Xanthoudakis S. Quantitative analysis of fluorescent caspase substrate cleavage in intact cells and identification of novel inhibitors of apoptosis. Cell Death Differ 2001;8:30–37.
37. Laxman B, Hall DE, Bhojani MS, Hamstra DA, Chenevert TL, Ross BD, Rehemtulla A. Noninvasive real-time imaging of apoptosis. Proc Natl Acad Sci USA 2002;99:16551–16555.
38. Uetz P, Finley RL Jr. From protein networks to biological systems. FEBS Lett 2005;579:1821–1827.
39. Figeys D. Combining different 'omics' technologies to map and validate protein–protein interactions in humans. Brief Funct Genomic Proteomic 2004;2:357–365.
40. Arkin MR, Wells JA. Small-molecule inhibitors of protein–protein interactions: progressing towards the dream. Nat Rev Drug Discov 2004;3:301–317.
41. Paulmurugan R, Umezawa Y, Gambhir SS. Noninvasive imaging of protein–protein interactions in living subjects by using reporter protein complementation and reconstitution strategies. Proc Natl Acad Sci USA 2002;99:15608–15613.
42. Ozawa T, Kaihara A, Sato M, Tachihara K, Umezawa Y. Split luciferase as an optical probe for detecting protein–protein interactions in mammalian cells based on protein splicing. Anal Chem 2001;73:2516–2521.
43. Grinberg AV, Hu CD, Kerppola TK. Visualization of Myc/Max/Mad family dimers and the competition for dimerization in living cells. Mol Cell Biol 2004;24:4294–4308.
44. Berg T, Cohen SB, Desharnais J, Sonderegger C, Maslyar DJ, Goldberg J, Boger DL, Vogt PK. Small-molecule antagonists of Myc/Max dimerization inhibit Myc-induced transformation of chicken embryo fibroblasts. Proc Natl Acad Sci USA 2002;99:3830–3835.
45. Krätzer F, Rosorius O, Heger P, Hirschmann N, Dobner T, Hauber J, Stauber RH. The adenovirus type 5 E1B-55K oncoprotein is a highly active shuttle protein and shuttling is independent of E4orf6, p53 and Mdm2. Oncogene 2000;19:850–857.
46. Knauer SK, Carra G, Stauber RH. Nuclear export is evolutionarily conserved in CVC paired-like homeobox proteins and influences protein stability, transcriptional activation, and extracellular secretion. Mol Cell Biol 2005;25:2573–2582.
47. Liebel U, Starkuviene V, Erfle H, Simpson JC, Poustka A, Wiemann S, Pepperkok R. A microscope-based screening platform for large-scale functional protein analysis in intact cells. FEBS Lett 2003;554:394–398.
48. Kino T, Gragerov A, Kopp JB, Stauber RH, Pavlakis GN, Chrousos GP. The HIV-1 virion-associated protein Vpr is a coactivator of the human glucocorticoid receptor. J Exp Med 1999;189:51–61.

Supplementary Online Information

Supplementary Methods

Plasmids

Plasmid p3-Exportin 1-HA, encoding HA-tagged Exportin 1 (7), pc3-E1B55K, encoding the Adenovirus type 5 E1B-55K protein (45), pc3-Vpr, encoding the HIV-1 Vpr protein (48), pc3-GR, encoding the human glucocorticoid receptor alpha (48), pc3-PKI-BFP, encoding a PKI-BFP fusion (7), pc3eIF-5A, encoding the eukaryotic initiation factor 5A (eIF-5A) (45), pc3p53, encoding human p53 (45), pc3mdm2, encoding the human mdm2 protein (45), pc3-E1BAP5, encoding the human E1B-AP5 protein (45), p3CANc/VSV-G, encoding the carboxy terminus of CAN/Nup214 (7) have been described. Plasmid pBrev14-GFP produces a cytoplasmic Rev-GFP mutant (Rev14-GFP) (23). pSTAT1-GFP encodes a human STAT1-GFP fusion (4). pDS-RED-N1 encodes the red-fluorescent protein (RFP) (BD Biosciences). pBABE confers puromycin resistance. pCaspase3-Sensor (BD Biosciences) encodes a fusion protein composed of the mitogen-activated kinase kinase (MAPKK) NES (26), followed by CS3, GFP and three copies of the SV40 NLS. pHA-CMV-bFosGC (FosGC) and pFLAG-CMV2-bJunYN (JunGN), encoding the IDs of human Fos and Jun fused to a C- (aa 155-238) or N-terminal (aa 1-154) fragment of GFP, respectively, have been described (12).

Supplementary Online Tables

Supplementary Table S1

Sequence and activity of the nuclear transport signals quantified by microinjection of recombinant GST-GFP-NES or -NLS substrates.

Signal	Sequence	Import/export activity
SV40 NLS	PPKKKRKVEDP	60+/- 5 min/neg.
PKI-NES	LALKLAGLDI	neg./5+/- 2 min
HIV-1 Rev NES	LQLPPLERLTL	neg./15+/- 3 min
STAT1 NES	LAAEFRHLQL	neg./20+/- 3 min
Abl NES	LENNLRELQI	neg./30+/- 5 min
MAPKK NES	LQKKLEELEL	neg./40+/- 3 min
p53 NES	MFRELNEALEL	neg./14+/- 1 h

Supplementary Table S2

Quantitation of the intracellular localization and of the translocation index T_i of the tested transport sensors in several cell lines (see Methods for details). H: HeLa, M: MCF-7, K: K562, H9: HRL9; SP: staurosporin.

Sensor	%C	%C/N	%N	T_i (in %)
RevNES-sensor	96,8±2,4 (H), 95,1±2,9 (M), 89,6±4,1 (K)	2,3±1 (H), 3,1±2,0 (M), 6,4±2,9 (K)	0,9±0 (H), 1,8±1,1 (M), 4,0±1,6 (K)	93,1± 3,9 (H) 92,3±4,1 (M) 86,9±5,6 (K)
RevNES-sensor +LMB	0,7±0,5 (H), 1,0±0,9 (M), 2,5±1,3 (K)	2,7±1,4 (H), 1,9±1,2 (M), 6,2±2,0 (K)	96,6±1,2 (H), 97,1±3,5 (M), 91,3±2,7 (K)	
RevNES-sensor (fixed cells)	97,1±2,1 (H), 94,8±3,9 (M), 88,3±5,2 (K)	2,3±1,5 (H), 2,7±1,4 (M), 8,6± 2,3 (K)	0,6±0,2 (H), 2,5±1,3 (M), 3,1±2,0 (K)	92,5± 3,4 (H) 91,4±6,0 (M) 85,7±4,7 (K)
RevNES-sensor +LMB (fixed cells)	1,2±0,3 (H), 2,3±1,1 (M), 2,3±1,4 (K)	2,3±0,8 (H), 3,5±1,8 (M), 8,0±2,0 (K)	96,5±1,4 (H), 94,2±4,1 (M), 89,7±3,4 (K)	
RevNES-GFP/GST-NLS	1,8±0,9(H), 3,5±3,0 (M), 5,1±2,8 (K)	4,1±1,0 (H), 3,5±2,0 (M), 6,3±4,1 (K)	94,1±0,8 (H), 93,0±1,9 (M), 88,6±5,2 (K)	n.d.
Rev14-GFP	21,3±3,3 (H), 22,5±5,3 (M), 30,7±2,0 (K)	75,1±4,9 (H), 73,0±4,2 (M), 66,9±6,9 (K)	3,6±3,9 (H), 4,5±2,0 (M), 2,4±2,0 (K)	73,7± 4,1 (H) 68,8±7,2 (M) 63,2±6,9 (K)
Rev14-GFP +LMB	1,0±0,7 (H), 3,2±2,4 (M), 5,7±2,3 (K)	30,2±3,9 (H), 35,9±5,4 (M), 45,7±2,1 (K)	68,8±2,8 (H), 60,9±6,4 (M), 48,6±7,2 (K)	
PKINES-sensor	97,7±2,3 (H), 95,0±3,3 (M), 88,8±4,2 (K)	2,0±1,0 (H), 3,7±1,0 (M), 10,1±4,3 (K)	0,3±0,0 (H), 1,3±0,9 (M), 1,1±0,7 (K)	91,4± 3,7 (H) 92,6±4,3 (M) 89,3±5,0 (K)
PKINES-sensor +LMB	0,5±0,3 (H), 1,1±1,1 (M), 3,5±2,8 (K)	1,9±1,2 (H), 3,4±2,3 (M), 7,4±4,0 (K)	97,6±3,9 (H), 95,5±1,1 (M), 89,1±5,2 (K)	
PKI-BFP	98,0±0,6 (H), 97,5±4,4 (M), 93,8±4,7 (K)	0,8±0,1 (H), 1,5±1,2 (M), 4,2±2,8 (K)	1,2±0,9 (H), 1,0±0,1 (M), 2,0±1,1 (K)	45,9± 2,8 (H) 42,4±3,9 (M) 36,6±6,1 (K)
PKI-BFP +LMB	1,0±0,5 (H), 0,9±0,3 (M), 1,8±1,2 (K)	98,5±2,8 (H), 97,6±3,7 (M), 94,9±2,2 (K)	0,5±0,1 (H), 1,5±0,7 (M), 3,3±1,7 (K)	
StatNES-sensor	80,3±3,3 (H), 82,6±4,9 (M), 78,4±5,2 (K)	15,0±1,0 (H), 13,9±2,5 (M), 17,5±3,7 (K)	4,7±2,0 (H), 3,5±2,1 (M), 4,1±3,4 (K)	78,3± 4,2 (H) 78,4±7,0 (M)

StatNES-sensor+LMB	0,9±0,5 (H), 1,4±0,9 (M), 2,3±1,6 (K)	6,4±2,5 (H), 5,5±2,2 (M), 8,1±3,3 (K)	92,7±3,7 (H), 93,1±4,0 (M), 89,6±5,1 (K)	65,8±8,7 (K)
STAT1-GFP	25,8±6,0 (H), 27,2±3,9 (M), 19,9±4,6 (K)	69,2±3,8 (H), 66,5±2,7 (M), 73,3±4,2 (K)	5,0±2,3 (H), 6,3±3,1 (M), 6,8±2,5 (K)	31,8± 2,9 (H) 33,1±5,5 (M) 28,7±8,9 (K)
STAT1-GFP + LMB	3,3±1,3 (H), 2,1±1,3 (M), 4,8±2,7 (K)	93,3±6,2 (H), 96,7±5,9 (M), 91,5±6,7 (K)	3,4±1,0 (H), 1,2±0,5 (M), 3,7±3,4 (K)	
AblNES-sensor	80,7±3,3 (H), 78,6±2,5 (M), 79,7±5,1 (K)	16,1±3,1 (H), 17,7±4,2 (M), 15,3±4,4 (K)	3,2±1,0 (H), 3,7±1,6 (M), 5,0±2,8 (K)	81,9± 4,8 (H) 80,4±4,2 (M) 70,7±6,7 (K)
AblNES-sensor+LMB	2,1±0,3 (H), 1,6±0,3 (M), 4,0±2,0 (K)	13,4±2,5 (H), 14,7±3,9 (M), 16,1±6,2 (K)	84,5±4,0 (H), 83,7±5,3 (M), 79,9±6,2 (K)	
RevNES-sensor+Dox	93,2±3,9 (H9)	4,1±2,7 (H9)	2,7±1,1 (H9)	91,7± 2,6 (H9)
RevNES-sensor+Dox+LMB	2,9±0,9 (H9)	2,7±1,5 (H9)	94,4±3,8 (H9)	
StatNES-sensor+Dox	81,3±5,6 (H9)	13,3±4,5 (H9)	5,4±2,2 (H9)	79,4± 5,1 (H9)
StatNES-sensor-Dox+LMB	2,6±1,8 (H9)	8,7±3,0 (H9)	88,7±6,3 (H9)	
AblNES-sensor+Dox	79,9±5,3 (H9)	16,5±6,4 (H9)	3,6±1,1 (H9)	77,3± 6,2 (H9)
AblNES-sensor-Dox+LMB	4,1±2,4 (H9)	17,6±3,9 (H9)	78,3±7,0 (H9)	
Casp3-sensor	93,1±5,2 (H)	5,3±2,9 (H)	1,6±0,7(H)	90,2± 2,9 (H)
Casp3-sensor+SP	9,4±7,8 (H)	10,3±7,0 (H)	80,3±5,5 (H)	
MKNES-CS3-GFP-NLS	80,2±5,7 (H)	11,9±4,1 (H)	7,9±4,8 (H)	56,5± 4,9 (H)
MKNES-CS3-GFP-NLS+SP	14,4±4,0 (H)	72,9±8,3 (H)	12,7±6,3 (H)	
Casp3mut-sensor	95,6±2,4 (H)	2,5±1,1 (H)	1,9±0,9 (H)	5,0± 2,9 (H)
Casp3mut-sensor+SP	93,8±3,8 (H)	3,4±2,0 (H)	2,8±1,3 (H)	

Supplementary Table S 3

Collective assay results for the effects of compounds or overexpressed proteins on nucleo-cytoplasmic transport. Expression of the indicated translocation sensor was induced by Dox. Cells were either incubated with the indicated compounds for 8 h and fixed or transfected with the indicated plasmids (see **Supplementary Methods** for details) and analyzed 16 h later by fluorescence microscopy. IH: inhibitor; -: no effect, +: inhibition of transport. The main target protein of the kinase IHs is indicated in brackets.

Substance	RevNES-sensor		StatNES-sensor		AblNES-sensor	
	Interference with					
	export	import	export	import	export	import
Exportin1 IH						
LMB	**+**	-	**+**	-	**+**	-
RatA	**+**	-	**+**	-	**+**	-
Transcription IH						
ActD	-	-	-	-	-	-
DRB	-	-	-	-	-	-
Cytoskeleton IH						
Taxol	-	-	-	-	-	-
Nocodazol	-	-	-	-	-	-
LAT-B	-	-	-	-	-	-
HDAC IH						
TSA	-	-	-	-	-	-
VPA	-	-	-	-	-	-
Kinase IH						
Wortmannin (PI(3)K)	-	-	-	-	-	-
LY294002 (PI(3)K)	-	-	-	-	-	-
Staurosporin (PKC)	-	-	-	-	-	-
SB203580 (p38-MAPK)	-	-	-	-	-	-
U-73122 (PLC)	-	-	-	-	-	-
IC261 (casein kinase)	-	-	-	-	-	-
STI571 (Bcr-Abl)	-	-	-	-	-	-
AG 1478 (EGFR)	-	-	-	-	-	-
UO126 (MEK)	-	-	-	-	-	-
Others						
INFg	-	-	-	-	-	-
CsA (calcineurin)	-	-	-	-	-	-
Rapamycin (mTOR)	-	-	-	-	-	-
Protein						
p53	-	-	-	-	-	-
PKI-BFP	**+**	-	**+**	-	**+**	-
Exportin 1	-	-	-	-	-	-
E1B-AP5	-	-	-	-	-	-
eIF-5A	-	-	-	-	-	-
RevM10BL	-	-	-	-	-	-
GR	-	-	-	-	-	-
Vpr	-	-	-	-	-	-
E1B55K	-	-	-	-	-	-
mdm2	-	-	-	-	-	-
CANc	+	-	**+**	-	**+**	-

Cells were treated with the following chemicals: LMB (10 nM), interferon gamma (IFNg) (10 ng/ml), wortmannin (20 μM), actinomycin D (ActD) (5 μM), 5,6-dichlororibofuranosylbenzimidazole (DRB) (5 μM), taxol (2 mM), nocodazol (50 μg/ml), latrunculin-B (LAT-B) (1 μM), rapamycin (50 nM), cyclosporin A (2 μM), staurosporin (1 μM) were purchased from Sigma (Sigma-Aldrich, Munich, Germany). Inhibitors NL-71-101 (20 μM), LY294002 (50 μM), IC261 (20 μM), SB203580 (20 μM), AG 1478 (10 μM), U-73122 (2 μM), valproic acid (VPA) (5 mM) and trichostatin A (TSA) (200 nM) were purchased from Calbiochem (St. Louis, MO, USA). Ratjadone A (10 nM) was purchased from Alexis Biochemicals (San Diego, CA, USA), UO126 (50 μM) from Promega (Madison, WI, USA) and STI571 (20 μM) was provided by Novartis (Basel, Switzerland).

Supplementary Figures

Supplementary Figure S1

Application of transport biosensors to identify compounds or proteins that interfere with nucleo-cytoplasmic transport. Expression of the RevNES sensor was induced by Dox and (**A**) cells were incubated with taxol or nocodazol or (**B**) transfected with the PKI-BFP or the CanC expression plasmids (3 μg each) together with 0.3 μg of the RFP expression plasmid and analyzed by fluorescence microscopy. (**A**) Inhibition of microtubule metabolism resulted in cell rounding but did not block nuclear export (upper panel) nor interfered with nuclear import (lower panel). (**B**) Overexpression of PKI-BFP or CanC inhibited nuclear export and resulted in the nuclear accumulation of the RevNES-sensor. Scale bars, 10 μm.

Supplementary Figure S2

Nuclear translocation of the biosensors as the principle for cell based screening applications. The cellular biosensors are composed of GST, GFP and rational combinations of nuclear import and export signals. Addition of regulatory sequences resulted in three classes of biosensors applicable for the identification of signal specific nuclear transport inhibitors, small molecules that interfere with protease activity and compounds that modulate protein-protein interactions in living cells. Nuclear accumulation of the cytoplasmic biosensors serves as the indicator, which can be induced by interference with nuclear export, induction of protease activity or formation of highly specific protein complexes.

Supplementary Figure S1

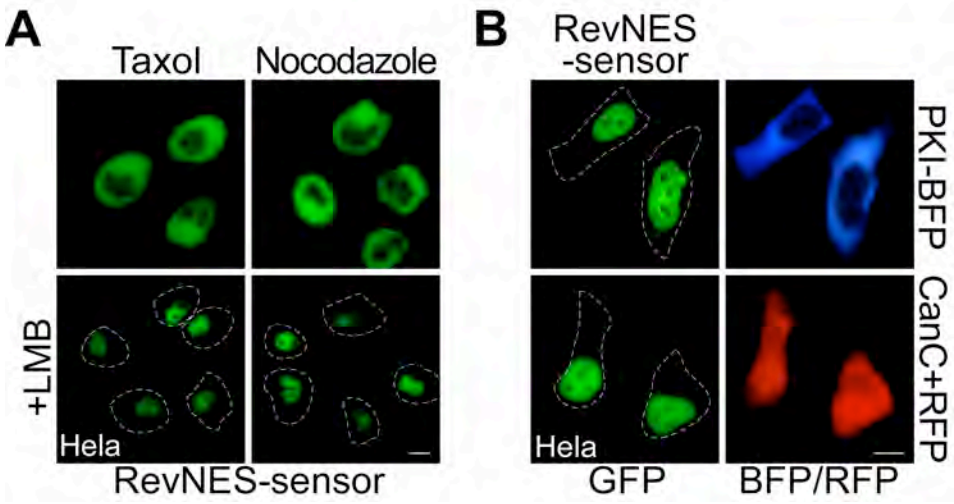

Supplementary Figure S2

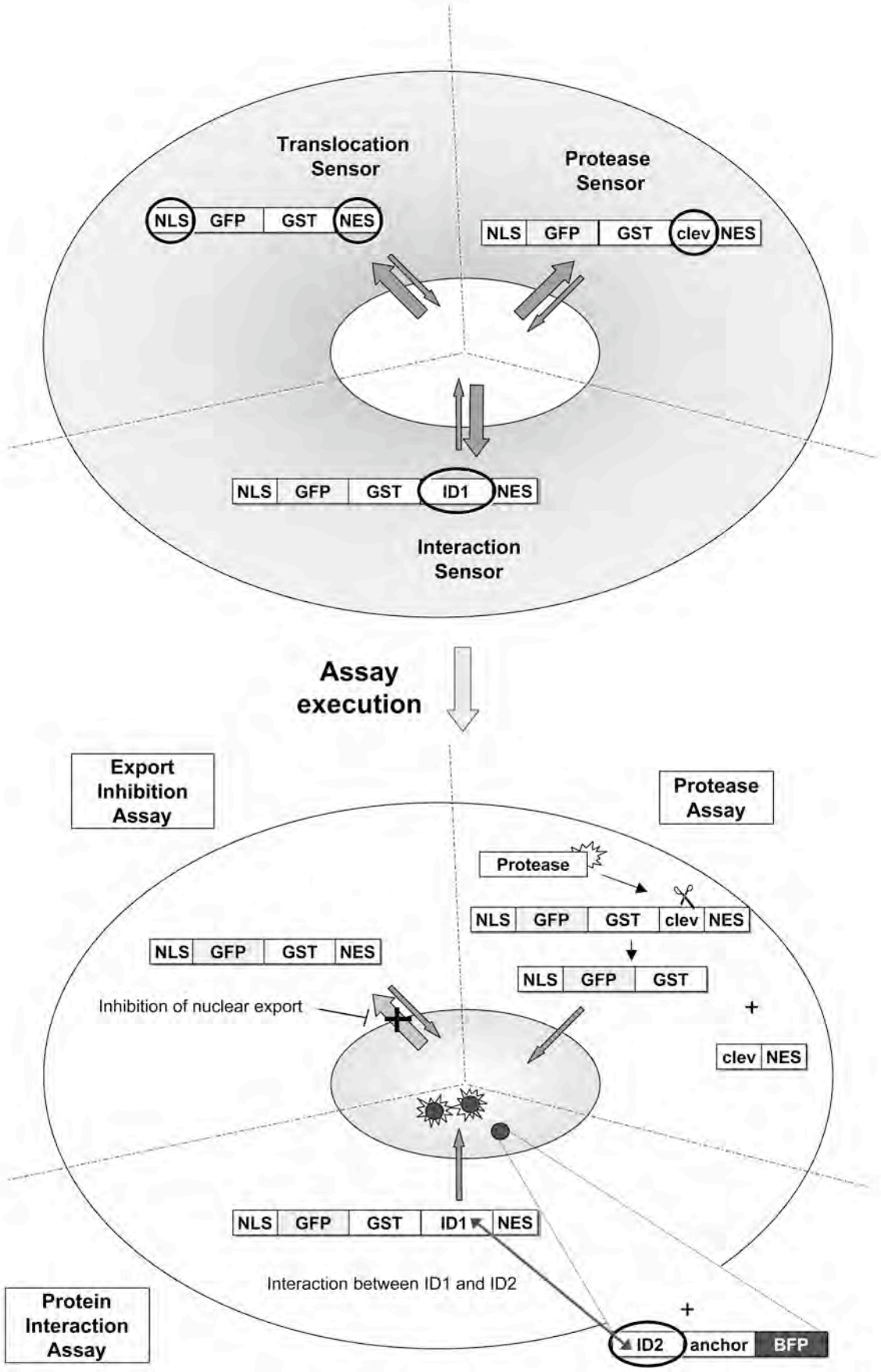

5

Development of an Autofluorescent Translocation Biosensor System To Investigate Protein−Protein Interactions in Living Cells

Shirley K. Knauer* and Roland H. Stauber

Georg-Speyer-Haus, Paul-Ehrlich-Strasse 42-44, D-60596 Frankfurt, Germany

Protein−protein interactions are crucial for all cellular events. To analyze protein−protein interactions in live mammalian cells, we developed novel protein translocation biosensors composed of glutathione *S*-transferase, mutants of GFP, and a rational combination of nuclear import and export signals. Nuclear accumulation of the cytoplasmic biosensors served as the reliable indicator, which was induced by the formation of protein complexes and could easily be detected by fluorescence microscopy. The efficacy of the system was systematically investigated by mapping the p53/mdm2 protein interaction interface. Specificity and general applicability of the biosensors were confirmed by studying additional classes of protein interaction domains (IDs), e.g., the leucine zipper IDs of Jun/Fos and the coiled-coil ID of Bcr-Abl in different cell lines. Importantly, we found that, in comparison to protein complementation assays, our system proved highly efficient and reversible and thus suited for the identification of molecular decoys to prevent specific protein−protein interactions in living cells. Reversibility was demonstrated in competition experiments by overexpressing the specific IDs or by the application of a p53/mdm2 protein interaction inhibitor. Thus, besides the convenient mapping of protein IDs in living cells, the modular translocation system has great potential to be employed in numerous cell-based assays for the identification of small-molecule protein interaction inhibitors as potential novel therapeutics.

Cellular homeostasis and communication strictly require regulated protein−protein interaction networks. Identification of these interactions and characterization of their physiological significance is one of the main goals of current research in a wide range of biological fields.[1,2]

In addition, abolishing or inducing specific protein−protein interactions by molecular decoys offers tremendous possibilities for the treatment of human diseases.[3] In cancer, cellular transformation and maintenance of the transformed phenotype often depend on the formation of high molecular weight complexes (HMWCs). For example, the proto-oncogenes *jun* and *fos* encode oncogenic transcription factors that bind DNA as dimers and can promote malignant transformation by activating or repressing gene expression (see ref 4 and references therein). As Jun and Fos are members of the basic leucine zipper (bZip) protein family, their dimerization is mediated by a parallel association of bZip IDs. Inhibitors that prevent Jun−Fos dimerization and thus DNA binding are currently under intense investigation as potential anticancer drugs.[5]

Likewise, the importance of protein interactions is further exemplified by the leukemia-inducing oncoprotein BCR-Abl. Oligomerization of BCR-Abl is mediated by the N-terminal coiled-coil region of BCR, and targeting this oligomerization domain by peptides was shown to inhibit the leukemic activity of BCR-Abl (ref 6 and references within).

In addition, the tumor-suppressor protein p53 forms an autoregulatory feedback loop with mdm2, in which the latter inhibits p53 transcriptional activity and stimulates its degradation (ref 7 and references therein). Inhibition of the p53−mdm2 interaction with synthetic molecules can lead to the nuclear accumulation and the activation of p53 followed by the death of the tumor cells from apoptosis.[8]

Therefore, modulating protein−protein interactions in general as a novel therapeutic principle has recently attracted major interest by academia and industry (reviewed in ref 3).

To date, numerous methods have been described to analyze protein−protein interactions in vitro, in cell culture, and in vivo.[9] Besides biochemical techniques, these include the yeast two-hybrid (YTH) system, several split-enzyme complementation/reconstitution assays (ref 10 and references therein), fluorescence resonance energy-transfer (FRET),[1,11] and bimolecular fluorescence complementation (BiFC) (see refs 12 and 13). Although

* To whom correspondence should be addressed. E-mail: s.knauer@em.uni-frankfurt.de. Phone: (+49) 69 63395-149. Fax: (+49) 69 63395-145.

(1) Ozawa, T.; Kaihara, A.; Sato, M.; Tachihara, K.; Umezawa, Y. *Anal. Chem.* **2001**, *73*, 2516−2521.
(2) Mendelsohn, A. R.; Brent, R. *Science* **1999**, *284*, 1948−1950.
(3) Arkin, M. R.; Wells, J. A. *Nat. Rev. Drug Discovery* **2004**, *3*, 301−317.
(4) Vogt, P. K. *Nat. Rev. Cancer* **2002**, *2*, 465−469.
(5) Berg, T. *Angew. Chem., Int. Ed.* **2003**, *42*, 2462−2481.
(6) Beissert, T.; Puccetti, E.; Bianchini, A.; Guller, S.; Boehrer, S.; Hoelzer, D.; Ottmann, O. G.; Nervi, C.; Ruthardt, M. *Blood* **2003**, *102*, 2985−2993.
(7) Chene, P. *Mol. Cancer Res.* **2004**, *2*, 20−28.
(8) Vassilev, L. T.; Vu, B. T.; Graves, B.; Carvajal, D.; Podlaski, F.; Filipovic, Z.; Kong, N.; Kammlott, U.; Lukacs, C.; Klein, C.; Fotouhi, N.; Liu, E. A. *Science* **2004**, *303*, 844−848.
(9) Meng, J. J.; Rojas, M.; Bacon, W.; Stickney, J. T.; Ip, W. *Methods Mol. Biol.* **2005**, *289*, 341−358.
(10) Paulmurugan, R.; Umezawa, Y.; Gambhir, S. S. *Proc. Natl. Acad. Sci. U.S.A.* **2002**, *99*, 15608−15613.
(11) Wehrman, T.; Kleaveland, B.; Her, J. H.; Balint, R. F.; Blau, H. M. *Proc. Natl. Acad. Sci. U.S.A.* **2002**, *99*, 3469−3474.
(12) Hu, C. D.; Kerppola, T. K. *Nat. Biotechnol.* **2003**, *21*, 539−545.

10.1021/ac050413o CCC: $30.25
Published on Web 00/00/0000

the various methods have been valuable tools in analyzing protein interactions, several intrinsic limitations apply (see ref 1 and references within). For example, the YTH detects only protein interactions in the nucleus of yeast cells, and FRET and BiFC require demanding technological assay platforms.

In particular, since biologically relevant protein−protein interactions or any potential drug therapy targeting protein interactions must be effective at the cellular level, cell-based assays (CBAs) have to be employed to complement in vitro data. Recently, several methods have been developed to facilitate the implementation of CBAs.[14] However, for any realistic application of high-content (HCS) and high-throughput screening (HTS), CBAs depend on robust and reliable biological readout systems with a high signal-to-noise ratio.

Facing the clear need for facile cellular protein−protein interaction assays, the present study describes a novel biosensor system that has been tailored to also meet crucial requirements of cell-based HCS/HTS assays. Combining autofluorescent proteins as imaging tools with regulated nucleocytoplasmic transport resulted in a mammalian two-hybrid protein translocation biosensor (PTB) system, composed of a shuttling GFP-tagged molecule I (GFP-prey) and a nucleolar anchored blue fluorescent protein (BFP)-tagged molecule II (BFP-bait). The expression of active protein IDs as fusions with the prey/bait constructs allowed the co-localization of the GFP-prey with the BFP-bait, resulting in cytoplasmic to nuclear prey translocation. Thus, our system exploited the spatial division of the cell into the nucleus and the cytoplasm as two intracellular compartments that can easily be distinguished by microscopy. In contrast to existing protein interaction assays, the presented strategy proved highly efficient, flexible, and reversible and thus represents a straightforward approach to characterize novel protein IDs and to identify low molecular weight protein interaction inhibitors in living cells.

EXPERIMENTAL PROCEDURES

Plasmids. To construct pc3GFP/GST, the coding region for GST was PCR amplified using primers containing *Kpn*I-restriction sites, pGEX-GFP[15] as the template, and cloned into the vector pc3-GFP.[15] Subsequently, complementary oligonucleotides encoding the SV40 NLS and the NES of the HIV-1 Rev were cloned into the *Hind*III-/*Bam*HI- or the *Kpn*I-/*Eco*RI-restriction sites to generate pNLS-GFP/GST-RevNES. Plasmids pNLS-GFP/GST-bZipJun-RevNES (GFP-prey_Jun), pNLS-GFP/GST-bZipFos-RevNES (GFP-prey_Fos), pNLS-GFP/GST-BCR−RevNES (GFP-prey_BCR), pNLS-GFP/GST-p53-RevNES (GFP-prey_p53), and pNLS-GFP/GST-mdm2-RevNES (GFP-prey_mdm2) encode NLS-GFP/GST-ID-RevNES fusions, containing the interaction domains (IDs) of human Jun (aa 222−331), human Fos (aa 118−209), and human BCR (aa 1−72), of the human p53 (aa 1−42) and the human mdm2 protein (aa 1−118). The expression vectors were constructed by inserting the IDs N-terminal to the RevNES by PCR amplifying the respective domains[15,16] using oligonucleotides containing *Not*I- and *Xho*I-restriction sites. pRevM10-BFP (BFP-_bait) encodes a NES deficient HIV-1 Rev-BFP fusion protein (RevM10-BFP).[17] Plasmids pFos-RevM10-BFP (Fos_BFP-bait), pJun-RevM10-BFP (Jun_BFP-bait), pBCR-RevM10-BFP (BCR_BFP-bait), pp53aa1-131-RevM10-BFP (p53 aa 1−131_BFP-bait), pp53aa132−262-RevM10-BFP (p53 aa 132−262_BFP-bait), pp53aa263−393-RevM10-BFP (p53 aa 263−393_BFP-bait), pp53-RevM10-BFP (p53_BFP-bait), and pmdm2-RevM10-BFP (mdm2_BFP-bait) encode N-terminal fusions of the respective IDs, the human p53 protein aa 1−131, aa 132−262, or aa 263−393 fused to RevM10-BFP. Plasmids were constructed by PCR amplification and cloning of the IDs 5′ to the Rev ORF by using oligonucleotides containing *Kpn*I-restriction sites. pc3Fos-bZip and pc3BCR_ID encode the untagged Fos bZip or the BCR aa 1−72, respectively, and were constructed by PCR amplifying the IDs using oligonucleotides containing *Hind*III-/*Bam*HI-restriction sites and cloning into pc3.[15] The plasmid pNLS-EYFP/GST-bZipJun-RevNES (YFP-prey_Jun) was constructed by replacing the GFP with the ORF of the yellow fluorescent protein (YFP) by PCR amplification and cloning using pEYFP−N1 (BD Biosciences) as template and oligonucleotides containing *Bam*HI-/*Kpn*I-restriction sites. Plasmid pc3p53, encoding human p53,[15] pc3mdm2, encoding the human mdm2 protein,[15] pHA-CMV-bFosYC (FosYC), and pFLAG-CMV2-bJunYN (JunYN), encoding the IDs of human Fos and Jun fused to a C- or N-terminal fragment of YFP, respectively,[18] have been described. pDS-RED-N1 encodes the red fluorescent protein (RFP) (BD Biosciences).

Cell Culture, Microinjection, and Fluorescence Imaging of Cells. 293, HeLa or Vero cell lines were maintained in DMEM medium (GIBCO) supplemented with 10% (v/v) fetal calf serum and 2 mM glutamine at 37 °C and 5% CO_2. Cells were transfected with Lipofectamine 2000 (Invitrogen) according to the manufacturer's instructions and analyzed 16 h later as described to avoid potential artifacts caused by protein overexpression.[19] Twelve-bit black and white images were captured using a digital Axiocam CCD camera (Zeiss) and appropriate excitation and emission filters to detect GFP, YFP, or BFP fluorescence.[20] Quantitation, image analysis, and presentation were performed using IPLab Spectrum (Scanalytics) and Axiovision software (Zeiss). The total cellular GFP signal was measured by calculating the integrated pixel intensity in the imaged cell multiplied by the area of the cell. The nuclear signal was similarly obtained by measuring the pixel intensity in the nucleus. To quantify the degree of protein interaction, the percentage of 200 BFP- and GFP-positive cells in which BFP and GFP co-localized to the nucleus from three separate images was determined with standard deviations (SD). To compare PTB and BiFC, 200 cells from three separate images were inspected, and the number of cells in which nuclear YFP fluorescence could be detected with equal CCD camera settings was counted. Nuclei were marked by staining with TO-PRO-3-iodide (Molecular Probes) according to the manufacturer's recommendations. All pixel values were measured below the saturation

(13) Yu, H.; West, M.; Keon, B. H.; Bilter, G. K.; Owens, S.; Lamerdin, J.; Westwick, J. K. *Assay Drug Dev. Technol.* **2003**, *1*, 811−822.
(14) Hemmila, I. A.; Hurskainen, P. *Drug Discovery Today* **2002**, *7*, S150−156.
(15) Krätzer, F.; Rosorius, O.; Heger, P.; Hirschmann, N.; Dobner, T.; Hauber, J.; Stauber, R. H. *Oncogene* **2000**, *19*, 850−857.
(16) Berg, T.; Cohen, S. B.; Desharnais, J.; Sonderegger, C.; Maslyar, D. J.; Goldberg, J.; Boger, D. L.; Vogt, P. K. *Proc. Natl. Acad. Sci. U.S.A.* **2002**, *99*, 3830−3835.
(17) Stauber, R. H.; Afonina, E.; Gulnik, S.; Erickson, J.; Pavlakis, G. N. *Virology* **1998**, *251*, 38−48.
(18) Hu, C. D.; Chinenov, Y.; Kerppola, T. K. *Mol. Cell.* **2002**, *9*, 789−798.
(19) Heger, P.; Lohmaier, J.; Schneider, G.; Schweimer, K.; Stauber, R. H. *Traffic* **2001**, *2*, 544−555.
(20) Stauber, R. H.; Horie, K.; Carney, P.; Hudson, E. A.; Tarasova, N. I.; Gaitanaris, G. A.; Pavlakis, G. N. *BioTechniques* **1998**, *24*, 462−471.

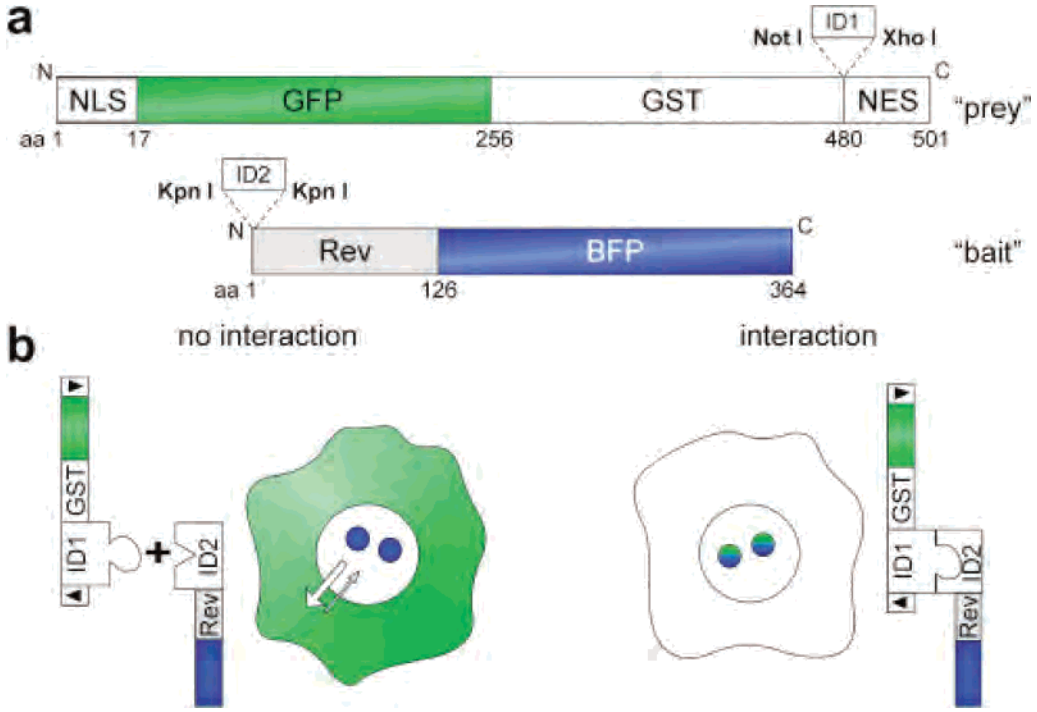

Figure 1. (a) Schematic representation of the domain organization of the GFP-prey and BFP-bait proteins. The GFP-prey is composed of the SV40 NLS, GST, GFP and the HIV-1 RevNES. The BFP-bait comprises a fusion of the HIV-1 RevM10BL protein fused to BFP. Unique restriction sites for the cloning of interaction domains are indicated. (b) Principle of the translocation based protein−protein interaction assay. GFP-prey fusions are continuously shuttling between the nucleus and the cytoplasm and do not interact with nucleolar BFP-bait proteins lacking matching IDs. In contrast, in case of efficient protein interaction, coexpression of a GFP-prey-ID1 fusion together with an ID2-BFP-bait protein results in translocation of the prey, being tethered to the nucleolus by the bait. Filled forward triangle, NLS; filled reverse triangle, NES.

limits, and the background signal in an area with no cells was subtracted from all values.

Drug Treatment. Cells were treated with 0.2 μM nutlin-3 (Alexis Biochemicals) for 8 h.

Immunoblotting. 5×10^5 HeLa cells were transfected with the indicated plasmids. Whole cell lysates, analysis of the complexes by SDS−PAGE, and immunoblotting using a polyclonal anti-GFP antibody (BD Biosciences) and a polyclonal anti-β-actin antibody (Sigma Aldrich) were performed as described.[19]

RESULTS

Rational Design of PTBs To Visualize Specific Protein−Protein Interaction in Living Cells. A facile and reliable system that allows visualization of protein interactions in living cells applicable also for drug screening CBAs has to fulfill the following criteria: (1) The GFP-tagged molecule I (GFP-prey), although continuously shuttling between the nucleus and the cytoplasm, should localize predominantly to the cytoplasm. (2) The BFP-tagged molecule II (BFP-bait) should be confined to the nucleus. (3) Upon specific protein interaction between molecule I and II, the GFP-prey should redistribute to the nucleus and co-localize with the BFP-bait (Figure 1b). (4) The system should be reversible and should allow the modular exchange of interaction domains. (5) Inhibitors/inductors of protein interactions should prevent/induce the cytoplasmic to nuclear translocation.

Previously, we showed that the intracellular localization of a GST−GFP fusion strictly depends on the presence of nucleocytoplasmic transport signals and is not flawed by passive diffusion.[19] In addition, GST−GFP is highly fluorescent, nontoxic, and stable. To design a GFP−GST shuttle protein with a predominantly

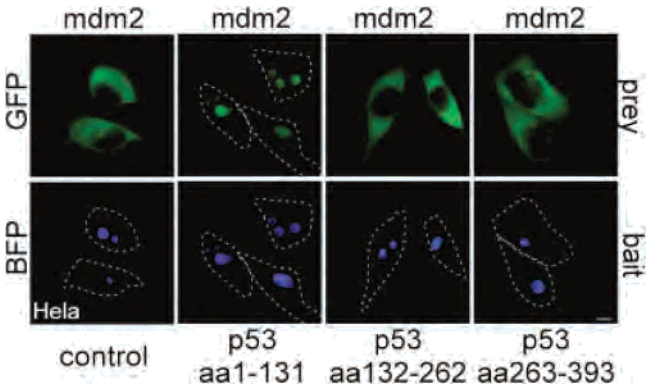

Figure 2. PTB-based mapping of the mdm2 protein interaction interface on p53. HeLa cells coexpressing the indicated prey/bait proteins were analyzed by fluorescence microscopy. The GFP-prey-mdm2 protein localized predominantly in the cytoplasm, and no co-localization was detectable by coexpression of the empty BFP-bait protein (left panel). In contrast, coexpression of the p53 aa 1−131, but not of aa 132−262 or aa 263−393_BFP-bait induced the cytoplasmic to nuclear translocation of GFP-prey_mdm2, indicative for protein−protein interaction. Scale bars, 10 μm.

cytoplasmic steady-state localization, an appropriate combination of nuclear import (NLS) and nuclear export signals (NES) had to be used. Based on our kinetic classification studies,[19] we choose the SV40 large T-antigen NLS (SV40NLS) and the NES from the HIV-1 Rev protein (RevNES). Subsequently, we engineered a cassette that allows the expression of any ORF **X** as a NLS-GFP/GST-**X**-NES fusion protein (GFP-prey) via cloning into the unique *Not*I-/*Xho*I-restriction sites of the expression vector (Figure 1a). Our previous work[17] demonstrated that a NES deficient HIV-1 Rev-

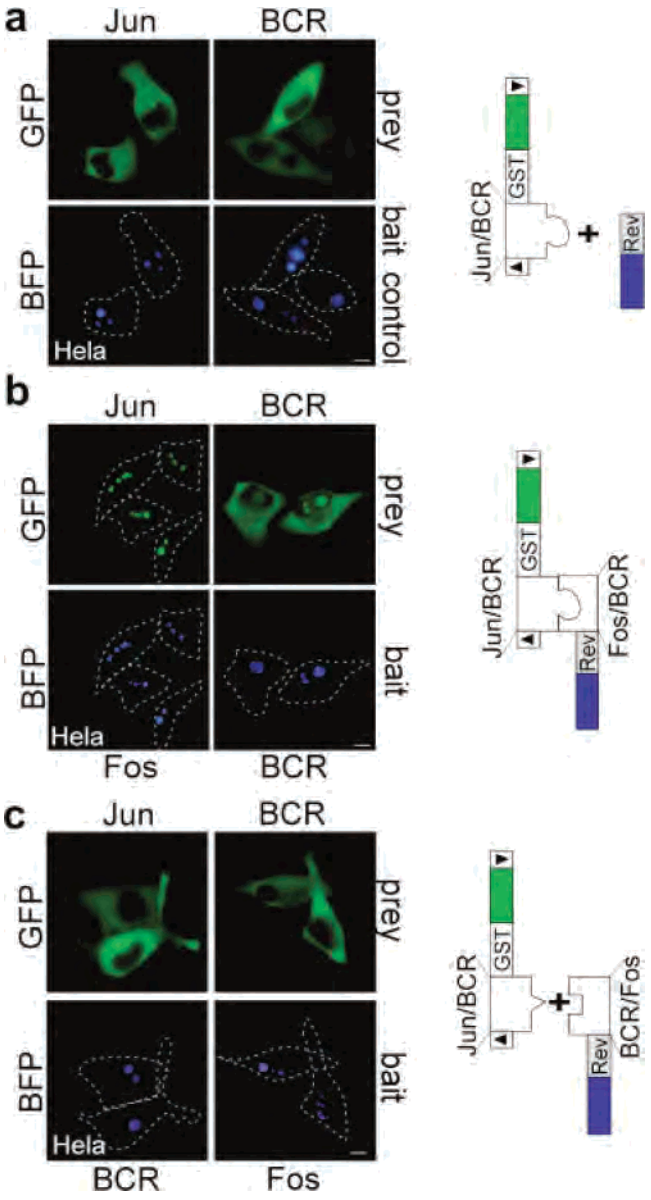

Figure 3. Application of PTBs to visualize specific protein−protein interaction in living cells. HeLa cells coexpressing the indicated prey/bait proteins were analyzed by fluorescence microscopy. (a) The GFP-prey-Jun/BCR proteins localized predominantly in the cytoplasm (upper panel) and no co-localization was detectable by coexpression of the empty BFP-bait proteins (lower panel). (b) In contrast, the GFP-prey proteins accumulated in the nucleolus upon coexpression of the matching BFP-bait interaction partners. (c) No significant co-localization was detectable by coexpression of GFP-prey_Jun together with BCR_BFP-bait or of GFP-prey_BCR and the Fos_BFP-bait fusion proteins. Dashed lines mark the cell boundaries visualized from the corresponding phase-contrast images. Scale bars, 10 μm. Filled forward triangle, NLS; filled reverse triangle, NES.

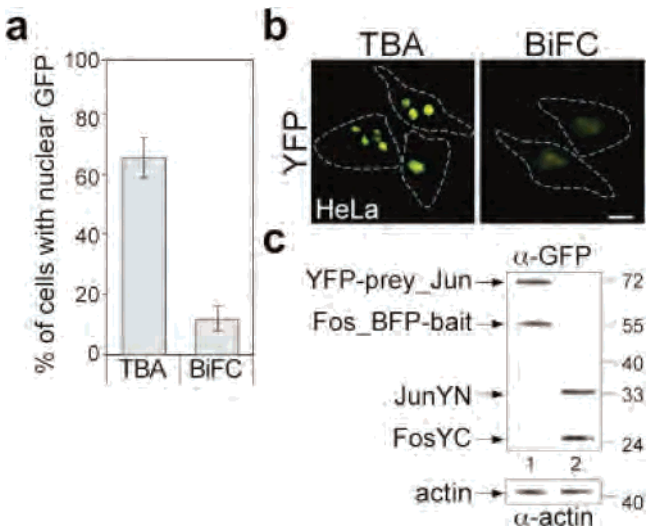

Figure 4. Superiority of AFP-based protein−protein interaction assay to bimolecular fluorescence complementation. HeLa cells were cotransfected with 1 μg of each of the GFP-prey_Jun and Fos_BFP-bait or the FosYC and JunYN expression plasmids and analyzed by fluorescence microscopy (see Experimental Procedures). Cells were recorded using identical camera settings. (a) A significantly higher percentage of cell displaying nuclear GFP fluorescence indicative for protein interaction was observed using the PTB assay. Mean values ± SD from two independent experiments are shown. Error bars, SD. (b) In addition, randomly selected cells displayed a higher fluorescence intensity on average in the PTB assay. Scale bars, 10 μm. (c) Equal expression levels of the indicated fusion proteins were verified by Western blot analysis of cellular lysates using a polyclonal anti-GFP antibody. β-Actin served as the loading control.

BFP fusion (RevM10-BFP) localized to the nucleolus and thus represented an ideal frame to express nucleolar anchored **Y**-BFP fusion proteins (BFP-bait) by cloning into the unique *Kpn*I-restriction site of the expression vector. Of note, the distinct emission and excitation spectra of the used GFP and BFP mutants[20] allowed the detection of the localized GFP-prey and the BFP-bait independently from each other in the same cell.

Mapping the mdm2 Protein Interaction Interface on p53. To demonstrate that our system was applicable for the identification of protein IDs, we first expressed the mdm2 aa 1−118, known to mediate p53 binding, as a GFP-prey_mdm2 fusion. As expected, the GFP-prey_mdm2 fusion localized to the cytoplasm and did not co-localize with the empty BFP-bait at the nucleolus upon coexpression in HeLa, 293 or Vero cells (Figure 2, left panel and data not shown). Next, we expressed the p53 aa 1−131, 132−262, or 263−393 in the context of the BFP-bait construct. Following transient expression, the p53-bait fusions were correctly tethered to the nucleolus. Although protein expression increased over time, the observed prey/bait-translocation patterns were similar when inspected at 16, 24, or 26 h posttransfection (data not shown). However, only the p53 aa 1−131 induced the cytoplasmic to nuclear translocation of the GFP-prey_mdm2 indicative of efficient protein interaction (Figure 2). Similar results were observed in 293 and Vero cells (data not shown). Since the p53/mdm2 ID has previously been assigned to the p53 aa 1−42,[7] our PTB could be successfully applied for the protein ID identification. Of note, we have not experienced limitations of our system due to protein size, since we used the PTB system to analyze homomultimerization of prey/bait proteins with 180 kDa in size (unpublished observation).

PTBs Are Generally Applicable and Specific. Subsequently, we confirmed the performance of our system by analyzing additional structurally unrelated protein IDs. As representatives of the basic bZip protein ID family we examined the bZip IDs of Jun and Fos. Expression of GFP-prey_Jun revealed a cytoplasmic localization even in the presence of the empty BFP-bait (Figure 3a, left panel, and Figure 4b). In contrast, coexpression of the Fos_BFP-bait resulted in nuclear translocation and co-localization

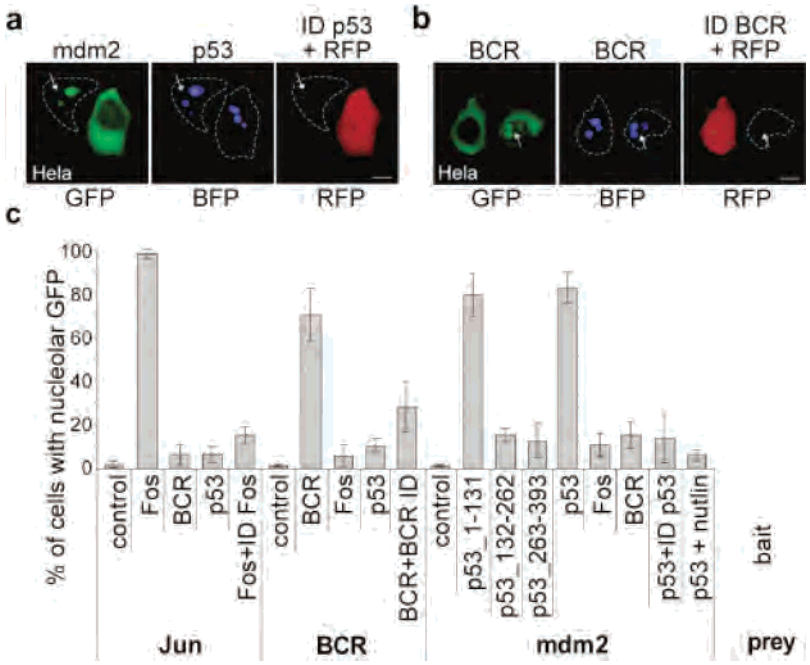

Figure 5. Reversibility of the PTB assay and suitability for the identification of SMPIIs. (a) Overexpression of the untagged p53 ID in GFP-prey_mdm2 and p53_BFP-bait coexpressing cells competes with p53/mdm2 interaction. RFP served as the transfection control. In RFP positive cells, expression of the competitor partially relieved the nucleolar accumulation of GFP-prey_mdm2, in contrast to nontransfected cells (marked by the arrow). (b) Overexpression of the untagged BCR ID in GFP-prey_BCR and BCR_BFP-bait coexpressing cells competes with BCR ID interaction. RFP served as the transfection control. In RFP positive cells, expression of the competitor relieved the partially nucleolar accumulation of GFP-prey_BCR in contrast to nontransfected cells (marked by the arrow). Scale bars, 10 μm. (c) To quantify the degree of protein interaction, 200 cells coexpressing the indicated GFP-prey and BFP-bait proteins together with the indicated competitors/compound were inspected. The percent of cells in which BFP and GFP co-localized at the nucleolus was determined. Mean values $\pm$ SD from two independent experiments.

of the GFP-prey_Jun fusion with the bait at the nucleolus (Figure 3b, left panel, and Figure 4b). Similar results were observed when swapping the Jun/Fos IDs in the prey/bait constructs (data not shown). As a further example for a non-leucine zipper protein ID, we investigated the N-terminal coiled-coil oligomerization interface of the BCR-Abl protein. The steady-state localization of the GFP-prey_BCR was cytoplasmic, and as required, no co-localization was induced upon coexpression of the empty BFP-bait (Figure 2a, right panel, and Figure 4b). Importantly, although the BCR-Abl ID is able to form homodimers, coexpression of the BCR_BFP-bait still resulted in a significant co-localization of the GFP-prey_BCR at the nucleolus (Figure 2b, right panel, and Figure 4b). Importantly, we did not observe protein interaction upon coexpression of the GFP-prey_Jun together with the BCR_BFP-bait (Figure 2c, left panel, and Figure 4b) or of the GFP-prey_BCR together with the Fos_BFP-bait (Figure 2c, right panel, and Figure 4b), which underlines the specificity of the interaction assay. All results could be confirmed in 293 and Vero cells (data not shown).

PTB Assay Is facile and Highly Efficient. A prerequisite for the routine use of live cell assays to detect protein−protein interaction is that the system is robust and does not require demanding technological assay platforms. Consequently, we compared our translocation assay to BiFC as another fluorescence microscopy-based assay system. BiFC is based on the fluorescence complementation between two nonfluorescent fragments of GFP when brought together by the interaction between proteins IDs fused to each fragment.

To compare the performance of the two assay systems, we cotransfected equal amounts of the GFP-prey_Jun and Fos_BFP-bait or the FosYC and JunYN expression plasmids into HeLa cells and quantitated the number of cells displaying nuclear GFP fluorescence indicative for active protein interaction (Figure 4a). Using identical CCD camera settings, not only the number of individual protein interaction events but also the average fluorescence signal was significantly higher for the PTB assay when compared to BiFC (Figure 4a,b). Similar transfection efficiencies and expression levels were confirmed by immunblot analysis (Figure 4c).

PTB Assay Is Reversible and Suited for the Identification of Small-Molecule Protein Interaction Inhibitors. Besides efficacy and specificity, reversibility is an important criterion for cellular protein interaction assays, in particular when applied for HCS/HTS to identify SMPIIs. Thus, we confirmed the reversibility of our assay by overexpressing the untagged ID of p53 (ID p53) in cells coexpressing the GFP-prey_mdm2 and p53_BFP-bait, which resulted in a significantly reduced nucleolar co-localization of the GFP-prey_mdm2 protein (Figure 5a,c). Similar results were obtained in competition experiments for the BCR-Abl ID using the untagged BCR aa 1−72 (Figure 5b,c).

As a case study for the application of a SMPPII, we attempted to disrupt the p53/mdm2 interaction by the use of nutlin-3, which had been described as a synthetic inhibitor of p53/mdm2 interaction in vitro and in vivo.[8] Treatment of transfected HeLa cells resulted in a significant cytoplasmic redistribution of the GFP-prey_mdm2 fusion, due to interference with p53/mdm2 interaction (Figure 5c). Of note, nutlin-3 treatment had no effect on Jun/Fos or BCR/BCR mediated translocation (data not shown), excluding the formal possibility that the GFP-prey_mdm2 redistribution was caused by nutlin-3-mediated inhibition of nuclear import.

DISCUSSION

This study validates the advantages of the AFP-based protein translocation biosensors as a straightforward approach to investigate protein−protein interactions in live cells. Recently, it has become clear that molecules that inhibit specific protein−protein interactions have great potential as therapeutics with new modes of action[3]. Consequently, numerous methods have been developed to analyze protein−protein interactions in vitro, in cell culture, and in vivo (see ref 21 and references therein). Paulmurugan et al.[10] reported a noninvasive system to detect protein−protein interaction in whole animals based on the reconstitution of split luciferase fragments. However, the experimental procedures required to quantify luciferase activity argue against its routine use in high-throughput CBAs. Fluorescence methods to study protein interactions in living cells involve inter- and intramolecular FRET as well as BiFC.[12] In contrast to in vitro FRET applications, the use of FRET in cellular assays is often inefficient, affected by background fluorescence, and requires demanding technological assay and analysis platforms in order to perform HTS. Although BiFC represents a powerful method, the efficiency and signal intensity is low, which could be also demonstrated in our study. In addition, BiFC depends on the proper orientation of the two AFP fragments, and the likelihood of complementation is expected to decrease with protein size and distinct intracellular localization of the interaction partners, which will limit its application for the characterization of HMWCs. Moreover, BiFC as well as other reconstitution/complementation assays appears to be irreversible[18] which hampers the screening for inhibitory protein interaction decoys. All these limitations do not apply to the described AFP-based cellular "two-hybrid" interaction system. We showed that the cytoplasmic to nuclear/nucleolar redistribution was easily detectable, highly specific, and reversible for the IDs investigated. In contrast to FRET, no specific linkers connecting the IDs to the prey/bait backbone were required. Importantly, the distinct intranuclear (co)localization patterns observed were characteristic for the IDs used and, in the case of the Jun-Fos IDs, exhibited a similar granular pattern as reported for full length Jun-Fos heterodimers.[18] This suggests that the IDs displayed by the prey/bait backbone can mimic the conformation of the IDs in the full length proteins in vivo. Besides specificity, reversibility is an important issue in CBAs in order to identify potent SMPIIs. Since overexpression of the untagged Fos or BCR ID was able to chase the respective prey fusion proteins out of the Jun/Fos or BCR/BCR complexes, our interaction system fulfills this criterion. Importantly, as a bona fide application of a SMPII treatment with nutlin-3 was able to successfully compete with p53/mdm2 ID interaction in living cells. Thus, the introduction of the AFP-based PTB system, combined with novel computer-driven, automated image acquisition and pattern-recognition systems, will help to realize cell-based high-throughput SMPIIs identification. Already to date, the defined disease relevant targets are numerous (see refs 5 and 21) and are expected to multiply by the systematic analysis of the human proteom.

In conclusion, the assay presented proved flexible, robust, facile, and highly amenable to academic-scale screens with the potential to be employed in novel HCS/HTS applications. Since the majority of GFP-prey fusions are not expected to intrinsically localize to the nucleolus, our system is applicable to also map the IDs of novel proteins. The modular composition of the PTB guarantees their application in numerous biological systems and will not only help to elucidate basic biological mechanisms but also stimulate the screening and discovery of pharmaceuticals that modulate protein−protein interactions as novel therapeutic strategies.

(21) Pagliaro, L.; Felding, J.; Audouze, K.; Nielsen, S. J.; Terry, R. B.; Krog-Jensen, C.; Butcher, S. *Curr. Opin. Chem. Biol.* **2004**, *8*, 442−449.

ACKNOWLEDGMENT

We thank B. Groner for support and G. Carra and Y. Fernandez for technical assistance. This work was supported by the Deutsche Forschungsgemeinschaft (Sta 598/1-2.), the BMBF (NGFN 01GS0451), and the Studienstiftung des Deutschen Volkes (S.K.K.).

Received for review March 9, 2005. Accepted May 22, 2005.

AC050413O

10 Curriculum Vitae

Persönliche Angaben

Name:	Shirley Knauer
Geburtstag:	09. August 1976
Geburtsort:	Fürth / Deutschland
Staatsangehörigkeit:	deutsch
Familienstand:	ledig

Schulausbildung

1982 - 1986	Grundschule Soldnerstraße in Fürth
1986 - 1995	Heinrich-Schliemann-Gymnasium in Fürth
30.06.1995	Allgemeine Hochschulreife (Note 1,1)

Hochschulausbildung

10/1995 - 09/1997	Grundstudium der Biologie an der Friedrich-Alexander-Universität in Erlangen
09/1997	Vordiplom der Biologie (Note 1,2)
10/1997 - 06/1999	Hauptstudium der Biologie mit dem Hauptfach Genetik und den Nebenfächern Virologie, Zoologie und Physikalische Chemie an der Friedrich-Alexander-Universität in Erlangen
07/1999	Diplomprüfung in den Fächern Genetik (Note 1,3), Virologie (Note 1,0), Zoologie (Note 1,3), Physikalische Chemie (Note 1,0)
11/1999 - 08/2000	Diplomarbeit am Institut für klinische und molekulare Virologie, Erlangen, Titel: „Charakterisierung von Domänen im HIV-1 Nef-Protein, welche die virale Infektiosität und Replikation beeinträchtigen“ (Note 1,0) Diplom-Gesamtnote 1,1
10/2000 - 08/2001	Bearbeitung eines wissenschaftlichen Projektes an der Universität Erlangen und später der Universität Ulm (ab 01/2001), Thema: „Modulation der HIV-1 Nef-Funktion während der AIDS-Progression“
Seit 09/2001	Doktorarbeit im Chemotherapeutischen Forschungsinstitut Georg-Speyer-Haus in Frankfurt am Main (voraussichtlicher Disputationstermin Ende Juni 2005)
Seit 1999	Im Rahmen der Diplom- und Promotionsarbeit in der HIV-1- und Krebsforschung tätig, aktive Teilnahme an verschiedenen nationalen und internationalen Kongressen (siehe Kongreßliste)

Nebentätigkeiten während der Schul- und Studienzeit

08/1991 - 03/1998	Lagertätigkeiten Arzneimittel, adäquater Versand rezeptpflichtiger Medikamente, Impf- und Gefahrstoffe an Apotheken bei der STUMPF AG, später PHOENIX AG
1992 - 2000	Nachhilfeunterricht für Real- und Gymnasialschüler in den Fächern Mathematik, Physik, Chemie, Englisch, Deutsch und Latein

Berufsbezogene Tätigkeiten

11/1998 - 12/1998	Industriepraktikum bei der Firma Merck in Darmstadt, Abteilung Biomed FO Target Research, Kardiovaskuläre Erkrankungen, Titel: „Alternative zum reverse Northern Blot“
01/2003	Für die Studienstiftung des deutschen Volkes als Mitglied der Prüfungskommission im Rahmen eines Auswahlseminars in Bad Homburg

Stipendien

09/2000 - 12/2000	Stipendium im Graduiertenkolleg „Kontrolle der Transkription“ TP PD Dr. Grassmann / PD Dr. Kirchhoff, 3. Förderperiode des GK
03/1998 - 10/2000	Stipendium der Studienstiftung des deutschen Volkes
01/2001 - 02/2001	Stipendium der Erika-Giehrl-Stiftung zur Förderung des wissenschaftlichen und künstlerischen Nachwuchses (Graduiertenförderung)
03/2001 - 03/2004	Promotionsstipendium der Studienstiftung des deutschen Volkes
05/2005	Stipendium zur Teilnahme an der 25. Blankenese-Konferenz „Signaling in Sensory Systems“ in Hamburg

Auszeichnungen

1995	Grete-Schickedanz-Preis
1995	Buchpreis des Fonds der Chemischen Industrie
1995	Bücherstipendium der Oskar-Karl-Forster-Stiftung
1996	Bücherstipendium der Oskar-Karl-Forster-Stiftung

Weiterbildung und Workshops

09/1998	Sommerakademie, Alpbach, Österreich „Regulatory mechanisms in malignant cells and cancer“
08/1999 - 09/1999	Hilderstone College, Broadstairs, Kent, UK „Intensive English Language Course for University Students“
03/2000 - 04/2000	Universität Erlangen „Einführung in die Versuchstierkunde“
03/2004	DECHEMA-Kurs Gentechnikrecht: Gefährdungspotentiale, Sicherheitsmaßnahmen und Rechtsvorschriften, anerkannt nach §15 Abs. 4 Satz 2 GenTSV
10/2002	Heidelberg, DKFZ, „Gene expression profiling“
10/2004	Karlsruhe, Forschungszentrum, EU 6th framework program BRECOSM „Women in science“

Ausbildungstätigkeit (Co-Betreuung von Diplomanden)

Sylvia Pesth	„Etablierung eines *in vivo* Selektionssystems zur Identifizierung regulatorischer mRNS Elemente“ (Diplomarbeit, Fachbereich Biologie und Informatik 2002-2003; Univ. Frankfurt)
Nariman Ansari	„Identifizierung von Peptidaptameren mit Spezifität für nukleäre Exportsignale“ (Diplomarbeit, Fachbereich Biologie und Informatik 2003; Univ. Frankfurt)
Sabrina Moodt	„Etablierung von GFP-basiereten zellulären Testsystemen zur Identifizierung krebstherapeutischer Substanzen“ (Diplomarbeit; Fachbereich Biochemie 2003-2004; Univ. Frankfurt

Soziales Engagement

1993 - 1995	VCP, Verein Christlicher Pfadfinder/innen, Gruppenleitung
1997 - 1999	Aktives Mitglied der Fachschaftsinitiative Biologie, Friedrich-Alexander-Universität Erlangen
12/2002 - 12/2003	Doktorandensprecherin am Georg-Speyer-Haus, Frankfurt am Main
Seit 10/2004	Mitglied des Betriebsrates des Georg-Speyer-Hauses, Frankfurt am Main

Sprachen

Deutsch (Muttersprache)
Englisch (verhandlungssicher)
Latein (großes Latinum)
Französisch (fundierte Grundkenntnisse)

Kongresse

2001, Dresden, Jahrestagung der Gesellschaft für Virologie: Knauer, Jafrate, Skowronski, Münch, Kirchhoff. „Characterization of domains in the HIV-1 Nef protein that affect viral infectivity and replication“ (Vortrag)

2001, Toulon, France, International AIDS Congress: Heger, Lohmeier, Knauer, Stauber. „Qualitative divergent nuclear export signals can modulate the post-transcriptional control of HIV-1“ (Poster)

2001, Strasbourg, France, First Joint French-German Congress on Cell Biology: Knauer, Stauber. „The tumor suppressor protein E1B-AP5: A mobile hnRNP protein containing cooperative nuclear import signals and a CRM1-dependent export signal“ (Poster)

2002, Bonn, Jahrestagung der Gesellschaft für Zellbiologie: Knauer, Carra, Stauber. „CVC paired-like homeobox genes encode active nucleo-cytoplasmic shuttle proteins“ (Vortrag)

2003, Wien, Österreich, 8th annual meeting of the RNA Society: Knauer, Pesth, Stauber. „Identification and characterization of regulatory mRNA elements in disease relevant genes“ (Poster)

2005, Braunschweig, 7th German Peptide Symposium, GBF - German Research Centre for Biotechnology: Knauer, Moodt, Berg, Liebel, Pepperkok, Stauber. „Development of Novel Translocation Biosensors to Study Signal Specific Nucleo-Cytoplasmic Transport, Protease Activity and Protein-Protein Interactions of Disease Relevant Targets“ (Poster)

2005, Würzburg, 13th AEK/AIO Cancer Congress: Knauer, Carra, Stauber. „Translocation Biosensors to Study Signal Specific Nucleo-Cytoplasmic Transport and Protein-Protein Interactions of Cancer Relevant Targets“ (Poster)

2005, Heidelberg, 28th Annual Meeting of the German Society for Cell Biology: Knauer, Carra, Stauber. „Nuclear export is evolutionary conserved in CVC paired-like homeobox proteins and influences protein stability, transcriptional activation and extracellular secretion“ (Poster)

2005, Hamburg, 25th Blankenese Conference, Signaling in Sensory Systems: Knauer, Carra, Stauber. „Nuclear export is evolutionary conserved in CVC paired-like homeobox proteins and influences protein stability, transcriptional activation and extracellular secretion“ (Poster)

Publikationen

Knauer, S.K., Carra G. and Stauber, R.H. (2005) Nuclear export is evolutionary conserved in CVC paired-like homeobox proteins and influences protein stability, transcriptional activation and extracellular secretion. ***Mol Cell Biol**, 25*: 2573–2582.

Knauer, S.K., Moodt, S., Berg, T., Liebel, U., Pepperkok, R. and Stauber, R.H. (2005) Translocation biosensors to study signal specific nucleo-cytoplasmic transport, protease activity & protein interactions. ***Traffic**, 6*:594-606.

Knauer, S.K. and Stauber R.H. (2005) Application of Autofluorescent Translocation Biosensors to Investigate Protein-Protein Interactions in Living Cells. ***Anal Chem**, DOI 10.1021/ac050413o*.

Dälken, B., Giesübel, U., **Knauer, S.K.** and Wels, W. (2005) Targeted induction of apoptosis by chimeric granzyme B fusion proteins carrying antibody and growth factor domains for cell recognition. ***Cell Death Differ***, *in revision*.

Krämer, O., Baus, D., **Knauer, S.K.**, Stein, S., Jäger, D., Stauber, R.H., Grez, M., Pfitzner, E. and Heinzel, T. (2005) Acetylation of STAT1 modulates NF-κB signaling. ***Genes Dev***, *submitted.*

Knauer, S.K., Krämer, O., Knösel, T., Engels, K., Rödel, F., Walendzik, H., Kovács, A.F., Habtemichael, N., Brieger, J., Mann, W., Heinzel, T., Petersen, I., and Stauber, R.H. (2005) Nuclear export is essential for the biological activity of survivin - Novel aspects to target the survivin pathway in cancer. *Cancer Research, submitted*.

Knauer, S.K. and Stauber, R.H. (2005) The tumor suppressor protein E1B-AP5: A mobile hnRNP protein containing cooperative nuclear import signals and a CRM1-dependent export signal, *in preparation*.

Meine akademischen Lehrer waren

Georg Fey, Frank Kirchhoff, Rolf Marschalek, Roland Stauber, Bernd Groner, Thorsten Heinzel,

11 Eidesstattliche Versicherung

Ich erkläre hiermit an Eides statt, daß ich die vorliegende Arbeit selbständig angefertigt und mich anderer Hilfsmittel als der in ihr angegebenen nicht bedient habe, insbesondere, daß aus Schriften Entlehnungen, soweit sie in der Dissertation nicht ausdrücklich als solche mit Angabe der betreffenden Schrift bezeichnet sind, nicht stattgefunden haben.

Frankfurt am Main, den 25.Juli 2005

Shirley Knauer

Erklärung

Ich erkläre hiermit, daß ich mich bisher keiner Doktorprüfung unterzogen habe.

Frankfurt am Main, den 25.Juli 2005

Shirley Knauer

12 Danksagung

Mein Dank gilt allen, die zum Gelingen dieser Arbeit beigetragen haben.

Bedanken möchte ich mich bei Herrn Prof. Dr. Bernd Groner für die Möglichkeit, diese Arbeit im Georg-Speyer-Haus anfertigen zu können. Ebenso danke ich Prof. Dr. Rolf Marschalek für die Übernahme der Betreuung von Seiten der Fakultät.

Mein besonderer Dank gilt PD Dr. Roland Stauber für die Vergabe des Themas, sein Interesse am Fortgang der Arbeit und seiner steten fachlichen sowie persönlichen Unterstützung. Die ständige Bereitschaft zur Diskussion, die vielen Anregungen und unzähligen Ideen, aber auch die Möglichkeit, eigene Ideen zu verwirklichen, haben die Motivation zum Denken und Forschen sehr leicht gemacht.

Mein besonderer Dank gilt auch der Studienstiftung des deutschen Volkes für die finanzielle Unterstützung während des Studiums sowie der Promotion.

Ebenso gilt mein Dank allen Mitgliedern der Arbeitsgruppe Stauber, mit denen das Arbeiten wirklich großen Spaß gemacht hat. Besonders danke ich Inka, Negusse, Silke und Silvia dafür, daß sie mir immer mit Rat und Tat zur Seite standen, und natürlich Gert und Yolanda für ihre unermüdliche Hilfe im Labor sowie ihren ständigen Einsatz als „Gute-Laune-Garanten".

Oliver Krämer danke ich vielmals für die allzeit gute und sehr fruchtbare Zusammenarbeit inklusive stundenlanger hochwertiger wissenschaftlicher Diskussionen.

Matthias und Elke möchte ich dafür danken, daß sie mir immer zugehört und mir Mut gemacht haben, wenn es im Labor mal nicht so gut lief.

Allen anderen, die mich inspiriert oder mir geholfen haben, aber nicht persönlich erwähnt werden, danke ich nicht minder.

Ganz besonderer Dank gilt natürlich meiner Familie, meinen Freunden und vor allem Roland für alles, was sie mir Gutes tun und getan haben. Meinen Großeltern möchte ich im Besonderen dafür danken, daß sie stets an mich geglaubt haben und dies alles erst möglich gemacht haben